MINERALOGICAL AND GEOCHEMICAL COMPARISON OF SKARNS IN THE AKDAĞMADENİ, AKÇAKIŞLA AND KESKİN DISTRICTS, CENTRAL ANATOLIA, TURKEY

A THESIS SUBMITTED TO
THE GRADUATE SCHOOL OF NATURAL AND APPLIED SCIENCES
OF
THE MIDDLE EAST TECHNICAL UNIVERSITY

BY

İLKAY KUŞCU

IN PARTIAL FULLFILMENT OF THE REQUIREMENTS FOR THE DEGREE OF

DOCTOR OF PHILOSOPHY

IN

THE DEPARTMENT OF GEOLOGICAL ENGINEERING

OCTOBER 1997

Approval of the Graduate School of Natural and Applied Sciences

Prof. Dr. Tayfur ÖZTÜRK
Director

I certify that this thesis satisfies all the requirements as a thesis for the degree of Doctor of Philosophy.

Prof. Dr. Vedat DOYURAN
Head of the Department

This is to certify that we have read this thesis and that in our opinion it is fully adequate, in scope and quality, as a thesis for the degree of Doctor of Philosophy.

Prof. Dr. Ayhan ERLER
Supervisor

Examining Committee Members

Prof. Dr. Hasan BAYHAN

Prof. Dr. Ayhan ERLER

Prof. Dr. M. Cemal GÖNCÜOĞLU

Prof. Dr. Taner ÜNLÜ

Assoc. Prof. Dr. Nilgün GÜLEÇ

ABSTRACT

MINERALOGICAL AND GEOCHEMICAL COMPARISON OF THE SKARNS IN THE AKDAĞMADENİ, AKÇAKIŞLA AND KESKİN DISTRICTS, CENTRAL ANATOLIA, TURKEY

KUŞCU, İlkay

Ph.D., Department of Geological Engineering

Supervisor: Prof. Dr. Ayhan ERLER

October 1997, 192 pages

The purposes of this study are (1) determination of the mineral assemblages and compositions, (2) establishment of mineralogical and geochemical differences, and (3) investigation of the physical and chemical changes in the evolution of hydrothermal system during skarn formation using the mineral chemistry data. It is based on petrographical, mineralogical and geochemical study of samples from 11 skarn occurrences in the Akdağmadeni, Akçakışla and Keskin districts within the Central Anatolian Crystalline Complex (CACC). The skarns in these districts are exoskarns and endoskarns. Endoskarns are present only in the Akçakışla district and represent the skarnization of the Akçakışla Granite. Exoskarns are observed at all districts. Three types of exoskarns were identified as garnet-pyroxene, epidote and wollastonite skarns.

The optical examination shows that many are narrow, and exhibit sharp contacts between the dark and light colored bands giving rise to a fluctuating pattern, due to the cyclical variations in the composition of the hydrothermal solutions controlled by fracturing. The garnets also exhibit dissolution structures, striations, and cellular structures and morphological transitions from planar to cellular structures due to high flow rates and rapid crystal growths. The main reasons of high growth rates are the periodic changes in the chemical potentials of the garnet forming components and in the oxygen fugacity of the system. The EMP analyses of garnets show that they are grossular-andradite (grandite) garnets ranging from Ad_{100} to $Gro_{92.01}Sp_{0.43}$. The Al_2O_3 and $Fe_2O_{3(T)}$ contents of garnets fluctuate from core to rim and as do the andradite and grossular contents. The oscillatory zoning reflects changes in the activity ratio of Al to Fe, changes in the distribution of Al and Fe between fluid and mineral, and changes in the oxidation potential controlled mainly by the changes in the oxygen fugacity of the hydrothermal system. There is a relative enrichment of andraditic garnets in the rims of Evciboyuntepe (Akdağmadeni district) and Barajdoğusu (Akçakışla district) samples indicating that the garnet compositions were controlled partly by a system with lower temperatures, higher oxygen fugacities, and lower salinities compared to that of cores. The relative enrichment of grossularitic garnets in the Özgebaca (Akçakışla district) and Karamağara (Keskin district) occurrences is related to the initial contact metamorphism controlled by Al-rich protolith.

Pyroxenes from the district are diopsides and hedenbergites, and those in the Akçakışla are diopsides. They are also classified as johannsenitic (typical for Pb-Zn sulfide associations) in the Bayramali occurrence and diopsidic in the Çiçeklitepe and Radarbaca (Akdağmadeni district) occurrences. In the Akçakışla district, the pyroxenes in the Barajdoğusu and Özgebaca occurrences range from hedenbergite to diopside.

The correlations between skarns and associated granitoids within the studied districts are evaluated using Harker type diagrams with major and trace elements. The granitoids within the Akdağmadeni Akçakışla and Keskin districts exhibit characteristic distribution patterns of the plutons associated with W, Zn, Cu, Mo and Sn skarns.

Keywords: Akdağmadeni, Akçakışla, Keskin, Central Anatolia, geochemistry, garnets, pyroxenes, skarn, oscillatory zoning.

ÖZ

AKDAĞMADENİ, AKÇAKIŞLA VE KESKİN BÖLGELERİNDEKİ SKARN YATAKLARININ MİNERALOJİK VE JEOKİMYASAL KARŞILAŞTIRILMASI, ORTA ANADOLU, TÜRKİYE

KUŞCU, İlkay

Doktora, Jeoloji Mühendisliği Bölümü

Tez Yöneticisi: Prof. Dr. Ayhan Erler

Ekim, 1997, 192 sayfa

Çalışmanın amacı skarn oluşumu sırasındaki (1) mineral topluluklarını ve bileşimlerini tespit etmek, (2) mineralojik ve jeokimyasal farklılıkları ortaya koymak (3) hidrotermal sistemdeki fiziksel ve kimyasal değişiklikleri araştırmaktır. Orta Anadolu Kristalen Karmaşığı içinde yeralan Akdağmadeni, Akçakışla ve Keskin bölgelerindeki 11 skarn zuhurundan alınan örnekler petrografik, mineralojik ve jeokimyasal olarak incelenmiştir. Çalışılan bölgelerdeki skarnlar Gümüşler ve Aşıgediği metamorfiklerinin mermerleri ile granitoyidlerin dokanakları boyunca gözlenir. Endoskarnlar sadece Akçakışla bölgesinde vardır ve Akçakışla Graniti'nin skarnlaşmasını temsil eder. Garnet-piroksen, epidot ve vollastonit skarn olmak üzere üç tip ekzoskarn tanımlanmıştır.

Granat-piroksen skarnlar ilerleyen skarn topluluğunu temsil eder ve baskın mineral garnet olmak üzere piroksen, hematit, manyetit, pirotin, ve pirit I minerallerinden oluşmaktadır. Epidot skarnlar, öncel garnet-piroksen skarnların hidrotermal çözeltilerle yeniden dengeye ulaştığı skarn topluluğunu temsil etmektedir. Bu skarnlar epidot, piroksen, wollastonit, tremolit, kalsit, klorit, kuvars, sfalerit, galen, kalkopirit, pirit II minerallerini içermektedir. Vollastonit skarnlar çoğunlukla vollastonit ve onunla birlikte bulunan pirit, sfalerit hematit ve manyetit minerallerinden oluşmaktadır.

Granat-piroksen skarnlarındaki garnetler salınımlı zonlar gösterirler. Salınımlı zonların optik incelenmeleri çoğunun dar, ve dalgalanmalı zonlanma

örgüsüne yolaçan koyu ve açık zonlar arasındaki geçişin keskin olduğunu göstermektedir. Dalgalanmalı zonlanma, skarn hidrotermal sistemi içinde kırıklanmaların başlamasıyla kontrol edilen hidrotermal çözeltilerdeki periyodik değişimlerle açıklanmaktadır. Granatlar, hücreli yapısı, çözünme yapısı ve çizikler gibi yüksek akış oranları ve hızlı kristal büyümesi sonucu gelişen bazı morfolojik yapılar göstermektedir. Hızlı kristal büyümesinin nedenleri granat oluşturan bileşenlerin kimyasal potansiyelindeki ve oksijen fugasitesindeki periyodik değişimlerdir. Granatların EMP analizleri, granatların Ad_{100} ile $Gro_{92.01}Ad_{7.50}Sp_{0.43}$ arasında değişen grossular andradit (grandit) olduklarını göstermektedir. Granatların Al_2O_3 ve $Fe_2O_{3(T)}$ miktarları, andradit ve grossular miktarlarında olduğu gibi merkezden çepere doğru dalgalanma gösterir. Dalgalanmalı zonlanma, Al'nin Fe'ye karşı aktivite oranındaki değişimlerin, sıvı ile mineral arasındaki Al ve Fe dağılımındaki değişimlerin ve oksijen fugasitesindeki değişimlerden kaynaklanan oksidasyon potansiyelindeki değişimlerin göstergesidir. Barajdoğusu ve Evciboyuntepe yataklarındaki gametlerin çeperlerinde andradit bileşimlerinde göreceli bir artış vardır. Bu da bu çeperlerdeki garnet bileşimlerinin merkezdekilere göre sıcaklığın daha düşük, oksijen fugasitesinin daha yüksek, tuzluluğun daha düşük olduğu bir sistem tarafından kontrol edildiğini göstermektedir. Özgebaca ve Karamağara yataklarındaki gametlerin grossularca zengin olmasının sebebi Al' ce zengin bir protolit tarafından kontrol edilen ilksel metamorfizmaya bağlanmaktadır.

Akdağmadeni bölgesindeki piroksenler hedenberjit ve diyopsit, Akçakışla'dakiler ise diyopsittir. Piroksenler ayrıca Bayramali'de Johansenitik (Pb-Zn sülfid birlikteliğinin tipik minerali), Çiçeklitepe ve Radarbaca'da diyopsitik olarak sınıflandırılmaktadır. Barajdoğusu ve Özgebaca yataklarındaki piroksenler hedenberjit ve diyopsit arasında değişmektedir.

Skarnlar ve onlarla birlikte bulunan granitoyidler arasındaki korelasyonlar, majör ve iz elementlerle Harker tipi diyagramların kullanılmasıyla yapılmıştır. Akdağmadeni, Akçakışla ve Keskin bölgelerindeki granitoyidler W,Zn,Cu,Mo ve Sn skarnlarıyla birlikte bulunan granitoyidlerin dağılım şekillerini vermektedir.

Anahtar Kelimeler: Akdağmadeni, Akçakışla, Keskin, Orta Anadolu, Garnet, piroksen jeokimya, skarn, dalgalanmalı zonlanma.

Of all the friends
Who know me the best
Among them one and other
Dearer by far
Than all the rest
Was just this one,-

(J.H. Rhoades; Random thoughts of a man at fifty)

To My Wife, Gonca;

ACKNOWLEDGMENTS

I would like to express my sincere gratitude to my supervisor, Prof. Dr. Ayhan Erler, for his patience, support, guidance and helpful suggestions during the preparation of this thesis.

I extend my thanks to Dr. Peter A. Floyd for providing the use of the Geochemistry Laboratories of the Department of the Earth Sciences, Keele University.

Thanks also go to Mr. David Emley for his help with the SEM and XRF analytical work, and solving my software problems; Mr. Peter Greatbach and Mr. David Wilde for fast thin and polished section service; Ms. Margaret Aikin for sincere helps for pressed powder pellet preparation and XRF analysis; Mr. Orhan Karaman for thin section preparation.

The major part of the research for this thesis was carried out with financial support by the METU Research Fund, which I acknowledge with thanks.

I am indebted to Prof. Dr. M. Cemal Göncüoğlu of the Department of Geological Engineering, METU, for his criticisms about the geological evolution of the Centrai Anatolian Crystalline Complex.

Last, but not the least, I must thank to my dearest wife Gonca , my sisters Selma, Gülsüm and Nuray, my parents Mehmet and Perihan for their continuous support and encouragement throughout the preparation of this thesis.

TABLE OF CONTENTS

LIST OF FIGURES

FIGURES

LIST OF TABLES

TABLE

CHAPTER 1

INTRODUCTION

1.1. Purpose and scope

The main purposes of this study on lead-zinc skarns in Akdağmadeni, Akçakışla and Keskin districts are (1) to determine the mineral assemblages and mineral compositions, (2) to establish mineralogical and geochemical differences, (3) to investigate the physical and chemical changes in the evolution of hydrothermal system during skarn formation using the mineral chemistry data, and (4) to examine the effect of compositional variations of associated igneous rocks on the lead-zinc skarns. The studies that dealt with lead-zinc skarns within these districts date back to early 20th Century. The general characteristics of lead-zinc skarn deposits in these districts can be found in several studies (Çağatay and Teşrekli, 1979; Tülümen, 1980; Sağıroğlu, 1982; 1984a; 1984b; 1984c). They did not investigate the possible answers to the questions such as "whether a relationship exists between several lead-zinc skarns distributed over wide ranges of geologic and geographic settings ", or "whether the composition of intrusive bodies influence the distribution of skarn deposits". The Akdağmadeni, Akçakışla and Keskin districts in Central Anatolia, are three well known districts that contain several lead-zinc skarn occurrences. Therefore, the understanding of their mineralogical and geochemical characteristics will contribute to better understanding of the differences and similarities between these occurrences, skarn forming processes and related mineralizations in these regions. Since, the skarn mineralogy includes a wide variety of calc-silicate minerals, it is not only the key to recognizing and defining skarns, but also critical in understanding their origin, and in distinguishing economically important mineral occurrences. This study highlights the mineralogical and geochemical characteristics of the lead-zinc skarn occurrences in the Akdağmadeni, Akçakışla and Keskin districts, and evaluates them from geochemical and mineralogical points of view.

The geological maps and geological data for the lead-zinc skarns in the studied districts were compiled from the previous works. In order to establish geochemical, mineralogical and physical and chemical framework of the lead-zinc skarns in the Akdağmadeni, Akçakışla and Keskin districts, the samples were collected from the skarns and igneous rocks. Petrographic features were investigated by the study of thin sections and polished sections prepared from the samples. The mineral compositions of the skarn mineral assemblages from the selected skarn samples were determined by electron microprobe studies, and the major and trace element contents of the granitic rocks in the Akçakışla by XRF spectrometry.

1.2. Geographic setting

The Akdağmadeni, Akçakışla and Keskin districts in which at least 11 Pb-Zn skarn occurrences are found, lie within the northern Central Anatolia (Figure 1.1). The Akdağmadeni and Akçakışla districts are in Yozgat, and Keskin in Kırıkkale. Akdağmadeni district is located at about 100 km east of Yozgat and Akçakışla at about 25 km southwest of Akdağmadeni. The Keskin district is situated at about 15 km southeast of Kırıkkale.

Akdağmadeni lies on the Yozgat-Sivas highway at about equal distances from both cities. The lead-zinc skarns in the Akdağmadeni district are found within an area of about 28 sq. km, and occupies the area between Karapir village, Evciboyuntepe and Oyumçayırtepe (Figure 1.2). The lead-zinc skarns in the Akçakışla district are distributed in an area of approximately 10 sq.km to the east of Akçakışla village (Figure 1.3). The Keskin district covers an area of about 8 sq.km between Keskin town and Ömerağa village (Figure 1.4).

In the Akdağmadeni district, six Pb-Zn occurrences are sampled (Figure 1.2). Of these, Bayramali is still producing, Çukurmaden and Peynirliktepe produced in the past, whereas Evciboyuntepe, Radarbaca, and Çiçeklitepe are still in prospect stage. The lead-zinc occurrences in the Akçakışla district are situated between two streams called Karahocadere and İğdirdere. Three occurrences with past production histories were studied in this district; from east to west these are Akçakışla, Barajdoğusu and Özgebaca. The Akçakışla lies on the southwestern foothills of the Büyükgüneytepe and northern bank of the Karahocadere, Özgebaca lies at the southeastern foothills of

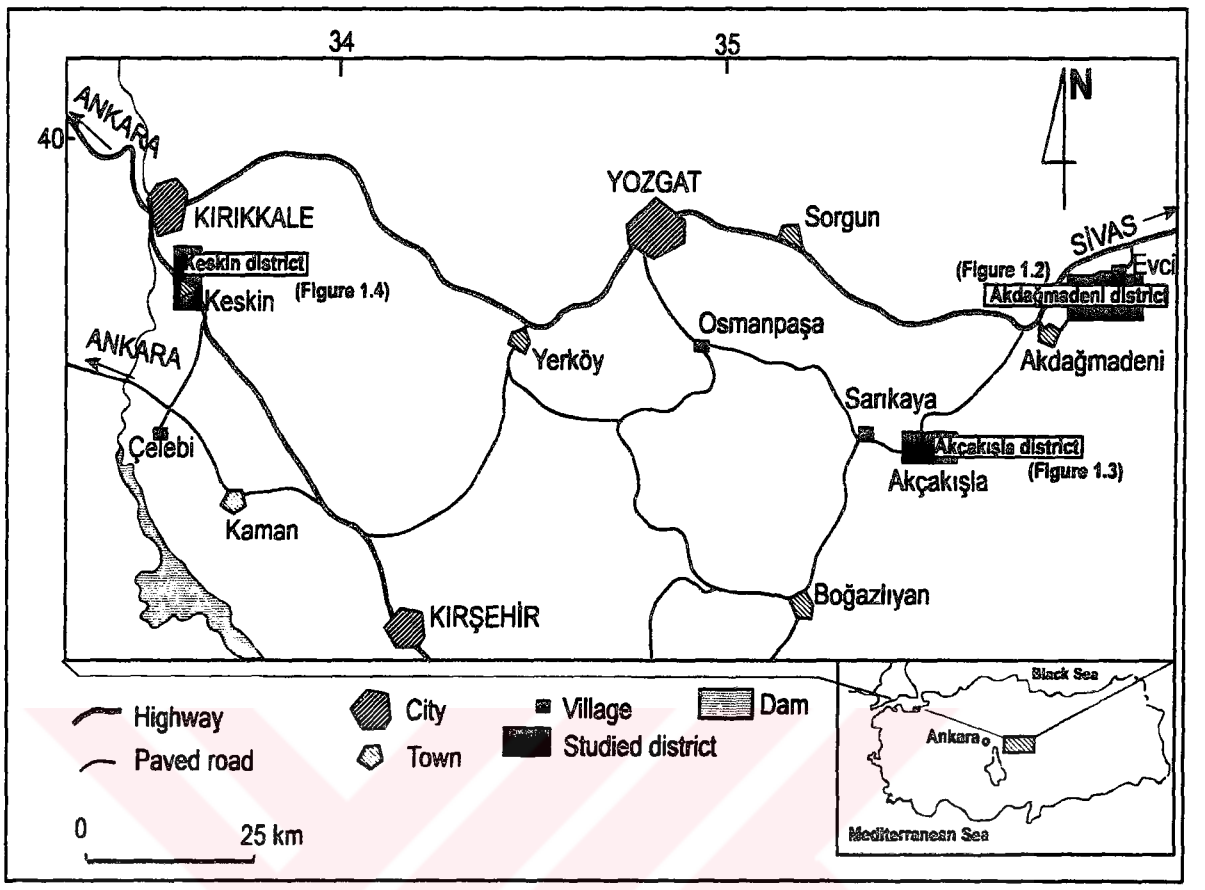

Figure 1.1. Location map of the studied areas

the Saytepe, and Barajdoğusu lies at southern bank of the Kurşunlukdere (Figure 1.3). The Keskin District is located on the western side of N-S trending hills. Within the Keskin area, two occurrences were studied. These are Karamağara at the southern end, and Simlikurşun at the northern end of the district (Figure 1.4) with past production histories.

1.3. Previous works

Economically important lead-zinc skarn mineralizations in the Akdağmadeni and Keskin regions have attracted interests of geologists since early 1900's. Most of the studies dealt with the geology of the mineralizations as well as general geology of the regions. Majority of these studies were done by the General Directorate of Mineral Research and Exploration (M.T.A), and are found as unpublished exploration reports

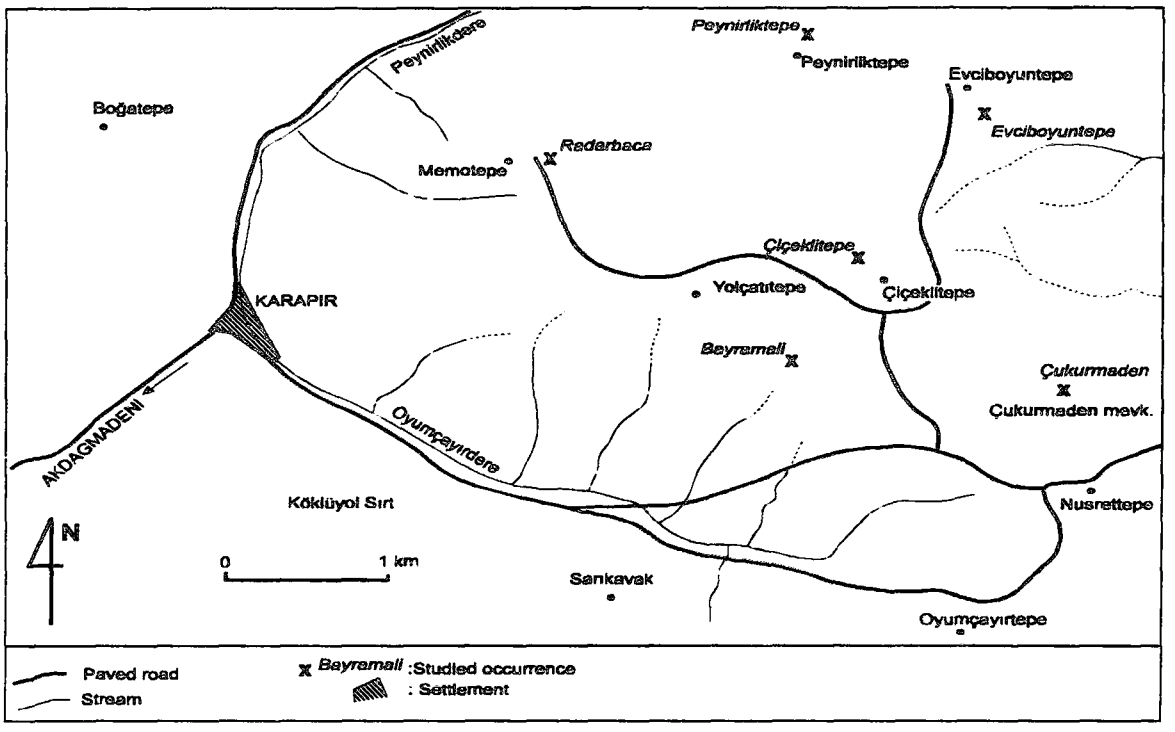

Figure 1.2. Location map of the Akdağmadeni district.

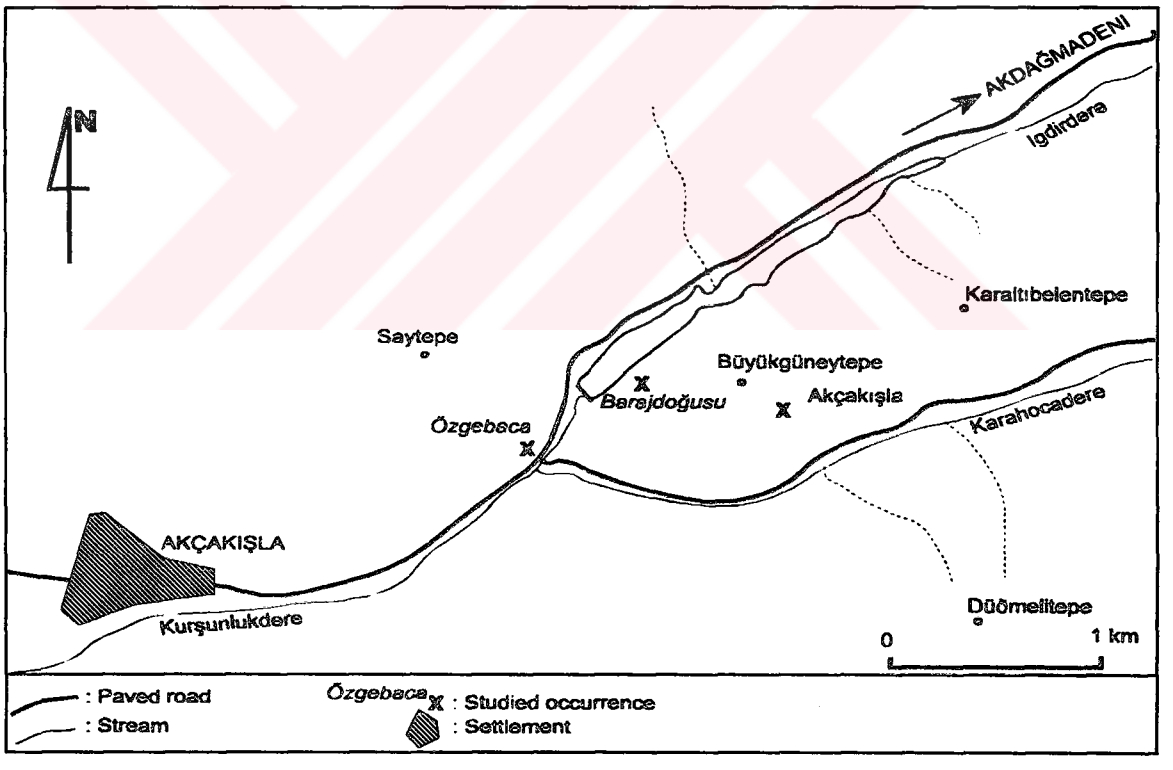

Figure 1.3. Location map of the Akçakışla district

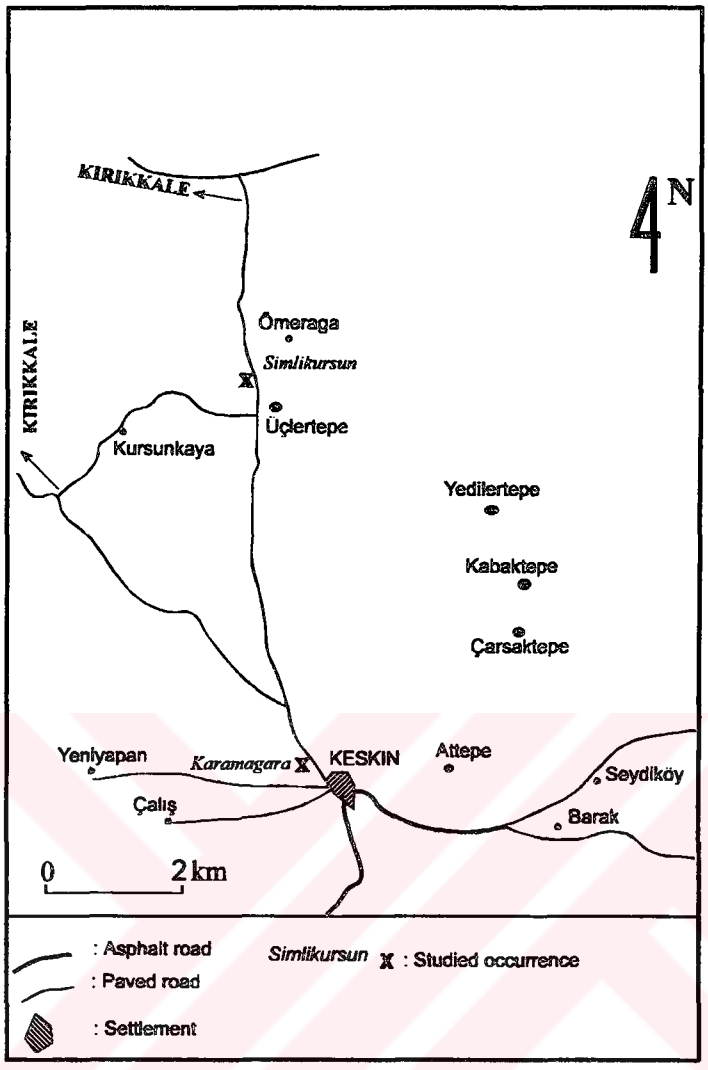

Figure 1.4. Location map of the Keskin district

within the M.T.A Library. Of these studies, only those related to general geology, mineralizations, and skarn related granitoids in the Akdağmadeni, Akçakışla and Keskin districts or nearby regions, are summarized.

The oldest known study was done by Paolo (1909). He explained the mineral content of a silver bearing skarn occurrence in the Akdağmadeni district.

Pilz (1936) studied in the Akdağmadeni district, and defined the geological features of the Akdağmadeni region. In this study, the ore minerals of the mineral deposits were also described.

Millet (1938) made reconnaissance studies in the Keskin district, and defined the geological setting of the Pb-Zn mineralizations. He defined that the ore body was found along the western contact between diabase tuffs and marbles.

Kovenko (1939a,b) made reconnaissance studies in the Keskin region. He suggested that the mineralizations in the Keskin were of mesothermal type. He explained that the mineralizations occur in the form of small veins collectively forming a thick ore body. He also explained that the mineralizations are found within a 10 km long N-S trending zone.

Kovenko (1940) described the form and style of mineralizations in the Keskin district. He also pointed out that the mineralization occurs mainly along the contacts between marble and granite, and he proposed that there is no chance of finding new mineralization in the district.

Kovenko (1947) discussed the metallogeny of lead-zinc skarn mineralizations in the Akdağmadeni, Akçakışla and Keskin districts. He proposed that the mineralizations are associated with skarns developed within the fracture zones of metacarbonates. He proposed that the mineralizations in these regions form a metallogenic province that can be correlated to the metallogenic lead province of Şebinkarahisar (Giresun).

Pollak (1958) studied around Akdağmadeni and Yıldızeli to highlight problems related to the mineralizations in these regions. In his study, he described the stratigraphic relationships between the rock units exposed in these regions. He mainly concentrated on the metamorphic basement, and proposed that a local unconformity exists between the gneissic basement and the overlying metacarbonate sequences.

CENTO (1964) reviewed the studies about the Akdağmadeni district and summarized structural control, paragenesis and mode of formation of mineralizations in this district. The skarns replaced the country rocks during the early hydrothermal period. The mineralization in skarn zones was introduced probably using faults as

main conduits. The faults were described as probably related to the emplacement of granite into the country rocks.

Vache (1963) outlined the geologic and tectonic setting of the Akdağmadeni contact metasomatic lead-zinc-silver deposits in the Central Anatolian Massif. He said that the metamorphic basement, and metamorphism related deformations were formed during Variscan Orogeny. The granites then intruded the metamorphics, and crystallized at shallow depths. He proposed that the fluids released from the granites just before crystallization moved upward through the fractures and caused extensive metasomatism producing calc-silicate minerals in the skarn zones. He termed the skarn zones as the metasomatized areas. During the advanced stages of cooling and crystallization, the metals transported by the fluids were deposited within the skarn zones. In his study, he suggested that deposits can be accepted as late pneumatolytic hydrothermal contact type deposits.

Çavuşoğlu (1967) studied the geology of the Pb-Zn mineralizations to the north of the Keskin, and argued that the mineralizations are lithologically controlled by marbles. He suggested that the marbles in the region occur as small blocks, and hence it is not possible to expect large mineralizations in this region.

Arslanpay and Yıldırım (1978) conducted a series of induced polarization studies in the Keskin region to find out the vertical and lateral distribution of the skarn mineralizations in this region. They determined three main anomalies and suggested 8 drilling sites within the anomalous areas as well as 6 more drilling sites for the entire region.

Çağatay and Teşrekli (1979) studied the mineralogy and paragenesis of the Karamağara lead-zinc occurrence in the Keskin district. They found that the mineral assemblage consists of galena (two types as galena I and II), sphalerite, hematite, chalcocite, and wittichenite. Galena I represents an earlier phase, and associated closely with the early forming minerals of sphalerite, chalcocite, and wittichenite. The microprobe analyses of galena I showed that it contains Ag and Bi indicating its formation at high temperatures.

Özkazanç (1980) conducted the magnetic surveys within the Keskin district to test the extent of mineralization within the marbles in contact with the granites at the

eastern and western parts of the N-S trending narrow skarn zone. He concluded that the marbles become wider on either side of the skarn zone and this causes the anomalies to be small compared to skarn zone, however, mineralization probably continues below the surface although the magnetic anomalies are small.

Tülümen (1980) studied the petrography and petrology of metamorphic rocks, granites and skarns in the Akdağmadeni region. The petrographical and mineralogical studies indicated that granitic rocks are mainly monzogranites, and cause the formation of skarns. The skarns are accepted as one of the major rock units in the region. Distinct zones are displayed from granite to metacarbonate as granite body, garnet zone, garnet-clinopyroxene-epidote zone, clinopyroxene-epidote zone, epidote-calcite zone, and metacarbonate. He also studied the zoning in the garnets.

Sağıroğlu (1982) studied the constraints on ore deposition and skarnization (skarn formation) related to lead-zinc ores in the Akdağmadeni region. He showed that the skarnization was formed in four successive stages each of which is characterized by a distinct assemblage. These stages are, magnetite-garnet-pyroxene, epidote-amphibole, epidote-chlorite, and kaolinite-muscovite. The early stage, magnetite-garnet-pyroxene represents release of early iron and aluminum rich solutions from the granite. This stage took place at temperatures between 500°-550°C without mineralization. The epidote-amphibole stage and its mineralogical assemblages were overprinted on the former minerals marked by alteration of garnets to epidote and pyroxenes to amphiboles and epidotes. He defined that this stage was the first stage at which sulfide precipitation was observed and early sulfide minerals, sphalerite, pyrrhotite, and pyrite were formed. The corresponding temperature for this stage is given as about 500°C. The third stage is the most important stage for the ore mineralization that occurred at temperatures between 490 to 330°C. Pyrite was the first mineral to form followed by arsenopyrite and chalcopyrite. Sphalerite started to form just before chalcopyrite formation was completed. Galena formation was partly accompanied by sphalerite. The final kaolinite-muscovite stage marks the onset of hydrothermal waters ascending through the wall rocks. This stage took place at temperatures less than 320°C

Sağıroğlu (1984a, b) proposed that the lead-zinc mineralizations in the Akdağmadeni occur along the contacts between adamellites and metacarbonates.

Three types of ore are observed as massive, "disseminated" and "cavity" ores. The paragenetic studies indicated a sequence of formation as pyrite, arsenopyrite, chalcopyrite, fluorite, sphalerite and galena. In addition, scheelite, chalcocite-covellite, goethite and smithsonite are mentioned. Pyrrhotite geothermometry and sphalerite geobarometry studies showed that the sulfide mineralizations occurred at temperatures between 390° and 430°C and pressures of nearly 500 bars.

Sağıroğlu (1984c) studied fluid inclusions in the lead-zinc skarns of the Akdağmadeni region. He found that the salinity of the hydrothermal fluids was high during the early stages of skarnization (20%NaCl equivalent) (magnetite-garnet-pyroxene and epidote-amphibole stages), and gradually decreased during the following stages (10% NaCl equivalent). The homogenization studies indicated that the homogenization temperatures for magnetite-garnet-pyroxene stage was more than 500°C, for epidote-amphibole stage it was 460-490°C, for epidote-chlorite-sulfide stage it was 390°-430°C, and for the final stage, kaolinite-muscovite stage it was less than 320°C

Ergintav (1987) studied the area between Akçakışla and Eynelli villages, and identified four rock units as İğdir limestone, Akçakışla granite, Kurtören formation and alluvial deposits. He also described the petrographical characteristics of the rock units

Bayhan (1989) studied petrographical, mineralogical and chemical characteristics of the Keskin Pluton, and showed that the Keskin Pluton is characterized by two mineralogically and chemically different groups, as light and dark colored groups. Dark colored, medium grained group is quartz monzonite to quartz monzodiorite in composition with metaluminous character. He said that this group displays characteristics intermediate between subalkaline (monzonitic) and calcalkaline and it belongs to cafemic rock association. Light colored, coarse grained group is granite-adamellite to granodiorite in composition with metaluminous to peraluminous characters. It exhibits a transition between cafemic and alumino-cafemic and between subalkaline and calcalkaline rock associations. He stated that the Keskin Pluton was formed due to partial melting of mantle and crustal materials.

Göncüoğlu et al.(1994) studied the geology of the eastern Central Anatolian Massif, and defined the relationships between the Central Kızılırmak Basin and the Sivas Basin. They suggested that general stratigraphic, and petrographic features of

the metamorphics within the Akdağmadeni are more or less the same with those exposed at different parts of the massif. The metamorphics in this region were correlated to the sequences in the Tauride Belt, and they suggested that they were the northern continuation of the Tauride-Anatolide Platform (TAP) before metamorphism.

Erler et al. (1996) studied the metallogeny of the Central Anatolian Crystalline Complex, and classified the mineral deposits into four major types based on their genesis as meta-sedimentary, skarn, vein, and sedimentary-volcanic types. They suggested that the deposits are related to the Alpine Orogeny, and are direct consequences of the southward obduction of the Upper Cretaceous ophiolitic rocks onto the Tauride-Anatolide Platform during Uppermost Cretaceous period. They proposed that the skarn type deposits are related to post collisional S-and I-type granitoids.

Kuşcu and Erler (1996, 1997) studied the space-time distribution and geologic setting of mineral deposits in the Central Anatolia, and classified them according to their host rocks as metamorphic hosted, granitoid hosted, sedimentary hosted and, volcano-sedimentary hosted deposits. They explained the evolutionary history of the mineral deposits in conjunction with the evolution of the complex.

1.4. Methods of study

1.4.1. Field work

Field work was done during summers of 1994 and 1995. It included mapping and sampling in the Keskin district and only sampling in the Akdağmadeni and Akçakışla districts. Sampling constitutes one of the major parts of this study, since the comparison of the Pb-Zn occurrences in the studied area depends largely on the mineralogy and geochemistry of individual skarn bodies. The sampling consisted of two successive stages; in the first stage only ore mineral-rich samples were collected, with at least four samples from each occurrence. In the first stage a total of 56 samples were collected. In the second stage the wall rocks (including skarns, and granitic rocks) were sampled during the summer of 1995. In this stage, garnet, pyroxene, amphibole, and epidote bearing samples were collected from the dumps in front of the mine workings. Since the garnet and pyroxene compositions are very helpful tools for the study of the physical and chemical conditions of skarn formation,

pyroxene and garnet bearing samples were collected with extra care. A total of 87 samples were collected in the second stage for geochemical and mineralogical studies.

1.4.2. Laboratory work

Laboratory work plays an important part in this study, and was done both at the Department of Geological Engineering, METU, and at the Department of Earth Sciences, Keele University. This part involved sample preparation, mineralogical studies, and chemical analyses.

1.4.2.1. Sample preparation

The thin and polished sections of the samples were prepared in the laboratories of the Department of Earth Sciences, Keele University, Keele, and the Department of Geological Engineering, Middle East Technical University, Ankara. A total of 130 thin sections were prepared, and 43 samples are polished for ore microscopy. Of the 130 thin sections, 21 samples were selected for microprobe analyses and they were doubly polished in laboratories of M.T.A. Then, they were coated with carbon before the analyses at the Department of Earth Sciences, Keele University. A total of 6 samples from the granitoids within the Akçakışla district were ground for XRF analyses.

1.4.2.2. Mineralogical studies

The samples were first examined by petrographic microscope and ore microscopy techniques. This was the crucial stage of this study, because the rest of the laboratory studies were based largely on the mineral content and their associations with each other. Mineralogical assemblage of the samples collected during first phase (ore mineral-rich samples) were determined by ore microscopy. The thin sections were examined by petrographic microscope. At this stage, although the purpose was to determine the mineral content of the samples and the association of the minerals with each other, the main objective was to select the pyroxene and/or garnet bearing samples for microprobe studies. At the end of these studies, 21pyroxene and garnet bearing samples were selected.

1.4.2.3. Chemical analyses

Chemical analyses include the whole rock chemistry and mineral chemistry. Whole rock chemistry was used to detect the major and trace element contents of the samples from the Akçakışla Granite. This was done by using XRF spectrometer (ARL 8420 Spectrometer) in the Department of Earth Sciences at the Keele University. It is fitted with two goniometers enabling simultaneous measurement of two analytical lines. The XRF is controlled by a DEC PDP 11/23 plus computer using ARL's DPS software running under multi-tasking operating system.

The compositional constituents of garnet and pyroxene bearing samples were analyzed by microprobe studies using the scanning electron microscope, JEOL JSM-35 linked to QX2000 energy dispersive analyzer specially designed for microprobe analyses at the Department of Earth Sciences, Keele University. The determination of compositional constituents helps to calculate the garnet and pyroxene compositions in terms of mole percent of their end members. The compositional information are summarized and evaluated graphically. Triangular plots are used to express variations in compositionally complex minerals such as pyroxene and garnet.

CHAPTER 2

REGIONAL GEOLOGY

The lead-zinc skarn occurrences in the Akdağmadeni, Akçakışla and Keskin districts are located along the northwestern and northeastern parts of Central Anatolian Crystalline Complex (CACC). The CACC is exposed within a wedge connecting the lines between Sulakyurt, , Yozgat, Sivas, Kayseri, and Niğde (Figure 2.1). It is simply an assemblage of ophiolitic, intrusive and extrusive rocks, and medium to high grade metamorphic basement that represents the northern passive margin of the Tauride-Anatolide Platform. This wedge or its subsidiary parts were named differently by several authors as Kırşehir Massif (Seymen, 1982) or Kırşehir Crystalline Massif (Bailey and McCallien, 1950; Egeran and Lahn, 1951), Central Anatolian Massif or Kızılırmak Massif (Ketin, 1955;1963; Erkan and Ataman, 1981). Locally, the same assemblage is called as Niğde Massif (Göncüoğlu, 1977), and Akdağmadeni Massif (Vache, 1963). The Central Anatolian Crystalline Complex was proposed by Göncüoğlu et al. (1991; 1992) as a combination of three well-documented sub-massifs, Akdağmadeni Massif to the northeast, Kırşehir Massif at the center, and Niğde Massif to the south. The CACC forms the central part of the Anatolide tectonic unit of Ketin (1966), and Anatolide-Tauride Platform of Şengör and Yılmaz (1981).

The assemblage is bounded by Upper Cretaceous (Campanian-Turonian) ophiolitic melange of İzmir-Ankara-Erzincan Suture Zone to the north, Sivas Basin sediments of Tertiary age to the northeast and east, Tuzgolü Basin sediments of Tertiary age to the west and southwest, Mio-Pliocene sedimentary rocks and Pliocene volcanic rocks to the south and southwest (Figure 2.1). Three distinctive structures outline the triangular figure of the area; Tuzgölü Fault Zone to the west, Ecemiş Fault Zone to the east, and İzmir-Ankara-Erzincan suture zone to the north.

2.1. Central Anatolian Crystalline complex

The CACC consists of five main rock units, metamorphic, ophiolitic, plutonic and volcanic rocks, and the cover units. The metamorphic rocks exhibiting a metamorphosed platform type sequence are called the Central Anatolian

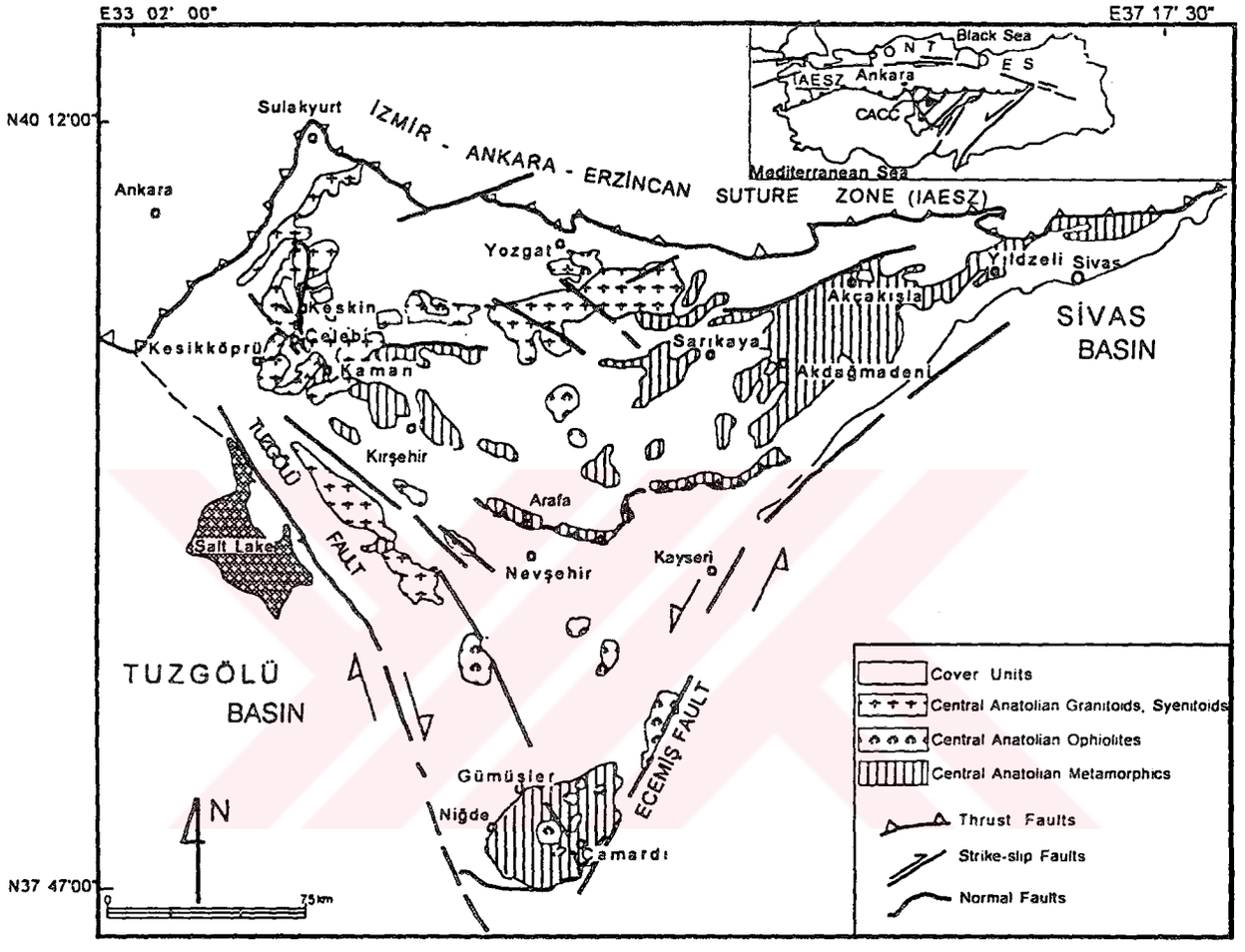

Figure 2.1. The simplified geological map of the CACC (Modified from Erentöz, 1961; Erentöz and Ternek, 1962; Ketin and Erentöz, 1961; Ketin, 1963, Göncüoğlu et al., 1991; 1993)

Metamorphics (CAM); the ophiolitic rocks are called the Central Anatolian Ophiolites (CAO), and the felsic to intermediate plutonic rocks intruding the CAM and partly CAO are called the Central Anatolian Granitoids (CAG) by Göncüoğlu et al. (1991; 1992;

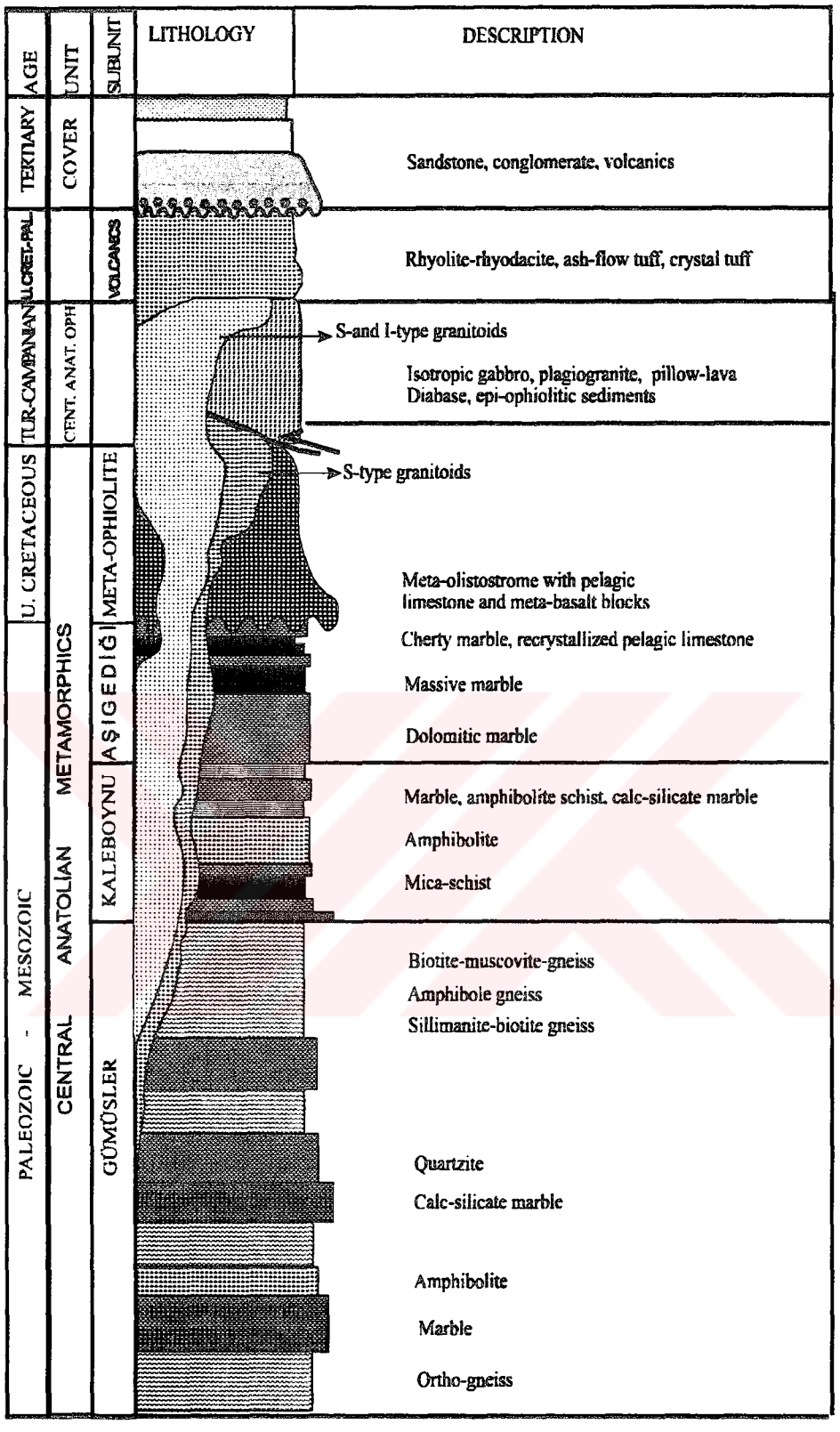

Figure 2.2. Generalized columnar section of the CACC (After Göncüoğlu et al.,1994)

1993) (Figure 2.2). Apart from these, the alkaline volcanic rocks younger than CAG represents younger volcanic activities within the CACC. These are called the Karahıdır Volcanics. The complex is overlain by sedimentary and volcano-sedimentary rocks called the cover units

2.1.1. Central Anatolian Metamorphics

The CAM is the assemblage of medium to high grade metamorphic rocks of Paleozoic-Mesozoic age. They are commonly exposed around Kırşehir, Akdağmadeni, and to the east of Niğde, along horst-like terranes that are bounded by faults of post-Eocene age, and/or at the central parts of anticlines. They are commonly subdivided into four main units (Göncüoğlu, 1977;Göncüoğlu et al., 1993); (1) Gümüşler Metamorphics, the lowermost unit is composed of ortho- and para-gneisses,and metamorphic equivalents of a mafic volcanic- and sediment-rich sequence, (2) Kaleboynu Metamorphics represent the metamorphic equivalents of carbonate-rich sequence alternating with sandstone-shale-marl and marly limestone; (3) Aşıgediği Metamorphics are characterized by metamorphosed platform carbonates grading upward to pelagic limestones then to calci-turbidites ; and (4) the uppermost unit is a meta-ophiolite composed of metagabbro, serpentinite, amphibolite and various metamorphosed ultramafic and mafic rocks locally within a meta-olistostromal unit (Göncüoğlu et al., 1991; 1992; 1993).

The Gümüşler Metamorphics consist of biotite-muscovite, biotite-garnet, kyanite-sillimanite, and quartzo-feldspathic gneisses. Amphibolite bands, marble and quartzite are often interlayered with the gneisses. This unit is correlated to the Gümüşler Formation (Göncüoğlu,1977) and to Kalkanlıdağ Formation (Seymen,1981). Kaleboynu Metamorphics contain marbles alternating with mica-schist, calc-silicate marble, biotite gneiss, quartzite, and amphibole schist. This unit is correlated to the Kaleboynu Formation (Göncüoğlu, 1977) and Tamadağ Formation (Seymen,1982). The Aşıgediği Metamorphics contain several types of massive and thick bedded marbles alternating with calcsilicate-amphibolites and occasional layers of meta-cherts. The grain size and bed thickness decrease upward, and the whole sequence grade into pinkish calc-silicate marble, pinkish-red quartz muscovite calc-schist interlayered with meta-cherts.

This unit is correlated to the Aşıgediği Formation (Göncüoğlu,1977). The lower part of the unit is correlated to Bozçaldağ Formation of Seymen (1982). The meta-ophiolite rests on the Aşıgediği Metamorphics with or without an olistostromal unit.

The main metamorphic event during the evolution of the CAM is of progressive type, and is represented by succeeding episodes of medium pressure-medium/high temperature, and medium/low pressure-high temperature type metamorphisms (Göncüoğlu, 1977; Seymen, 1982). The first event is accompanied by cataclastic deformation (Göncüoğlu, 1977; Göncüoğlu et al., 1993) with kyanite-biotite-garnet paragenesis within the Gümüşler Metamorphics. The second is a product of a recrystallization related to intrusive events resulting from partial melting and crustal extension (Göncüoğlu et al., 1991) This second episode is represented by an andalusite-sillimanite-cordierite paragenesis

The age data on the main metamorphism events within the complex are limited and inconclusive at present. The age of these metamorphics is given by Seymen (1982) as pre-Mesozoic. U-Pb dating on zircons from the gneisses of the same area yield an age of 2059±77 Ma for the protolith of the metamorphics (Göncüoğlu, 1986). The K/Ar dates of biotites range 74.9-77.4±1.2 Ma, and Rb/Sr mineral-whole rock isochron give 77.8±1.2 Ma (Göncüoğlu, 1986); the K/Ar dating of biotite and hornblende give 69.7±1.7 Ma and 71.4 3.2 Ma, respectively (Erkan and Ataman, 1981). However, Göncüoğlu (1986) obtained, using whole rock Rb/Sr isochron, an age of 95±11 Ma for the S-type Üçkapılı Granodiorite that intruded the metamorphics. All these data indicate a pre-Cenomanian age for the main metamorphism (Göncüoğlu et al.,1991). Göncüoğlu et al. (1991) proposed that the metamorphism was renewed by intrusive rocks.

2.1.2. Central Anatolian Ophiolites

The ophiolitic rocks, observed as a number of isolated outcrops, and found as allocthonous bodies in CACC, are termed as the Central Anatolian Ophiolites (CAO) (Göncüoğlu et al., 1993). They consist of ultramafic rocks, isotropic gabbro, plagiogranite, diabase, pillow lava, and epi-ophiolitic sediments. They are exposed as partial to almost complete sequences within the tectonic slices (Yalınız et al., 1995). Although, meta-ophiolite is regarded as a member of the metamorphic basement (Göncüoğlu et al., 1991; 1992), Yalınız et al. (1996) included the meta-ophiolite in the

CAO. Therefore, they subdivided the CAO into two main groups; (a) metamorphic ophiolites, deformed and metamorphosed at the same time as the CAM basement (meta-ophiolite), and (b) essentially non-metamorphic or weakly metamorphosed ophiolites thrusted over the basement (Göncüoğlu et al., 1992).

Geochemical data indicate that the non-metamorphic ophiolites are of supra-subduction zone (SSZ) type (Yalınız et al., 1996). They are related to an ensimatic arc located to the north of the Tauride-Anatolide Platform (TAP), which was active during the closure of Northern Branch of Neotethyan Ocean (NBN) (Göncüoğlu et al., 1992; Yalınız et al., 1995; Yalınız et al., 1996) The ophiolites display geochemical characteristics similar to other Late Cretaceous Neotethyan ophiolites in the Eastern Mediterranean area (Yalınız et al., 1996). The field relationships and paleontological dating of the ophiolite-related sediments (red-pink colored pelagic limestones intercalated with pillow lavas) indicate that the ophiolitic rocks are older than Late Cretaceous (Turonian-Santonian) (Yalınız et al., 1996).

2.1.3. Central Anatolian Granitoids and Syenitoids

In the CACC, the Central Anatolian Granitoids and Syenitoids are commonly exposed along the northern and western margins. Geographically, they are also divided into three groups: (1) a number of large plutons which form an arcuate set and curve from NE-SW to NW-SE and extend from Sulakyurt to Niğde along the western margin, (2) a relatively narrow and smaller set of isolated plutons extending from Sivas to Çamardı along the eastern margin, and (3) a very large batholith exposed around Yozgat (Erler et al. ,1991; Akıman et al. 1993; Erler and Bayhan, 1995). They intrude the CAM and CAO, and are overlain by the Tertiary sedimentary rocks of the cover units. The granitoids are classified as (1) leucogranites, (2) biotite/hornblende granites, (3) alkali-feldspar megacryst granites, and (4) aplitic-alkali feldspar granites, based on field observations (Göncüoğlu et al., 1992;1993). The syenitoids consist of nepheline syenite and quartz syenite.

Leucogranites are probably the oldest of all, and are subjected to most intense alteration. Biotite/hornblende granites are of two types; (1) as outcrops with different sizes, and (2) as the marginal zones of alkali-feldspar megacryst granites. The aplitic alkali-feldspar granites represent the youngest group, and occur as dike swarms or as individual large dikes intruding the other groups. The granitoids are generally

monzonitic, quartz monzonitic and granodioritic in composition. They include enclaves of both metamorphic and mafic rocks, and enclaves of earlier granites (Göncüoğlu et al., 1993; Kadıoğlu, 1996).

The granitoids and syenitoids were generated during and after the southward obduction of the ophiolitic rocks from the NBN , onto the TAP during Late Cretaceous period (Erler et al., 1991; Akıman et al., 1993) and before Upper Maastrichtian (Yalınız et al., 1996). They are the consequences of crustal thickening due to arc to arc or arc to continent collision (Göncüoğlu et al., 1992; 1993). In general, the Central Anatolian Granitoids are members of two broad classes; granitoids with S-type characteristics and granitoids displaying both S-and I-type characteristics. In other words, they display distinctive features of H-type (hybrid) granites, and plot both in island arc and collision fields with within plate signatures on trace element discrimination diagrams (Bayhan, 1987; Erler et al., 1991; Akıman et al., 1993; Erler and Bayhan, 1995), and may be accepted as collision granitoids. The geological evidence indicates a two-fold obduction resulting in two phases of magmatism producing two different types of plutonics (Göncüoğlu et al., 1991). The earlier obduction that generated S-type syncollisional granitoids of 84-106 Ma (95±11) age (?Albian-Santonian) (Göncüoğlu, 1986), is due to the obduction of ophiolitic melange (Göncüoğlu et al., 1992; Yalınız et al., 1996) onto the protoliths of the CACC, and the latter is due to obduction of supra-subduction zone ophiolites (SSZ) onto the metamorphics and previously obducted ophiolitic melange (collision of ensimatic arc with TAP and CACC). The second phase is characterized by post-collisional granitoids and syenitoids, granitoids displaying both S and I-type characters (Erler et al., 1991; Geven, 1992; Göncüoğlu et al., 1993). These were generated by post collisional extension after the second obduction event ceased (Erler and Göncüoğlu, 1996). Both syn-collisional and post-collisional varieties cut across the CAM; however, the ophiolites are cut only by the post-collisional intrusives.

The radiometric data on the CAG are rather scarce. Ayan (1963) reported an age of 54 Ma for the Baranadağ Monzonite using total Pb method. Ataman (1972) and Gündoğdu et al. (1988) dated Cefalıkdağ quartz monzonite using Rb-Sr wholerock-mineral isochron method as 71±1 Ma, and 71.8±1.1, respectively. Göncüoğlu (1986) using whole rock Rb-Sr isochron obtained an age of 95±11 Ma for the granitoid in Niğde area, and K-Ar age dating on minerals of granitoids yielded ages of 76.5±1.1 Ma

age. Zeck and Ünlü (1988) dated Murmano Pluton using Rb-Sr whole rock isochron method as 110±5 Ma. Güleç (1994) found that the age of Ağaçören granitoids is of 110±14 Ma age based on whole rock Rb-Sr isotope dating on three samples.

The syenitoids are regarded as a separate unit as the products of alkaline magmatism (Göncüoğlu et al.,1993). They comprise mainly the syenitic rocks that intrude the granites, and that are intruded by the rhyolitic rocks of younger ages. Petrographical studies showed that they are nepheline syenite and quartz syenites (Dalkılıç, 1986; Bayhan, 1987; 1988). They are supposed to be formed as a result of differentiation of the silica-undersaturated K-rich magma at the expense of crustal contamination (Özkan and Erkan, 1994).

2.1.4. Karahıdır Volcanics

The felsic volcanic and volcanoclastic rocks alternating with the continental clastics, and overlying the units of the CACC are termed as the Karahıdır Volcanics (Göncüoğlu et al., 1993). They consist of two distinctive sections as volcanic and volcanoclastic sections. Volcanic sections includes volcanics like rhyolite, rhyo-dacite and/or trachy-andesite (Gençalioğlu-Kuşcu and Floyd, 1995) and basaltic dikes. The volcanoclastic section, on the other hand comprises ignimbrite, crystal tuff, ash-flows and accretionary lapilli tuffs (Gençalioğlu-Kuşcu and Floyd, 1996).

The rhyolitic rocks of the volcanic section occur as domes and flows. Rhyolite flows occasionally contain spherulite bearing levels. The upper surfaces are typically blocky and rubbly. Majority of flows are laminar flows with well-developed flow banding. The domes are characterized by radiating columnar joints, and surface breccias. "Flushing-up" structures at some individual outcrops represent the initial dome growth stage (Gençalioğlu-Kuşcu and Floyd, 1995). The volcanoclastic section consists mainly of ignimbrites. The ignimbrite eruption followed the formation of rhyolites, resulting in cast-like structures all over the ignimbrite-rhyolite contact (Gençalioğlu-Kuşcu and Floyd, 1995).

2.1.5 Cover Units

Cover units include the sedimentary, volcanic, and volcanoclastic rocks of Lower and Upper Tertiary age. They generally overlie the CACC units, however CAM and CAG are locally thrusted over Lower Tertiary rocks. In general, Lower Tertiary rocks represent the sedimentary units within the basins formed over the CACC, and

they are named as the Central Kızılırmak Basin Sediments by Göncüoğlu et al., (1993). They consist of Göynük and Elmalıdere formations (Upper Maastrichtian-Lower Paleocene?), Yeşilöz Formation (Middle-Late Paleocene?), and Mucur Formation (Lower-Middle Eocene).

Göynük formation represents a volcanoclastic olistostromal to sedimentary sequence resting on the Karahıdır Volcanics (Köksal, 1996). The volcanoclastic sequence dominates at lower parts and they grade upward into an olistostromal section at middle parts. Then, they grade into fossiliferous sedimentary rocks. The age of the unit is said to be Paleocene to Lower Eocene based on the fossil assemblage (Köksal, 1996).

The red clastics formed as debris flow and/or alluvial sediments at the southern parts of the Kızılırmak Basin are named as the Yeşilöz Formation (Göncüoğlu et al., 1993). The Yeşilöz Formation contains fossil assemblages dating the unit as Upper Danian-Lower Thanetian.

The sedimentary unit starting with conglomerate at the bottom grading upward to fossiliferous clayey limestone and sandy limestones within a blocky flysch sequence is called the Mucur Formation (Göncüoğlu et al., 1993). The Mucur Formation contains fossil assemblage dating the unit as Middle Eocene (Göncüoğlu et al., 1993)

The Upper Tertiary rocks are represented by the sedimentary, volcanic and volcanosedimentary rocks. They are grouped into two as the Gümüşyazı Group of Early Neogene and the Kızılırmak Group of Late Neogene age (Akgün et al., 1995).

The Gümüşyazı Group is exposed mainly around the north of Kırşehir, Mucur, Hacıbektaş and Tuzköy. It consists of Kızılöz, Tuzköy, and Avcıköy formations (Göncüoğlu et al., 1993; Akgün et al., 1995). These units unconformably overlie the Yeşilöz and Mucur formations of Lower Tertiary age, but they are unconformably overlain by the Miocene-Pliocene Kızılırmak Group. In general, the Gümüşyazı Group contains lacustrine deposits, mainly conglomerate, sandstone, siltstone and gypsum. The age of the Gümüşyazı Group is assigned by the palinological studies as Middle Miocene (Akgün et al., 1995).

The Kızılırmak Group is exposed mainly around the central and northern parts of the CACC. It unconformably overlies the Gümüşyazı Group, and is unconformably overlain by the Plio-Quaternary volcanics and alluviums. The Kızılırmak Group consists

mainly of conglomerate, cross-bedded sandstone alternated with marl and shale, tuffs, and limestone.

2.2. Geological evolution

The complex has been studied by several researchers since late 1970's (Erkan, 1976; Göncüoğlu, 1977; Seymen, 1982; Görür et al., 1984; Bayhan, 1987; 1988; Göncüoğlu, 1986; Bayhan and Tolluoğlu, 1987; Erler et al., 1991; Akıman et al., 1993; Göncüoğlu et al., 1991; 1992; 1993; 1994: Türeli, 1991; Geven, 1992; Türeli and Göncüoğlu, 1993; Yalınız et al., 1994 Yalınız et al., 1996; Erler and Bayhan, 1995; Erler et al., 1996; Kadıoğlu, 1996). Each work described different aspects of the region, and proposed a model to explain the evolution of the complex. Majority of the models are based on geochemical and geochronological data obtained from the metamorphics, granitoids, and ophiolites in the assemblage. In this sense, the models for the evolution of these rocks can also serve to understand the geological evolution of the region. This summary highlights commonly accepted models, and discusses them in the light of present data.

In general, models about the geologic and geodynamic evolution of the CACC include (1) island-arc model (Seymen, 1982; Görür et al., 1984; Erler et al., 1991), and (2) collision model (Erler et al., 1991; Göncüoğlu et al., 1991; 1992; 1993; Geven, 1992; Akıman et al., 1993; Erler and Bayhan, 1995). They also differ in age constraints.

The subscribers of the island arc model suggested that the granitoids at the western margin of CACC were generated as the cores of island arc/arcs formed during the closure of Inner Tauride Ocean, and subduction beneath the Kırşehir Block. This model requires the presence of a so-called "Inner Tauride Ocean" that opened at Late Triassic time, and that closed during Cretaceous time due to the subduction toward northeast (Şengör and Yılmaz, 1981; Görür et al. 1984). In this model, the granitoid belt along the western margin of CACC is therefore, accepted as the product of an island arc. However, this proposal still does not explain the granitoids along the northern margin of CACC, so Tüysüz (1993) and Tüysüz et al. (1995) proposed an oblique subduction model to explain the granitoids at the western and northern margins of CACC.

On the contrary, the subscribers of the collision model proposed that the granitoids were produced during and after the collision between Kırşehir Block and Sakarya Block. This model suggests two possible cases of collision; (1) the Kırşehir Block is an active margin, and (2) Kırşehir Block is a passive margin. In the first case, the Northern Branch of Neotethyan (NBN) Oceanic crust is said to be subducted southward beneath the Kırşehir Block, and therefore, the granitoids are supposed to be derived from collision of Kırşehir Block with the Sakarya and/or Pontide Block. This model is similar to island arc model and needs verification and acceptance of that model. In the second case, the granitoids are said to be produced by a collision between Kırşehir Block and Sakarya/Pontide Block. In this case, the Kırşehir Block which is supposed to be the northern extension of the Tauride Platform, subducted northward beneath the Sakarya Block. The granitoids, then, generated by partial melting as a result of crustal thickening during and after collision.

The geochemical and geochronological data (Erler et al., 1991, Göncüoğlu et al., 1991; Geven, 1992; Türeli, 1991; Türeli and Göncüoğlu, 1993) highlight two important points related to the evolution of CACC. First and perhaps the most significant one is that the magmatism in the complex is not of arc magmatism as suggested by Seymen (1982) and Görür et al. (1984), but are of collisional to post-collisional type. This is important in terms of general explanation of geological evolution of the region. Because if the granitoids along the western and northern margins of the complex are not accepted as arc-related, it becomes difficult to explain the consumption and closure of "Inner Tauride Ocean" during the subduction beneath the Kırşehir Block. In this respect, collision-type granitoid producing events, such as crustal thickening, should be discussed in detail when discussing the geological evolution of CACC.

The evidences for crustal thickening are obtained by studying the deformation and recrystallization histories of metamorphic rocks in the complex. The studies of metamorphic rocks showed that the main metamorphism event is of progressive type completed in two successive sub-phases (Göncüoğlu, 1977; Seymen, 1982; Göncüoğlu et al. 1991). The evolution paths of the metamorphics on the pressure, temperature and time diagrams trend in a clockwise direction (Göncüoğlu, 1977; Göncüoğlu et al., 1991). Such kind of trends represent collisional, and post-collisional extensional regimes (Göncüoğlu et al. 1994). Hence, when combined with

geochronological data from the metamorphics (Erkan and Ataman, 1981; Göncüoğlu, 1986) and from the granitoids (Göncüoğlu, 1986), metamorphics in the complex contain mineral assemblages indicating an earlier crustal thickening, and a later crustal extension during main metamorphism.

The triggering event for crustal thickening and resultant partial melting is the closure of the NBN Ocean during Late Cretaceous time, and northward subduction of the oceanic crust beneath the Sakarya Block. During the closure oceanic crust was mainly consumed, but also the oceanic crust and ophiolitic rocks were obducted over the passive margins of the Tauride-Anatolide Platform (TAP) (Göncüoğlu et al., 1991; 1992).

To conclude, the data and interpretations related to granitoids and metamorphics suggest that the "collision model" appears to be more appropriate for the geological evolution of the complex. According to this model, metamorphics representing the metamorphosed equivalents of northern passive margin of the TAP underwent the same geological events together with the Tauride carbonate platform for at least during Mesozoic (Göncüoğlu et al, 1993; 1994). During the subduction, the northern margin of TAP was subjected to an internal deformation by the activities of thrust faults, and blocks of oceanic crust began to be emplaced onto the northern margin of TAP. This was followed by obduction of large ophiolite slabs and fragments. These two events caused the crustal thickening and medium pressure-medium/high temperature type metamorphism over the northern margins of TAP. When the metamorphism reached conditions sufficient for partial melting, S-type syn-collisional granitoids of 95±11 Ma (Göncüoğlu, 1986) age were generated. The geological (Göncüoğlu et al., 1992) and geochemical studies (Yalınız et al., 1996) showed that the NBN Ocean were consumed not only by a northward subduction but also by an intra-oceanic subduction that gave rise to supra-subduction zone ophiolites. These were later obducted over the metamorphics. After the obduction ceased, H-type (S- and I-type) post-collisional granitoids of 71± Ma (Ataman, 1972) age were produced. The field evidence showed that these intruded the metamorphics, and overlying supra-subduction zone ophiolites (Göncüoğlu et al., 1991; 1992).

CHAPTER 3

GENERAL OVERVIEW OF THE SKARNS

3.1. Terminology and classification of skarns

Skarn deposits are the world's premier sources of tungsten; important sources of iron, and zinc, and minor sources of gold, silver, lead, molybdenum, bismuth and tin. They also serve as sources of industrial minerals, such as graphite, wollastonite, phlogopite, talc and fluorite. This wide range of commodities, occurring in a broad range of environments, is unified under the title "skarn" deposits and related terms. Skarns that contain ore deposits are found at or near the contacts between igneous plutons and carbonate-rich rocks, or fractures in carbonate rocks. These deposits, in the literature, are termed hydrothermal metamorphic (Lindgren, 1905 in Einaudi et al., 1981), tactite (Hess, 1919 in Einaudi et al., 1981), pyrometasomatic (Lindgren, 1922 in Burt, 1982), igneous metamorphic (Park and McDiarmid, 1975), or contact metasomatic (Jensen and Bateman, 1979). These termes were used interchangeably for several decades, however, they seem to have been dropped by almost universal consent (Einaudi et al., 1981). This is because (1) none of these terms is appropriate, (2) igneous contacts are not always observed, (3) the formation of the deposits spans a broad range in temperature, and (4) the distinction between, and relative importance of metamorphic and metasomatic processes are not clear (Einaudi et al., 1981).

The first published use of the term "skarn" is by Tornebohm (1875 in Burt, 1982; Meinert, 1997), although there are earlier descriptions of deposits now known to contain skarn. His definition is as follows "As subordinate layers in the feldspar poor felsic volcanic rocks, there appear peculiar dark rocks which also are ore's host rock. These rocks are termed as "skarn", a word which likely can be used as a collective term for all such kind of rocks occurring alongside the ores". Tornebohm (1875 in Burt, 1982; Meinert, 1997) also defined the dark colored rocks associated with ores in the Persberg area as garnet-rich "brunskarn" (brown skarn), and pyroxene-rich "gronskarn" (green skarn).

The term "skarn" in present day usage was described by miners in Central Sweden where it was used to refer to the coarse grained calc-silicate gangue associated with iron ore and it was adopted by Goldschmidt (1911 in Einaudi et al., 1981) in his classic work on the Kristiania area, Norway. Since that time the term has been expanded to include a large variety of calc-silicate rocks that are rich in calcium, iron, magnesium, aluminum and manganese regardless of their association with economically interesting minerals, and that formed by replacement of originally carbonate-rich rocks (Einaudi et al., 1981). Therefore, in this study, the suggestions of Phan (1969 in Burt, 1982), Burt (1977), and Einaudi et al. (1981) will be adopted to simply refer to these rocks as "skarns", a term free of genetic implications.

There are several terms related to skarns, such as reaction skarn, calc-silicate hornfels, and skarnoid. The reaction skarn can form from isochemical metamorphism of thinly interlayered shale and carbonate units where metasomatic transfer of components between adjacent lithologies may occur on a small scale, perhaps centimeters (Meinert, 1993). In this respect the reaction skarn can be regarded as lithologically and structurally controlled small scale strata-bound skarn. Calc-silicate hornfels is a descriptive term often used for relatively fine-grained calc-silicate rocks that result from metamorphism of impure carbonate units such as silty limestone and limy shale. Skarnoid is also a descriptive term for calc silicate rocks that are relatively fine grained, iron-poor, and reflect, at least in part, compositional control of protolith (Zharikov, 1970). For all these terms, the composition and texture of protolith tend to control the composition and texture of the resulting skarn.

Skarns are classified according to the rocks they replaced, and the term exoskarn and endoskarn were applied originally to replacements of carbonate-rich rocks, and intrusive rocks respectively (Einaudi and Burt, 1982). Exoskarns are also classified according to dominant mineralogy they contain; as magnesian if they contain an important proportion of Mg-silicates such as forsterite and serpentine, and as calcic when Fe-Ca-silicates such as andradite, diopside and hedenbergite are predominant. The skarn deposits, on the other hand, are best classified on the basis of the dominant economic metal they contain; major subclasses occur in either magnesian or calcic skarns, consisting of Fe-Cu, Zn-Pb, Mo, and Sn. However, magnesian skarn deposits

of W, Cu and Zn-Pb are notably sparse, and majority of the world's economic skarn deposits occur in calcic exoskarns (Einaudi et al., 1981).

3.2. General overview of the developments in skarn concept

Skarn deposits have been scientifically recognized as a distinct class of mineral deposits for more than 100 years, but geologists still argue about terminology and processes of their formation. The skarns continue to intrigue the interests of geologists as an old but popular research topic. Most of the studies were about the geology and petrology of individual skarn deposits and skarn ore regions by the ends of early 1970's. Research on skarn deposits in last two decades using the advances in the fields of mineralogy, petrology, geochemistry and tectonics has greatly clarified our understanding of their general characteristics and mode of occurrences. A review of modern and ancient research on skarn deposits in particular suggests new framework for their exploration and study.

Skarn deposits are of world-wide distribution; they have been mined since the Middle Ages and studied since the nineteenth century. Early workers (Lindgren 1902; 1905; 1924; Barrell, 1907; Goldschmidt, 1911; Umpleby, 1916; Kato, 1917; Knopf,1918; and Hess, 1919; all in Burt, 1982) defined the geological features of skarn deposits and used different terms to define these deposits. It was after 1922 that Lindgren defined for the first time the term "pyrometasomatic" and also used the term "skarn". These terms were later adopted by many authors. Magnusson (1936 in Burt, 1982) defined the term reaction skarn for the mineral association, including ores. Korzhinskii (1936, 1945, 1948 and 1955; all in Burt, 1982) and Korzhinskii (1970) explained the mode and means of transportation of metals and deposition of ore and calc-silicate minerals, and put forward the constraints in mobility. He outlined the classic parameters on metasomatism and its results, including skarn formation. In his studies, he restricted "skarn" to phenomena directly associated with ore bodies. In the period between 1957 and 1968, the researchers (Shaw,1957; Cooper, 1957; Watanabe, 1958; Thompson, 1959; Guitard and Lafitte,1960; Titley, 1961; Greenwood, 1962; all in Burt, 1982; and Buseck, 1966) described in detail the development of metasomatic skarn zones next to intrusive rocks, and used Korzhinskii's terminology for skarn deposits for their studies. After late sixties, the objective of studies shifted from field geological studies to laboratory studies using the

tools of geochemistry. Zharikov (1970) was the first geologist who studied the element abundance and distribution in skarn pyroxenes and garnets to correlate pyroxene and garnet compositions with the skarn deposit. Later studies also dealt with the similar correlations, and they experimentally attempted to demonstrate how calc-silicate rocks are formed during regional metamorphism, and metasomatism (Vidale, 1969; Perry, 1969; Bartholome, 1970; Korzshinskii, 1970; Kerrick, 1974; Burt, 1977). Broad correlations between igneous composition and skarn type were noted by Shimazaki (1975). However, the contemporary works on igneous rocks associated with ore deposits including skarn and porphyry copper deposits (Kesler et al., 1975; Mutschler et al., 1981; White et al., 1977; Cornwall, 1982) indicated that there are strong connections between igneous petrogenesis and ore deposition. The research on skarns in the seventies concentrated on geochemistry of skarns, and accumulated data on the mineralogy, temperature, pressure and geochemistry of individual skarn deposits (James, 1976, Sato, 1980; Newbery, 1982). During and after late eighties, the studies aimed to make correlations between the skarn mineralogy and type of dominant ore metal. Some of the studies of this period used the skarn pyroxenes as an indicator in the classification of skarn deposits (Nakano, 1982; Einaudi, 1982a; 1982b; Einaudi and Burt, 1982; Meinert, 1987; Abrecht, 1985; Newbery et al., 1991; Nakano, 1991; Nakano et al., 1994). However, some of them studied the garnets for better understanding of the oxidation state, pH of the hydrothermal fluids, and timing of hydrofracturing and change in the composition of aqueous fluid at garnet-fluid interface, (Einaudi, 1982a; Kwak, 1986; Kato, 1991; Yardley et al., 1991; Jamtveit, 1991; Jamtveit and Andersen, 1992; Jamtveit et al., 1992; 1993; Jamtveit and Hervig, 1994; Jamtveit et al., 1995; Polvates et al., 1996). This is one of the most important

exploration stages. Details of skarn mineralogy and zonation can be used to construct deposit-specific exploration models as well as to develop exploration programs or regional syntheses. Although skarn minerals are typical rock-forming minerals, most of them have compositional signatures which can yield significant information about the environment of formation. The presence and association of these minerals in skarns vary with respect to the type of skarn. The skarn minerals include pyroxenes (such as diopside, hedenbergite, johannsenite, salite, ferrosalite), garnets (grossular, andradite, pyrope, almandine, spessartine), wollastonite, amphiboles (actinolite, tremolite, hornblende), epidotes (zoisite, clinozoisite, epidote), vesuvianite, tourmaline, plagioclases (oligoclase, albite), and scapolite. Some minerals like quartz and calcite are present in almost all skarns. However, others such as humite, periclase, phlogopite, talc, olivine, serpentine, and brucite are typical of magnesian skarns but are absent from most of the other skarn types (Meinert, 1992).

The modern analytical techniques, particularly electron microprobe, make it relatively easy to determine the accurate mineral compositions and consequently, to use precise mineralogical names (Zharikov, 1970; Burt, 1977). The minerals which are most useful for both classification and exploration are garnet, pyroxene, and amphibole. They are present in all skarn types and show marked compositional variability that can be shown graphically. Triangular plots commonly are used to express variations in compositionally complex minerals such as garnet and pyroxene (Einaudi et al, 1981). Amphiboles are difficult to show graphically because they have structural as well as compositional variations.

In most skarns there is a general zonation pattern of proximal garnet, distal pyroxene, and idocrase (or a pyroxenoid such as wollastonite, bustamite or rhodonite) at the contact between skarn and marble. In addition, skarn minerals may display systematic color or compositional variations within the larger zonation pattern (Meinert, 1993; 1997). For example, the proximal garnet is commonly dark red-brown, becoming lighter brown and finally pale green near the marble front (Atkinson and Einaudi, 1978). The change in pyroxene color is less pronounced but typically reflects a progressive increase in iron and and/or manganese towards marble front (Harris and Einaudi, 1982).

CHAPTER 4

ROCK UNITS

In the Akdağmadeni, Akçakışla and Keskin districts the units of the Central Anatolian Crystalline Complex (CACC) and overlying cover units are exposed. The observed units of CACC are Central Anatolian Metamorphics (CAM), Central Anatolian Ophiolites (CAO) and Central Anatolian Granitoids (CAG). In this section, only general field and petrographic features of the rock units will be summarized from the previous studies.

4.1. Central Anatolian Metamorphics.

The oldest rock unit exposed within the Akdağmadeni, Akçakışla and Keskin districts is the Paleozoic-Mesozoic CAM which are often intruded by relatively younger Upper Cretaceous CAG. The metamorphics are nonconformably overlain by Tertiary cover units.

The CAM are represented by Gümüşler and Aşıgediği metamorphics. In the studied districts, the Gümüşler Metamorphics have limited exposures, and are observed only within the Akdağmadeni district. In contrast to the Gümüşler Metamorphics, Aşıgediği Metamorphics are well exposed as forming the highlands in the Akçakışla and Keskin districts.

4.1.1. Gümüşler Metamorphics

The Gümüşler metamorphics, the lowermost unit of CAM, crops out in the Akdağmadeni region between Akdağmadeni, Karapir, Ortaköy and Peynirliktepe

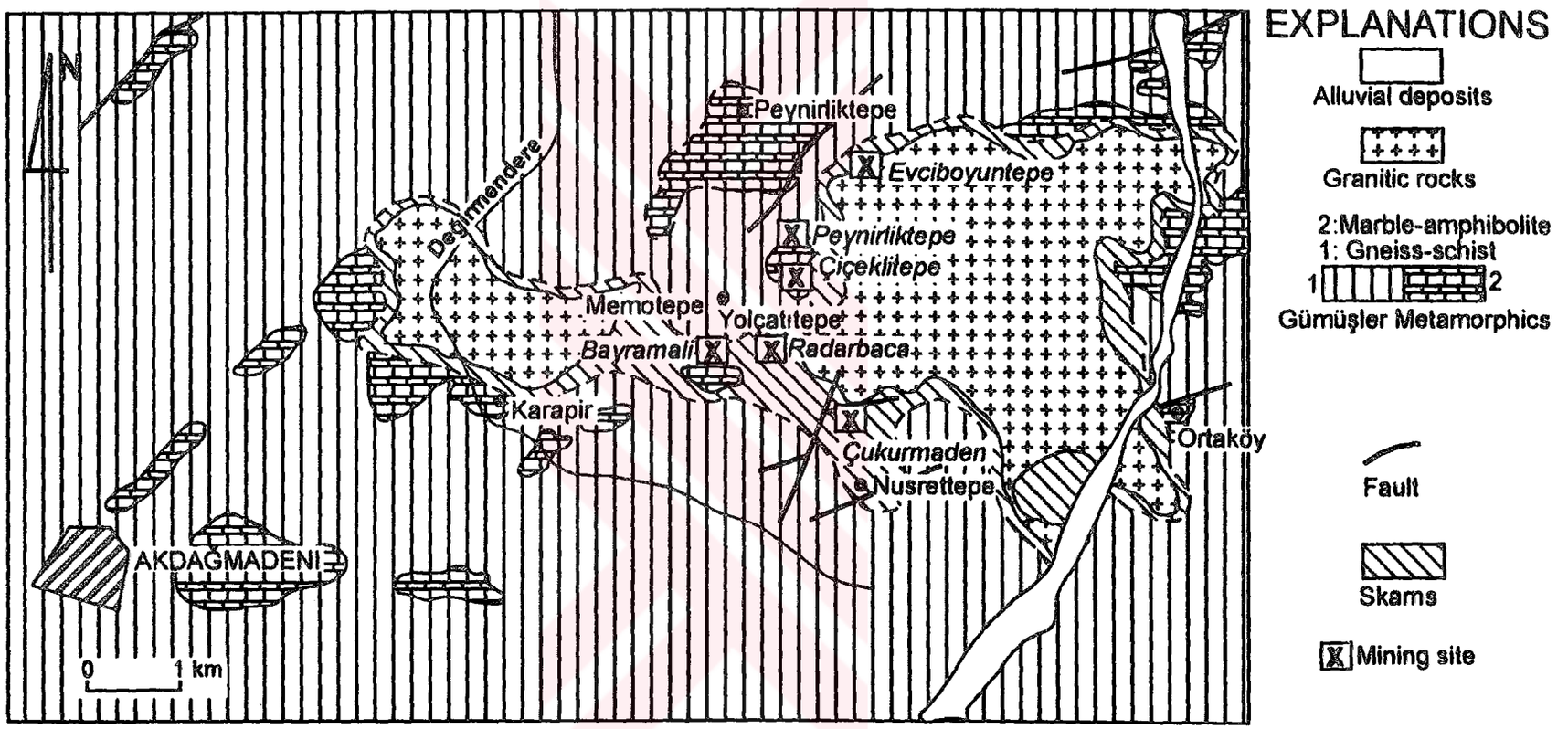

Figure 4.1. Geological map of the Akdağmadeni district (Simplified from Tülümen, 1980)

meters scale, although the marble layers are much more thicker and may reach up to 2-3 m thickness around Nusrettepe and Bayramali occurrences (Sağıroğlu, 1982). The gneisses of the Gümüşler Metamorphics are identified as muscovite gneiss, biotite gneiss, sillimanite-muscovite gneiss, sillimanite-biotite-muscovite gneiss, muscovite-biotite gneiss, scapolite gneiss, and almandine-biotite gneiss types (Tülümen, 1980). The amphibolites, quartzite and marbles are observed as intercalations and lenses within the sillimanite-biotite muscovite gneisses of the Gümüşler Metamorphics (Tülümen, 1980).

The marbles are observed at the southern parts of the district commonly around the lead-zinc occurrences (Figure 4.1). They occur as large lenses and intercalations within the gneisses around the Peynirliktepe and Çiçeklitepe occurrences, and as 2 m thick lenses around the Bayramali and Çukurmaden occurrences. The marbles are composed of coarse grained (1-2 cm in diameter) calcite crystals with some accessory minerals (Tülümen, 1980). Those around the Peynirliktepe and Çiçeklitepe are thick bedded and massive, and cover large areas. Similar exposures are also observed around the Evciboyuntepe.

The foliation planes of marbles and amphibolites are conformable with each other, and with the general foliation planes of the gneisses (Tülümen, 1980). They trend usually NE-SW (Tülümen, 1980). The intercalations of schist, gneiss, quartzite, and marble show that they were derived from sandstone-shale or clayey clastic rocks, and the amphibolites were probably derived from the metamorphism of volcanic or volcanogenic rocks in the protoliths of the Gümüşler Metamorphics.

A Paleozoic age is assigned for this unit by Göncüoğlu et al. (1994) by comparing and correlating this unit with the units of Kütahya-Bolkardağı Belt (Özcan et al., 1990) and lowermost section of Yahyalı Metamorphics (Göncüoğlu et al., 1991).

4.1.2. Aşıgediği Metamorphics

The Aşıgediği Metamorphics are exposed at Akçakışla and Keskin districts (Figure 4.2 and Figure 4.3). They either occur as roof pendants within the granitoids in

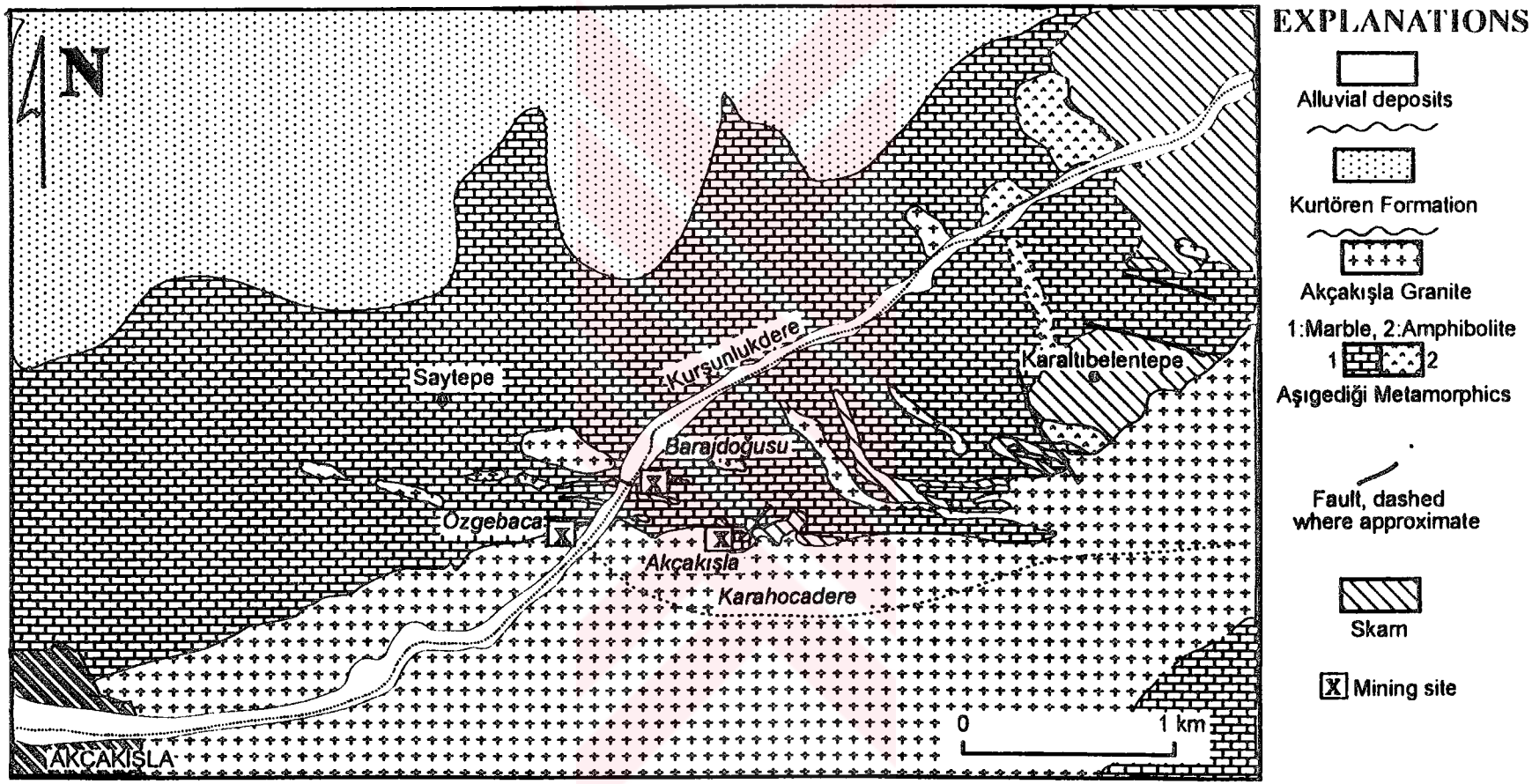

Figure 4.2. The geological map of the Akçakışla district (After Ergintav, 1987)

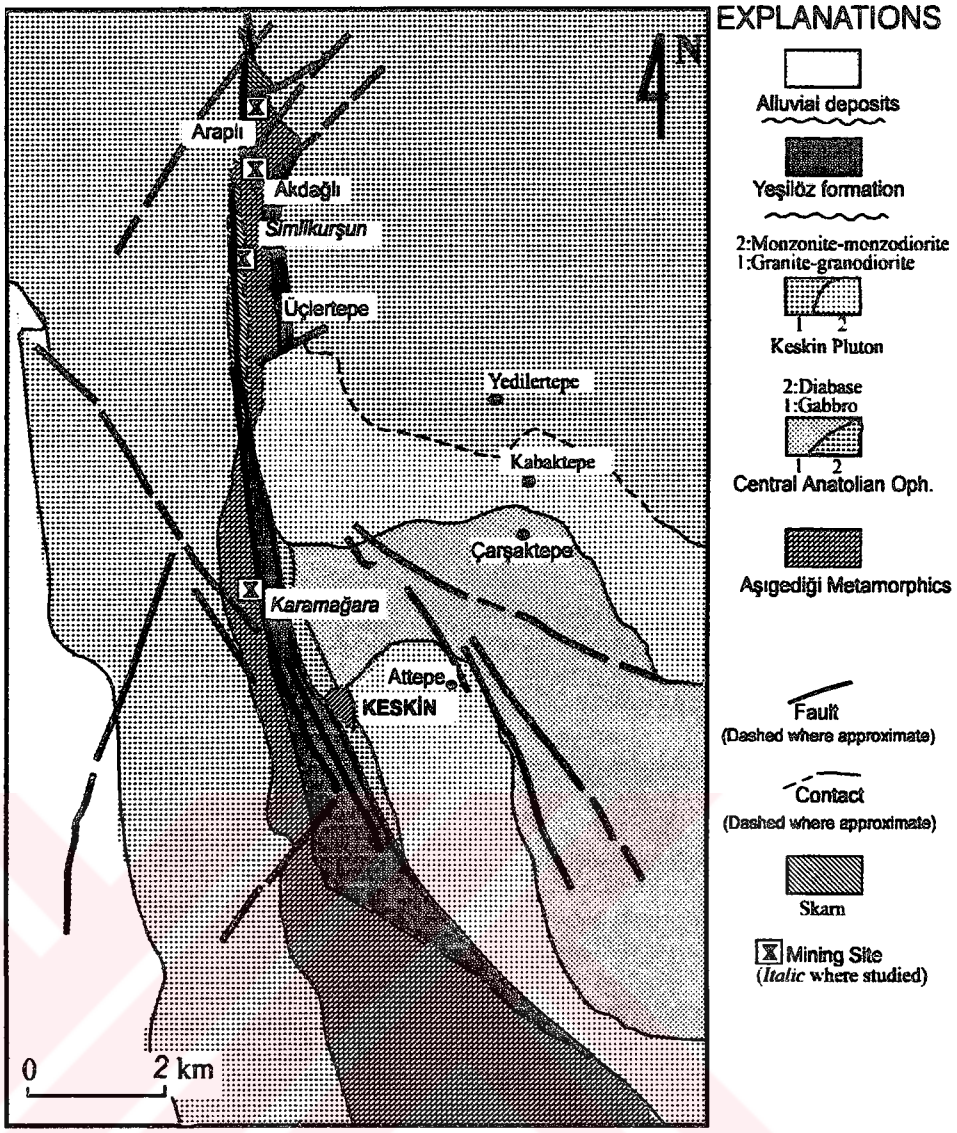

Figure 4.3. Geological map of the Keskin district (Modified from Kovenko, 1947)

the Keskin district (Figure 4.3), or they surround the granitoids in Akçakışla district (Figure 4.2 and Figure 4.3). They cover large areas in the Akçakışla district whereas they cover relatively small areas in Keskin district (Figure 4.3). In the Akçakışla district, they appear as thick, massive, and gray to white marbles intercalated with amphibolites (Tülümen, 1980; Sağıroğlu, 1982). The Aşıgediği Metamorphics in Keskin

The marbles in the Aşıgediği Metamorphics start with 5 to 50 m thick banded (yellowish-gray muscovite-quartz bearing bands) marbles in Keskin and Akdağmadeni (lower parts). They grade upward into gray-white colored massive marbles in Akçakışla (upper part). This section make up the thickest part of the unit, and composed mainly of coarse calcite crystals

The lower part is represented by thick bedded massive marble at and around the Keskin districts. In this part, the marbles start with coarse grained grayish-black banded marble, and grade upward into white to yellow coarse grained marble. Generally, the thickness of marbles range between 250 to 300 m (Sağıroğlu, 1982).

The age of this unit is debatable. Tülümen (1980) proposed that this unit is older than Eocene because they are unconformably overlain by sedimentary rocks Eocene in age. The volcanic and volcanoclastic rocks that overlies the metamorphic rocks to the south of Akçakışla are Pre-Late Cretaceous in age (Gençalioğlu-Kuşcu, 1996). Göncüoğlu et al. (1994) proposed that the age of the Aşıgediği Metamorphics should be Mesozoic mainly based on the regional correlation of this unit with the Triassic to Early-Late Cretaceous aged carbonate sequences in Tauride and Kütahya-Bolkardağ belts.

4.2. Central Anatolian Ophiolites

The Central Anatolian Ophiolites are observed only within the Keskin district as gabbroic roof pendants and/or large enclaves within large granitic bodies (Keskin Pluton, Bayhan, 1989), or appear as small diabase dikes intruding the gabbros. They are exposed at the eastern and southern parts of the Keskin district around Çarşaktepe (Figure 4.3).

The gabbro is not uniform, crystal size ranges from fine to medium. Fine grained gabbro is observed along the contacts between the Keskin Pluton and gabbro, and it is commonly cross-cut by diabase dikes, and monzonite and/or monzogranites.

The diabases are exposed only at Keskin district around Keskin as small dikes that cross cut each other. In the previous studies (Çavuşoğlu, 1967) the green colored rocks along marble-granite contacts along the western side of the N-S trending zone were erroneously referred to as diabases which are actually epidotized pyroxene-rich skarn rocks. The IP anomaly map (Arslanpay and Yıldırım, 1978) shows that these rocks (epidotized skarn rocks) are parallel to skarn outcrops in the district. The

distinction between these two is based on mineral composition and association with skarns. The diabases studied in this work are not mineralized, and are associated with the gabbros.

The gabbros and diabases in this area are correlated to gabbro and diabase of the Central Anatolian Ophiolites (CAO) of Göncüoğlu et al. (1991; 1992; 1993), and of Türeli and Göncüoğlu (1993). The gabbros are also correlated with the Ekecikdağ Hornblende Gabbro of Kocak and Leake (1994).

4.3. Central Anatolian Granitoids

The Central Anatolian Granitoids are represented by (1) the granitic rocks in the Akdağmadeni district (Tülümen, 1980), (2) Akçakışla Granite (Ergintav, 1987), and (3) Keskin Pluton (Bayhan, 1989) in the studied districts. These intrusive rocks were classified as granitoids of western and eastern groups based on their geographic settings (Erler et al., 1991; Akıman et al., 1993; Erler and Bayhan, 1995). In this study, both classification schemes will be used to describe their geographic and geologic settings.

4.3.1. Western Group

The granitoids in the Keskin district are named as the Keskin Pluton (Bayhan, 1989). They belong to granitoids of western group. The Keskin Pluton is exposed at and around the Attepe, Kabaktepe and almost northern half of the district (Figure 4.3). They are pinkish to gray, feldspar-rich monzonitic rocks (Bayhan, 1989). Those around Attepe and Kabaktepe are darker in color and finer grained, but those covering the northern and western parts are lighter in color and coarse grained. They represent outer belt granitoids of the Western Group (Erler et al., 1991; Akıman, et al., 1993) like Sulakyurt, Karacaali, Behrekdağı, Çelebi, Ağaçören and Ekecikdağı granitoids. They

represented by two groups as dark and light colored groups. Dark colored group is quartz monzonite and quartz monzo-diorite in composition with metaluminous character (Bayhan, 1989). It is composed of fine grained zoned plagioclase, perthitic orthoclase, quartz, biotite and accessory minerals. Light colored group is granite and granodiorite in composition with metaluminous and peraluminous characters (Bayhan, 1989). In contrast to the dark colored group, it is coarse grained and porphyritic. The size of orthoclase crystals sometimes reach up to 5 cm. It contains quartz, biotite, plagioclase, orthoclase, microcline, and muscovite.

This unit is well correlated to Ağaçören Granitoid of Kadıoğlu (1991; 1996) and Ekecikdağ Granitoid of Türeli and Göncüoğlu (1993).

4.3.2. Eastern Group

The eastern group granitoids include the granitoids in Akdağmadeni and Akçakışla districts. They are represented by the granitic rocks in Akdağmadeni district (Tülümen, 1980) and Akçakışla granite (Ergintav, 1987). The granitic rocks in Akdağmadeni district occurs as two separate plutons (larger and smaller plutons) (Figure 4.1). However, the Akçakışla granite is exposed as a relatively smaller pluton in Akçakışla district (Figure 4.2). (Sağıroğlu, 1982). In places, they are poorly exposed or weathered.

The larger pluton is exposed at the eastern part of the Akdağmadeni district to the east of the Çiçeklitepe, Peynirliktepe and Evciboyuntepe. The smaller pluton is exposed at the center of the district to the west of Memotepe. (Figure 4.1). Other exposures are observed at Boğatepe and Nusrettepe. The granitic rocks appear as granite to tonalite (Erler and Bayhan, 1995), hornblende granite, granite porphyry and aplitic granites (Vache, 1963), monzonite to adamellite (Sağıroğlu, 1982), and monzonite (Tülümen, 1980). The northern margin of the granitic rocks around the Karapir are fine grained (Tülümen, 1980). However, those around the Ortaköy are coarse grained, and the orthoclases are observed as coarse grained constituents.

In the Akçakışla district the Akçakışla Granite intrude the Aşıgediği metamorphics (marbles) (Figure 4.2). Vache (1963) and Sağıroğlu (1982) proposed that the granitic rocks in Akdağmadeni and Akçakışla Granite are the surface exposures of a single large pluton, and the country rocks between them are roof pendants. They proposed

that the intense skarnization and dense faulting of the country rocks lying between the plutons support this argument. The contacts between granitoid and marble are well exposed.

The mineral assemblage of the granitoids consists of orthoclase, plagioclase, quartz, biotite and hornblende with some accessory minerals like sphene and apatite (Sağıroğlu, 1982). The geochemical studies showed that the granitoids in the eastern group are of subalkaline type with metaluminous character, and are of cafemic-calcalkaline trend (Erler and Bayhan, 1995). They plot in late orogenic and syn-collisional field (Erler and Bayhan, 1995).

4.5. Cover units

4.5.1 Yeşilöz Formation

Dark red to brown polygenic conglomerate, conglomeratic sandstone and sandstone units overlying the CACC are named as the Yeşilöz Formation by Göncüoğlu et al. (1993). The formation crops out only within an approximately N-S trending zone in the Keskin district (Figure 4.3). The width of the unit becomes thinner from south to north. The upper contacts with the diabases and monzonitic rocks (Keskin Pluton) are fault controlled around Keskin, Karamağara and to the south of Üçlertepe, but the lower contacts are mainly unconformable with the Aşıgediği Metamorphics (Figure 4.3). Along the contact between granitoids and conglomerate, intense shearing and mylonitization are seen (Kuşcu and Demirci, 1995). The conglomerates are poorly sorted and graded, and contain well rounded clasts of metamorphic rocks, volcanic rocks, and granitoids. The sandstones are well bedded and show cross-bedding.

The base of the unit is characterized by several cycles of coarse clastic sedimentation. In general the clasts show imbrication in a direction from southwest to northeast (Kuşcu and Demirci, 1995). The size of clasts range from 1 to 20-30 cm. The coarse grained conglomeratic unit at the base grades into reddish conglomeratic sandstones then to grayish green sandstones and siltstones. The upper levels are also characterized by pinkish recrystallized limestones as lenses within the greenish siltstones. The sandstones are interlayered with chert and volcanogenic sandstone, and contain clasts of diabase about 1 cm in diameter.

The Yeşilöz Formation is correlated to the Kartal Formation of Seymen (1982). The

age of the Yeşilöz Formation is said to be Upper Danian-Lower Thanetian by Göncüoğlu et al. (1993). Seymen (1982) estimated the age of the Kartal Formation as Upper Maastrichtian.

4.5.2. Kurtören Formation

The conglomerates and fossiliferous limestones exposed mainly at the northern part of the Akçakışla district is called the Kurtören Formation (Ergintav, 1987) They unconformably overlie the Akçakışla Granite and the Aşıgediği marbles, and are unconformably overlain by the alluvial deposits.

The formation begins with 10 m thick semi-consolidated to consolidated basal conglomerate (Ergintav, 1987) containing clasts of metamorphic and granitic rocks. The conglomerates are conformably overlain by the Nummulitic limestones at the upper levels of this formation. Limestones consist of grayish yellow, thin to medium bedded turbiditic limestone and siltstones. The observed thickness of the formation ranges between 20-50 m (Ergintav, 1987).

This unit is correlated to the Mucur Formation of Göncüoğlu et al. (1994), Boztepe Member of Atabey et al. (1987), and Ortaköy Formation of Tekeli et al. (1992). Lower to Middle Eocene age is assigned to this unit based on its fossil content (Ergintav, 1987).

CHAPTER 5

LEAD-ZINC OCCURRENCES

Lead-zinc occurrences in Akdağmadeni, Akçakışla and Keskin districts have attracted infrequent exploration activities since the Byzantine times. Several lead-zinc occurrences are found within the districts. In this study, they are classified into two major types according to their configuration with respect to adjacent intrusive body. These are "skarn around intrusive" and "intrusive around skarn" types (Burt, 1977). The lead-zinc occurrences in skarn zones which surround the granitoids in the Akdağmadeni and Akçakışla, are termed as the "skarn around intrusive" type skarns. However, the skarn zones in the Keskin district are enveloped by the Keskin Pluton, and hosted by the marbles as roof pendants in the Keskin Pluton, and hence are termed as "intrusive around skarn" type skarns. It is an old but very important classification, since most of the economic skarn mineralizations occur in regions where "intrusive around skarn" type configuration appear (Burt, 1977). In this sense, the Keskin lead-zinc occurrences are supposed to have the higher grades of lead-zinc, because a relatively small (compared to those in Akdağmadeni, and Akçakışla) metacarbonate body was metasomatized by a huge intrusive rock.

The studied districts are characterized by two main types of skarns, endoskarns and exoskarns. Endoskarns are exposed in the Akçakışla district. Endoskarn mineralogy is limited and represents the skarnization of Akçakışla granite in the Akçakışla district. Exoskarns are the typical skarn types for each district, and could easily be identified at the field and under the microscope.

The mineralogical assemblage of the skarns consists of silicate minerals, and ore minerals (oxide and sulfide minerals). The lead-zinc occurrences are hosted by the exoskarns. Sağıroğlu (1982) distinguished three major types of exoskarns; (1) magnesian, (2) garnet, and (3) epidote skarns. Of these, the magnesian skarn is exposed only within the Akçakışla district, the garnet-pyroxene and epidote skarns are exposed at each district. The epidote skarn is the most widely exposed exoskarn type

in each district. The most typical exposures of the epidote skarns are found within the "densely faulted area" between Evciboyuntepe, Çiçeklitepe and Nusrettepe localities (Sağıroğlu, 1982).

5.1. Akdağmadeni district

The lead-zinc skarns in the Akdağmadeni district are observed around the granitoids that intruded the metamorphic rocks. The main ore deposition is found within the large skarnized area between Karapir, Peynirliktepe, Nusrettepe and Ortaköy (Figure 4.1). In this district, six occurrences are studied. In an alphabetical order, these are Bayramali, Çukurmaden, Çiçeklitepe, Evciboyuntepe, Peynirliktepe and Radarbaca occurrences (Figure 1.2 and Figure 4.1).

5.1.1. Mining History

The lead-zinc occurrences in the Akdağmadeni area have been the important mining sites since the Byzantine times. During the Byzantine Empire, the mines were operated for lead, silver, and zinc (Kovenko, 1940). Remains of zinc-rich slags can be seen in old mining sites around Oyumçayırdere and Çukurmaden. In the period between the second half of the last century and 1914, French companies operated the mines (Kovenko, 1947). The mining activities ceased due to beginning of the World War I (Kovenko, 1947).

The Rasih-İhsan Ltd. Şti. began the mining operations in late fifties, and has been mining in several sites in the Akdağmadeni area since then. Although they abandoned the mines because of economical reasons, they mined the lead-zinc ores in the Akdağmadeni district for about 40 years. At present, there is limited mining activity in the district.

5.1.2.Wall rocks

The lead-zinc occurrences are hosted within skarnized marbles that belong to the Gümüşler Metamorphics. The marbles occur both as lenses and intercalations within the gneisses. The skarnized marbles are light colored and thick-bedded. They are coarse grained, and have a few millimeter thick mica and quartz-rich bands. The skarnization is widespread where granite intrudes the banded marbles.

The granites that caused skarnization in the Akdağmadeni district are exposed

as two large mappable plutons aligned in E-W direction. The best exposures of the western granite body are observed along the course of Değirmendere (Figure 4.1).

5.1.3. Skarn zones

The contacts between marbles and granites display an extensive skarn formation in the Akdağmadeni district. In places, some skarn zones are away from granite contacts; but they are probably related to offshoots or mushrooms of granites which do not crop out at the surface. The skarn zones were developed along granite-marble contacts, or along fracture zones within the marbles (Sağıroğlu, 1982). The width of the skarn zones are up to 500 m, but not less than 200 m (Sağıroğlu, 1982). The skarn zones may also occur as lenses along the pre-existing fractures or bedding planes of marbles. The skarn zones are narrower in Akdağmadeni than those of Akçakışla (Vache, 1963). This is probably related to the depth of granite emplacement within the metamorphics. The skarn zones are of calcic exoskarn type. They are mainly of two types as garnet-pyroxene and epidote skarns. This classification scheme is mainly based on the predominant mineral in the skarn mineral assemblage. The sulfide mineralizations occur as replacing the epidote skarn assemblage. The iron-oxide mineralizations occur within the garnet-pyroxene skarns.

The exoskarns generally occur adjacent to plutons, and their thickness vary with respect to lithology and structure. For example, they become more widespread where they are found within the marbles associated with faults and fractures. The exoskarns are well developed in the area between Evciboyuntepe, Çiçeklitepe, and Nusrettepe. This is because of the faulting that caused extensive retrograde alteration in these areas (Figure 4.1). The skarn zones are well observed along the margins of the granitoids in contact with marbles at Karapir village, Memotepe, Yolçatıtepe, Çiçeklitepe, Peynirliktepe, Evciboyuntepe, Nusrettepe, Ortaköy line (Figure 4.1).

The garnet-pyroxene skarns of the Akdağmadeni district are observed only in Evciboyuntepe and Radarbaca occurrences. In the Evciboyuntepe occurrence, the garnet locally becomes so abundant that this gives a brownish to green spotted texture to the rock by naked eye. The garnets also appear in other occurrences of the Akdağmadeni district in epidote skarns, but in these, the garnets are subordinate, and they occur as altered minerals from which epidotes and calcites were derived. The

garnet-pyroxene skarns are composed of garnet as predominant mineral associated with pyroxene. Magnetite, hematite, pyrrhotite, and some pyrite are the characteristic ore minerals observed in the garnet-pyroxene skarns. The garnet-pyroxene skarns occur within the skarn zones next to or close to the granite contacts, and their thickness decreases away from the granites (Sağıroğlu, 1982). Hence by considering the relative amount of garnet in the skarns, it is possible to deduce that the Evciboyuntepe and Radarbaca are relatively proximal exoskarns compared to other skarns in the district.

The skarns which consist predominantly of epidote are termed as epidote skarns. The epidote skarns include epidote, pyroxene, wollastonite, tremolite, calcite, chlorite, quartz, and sulfide minerals (sphalerite, galena, chalcopyrite, pyrite). The early formed mineral assemblages (garnet and pyroxene) were re-equilibrated by subsequent hydrothermal solutions, and altered to mineral assemblage of epidote skarns.

In general, the epidote skarns are divided into two as sulfide-poor and sulfide-rich epidote skarns. This classification is based on the association of sulfide minerals with the assemblage of epidote skarns. In the sulfide-rich skarns, the sulfide minerals appear as replacing the assemblage of epidote skarns after the epidote skarns are formed. The minerals in the sulfide-poor epidote skarns are fresher than sulfide-rich epidote skarn. Both of these may be present in the same occurrence. The Radarbaca, Bayramali, and Çiçeklitepe are the occurrences with the sulfide-poor type epidote skarn, but Bayramali, Çukurmaden, Evciboyuntepe, and Peynirliktepe are the occurrences with the sulfide-rich type epidote skarn. In the sulfide-rich type, the skarn minerals are more altered. Some of the sulfide-rich epidote skarns are made up of three subzones, as pyroxene-epidote zone closer to granite side of the skarn zone, calcite-quartz zone at the middle, and quartz-sphalerite-galena zone closer to marble side of the skarn.

5.1.4. Mineralization

The mineralizations appear as a series of lenses parallel to each other, and the distances between them do not exceed a few meters (Vache, 1963). These are mainly parallel to the main trends of the fractures in the district (Vache, 1963). The

mineralizations in the Akdağmadeni district are of two types as mineralizations formed at high and low temperatures (Vache, 1963). The mineralizations formed at high temperatures (magnetite (martitized), hematite, pyrite and quartz) are observed mainly within the area between Memotepe, and west of Karapir village (Vache, 1963). The second type of mineralizations are found in the eastern part of the district , and they are observed within a "densely faulted area" between Evciboyuntepe, Çiçeklitepe, Çukurmaden and Nusrettepe (Vache, 1963). The mineralizations along the fault zones appear to be massive polymetallic type (Sağıroğlu, 1982). This area is characterized mainly by galena and sphalerite, with minor pyrite. The magnetite is subordinate and martitized (Vache, 1963). Andradite, grossular, epidote, calcite, and chlorite are the characteristic silicates associated with the ore minerals. The galena is silver-bearing (85 ppm to 1450 ppm Ag, Vache, 1963).The grade of the mineralization is high. The average grade of metals range from 18 to 29% Pb, and 30-35% Zn (Vache, 1963)

5.3.4. Structural control

The skarn zones and lead-zinc mineralizations in the Akdağmadeni district are associated with the structural features. These provide both channelways for passage of hydrothermal fluids, and sites of deposition for ore and gangue minerals. Faults, bedding planes and joints are the main agents that control the skarnization and ore deposition.

Small and large-scale normal faults are observed in the district. They generally trend NE-SW. Most of the faults occur along the peripheries of the granitoids displacing both the granitoids and metamorphics. Sağıroğlu (1982; 1984a) described that the thickness of the skarn zones are controlled mainly by faults in a way that dense faulting increased the permeability of the marbles (superimposed permeability). The superimposed permeability enhanced the transportation of the skarnizing fluids over large distances, and caused extensive skarnization. However, it is necessary to note that this could happen only where the granite emplacement takes place at shallower depths at which the rocks are subjected to brittle deformations. Otherwise, if the bedding planes are bent parallel to the peripheries of the granitoid during its emplacement, limited skarn zones develop only at the contacts between upper parts of the granitoids and carbonate-rich rocks (Meinert, 1983; 1992; 1993). Therefore, the skarns in the Akdağmadeni district should have been formed at shallow depths (2 to 4

km). The fault zones and fault gouges, or wall rocks on either side of the faults were mineralized and skarnized (Sağıroğlu, 1982). Çukurmaden and Bayramali are the principal occurrences controlled by the faults (Sağıroğlu, 1982).

The bedding planes of the marbles also control the skarnization and mineralization. In these, infiltration is the mechanism by which the fluids were transported, and the rocks were metasomatized. The orientation of bedding planes with respect to granitoid body plays an important role in the extent of skarnization. The orientation of bedding planes with respect to the granitic body is controlled largely by the depth of emplacement of the granitoid body (Einaudi et al., 1981; Meinert, 1983; 1992; 1993). The intrusive contacts at depth tend to be sub-parallel to the bedding; either the pluton intrudes along the bedding planes or the sedimentary unit flows or is folded until it is aligned with the intrusive contacts. In the regions where the intrusive contacts are sub-parallel to the bedding planes, skarn is usually confined to a narrow but vertically extensive zone (Meinert, 1983). Whereas in the regions where the intrusive contacts are not parallel or sub-parallel to the bedding planes that are more suitable to the flow of skarnizing fluids through the bedding planes, the skarn zone is wider. In the first case, the transportation of the fluids is mainly by diffusion, and hence limited skarns are formed. However, in the second case it is by infiltration. The skarn zones in the Akdağmadeni district are not limited (the width of skarn zones ranges between 200 to 500 m) and they are observed in widespread areas from the intrusive contacts. Therefore, it is possible to say that the metacarbonates are intruded at relatively shallow depths by the granitic rocks in such a way that the intrusive contacts are not parallel to the bedding planes. This resulted in formation of extensive skarn zones in this district. The mineralization controlled by bedding planes is termed as the "disseminated ore" (Sağıroğlu, 1982).

5.2. Akçakışla district

In the Akçakışla district, outcrops of skarns were destroyed by exploration and mining activities so that the nature of mineralization is obscured. The outcrops are in the mine workings (Sağıroğlu, 1982). The skarns are observed along the contact between the Akçakışla Granite and the Aşıgediği Metamorphics (Figure 4.2). The thickness of the skarns is about 200 m (Sağıroğlu,1982). In this district, three occurrences are studied. In an alphabetical order, these are Akçakışla,

Barajdoğusu and Özgebaca occurrences (Figure 4.2).

5.2.1. Mining history

The data about the mining and exploration activities in the Akçakışla district is very limited. The Rasih-İhsan Ltd. Şti. began the mining operations in 1978. They abandoned the mines because of economical reasons. They have mined the lead-zinc ores in the Akçakışla district for about 12 years between 1978-1990. At present, there is no mining activity in the district. The dumps in front of the mine workings are observed around the Özgebaca, Akçakışla and Barajdoğusu occurrences.

5.2.2. Wall rocks

The mineralizations in the Akçakışla district are hosted by the marbles that bound the Akçakışla Granite at the north (Figure 4.2). The thickness of marble is about 250-300 m (Sağıroğlu, 1982). The Akçakışla granite display geochemical characteristics similar to the granitic rocks in the Akdağmadeni district (Sağıroğlu, 1982), but the texture of Akçakışla granite is different, the decrease in grain size near contacts is more distinct (Sağıroğlu, 1982).

5.2.3. Skarn zones

Two types of skarn zones appear in the Akçakışla district, the endoskarn and exoskarn. Endoskarns are developed within the Akçakışla granite. The Özgebaca occurrence is characterized by a limited endoskarn development within the marginal parts of the granite. In this sense, the endoskarns appear in the regions where skarnizing fluids circulated along the periphery of granites in contact with marbles. Endoskarns appear as gray colored discontinuous lenses, or patches around densely jointed areas in the granites. The thickness of endoskarns does not exceed 0.5 m (Sağıroğlu, 1982). The endoskarns contain chalcopyrite, pyrite, pyroxene, epidote, biotite, plagioclase, garnet, quartz, chlorite and calcite. Similar to the exoskarns, the minerals formed at high temperatures are overprinted by the minerals formed at low temperatures.

The exoskarn zones are not widespread in the Akçakışla district compared to those in the Akdağmadeni district. In observable parts of the Akçakışla district faulting

is not dense, and the layers strike more or less parallel to the granite contact (Sağıroğlu, 1982). This means that the granite emplacement must have taken place at deeper levels where the wall rocks behave plastically during the intrusion. In these cases, the skarns are developed very close to the granite, commonly at the roof of the granite, or occasionally within the granite (Meinert, 1983; 1992 and 1993) and the skarns are termed as proximal skarns so as the skarn zones in the Akçakışla district.. Exoskarns mostly develop between marble-granite contacts, and rarely along the fault zones within marbles . The exoskarns are observed mainly as patches in association with the granites. The exoskarns in the Akçakışla district are classified as the magnesian and calcic skarns (Sağıroğlu,1982).The magnesian skarns have limited exposures only at the dolomitic marble-granite contacts (Sağıroğlu, 1982). They are composed of equidimensional olivine, clinopyroxene, spinel, phlogopite and magnetite (Sağıroğlu, 1982). They are very rare since the dolomitic marbles are subordinate compared to calcitic marbles. The calcic exoskarns in the districts are mainly of two types as garnet-pyroxene and epidote skarns.

The garnet-pyroxene skarns are commonly observed in the Barajdoğusu and Özgebaca occurrences. The magnetite, hematite, pyrrhotite, and pyrite are the characteristic ore minerals observed in the garnet-pyroxene skarns. Pyrite and pyrrhotite are not common, and appear only in the Özgebaca occurrence. They are associated with garnet and pyroxene. The formation of these minerals along the fracture planes, and replacement of garnet and pyroxenes, or formation of them rarely along the oscillatory zones within the garnets indicate that they are formed during the prograde stage of the skarnization just after the garnet and pyroxene formation.

The epidote skarns are also common in the Akçakışla district. They are are classified as sulfide-rich epidote skarns. The sulfide mineralizations occur as replacing the assemblage of the epidote skarns in the district.

5.2.4. Mineralization

The economic mineralizations in the Akçakışla district occur mainly in the exoskarns like those in the Akdağmadeni district. The mineralizations are observed along the contact between the Akçakışla Granite and the Aşıgediği Metamorphics. The thickness of the ore bodies in the exoskarns are more than 50 m (Sağıroğlu, 1982).

The mineralization is not homogeneous, and is made up of three different zones (Sağıroğlu, 1982). These are pyrite, pyrite-sphalerite-galena, and sphalerite-galena zones. In this study, pyrite-hematite, and hematite zones were also identified. The thickness of the pyrite zone is about 20-30 m, and in places pockets (up to 8-10 m in diamater) of galena and sphalerite are observed (Sağıroğlu, 1982). The sphalerite-galena zone becomes dominant toward the marble.

5.2.5. Structural controls

The skarn zones and skarnization are controlled to a large extent by the depth of granite emplacement, and the orientation of bedding planes of marbles with respect to the granite in the Akçakışla district. The faults are rare and are limited in the district. The bedding planes of the marbles in the Akçakışla district strike more or less parallel to the peripheries of the Akçakışla Granite. Therefore, the fluids were transported along the peripheries of the granite, and the skarn zones were developed close to the granite contacts. This also caused the formation of endoskarns where the hydrothermal fluids circulating along the periphery of the granite body penetrated into the granite and caused metasomatism of the granite body. In this area, only a few small-scale faults are observed at the surface, the skarnizing fluids could not be transported over large distances and the mineralization was developed in narrow zones as massive lenses (Sağıroğlu, 1982). Sağıroğlu (1982) proposed that the early skarn minerals formed by the rapid replacement of wall rocks by the fluids inhibited the later exchanges between the skarnizing fluids and the wall rocks.

5.3. Keskin district

The Keskin district includes four occurrences. In alphabetical order, these are

not restricted to this zone, and it is also observed elsewhere as lenses within the marbles away from the N-S trending zone.

5.3.1. Mining history

The mining activities in Keskin date back to late 1800's. Genoese conducted the earliest exploration and mining activities at Akdağlı and Araplı occurrences (Figure 4.3) (Çavuşoğlu, 1967)). The British miners also mined the same areas during the last quarter of the 19th Century. A Greek-French joint venture operated the mines until the end of 19th century (Çavuşoğlu, 1967). They abandoned the Akdağlı and Araplı occurrences just after the beginning of the World War I. There was no exploration activity until 1937. In 1937, the M.T.A. started new exploration and mining activities at Akdağlı and Araplı. M.T.A. initially intended to discharge the water filling the galleries and shafts opened by the previous miners (Çavuşoğlu, 1967). These activities continued in the period between 1937 and 1940, but they were not able to discharge the water from the galleries, and they abandoned the area in 1940. Between 1959 and 1964, the area was under the control of Cıngıllıoğlu Madencilik Ltd. Şti. The last mining activity in this area was started by Kesikköprü Madencilik Ltd. Şti. in 1959 (Çavuşoğlu, 1967). This company mined the Pb-Zn skarn ores in the Karamağara occurrence until 1974. In the period between 1974 and 1980, M.T.A. conducted geological and geophysical studies to determine the vertical and lateral extent of the mineralizations. At present, there is no mining activity in the district.

5.3.2. Wall rocks

The known Pb-Zn skarn mineralizations are hosted by the marbles (Figure 4.3). Here, the marbles appear as lens-shaped roof pendants within the granitoids. They pinch out and swell, but the widest exposures are about 1 km around the Karamağara occurrence, and about 3 km at the southern parts of the district. The initial isochemical metamorphism and skarnization after granitoid intrusion caused the deformation of the original bedding planes. A N-S striking strike-slip fault with a reverse component (Kuşcu and Demirci, 1995) is observed along the boundary between marble and granite. Along the same fault, the conglomerates are occasionally juxtaposed with marbles and the granitoids as well. The previous workers proposed that the known

mineralizations occur between diabases and the marble along the western side of the N-S trending zone (Millet, 1938; Kovenko, 1939a; 1939b;1940; Çavuşoğlu, 1967). However, the rocks called as diabases at the western margin of the marbles are not diabases, in fact they are altered pyroxene-rich skarn zones. The N-S trending marble exposure is displaced by approximately NE-SW trending smaller faults. This results in development of a blocky outcrop pattern for the marbles.

The geophysical studies by induced polarization method showed that the marbles become thicker eastward below the surface (Özkazanç, 1980). These studies also indicated that the thickness of the marble is about 125 m at its thickest section (Özkazanç, 1980). They have their widest surface area around the Karamağara occurrence resulting in more detailed exploration and mining activities around this occurrence. The geophysical studies showed that the total volume of the marbles subjected to skarnization is very small (Arslanpay and Yıldırım, 1978; Özkazanç, 1980). This could be the reason why the grade of the Pb-Zn mineralization is very high (40-45% Pb, Çavuşoğlu, 1967) in the Keskin district. This is also correct according to Burt's (1977) intrusive around skarn classification scheme stating that the smaller the replaced carbonate body within an intrusive the higher the grade of ore body.

5.3.3. Skarn Zones

The wall rocks are characterized by narrow and limited skarn development. The skarn zone is developed along the western margins of the N-S trending marble zone. The geophysical studies confirmed that the thickness of the skarn zones decreases with depth (Özkazanç, 1980). The observable part of the skarn zones on the surface is limited, and concealed by soil cover or mine dumps, except for the Karamağara occurrence where the marble has the widest exposure.

The exoskarns are of two types as garnet-pyroxene and wollastonite skarns. The garnet-pyroxene skarns are observed only in the Karamağara occurrence. The wollastonite skarns have limited exposures in the Keskin district. The skarns in the Keskin district are also subdivided into two as sulfide-rich and sulfide-poor types. The Karamağara is the occurrence with the sulfide-poor type, and Simlikurşun is the occurrence with the sulfide-rich type skarn. In general, the skarns contain garnet, pyroxene, epidote, actinolite, chlorite, calcite and quartz with less galena and

sphalerite (Çağatay and Teşrekli, 1979).

5.3.4. Mineralizations

The lead-zinc mineralizations is observed within the skarnized rocks (Millet, 1938; Kovenko, 1940;1947; Çavuşoğlu, 1967) extending from Keskin to Araplı occurrence (Figure 4.3). The mineralizations are observed along the contacts between the marble and granite (Arslanpay and Yıldırım, 1978; Çağatay and Teşrekli, 1979). However, Kovenko (1947) proposed that the mineralizations are found within the marbles in contact with diabase and green tuffs. The mineralizations occur as pockets and lenses within the skarnized rocks (Arslanpay and Yıldırım, 1978). The pockets and lenses are 0.20 to 1.5 m thick and 20-30 m long (Kovenko, 1947). The Keskin district is characterized by dominant galena and hematite, with subordinate sphalerite, magnetite and pyrite. The hematites are associated mainly with altered garnet and pyroxene in garnet-pyroxene, and wollastonite in the wollastonite skarn. The sulfide minerals are observed as replacing the assemblages of wollastonite and to some extent garnet-pyroxene skarns during the retrograde stages. The Akdağlı occurrence at the north of the district contains mainly galena with subordinate or without sphalerite, the Araplı occurrence contains mainly pyrite with hematite, galena and sphalerite (Arslanpay and Yıldırım, 1978). The Simlikurşun occurrence contains pyrite, sphalerite and galena, and the Karamağara occurrence contain galena, sphalerite and hematite, chalcocite, wittichenite, pyrite, chalcopyrite, malachite, and covellite (Çağatay and Teşrekli, 1979)

5.3.5. Structural Control

The most prominent structure in the Keskin district is the N-S trending strike slip fault with a reverse component (Kuşcu and Demirci, 1995). This fault is displaced by younger NE-SW trending smaller strike-slip faults. The previous workers (Millet, 1938; Kovenko, 1940; 1947; Çavuşoğlu, 1967; Arslanpay and Yıldırım, 1978; Çağatay and Teşrekli, 1979; Özkazanç, 1980) all agree that this is the main structure that controls the Pb-Zn mineralizations in this area. However, there is no evidence for that in the district. The field studies showed that this fault is younger than skarnization and mineralization, because the Tertiary aged (Early-Middle Paleocene) conglomerates nonconformably overlie the marbles elsewhere, and are thrusted by the Keskin Pluton

along this fault (Figure 4.3). The presence of granitic rock and marble pebbles within the conglomerates indicate that they are younger than granitoids and marbles, so the mineralization should predate the conglomerates. Since the conglomerates are thrusted by the Keskin Pluton, the mineralization should also predate faulting. Therefore, the alignment of the skarn zone more or less parallel to the dominant trend of this fault should be related to the original ellipsoidal shape of the marble body left as roof pendant within the pluton. The contacts on both sides of the marble were later faulted after Paleocene time due to regional compressional forces. Another possibility is that the present strike slip fault was formed by the re-activation of a pre-exiting fault which controlled the skarnization during the emplacement of the Keskin Pluton. However, there is no evidence to support this, and this needs further studies.

CHAPTER 6

MINERALOGY AND PETROGRAPHY

The studied lead-zinc occurrences have simple mineralogy. Each district is characterized by a mineralogical assemblage depending on the type of skarn, and the mineralogy of skarns differ from occurrence to occurrence. These differences may arise because of their distance to marble-granite contact, degree and extent of faulting, and the degree of retrograde alteration. In this section, the main objective is to describe mineralogical characteristics of the lead-zinc occurrences in Akdağmadeni, Akçakışla and Keskin districts. The mineralogical assemblage of the occurrences resemble the characteristic assemblages of the world-wide Pb-Zn skarns. In the studied districts, the minerals are found commonly in the exoskarns, and occasionally in the endoskarns.

The mineralogical assemblage of the skarns includes silicate minerals such as garnet, clinopyroxene, epidote, tremolite, chlorite, wollastonite and quartz, oxide minerals such as hematite and magnetite and sulfides such as sphalerite, galena, chalcopyrite, pyrite, and pyrrhotite. These minerals are found within the garnet-pyroxene and epidote skarns. Depending on the distance to granite contact, a zoning of minerals is apparent so as the high temperature minerals (prograde skarn minerals) like garnet and clinopyroxene (as well as iron oxides) appear close to granite contact, and low temperature (retrograde) minerals like epidote, chlorite, and sulfides away from the contact much closer to marble side (Sağıroğlu, 1982). However, it is difficult to locate the exact geological setting of these minerals in the skarns with respect to granites; because, early formed mineral assemblages were re-equilibrated by subsequent hydrothermal solutions, and altered to mineral assemblage of epidote skarns.

6.1. Akdağmadeni District

The Akdağmadeni district is characterized by garnet-pyroxene and epidote skarns. Both could be observed in a single occurrence, or only one skarn type could

be observed in a single occurrence. The mineralogy of the occurrences are controlled by the type of skarn, in which the occurrence is hosted. In general, the epidote skarns are termed as the sulfide-poor and sulfide rich epidote skarns depending on the sulfide minerals that replace the assemblage of epidote skarns later in the sulfide stage.

6.1.1. Bayramali occurrence

The sulfide-rich and sulfide-poor epidote skarns are observed within the Bayramali occurrence. The skarn minerals are mainly epidote and calcite with varying amounts of clinopyroxene, wollastonite, tremolite, and quartz. The ore minerals are sphalerite, galena and chalcopyrite.

Epidote is the dominant constituent of the skarns. It is fine to medium grained and commonly anhedral. It occurs as colorless to light yellow and/or pale green granular aggregates with weak pleochroism. Epidotes are the alteration products of pyroxenes. Locally, the alteration becomes so intense that only the relicts of pyroxenes are observed between the epidotes. Epidotes also replace tremolite, but are replaced by quartz. Those in the sulfide-rich epidote skarns are associated with calcite and tremolite, but those in the sulfide-poor epidote skarns are associated with clinopyroxenes.

Calcite is the second dominant mineral in the Bayramali occurrence. It is fine to medium grained with well developed rhombic cleavages. Calcites are secondary, formed by the alteration of pyroxenes during retrograde alteration stages. They replace clinopyroxene, but are replaced by quartz. They are associated with ore minerals.

Clinopyroxene is fine to medium grained, and it is colorless to pale green in color. It locally occurs as anhedral, subhedral and euhedral prismatic crystals or columnar aggregates. The cross sections of the euhedral crystals are four to eight sided (Figure 6.1). The optical characteristics of the pyroxenes resemble to those of diopsides. They are altered, and replaced by epidotes. The alteration is commonly developed along cleavage planes and fractures. Some of them are altered to tremolites. Clinopyroxenes occur both in the sulfide-poor and sulfide-rich epidote skarns. Clinopyroxenes in the sulfide-poor parts are those commonly altered to epidotes, but those in the sulfide-rich epidote skarns are altered to tremolites.

Wollastonite is observed as fine to medium grained radiating crystals. It is colorless to light brown in color. Wollastonites are locally associated with epidotes, and they are replaced by epidotes.

Tremolite occurs as fine to medium grained prismatic crystals and/or coarse grained fibrous aggregates (Figure 6.2). The tremolites are colorless to pale green, and the green varieties show weak pleochroism. They are the alteration products of pyroxenes. Locally, they also replace the epidotes. They are present in the sulfide-rich epidote skarns.

Quartz is fine grained and anhedral. It is observed within the veinlets associated with epidote. Quartz shows undulose extinction. The cross-cutting relationships with other minerals indicate that it is the last formed mineral in the Bayramali occurrence.

Sphalerite is the most common sulfide mineral replacing the assemblage of the epidote skarns of the Bayramali occurrence. Sphalerites, in general occur either as filling the interstitial spaces of altered epidote and tremolite or as replacing them. They are associated with calcite and quartz. They show dark brown to black or dark red to brown internal reflections along the fractures. Sphalerites are termed as heterogeneous sphalerite (Picot and Johan, 1982) based on the color of internal reflections. They are replaced by galena.

Galena is another common sulfide in the epidote skarns. It is fine to medium grained and anhedral to subhedral. Galena always coexists with sphalerite and it replaces sphalerite, it is evident from the unreplaced sphalerite islands within the galena.

Chalcopyrite is subordinate, and always coexists with sphalerite and galena. It is fine grained and anhedral. It occur either as minute exsolutions within sphalerite or as pockets along the contacts between galena and sphalerite.

6.1.2. Çiçeklitepe occurrence

In the region, an assemblage of epidote, clinopyroxene, chlorite, biotite, plagioclase and pyrite is observed within the alternating gneiss and marble lenses in the Gümüşler Metamorphics. These minerals may be regarded as the skarn minerals, however, such an assemblage in aluminous rocks like gneisses is likely to be called

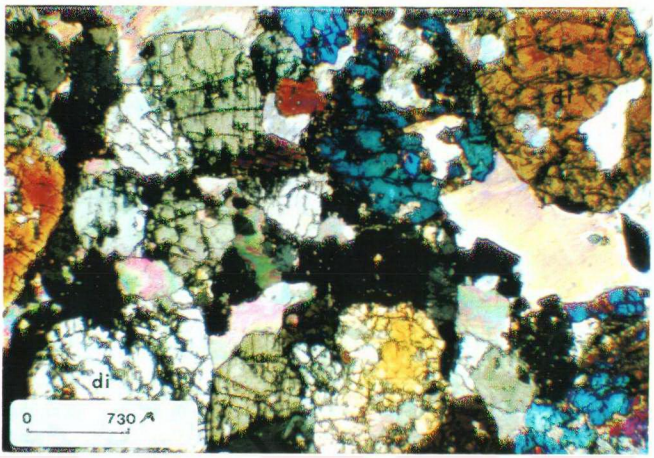

Figure 6.1. Photomicrograph showing euhedral to subhedral diopside(di) crystals

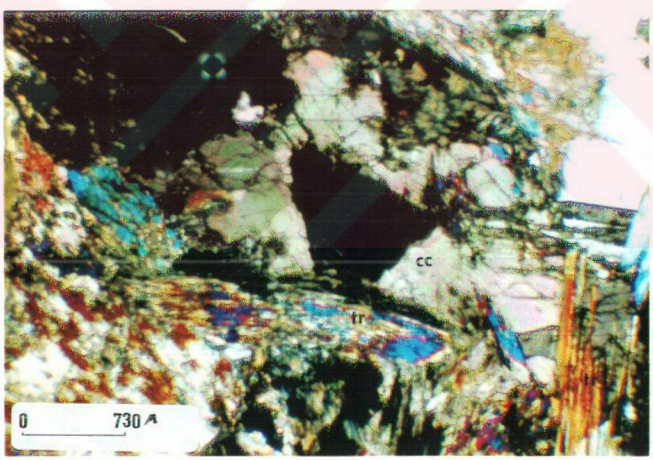

Figure 6.2. Photomicrograph displaying prismatic and fibrous tremolite (tr) crystals (cc: calcite)

skarnoid such as those at Yerington district (Harris and Einaudi, 1982). They are formed as result of metasomatism of alternating marble and aluminous rocks like gneiss.

The skarns in the Çiçeklitepe occurrence are sulfide-poor epidote skarns. They contain epidote, quartz, clinopyroxene, chlorite, tremolite, and calcite. In the skarns, limited lead-zinc mineralizations are observed along the marble and granite contacts (Sağıroğlu, 1982).

Epidotes are medium to coarse grained, pale green to yellow in color. They occur as euhedral to subhedral granular aggregates (Figure.6.3) replacing clinopyroxene, garnet and calcite. Some of the epidotes have the optical properties of zoisites, and are termed as zoisite. The zoisitic varieties occur as long prismatic crystals with deep blue to gray interference colors, and replace the epidotes. They both are replaced by quartz.

Clinopyroxene occurs as medium to coarse grained columnar aggregates or prismatic crystals. It is colorless to faint green in color. Clinopyroxenes are altered mainly to epidotes, and are replaced by quartz. They appear as the groundmass for the epidote and quartz crystals. The alteration is more intense along the fractures and cleavage planes.

Quartz is fine to medium grained, and occur as disseminations and aggregates of anhedral crystals. It is always associated with epidotes and replace them. The quartz locally contain minute inclusions and/or unreplaced islands of epidotes.

6.1.3. Çukurmaden Occurrence

The Çukurmaden occurrence is characterized by sulfide-rich epidote skarns. The skarn minerals in this occurrence are more altered compared to other occurrences in the Akdağmadeni district. The skarns contain quartz, calcite, epidote, chlorite, clinopyroxene, garnet, galena, sphalerite, pyrite, chalcopyrite, and hematite. The ore minerals occur as replacing the assemblage of epidote skarns.

Quartz is one of the major constituents of the skarns. It is fine to medium grained, subhedral to euhedral or anhedral. Quartz is observed as fine grained anhedral crystals (quartz I) where associated with ore minerals, and medium grained subhedral to euhedral crystals (quartz II) associated with calcite. The finer grains

enclose the medium grains. The first type replaces commonly clinopyroxene and epidote, and the ore minerals tend to occur along the contacts between quartz-clinopyroxene and/or quartz-epidote. In general, quartz replaces calcite. It is evident from the embayment of quartz I by the ore minerals that quartz I predates the mineralization in this occurrence.

Calcite is fine to coarse grained. Calcites are of primary and secondary calcites. The primary calcite is recrystallized and coarse grained, and since it was replaced by the mineral assemblage of epidote skarns, it is not common. The secondary calcite is commonly associated with pyroxenes, and it is formed by the alteration of pyroxenes. The primary varieties are characterized by well developed rhombic cleavages. The secondary calcites are associated always with medium grained quartz crystals and epidote. The calcites, in general, may locally be observed within veins together with quartz. They are associated with sphalerite and/or galena, and are replaced by quartz II crystals.

Epidote is yellowish to green in color, and fine to medium grained. It occurs as granular aggregates within the veinlets together with quartz II. The epidotes tend to be associated with secondary calcites. They are formed by the alteration of pyroxenes.

Chlorite is green in color, and fine grained. It is associated with epidote, clinopyroxene, calcite, and ore minerals. Chlorites are replaced by quartz II, and locally replace epidote. They predate the mineralization.

Clinopyroxenes are rarely observed in the Çukurmaden occurrence due to alteration during the retrograde stages of skarnization, and only relicts of them are seen under the microscope. They are mostly altered to epidotes and calcites. The calcitization seem to be more effective compared to epidotization. Locally, the pyroxenes are partly to completely converted into calcites, and pyroxenes may occur as unaltered patches and/or unreplaced islands within the calcite.

Garnet is observed as coarse grained and euhedral crystals. Although it is not common in the epidote skarns, it is present as remnants. Garnets are partly altered to calcites. They show oscillatory zoning, and the iron-oxides are found as very thin replacements between the zones (Figure 6.4) , or along the fracture planes.

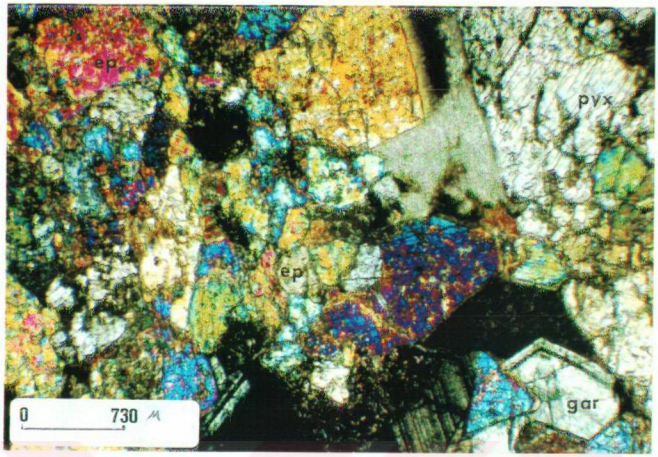

Figure 6.3. Photomicrograph showing granular aggregates of epidotes (ep) (pyx: pyroxene, gar: garnet)

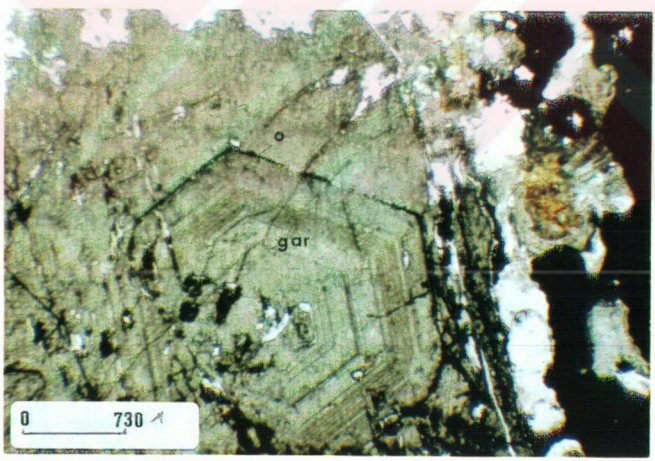

Figure 6.4. Photomicrograph showing the iron-oxide (o) minerals in the zoned garnet (gar).

Sphalerite is present as coarse to fine grained minerals that replace epidote and clinopyroxene. It is the major ore mineral constituent of the Çukurmaden occurrence and is always associated with galena. It is replaced by galena. Sphalerites contain minor amounts of chalcopyrite blebs, probably exsolutions. They show reddish internal reflections due to incipient alteration along the fracture zones.

Galena is medium to coarse grained, bright white to yellowish colored with high reflectance. Some of them are observed as inclusions within sphalerite. Galena sometimes contains pyrite as unreplaced islands. The triangular pits are rare or even absent. They are commonly associated with sphalerite with an interlocking texture, and occasionally associated with chalcopyrite.

Pyrite is not a common mineral in the Çukurmaden occurrence, and is locally observed along the contacts between galena and sphalerite, or within galena as unreplaced islands. It is fine to medium grained, and subhedral to anhedral. Pyrites are of two types as those associated with hematite (pyrite I) and those associated with sphalerite and galena (pyrite II). Pyrite I is represented by subhedral crystals that replace hematite, and pyrite II is represented by anhedral crystals replaced by galena and sphalerite.

Chalcopyrite is not common. It is observed in the form of structurally oriented rows of blebs and rods within the sphalerite. They are probably exsolutions along the pre-existing fractures within the sphalerite.

Hematite is subordinate and occurs as anhedral crystals associated with pyrite and galena. It is also commonly observed along the fracture planes of garnets as replacing them, or between the oscillatory zones in the garnets.

6.1.4. Evciboyuntepe occurrence

The Evciboyuntepe occurrence is characterized by garnet-pyroxene and sulfide-rich epidote skarns. The garnet-pyroxene skarn includes mainly garnet with or without clinopyroxene, and the sulfide-rich epidote skarn include calcite, tremolite, epidote, galena, sphalerite, pyrite, chalcopyrite, goethite, and chalcocite. The garnet-pyroxene skarn assemblage is overprinted by the sulfide-rich epidote skarn assemblage.

Garnet is the predominant constituent of the skarns in this occurrence. Garnets are commonly subhedral to anhedral, medium to coarse grained. They are green to pale brown in color. They are locally present as very coarse grained (larger than 1 cm) anhedral grains with a highly fractured appearance. They show oscillatory zoning, but the zoning is observed close to margins. The oscillatory zones consist of periodic alternations of light and dark colored bands of garnets yielding strong optical anomalies. The zoning begin with a light colored thin zone over a darker coarse grained isotropic garnet core. The growth and morphology of the zoning are locally controlled by microfractures. The number of oscillatory zones vary, but at least 3 and at most 22 bands are observed. The morphology of oscillatory zones change from regular planar structures to cellular and dissolution structures. The cellular morphology is commonly observed at the edges of garnets. However, the dissolution structures commonly appear between two individual bands. Clinopyroxenes which were later altered to tremolites replace garnets. Garnets are altered to epidotes, and veinlets of calcites cross garnets.

Clinopyroxene is medium to coarse grained, colorless to light green in color. Clinopyroxenes occur as subhedral to anhedral columnar aggregates. They are only observed as small patches in association with epidote and tremolite. Most of them are altered to epidote and tremolite. The alteration begins around the margin, and it proceeds along the cleavages.

Calcite is one of the dominant constituents of the skarns in the Evciboyuntepe occurrence. Calcite is either coarse grained, recrystallized with rhombic cleavages, or fine grained. The fine grained calcite replaces the mineral assemblage of the garnet-pyroxene and epidote skarns. These minerals are either veined by secondary calcite, or appear as unreplaced islands within the secondary calcite. The primary calcite is replaced by the assemblage of garnet-clinopyroxene skarn.

Tremolite is medium to coarse grained, colorless to pale green in color. The light green varieties are also observed, and they show faint pleochroism. They occur as long prismatic crystals replacing clinopyroxene and garnet. They are formed by the alteration of pyroxenes during the retrograde stages of skarnization. The tremolite is also present as long prismatic replacements within calcite.

Epidote occurs as fine to medium grained anhedral aggregates. It is pale green to yellow in color. It is less abundant than tremolite. Epidotes are only observed where the pyroxenes are altered. Their occurrence is strongly controlled by the alteration of clinopyroxene. They are not abundant where the pyroxenes are tremolitized. They appear commonly at the cores or around the margins of pyroxenes and garnets. Those observed around the margins of garnets show anomalous pale red to blue interference colors.

The mineralization in the Evciboyuntepe is characterized by sphalerite and galena. These two is commonly accompanied by pyrite, chalcopyrite, chalcocite and goethite. They occur as replacing the assemblage of epidote skarns.

Sphalerite is gray to dull grayish brown in color with low reflectance. It occurs as anhedral crystals mostly replacing pyrite. It contains fine to medium grained chalcopyrite rods and blebs. Many small lath-like or irregular galena inclusions are observed within sphalerite (Figure 6.5). They rarely show internal reflections. It is also observed as unreplaced islands within galena. They are replaced by galena, but they always coexist with galena, and this may indicate that they formed simultaneously.

Galena is white to grayish white in color with high reflectance. It occurs as very coarse grained anhedral crystals. Most of the other ore minerals are observed as unreplaced islands within the galena. Galenas do not contain triangular pits, and they are not fractured. The contacts with other minerals are commonly irregular. They replace pyrite, chalcopyrite and sphalerite.

Pyrite occurs as medium to coarse grained subhedral to euhedral crystals. It represents the earlier phase in the Evciboyuntepe occurrence. It is observed as unreplaced islands within sphalerite and galena, or replaced partly by sphalerite (Figure 6.6). Fractures in pyrite are filled by chalcopyrite which is altered to chalcocite and goethite.

Chalcopyrite is not common in the Evciboyuntepe occurrence. It is either observed as anhedral fine to medium grained crystals filling the fractures of pyrite, or as blebs within sphalerite. Chalcopyrite occurring as fracture filling is less abundant than those observed as blebs. Chalcopyrite blebs are not rounded or spherical. Instead, they have elliptical morphologies.

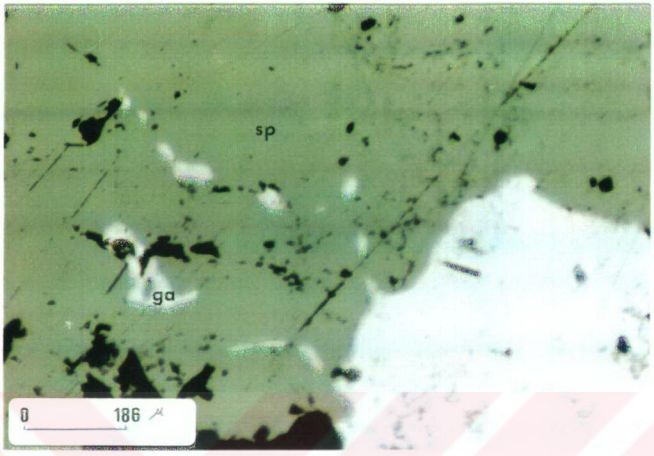

Figure 6.5. Photomicrograph showing galena (ga) inclusions within sphalerite (sp)

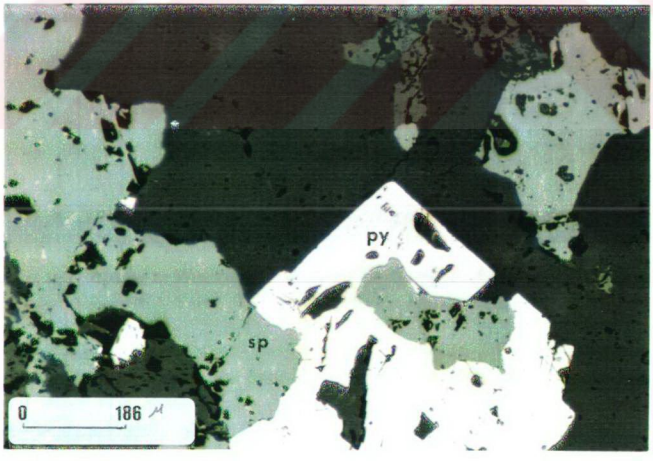

Figure 6.6. Photomicrograph showing replacement of pyrite (py) by sphalerite (sp)

Goethite is gray to grayish white in color with red to brown anisotropic colors. It occurs in zoned forms that replaces pyrite. It is a supergene mineral that was formed by the alteration ore minerals during the supergene stages. It is mainly found along the fracture planes of pyrite and sphalerite.

Chalcocite is the other supergene mineral formed by the alteration of chalcopyrite in the Evciboyuntepe occurrence. It is commonly gray to white in color with a characteristic bluish tint. It is associated with fractured chalcopyrite and pyrite.

6.1.5. Peynirliktepe occurrence

The Peynirliktepe occurrence is characterized by epidote skarns which are later replaced by the sulfide minerals. The mineral assemblage of this occurrence is very similar to other sulfide-rich epidote skarns in the Akdağmadeni district. It contains epidote, chlorite, and quartz as major constituents with subordinate calcite, tremolite and clinopyroxene. The ore minerals of the occurrence are sphalerite, galena, and chalcopyrite. They appear as replacing the assemblage of epidote skarns.

Epidote occurs as fine to medium grained granular aggregates that usually replace clinopyroxene. It is replaced by chlorite and calcite. Epidotes are locally associated with quartz, and they replace quartz where they both are observed

Chlorite occurs as fine to medium grained anhedral masses. It is usually associated with clinopyroxene. Chlorites are formed by the alteration of clinopyroxene. They replace tremolite, epidote and clinopyroxene.

The calcite occurs as fine grained anhedral crystals. It is associated with clinopyroxene, and tremolite and quartz. It replaces epidote, clinopyroxene and tremolite.

Tremolite is rare compared to epidotes. It occurs as fine to medium grained prismatic crystals. It is observed commonly at the margins of pyroxenes. Tremolite replaces clinopyroxene, and is replaced by calcite and tremolite.

Clinopyroxene occurs as medium to coarse grained subhedral to anhedral columnar aggregates. It is altered either to tremolite and epidote or to chlorite. The alteration is very distinct at the center of clinopyroxene.

The quartz is observed as fine to medium grained anhedral crystal aggregates. Quartzes are usually equigranular.

Sphalerite is gray to dull gray in color with low reflectance. It occurs as medium to coarse grained anhedral crystals. It is highly fractured, and shows incipient alteration along the fractures that caused various internal reflections within the sphalerites. The internal reflections become lighter within the sphalerites that are fractured. In general they are termed as heterogeneous sphalerites because of dark brown to black internal reflections. Sphalerites locally become so abundant that they appear to be the groundmass for other ore minerals. They are characterized by many chalcopyrite blebs, probably exsolutions that display systematic arrangements suggesting the existence of the pre-existing fractures. It is replaced by the galena and also contains many minute inclusions of galena.

Galena is bright white in color with high reflectance. It occurs as fine, medium to coarse grained crystals replacing the gangue minerals. The triangular pits are not always present or they are less compared to other occurrences. It replaces sphalerite. The sphalerite and galena contacts are locally occupied by chalcopyrite pockets (Figure 6.7) especially where sphalerite is replaced by galena.

Chalcopyrite is subordinate, and occurs either exsolutions within the sphalerite or as pockets along sphalerite and galena contacts. The occurrence of chalcopyrite as exsolutions are much more common than the chalcopyrite pockets.

6.1.6. Radarbaca occurrence

The Radarbaca occurrence includes garnet-pyroxene skarns that were later overprinted by the assemblages of epidote skarns The epidote skarns are later replaced by the sulfide minerals. Radarbaca occurrence contains calcite, epidote, garnet, clinopyroxene, quartz, tremolite and chlorite. The ore minerals are mainly galena with subordinate sphalerite and chalcopyrite.

Calcites are of two types, primary and secondary. Primary calcites are medium to coarse grained, and commonly occur as recrystallized aggregates. Most of them display typical rhombic cleavages. Secondary calcites are fine to medium grained. They are formed during the retrograde stage of skarnization. In general, both occur as the major mineral constituents of the occurrence Secondary calcites replace epidote,

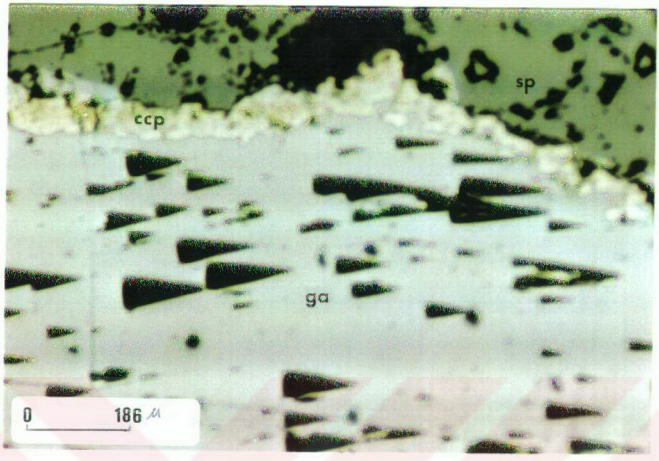

Figure 6.7. Photomicrograph showing the chalcopyrite (ccp) pockets along galena (ga) and sphalerite (sp) contacts

clinopyroxene and garnet, and contains very fine grained unreplaced islands of these minerals. However, primary calcites are replaced by the skarn assemblages. They do not show any deformation texture, and commonly vein clinopyroxenes.

Epidote is also very abundant in the skarns of the Radarbaca. It is yellowish to green in color with red to dark blue interference colors. The epidotes occur as fine medium grained granular to prismatic aggregates replacing clinopyroxene and garnet. They are formed mostly by the alteration of pyroxenes and garnets. The granular aggregates are commonly associated with the ore minerals. Opaque minerals are observed at the centers or along the cleavage planes of the granular epidote grains. Epidotes are replaced by calcite and quartz, and replace the clinopyroxene and garnet.

Garnet occurs as fine to medium grained subhedral to anhedral crystals. Since garnets in the garnet-clinopyroxene skarn zone are overprinted by the epidote and calcite, they are subordinate in this occurrence. They exhibit oscillatory zoning. The

zoning is in the form of alternating dark and light colored bands less than a millimeter wide. It is replaced by clinopyroxene. It is strongly altered to epidote and calcite, and only relicts of them are observed under the microscope.

Clinopyroxene is colorless to greenish in color. It occurs as medium to coarse grained, subhedral to euhedral, prismatic to columnar aggregates. Clinopyroxenes together with garnets belong to garnet-pyroxene skarn assemblage of the Radarbaca occurrence. Some of the pyroxenes have six or eight sided crystal outlines. The optical properties of these pyroxenes resemble to those of diopsides. They are altered, and diopsidic pyroxenes are more susceptible to alteration, and the epidotes are usually associated with these pyroxenes. The diopsidic pyroxenes are replaced by other pyroxenes. In general, they all are replaced by epidote, calcite and quartz. The pyroxenes with prismatic crystal outlines replace the garnets.

Quartz is a late stage or retrograde stage mineral that usually replace other silicate minerals in the skarns of the occurrence. It occurs as fine to coarse grained anhedral granular aggregates.

Tremolite and chlorite occur as fine to coarse grained anhedral aggregates. They both are the alteration products of pyroxenes. Chlorites replace the tremolites where they both are observed. Chlorite is commonly observed along the fractures of pyroxenes or within the pre-existing fractures.

The Radarbaca occurrence contains mainly galena with subordinate sphalerite. The mineralization occurs as replacing calcite and altered granular clinopyroxene crystals. Galena occurs as fine to coarse grained subhedral to anhedral crystals. Galenas have well developed cleavage planes. The triangular pits are rare. Galenas replace sphalerite where they both are observed. Many small unreplaced islands of sphalerite are present within galena. The cataclastic deformation that caused the formation of fractures in clinopyroxene and epidotes are not observed in the galena. This clearly indicate that they are formed after the gangue minerals.

6.2. Akçakışla district

The skarns in the Akçakışla district are of endoskarn and exoskarn types. The endoskarns are observed only within the Özgebaca occurrence but the exoskarns are

observed at each occurrence in this district. The exoskarns in this district are classified as garnet-pyroxene and epidote skarns.

6.2.1 Akçakışla occurrence

The Akçakışla occurrence is observed at about center of the district. The mineral assemblage of the Akçakışla occurrence is of the sulfide-rich epidote skarns. This occurrence contains calcite, epidote, quartz, clinopyroxene, sphalerite, galena, chalcopyrite, pyrite, magnetite, hematite and pyrrhotite.

The samples collected from the Akçakışla occurrence consists mainly of recrystallized calcite. Calcite is medium to coarse grained with well developed rhombic cleavages. It is possible to see primary calcites replaced by the skarn mineral assemblages, or the secondary calcites formed during the retrograde stage of skarnization. Primary calcites are replaced by pyroxenes and epidotes, and other skarn minerals. Secondary calcites replace commonly epidote, clinopyroxene, and quartz. Calcites are associated with mineralization where they replace quartz. The recrystallization is very clear with well developed crystals with 120° interfacial angles.

Epidote is not abundant in this occurrence compared to other occurrences in the Akdağmadeni and Akçakışla districts. It occurs as yellowish to green colored fine to medium grained granular aggregates. Fine grained epidotes are observed as prismatic crystals. They replace pyroxenes and primary calcites, but are replaced by the secondary calcite and quartz.

Quartz is very common, and it reaches its highest amount in this occurrence. It occurs as medium to coarse grained subhedral crystals. Quartz crystals locally contain minute impurities with well developed outlines (Figure 6.8). They are one of the last formed minerals in the skarns of the Akçakışla occurrence, and they occur as replacing the other minerals.

Clinopyroxene is very rare, and occurs as colorless to greenish subhedral to anhedral granular aggregates. It is closely associated with pyrite, epidotes and secondary calcites. Epidote and secondary calcite replace clinopyroxenes along the fracture and cleavage planes.

The Akçakışla occurrence is characterized by various ore minerals. These commonly occur as replacing the silicate minerals of the skarn zones. Locally, they are

observed in three major zones, hematite, pyrite-hematite, and sphalerite. Hematite zone includes radiating crystals of hematites with subordinate pyrite. Pyrite-hematite zone is characterized mainly by pyrite with abundant hematite. Sphalerite zone contains sphalerite, galena and chalcopyrite with subordinate magnetite and pyrrhotite. It occurs close to the marble side of the skarn.

Galena is one of the most common ore minerals of the Akçakışla district. It occurs as medium to coarse grained subhedral to anhedral crystals or as fine grained replacements within the sphalerite. It contains numerous triangular pits in different sizes. It is associated mostly with sphalerite and magnetite in the sphalerite zone. It replaces all other ore minerals, and the other minerals may occur as unreplaced islands within the galena.

Sphalerite is gray in color, and occur as anhedral crystals. Sphalerite is less abundant than galena. It is observed within the sphalerite zone. Sphalerites always contain chalcopyrite exsolutions. They are replaced by galena. Sphalerites do not show internal reflections. Picot and Johan (1982) classified such kinds of sphalerites as iron rich, massive sphalerites.

Chalcopyrite occurs either as anhedral crystals replaced by galena or as exsolutions within the sphalerite. The exsolutions occur either along pre-existing microfractures, or are aligned parallel to margins of sphalerites. They become finer grained from the center to the margin of the sphalerite (Figure 6.9). The shape of the exsolutions are ellipsoid with long axis parallel to microfractures, or irregular. The anhedral coarse grained crystals generally replace the sphalerite

The pyrite occurs as anhedral to subhedral crystals. The pyrites are replaced mainly by galena and chalcopyrite along their fracture planes. They are formed in two stages. Pyrites (pyrite I) observed in the hematite zone are the products of early generation stages, but those (pyrite II) observed in sphalerite zone are the products of the late generation stage. Pyrite II is subhedral to euhedral and coarse grained But pyrite I is relatively finer grained, and anhedral and are replaced by hematites, however pyrite II is replaced by chalcopyrites.

Magnetite occurs as fine to medium grained masses replacing gangue minerals, and that are replaced by galena, sphalerite and hematite. It is gray to dull

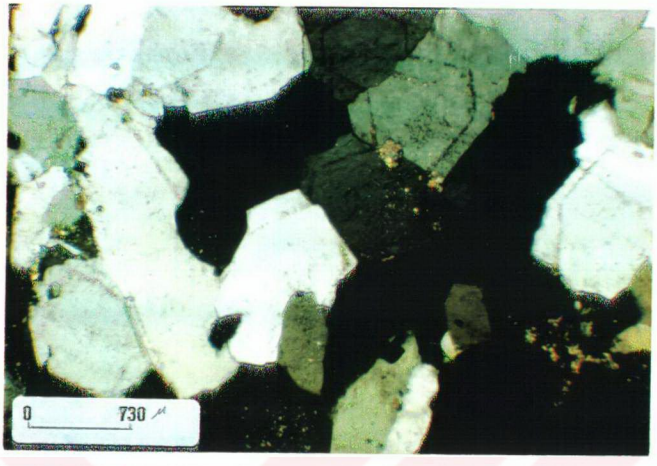

Figure 6.8. Photomicrograph showing impurities within subhedral quartz crystals

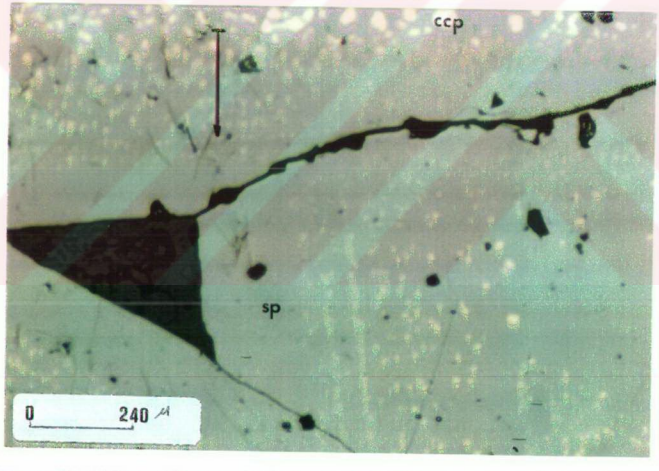

Figure 6.9. Photomicrograph displaying the decrease in grain size of the chalcopyrite (ccp) exsolutions from the margin to center of sphalerite (sp) (arrow indicates the direction from margin to center)

gray in color with low reflectance. They are locally observed as unreplaced islands within sphalerite (Figure 6.10). The contacts with the galena is characterized by a bluish tint.

Hematite occurs as radiating subparallel crystals. It is generally medium to coarse grained. The hematites replace the pyrite I and pyrrhotite, but they are replaced by sphalerite. The hematites may occur in pyrite-hematite, sphalerite and hematite zones. Hematites are rare in the first two zones, but they are commonly observed in hematite zone. In this zone they are radiated, and are associated also with sphalerite and galena. They are rarely associated with magnetites, but they replace the magnetites where both are observed.

The pyrrhotite is very rare, and is observed only within the sphalerite zone. It occurs as very fine grained minerals replaced by hematite, sphalerite and galena. It is moderately anisotropic, and shows magnetic properties.

6.2.2. Barajdoğusu occurrence

The Barajdoğusu occurrence is characterized by the mineral assemblage of the garnet-pyroxene and epidote skarns. Both skarn types are mineralized, however their ore mineral parageneses are different. The garnet-pyroxene skarns are characterized by garnet and clinopyroxene as major constituents with subordinate epidote, tremolite and calcite. The characteristic ore minerals are magnetite and hematite. However, the epidote skarns are characterized mainly by epidotes and wollastonite, with altered clinopyroxene, tremolite, calcite, quartz, galena, sphalerite, and chalcopyrite. The sulfide mineral assemblage replaces the epidote skarn assemblage.

Garnet in the garnet-pyroxene skarns is of two types, as very coarse grained (larger than 1 cm), anhedral crystals, and as medium to coarse grained euhedral to subhedral crystals (Figure 6.11). The anhedral garnets are not zoned, and are isotropic. They are replaced by clinopyroxene, epidote and calcite. The euhedral to subhedral garnets are fractured. The abrupt truncation of garnet euhedra by clinopyroxene crystals (Figure 6.12) provides evidence for the replacement by pyroxenes; these are also replaced by epidote and calcite. In contrast to the anhedral varieties, they show oscillatory zoning with strong optical anomalies. Similar to other garnets in the garnet-pyroxene skarn containing occurrences, the zoning begins with a

light colored thin garnet zone over a darker euhedral garnet core. The zoning tend to be symmetrical with respect to microfractures (Figure 6.13) and hence their growth seem to be controlled by fracturing. The number of zones forming the oscillatory zoning ranges between 2 to 46. The contacts between individual zones are very clear. The thickness of zones are generally less than a millimeter. Locally, a series of very thin alternations of dark and light colored bands (Figure 6.12 and 6.11) are observed between two dark colored zones. This structure is termed as striation (Jamtveit et al. 1993), and is used to understand how fast the physicochemical conditions of the hydrothermal fluids changed during the skarnization. These kinds of structures can only be observed in hydrothermal systems where the physicochemical conditions of the hydrothermal fluids changed rapidly. The planar structure of garnets changes gradually into non-planar structures called cellular morphology (Jamtveit et al., 1993) (Figure 6.14) towards the margins of garnets and end in contact with calcite or quartz. Dissolution structures (Jamtveit, et al, 1993) are also observed within the oscillatory zones (Figure 6.15) along the planar surfaces of the garnets. Locally, the morphology of the zoning may change. The pattern of zoning at individual crystals are different, they differ both in crystal shape, and thickness of bands.

Clinopyroxene occurs as colorless to greenish prismatic or columnar aggregates (Figure 6.16). It is medium to coarse grained, and subhedral to euhedral. clinopyroxenes occur either as replacing the garnets or as replaced by the epidotes and tremolite. The amount of epidote inclusions in clinopyroxenes is relatively less than that of tremolite. The ore minerals are observed as replacements or disseminations within the clinopyroxene. Some pyroxenes have well developed eight-sided crystal outlines, and they have optical properties resembling those of diopside.

Tremolite occurs as very fine grained fibrous to columnar aggregates. It is usually associated with clinopyroxene.

Wollastonite occurs typically as colorless radiating crystals. It is fine to medium grained. Wollastonites are associated with ore mineralization and the iron oxides are usually observed between the radiating crystals.

Epidote occurs as medium to coarse grained euhedral aggregates closely associated with clinopyroxene and garnet. It is pale green in color, weakly pleochroic, and shows bluish to red interference colors. Epidotes are present either in the garnet-

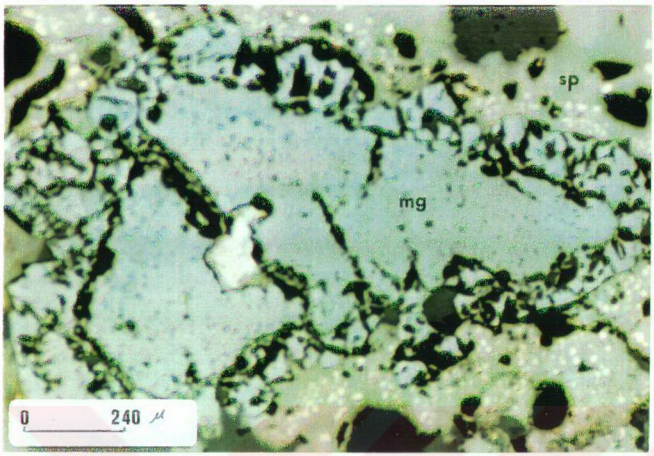

Figure 6.10. Photomicrograph displaying the unreplaced islands of magnetite (mg) in sphalerite (sp).

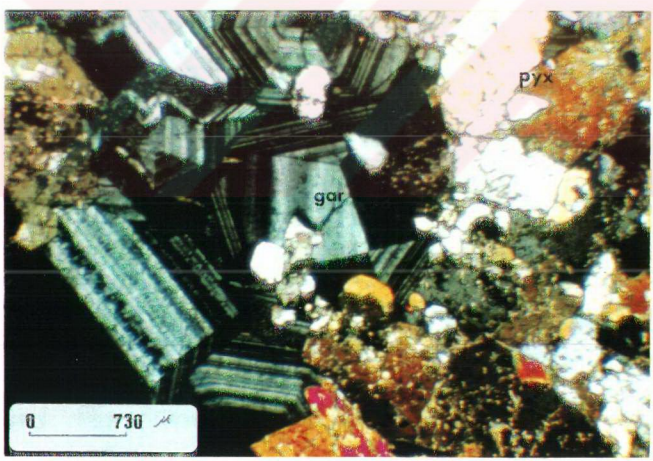

Figure 6.11. Photomicrograph displaying euhedral to subhedral garnets (gar) that show oscillatory zoning (pyx: pyroxene)

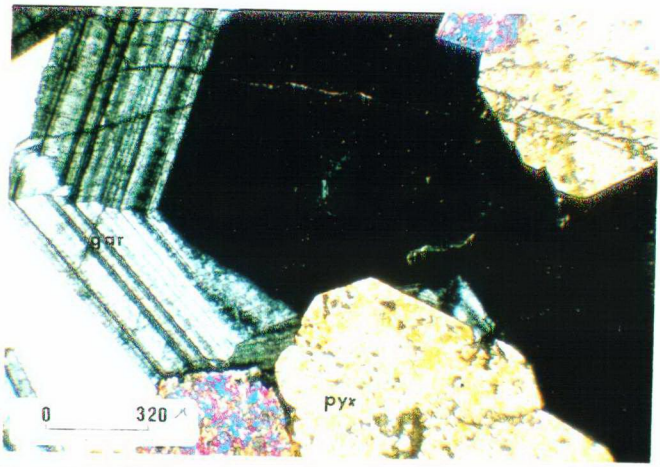

Figure 6.12 Photomicrograph showing the replacement of zoned garnets (gar) by clinopyroxene (pyx)

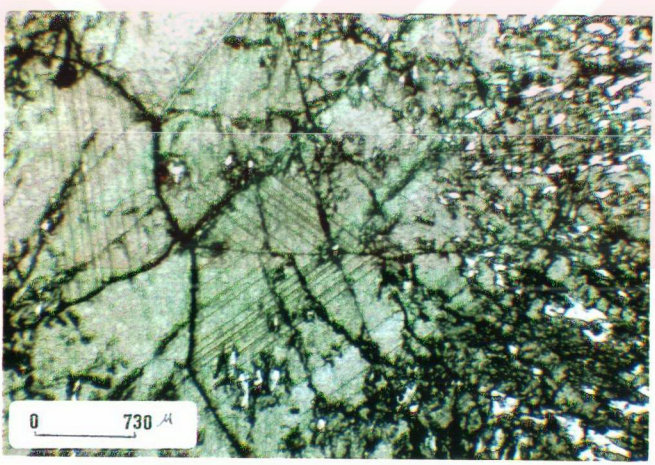

Figure 6.13. The photomicrograph showing the symmetrical development of oscillatory zones with respect to a microfracture zone.

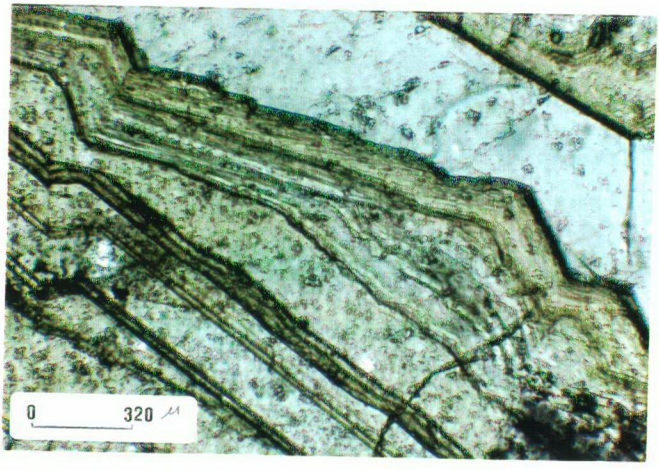

Figure 6.14. Photomicrograph showing transition from planar to cellular structure in zoned garnet

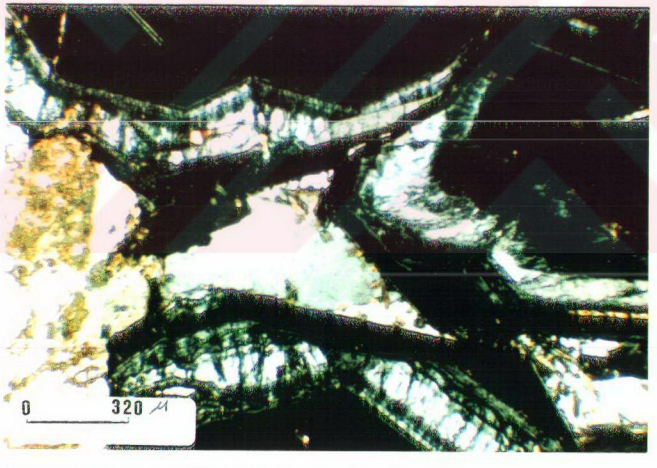

Figure 6.15. Photomicrograph showing the dissolution structures within the osciliatory zones

pyroxene skarns, or in the epidote skarns. Epidotes observed in the garnet-pyroxene skarns are fine to medium grained. They are observed along the fracture planes and/or margins of garnets. This type is not associated with mineralization. They replace garnet and clinopyroxene. However, those observed in the epidote skarns are medium to coarse grained. Their amount tend to increase where the pyroxenes are the major constituents. These completely replace the pyroxenes, and are associated with the mineralization. In these skarns they are replaced by quartz and calcite.

Calcite occurs as medium to coarse grained crystals. It is subhedral to euhedral and shows well developed rhombohedral cleavages. It is of two types as primary (those inherited from marbles) and secondary (those formed during the skarnization). The primary calcites are observed as coarse grained, and recrystallized crystals. They are replaced by the skarn mineral assemblage. They are separated from the calc-silicate assemblage with sharp contacts. The secondary calcites are fine to coarse grained mostly formed by the alteration of clinopyroxene and garnet. They may also show rhombohedral cleavages, but they are mostly observed as anhedral crystals. Some are replaced by quartz crystals.

The quartz is very rare, and occurs as fine to medium grained, subhedral to anhedral crystals. The fine grained quartz crystals are usually associated with secondary calcites. However, the medium grained constituents are associated with ore minerals.

The sphalerite is the major ore mineral constituent of the Barajdoğusu occurrence. It occurs as gray colored, anhedral crystals in polished sections. It contains numerous chalcopyrite exsolutions. The exsolutions are randomly dispersed rows of blebs and rods in the sphalerite. It also contains small inclusions of galena. Sphalerites show dark brown to dark red internal reflections are termed as heterogeneous sphalerite based on the classification by Picot and Johan (1982). They commonly replace calcite, and the mineralization is associated with calcite. They are observed together with coarse grained and recrystallized calcites.

Galena occurs as medium to coarse grained crystals with high reflectance. It is associated with pyrite, chalcopyrite and sphalerite. It replaces magnetite, hematite,

and sphalerite. It contains numerous triangular pits. Galenas locally contain unreplaced islands of sphalerite.

Magnetite occurs as medium to coarse grained anhedral masses commonly in contact with pyrite, or as unusual radiating lath-like crystals associated with hematites (Figure 6.17). It is evident from the radiating lath-like form of the magnetites that the magnetite replaced the hematite and retained its shape, and this pseudomorph is known as specular magnetite. (Ashley, 1980; Picot and Johan, 1982) However, the opposite is also observed, and magnetite is replaced by hematite. This is known as martite texture (Figure 6.17).

Hematite is not common compared to magnetite. The hematites occur always in association with magnetite as fine to medium grained lath-like or radiating crystals. They rarely show red internal reflections. They are replaced by sphalerite and galena. Most of the hematites observed in this occurrence are those replacing magnetites. Chalcopyrite is very rare in this occurrence. It is of two types as those observed as fine grained exsolutions in the sphalerite, and those observed as medium to coarse grained anhedral masses between galena and sphalerite contacts. The second type locally replace galena.

6.2.3. Özgebaca occurrence

The Özgebaca occurrence is characterized by the presence of the endoskarns and exoskarns. The exoskarns include garnet-pyroxene and epidote skarns. The mineralizations are usually observed in the exoskarns, those in the endoskarns are negligible.

The endoskarns represent the skarnized granite in contact with the exoskarns of the Özgebaca occurrence. The endoskarns are not widespread, and they occur mainly along the margins of the granites. The mineral assemblage of the endoskarns includes quartz, orthoclase, plagioclase and biotite with calcite, garnet, clinopyroxene, epidote, fluorite, pyrite and chalcopyrite.

Orthoclases are altered mainly to sericite. It is locally altered to clay minerals probably to kaolinite. Plagioclases occur as polysynthetically twinned and zoned crystals. Sericitization is very diagnostic at the central parts of the polysynthetically twinned plagioclase, and between the zones of zoned plagioclases. Epidotes are

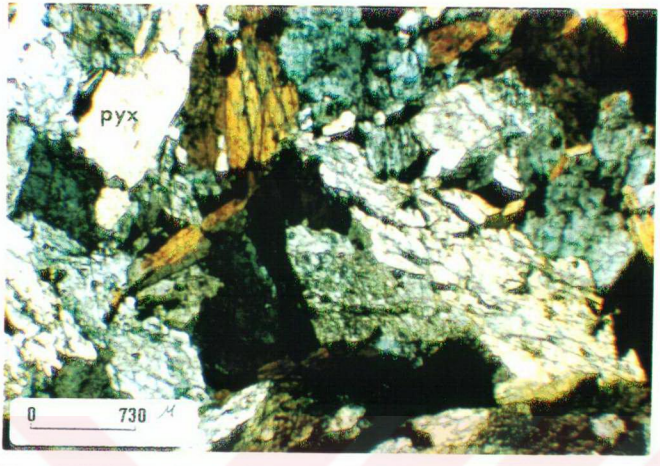

Figure 6.16. Photomicrograph showing the columnar aggregates of pyroxenes (pyx)

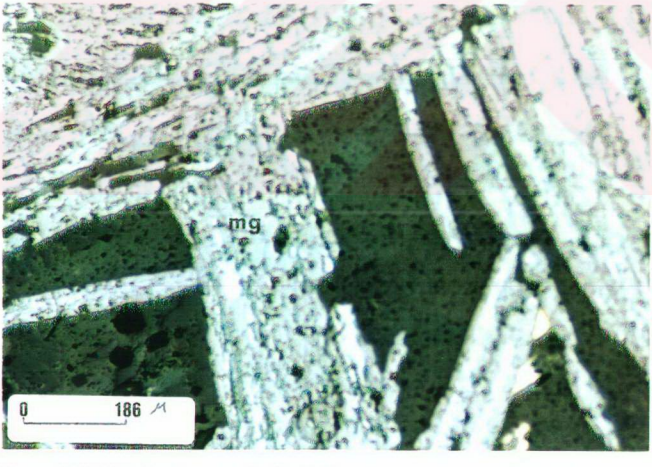

Figure 6.17. Photomicrograph displaying specular magnetite (mg)

observed as patches on both types of plagioclases, commonly along the margins. The association of sericite with plagioclases and orthoclases indicate the addition of potassium to the plagioclases, and leaching of potassium from the orthoclases, respectively. The sericitization is due to hydrogen ion metasomatism in the endoskarns

Quartz is of two types as original magmatic quartz that occurs as coarse grained crystals, and as hydrothermal quartz that occurs as fine grained anhedral crystals the amount of which increases where the plagioclases are sericitized. Biotite occurs as fine to medium grained altered crystals. Biotites are almost totally converted to chlorite. Pyrite is related to chloritization, and tends to be present in places where the biotites are chloritized.

Garnet in the endoskarns is very rare, and it occurs as medium to coarse grained subhedral to euhedral crystals. The size of garnets may reach up to 1 cm. These are associated with recrystallized calcite crystals. They are veined by calcites and are replaced by clinopyroxenes. Epidotes are minor constituents of the endoskarns, and associated mainly with pyroxenes. They are the alteration products of pyroxenes and plagioclases. Fluorite is rarely observed. It occurs as purple colored, fine to medium grained anhedral crystals. They are associated always with calcite and pyrite within the calcite veins that cross-cut the endoskarns. The amount of fluorite increases where the amount of calcite and pyrite increases.

Pyrite and chalcopyrite are the characteristic ore minerals in the endoskarns. They occur as subhedral to anhedral disseminations within the calcite veins. Pyrite is observed mainly within the sericitized and chloritized endoskarns. Chalcopyrite is less abundant than pyrite and associated with pyrite.

The exoskarns are represented by garnet-pyroxene and epidote skarns. Garnet, clinopyroxene, calcite, iron-oxides are the common minerals in the garnet-pyroxene skarns. Epidote, wollastonite, calcite, quartz, and sulfides are the common minerals in the epidote skarns.

Garnets occur as medium to coarse grained subhedral to anhedral crystals. The oscillatory zoning is very limited, and only a few garnets are zoned. The zoning is observed mostly along the margins of garnets. There are also garnets that are zoned from core to rim, but they are less in amount.. Similar to other zoned garnets at other

occurrences, the zoning is controlled by microfractures. The marginal parts that show zoning are anomalous, but cores are isotropic. The garnets may locally show twinning (Figure 6.18). They are replaced by clinopyroxene, epidote, calcite and quartz. The pyroxenes truncate the oscillatory zoning abruptly. The ore minerals (mainly iron-oxide minerals) are observed commonly as replacing the garnets or within the fracture planes of garnets.

Clinopyroxene occurs as subhedral to euhedral, colorless, medium to coarse grained crystals. The optical properties of the pyroxenes resemble to those of diopsides. They are characterized by six or eight-sided euhedral crystal outlines. Most of them are altered to epidote, calcite and chlorite. They replace garnets, and the pyroxenes replacing the garnet are surrounded by a calcite rim.

Calcite is of two types as primary and secondary. The primary calcites occur as medium to coarse grained crystals with well developed rhombic cleavages. They host the calc-silicate and ore mineral assemblage of the exoskarns. They are commonly observed within the garnet-pyroxene skarns. The secondary calcites occur as fine to medium grained subhedral to anhedral crystals. They are observed within the epidote skarns as replacing the calc-silicate assemblage. In places, they replace clinopyroxene and garnet completely and only pseudomorphs of these minerals can be seen.

Epidote is fine to medium grained, and occurs as yellow colored anhedral crystals. They are formed by the alteration of garnet and clinopyroxene. They are mostly associated with pyroxenes. They are replaced by secondary calcite and quartz.

Wollastonite occurs as fine to medium grained, subhedral to anhedral fibrous crystals. It replaces quartz ,and is associated with hematites. The ore minerals are observed between the wollastonite crystals.

Quartz occurs as fine to medium grained subhedral to anhedral crystals. It is associated with hematite, calcite epidote and garnet. It replaces epidote and garnet along the pre-existing fractures, and is replaced by secondary calcite.

The Özgebaca occurrence contains iron-oxide and sulfide ore mineral assemblages. The iron-oxide minerals include magnetite and hematite. They are hosted by the garnet-pyroxene skarns, and occur as replacing the assemblage of

garnet-pyroxene skarns. The sulfide minerals include sphalerite, galena, pyrite and chalcopyrite. They replace the epidote skarns.

The sphalerite is the predominant sulfide mineral in the Özgebaca occurrence. It is gray in color and has low reflectance. It occurs as medium to coarse grained, anhedral crystals. It contains fine grained chalcopyrite exsolutions. The exsolutions are observed mainly within the pre-existing fractures, along the crystallographic directions of the sphalerite or along the margins of sphalerites. The ellipsoidal exsolutions are mostly parallel to the trend of fractures. Sphalerites are replaced by galena and chalcopyrite, and replace magnetites, and preserve them as unreplaced islands.

Galena is less than sphalerite, but it is also one of the characteristic sulfide minerals in this occurrence. It occurs as medium to coarse grained subhedral to anhedral crystals. It is bright white in color and has high reflectance. It replaces sphalerite, and is replaced by chalcopyrite.

Magnetite is one of the major iron-oxide minerals in the garnet-pyroxene skarns. It is mostly observed as replacements commonly in the assemblage of hematite, pyrite, and garnet. It occurs as anhedral massive and/or radiating laths associated with hematite. Magnetites retain the shapes of hematites during the replacement of hematite (hematite I), and are termed as specular magnetite. However, the magnetite is replaced by hematite as well. Most of them occur as specular magnetite, only a few appear as massive forms. These are associated with pyrites. The martitization and specular magnetite formation is very common for all magnetites in this occurrence. Locally, the magnetite appears as fractured massive aggregates usually replaced by sphalerite and galena (Figure 6.19). The magnetite mineralization is local, and in places, it occurs as the dominant ore mineral in the garnet-pyroxene skarns. Magnetites replace pyrites (Figure 6.20), and are replaced by galena, sphalerite, and pyrite.

Hematite occurs as medium to coarse grained, radiating laths associated with magnetite. The radiating laths commonly spread out from a common center and terminate at the edge of another lath. They commonly replace the specular magnetite, and the specular magnetite is only observed along the marginal parts of the radiating laths. Hematites are often overprinted by sulfides in the epidote skarns. They are replaced by sphalerite and galena.

Chalcopyrite is of two types as fine grained exsolutions within the sphalerite or medium to coarse grained anhedral masses associated with sphalerite. Those observed as exsolutions are mostly observed within the pre-existing microfractures of sphalerite (Figure 6.21). The size of the exsolutions increases on both sides away from the microfractures (Figure 6.21). Those observed as massive, medium to coarse grained masses replace sphalerite and galena.

Pyrite occurs as fine to coarse grained, subhedral to euhedral crystals. Pyrites are of two types as early pyrite (pyrite I) and late pyrite (pyrite II) based on the relationships with other ore minerals. The early pyrites are commonly euhedral and represent those formed during the prograde stages of skarnization. These are commonly observed in the garnet-pyroxene skarns, and are replaced by magnetite and hematite. The late pyrites are usually subhedral to anhedral, and represent those formed during the retrograde stage of skarnization. They occur in the epidote skarns, and locally replace magnetite, galena and chalcopyrite.

6.3. Keskin district

The skarns in the Keskin district include garnet-pyroxene and wollastonite skarns. Garnet-clinopyroxene skarns are observed in the Karamağara occurrence, and wollastonite skarns in the Simlikurşun occurrence. The mineral assemblage of the occurrences differ depending on the type of skarn with which they are associated.

6.3.1. Karamağara occurrence

The Karamağara occurrence lies at the south of the district.. The mineral assemblage of the Karamağara occurrence includes garnet as the predominant constituent. Clinopyroxene, epidote, quartz, and calcite are subordinate. The epidotes are observed as finer grained patches within the garnets observed in this occurrence, and the epidote skarns are not present in this occurrence The ore minerals are mainly sphalerite and hematite with some chalcopyrite, galena and pyrite. The ore minerals replace the assemblage of the garnet-pyroxene skarns.

Garnet occurs as medium to coarse grained, subhedral to euhedral crystals. The medium grained varieties are usually euhedral compared to coarse grained varieties. They show oscillatory zoning. The number of alternating dark and light colored zones changes based on the size of the garnet. But in general, it ranges

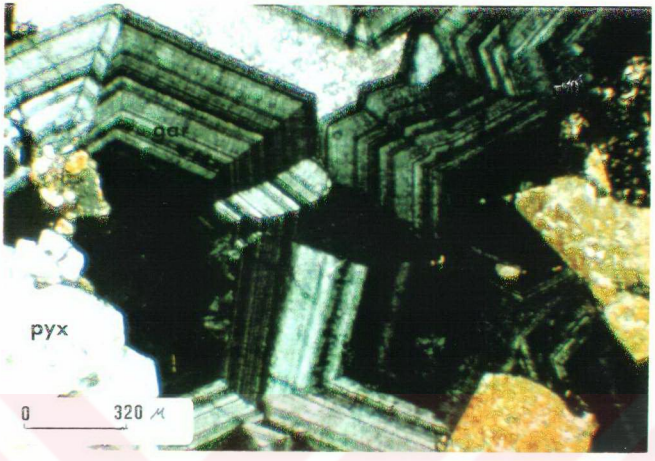

Figure 6.18. Photomicrograph showing twinning in the garnet (gar) (pyx: pyroxene).

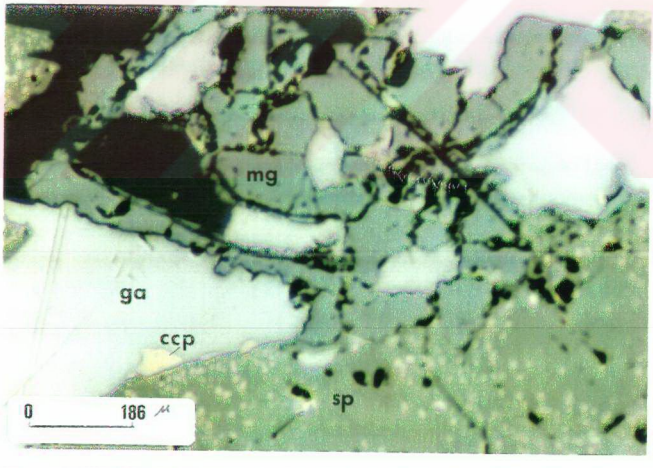

Figure 6.19. Photomicrograph showing the replacement of magnetite (mg) by galena (ga)

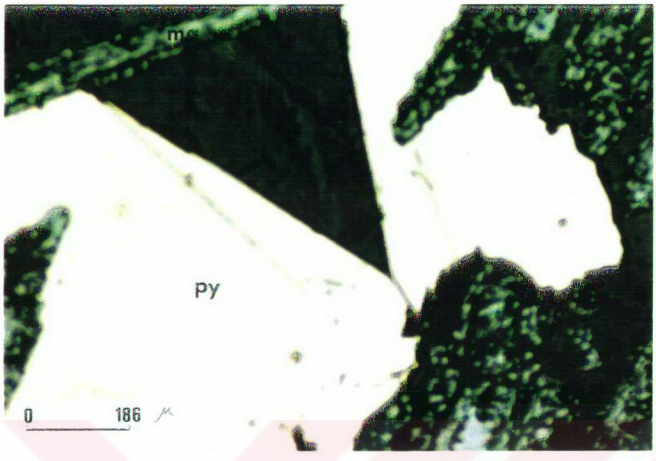

Figure 6.20. Photomicrograph displaying the replacement of pyrite (py) by specular magnetite (mg)

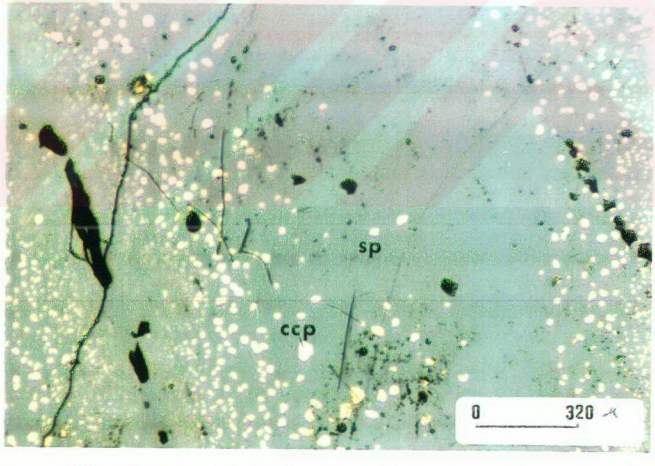

Figure 6.21. Photomicrograph of chalcopyrite (ccp) exsolutions along the pre-existing fractures in the sphalerite (sp)

between 22 to 58. The zoning is symmetrical with respect to microfractures, and hence their generation is controlled by the fracturing. Garnets are locally replaced by epidotes which are very much finer than garnets. The mineralization is restricted to narrow zones across the garnets. They are altered to calcites, and locally the calcites vein them.

Clinopyroxene is rare compared to garnet. It occurs as fine grained, subhedral to anhedral columnar aggregates. It replaces the garnet, and is observed as patches in the garnets. It is replaced by epidote and calcite. Epidote occurs as yellowish to green colored, fine grained, anhedral aggregates which are usually associated with garnet and clinopyroxene. Calcite is observed as the alteration product of garnet and pyroxenes. The calcites usually vein these minerals, and are associated with mineralization.

The ore minerals of the occurrence include hematite, sphalerite, galena chalcopyrite and pyrite. The mineralization is related to the calcitization. The occurrence is poor in galena, chalcopyrite and pyrite.

Hematite is the most striking mineral of the occurrence in the garnet-pyroxene skarns. Locally, the ore minerals are dominantly hematite associated with sphalerite. It occurs either as medium to coarse grained radiating laths and/or fibrous crystals that cross-cut each other, or anhedral masses. The radiating laths of hematite show more or less bending, or a folded structure, and the hematites that show these structures are termed as sinuous hematite (Picot and Johan, 1982) (Figure 6.22). The radiating laths are replaced by sphalerite, galena and chalcopyrite. However, the hematites observed as anhedral masses are the products of oxidation of iron-bearing minerals, they replace sphalerite, galena and chalcopyrite.

Sphalerite is the second predominant constituent of the Karamağara occurrence. It occurs as gray colored anhedral crystals. Sphalerite does not contain chalcopyrite exsolutions, but contains finer grained inclusions of galena. They show red to brown internal reflections along the fracture planes. They are replaced by galena and anhedral hematite as well.

Galena is not common compared to sphalerite. It occurs as fine to medium grained subhedral to anhedral crystals. Galenas are observed either within the

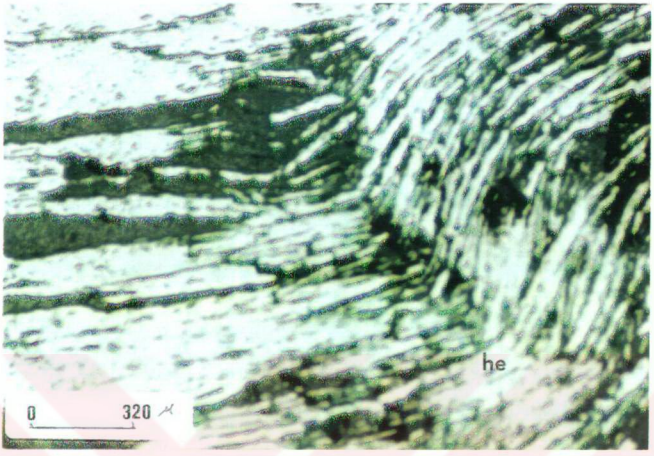

Figure 6.22. Photomicrograph showing sinuous hematite (he)

sphalerite as replacements or as disseminated grains. Some of the galenas are folded, the folds are small scale structures observed as folding of the traces of the triangular pits.

Chalcopyrite and pyrite are not common. Chalcopyrite is rarely observed, and occurs as anhedral crystals which are usually replaced by sphalerite and galena. Pyrite occurs as fine grained subhedral to euhedral crystals. It is usually associated with sphalerite, and is replaced by sphalerite and galena.

6.3.2. Simlikurşun occurrence

The Simlikurşun occurrence is at the north of the Keskin district. It is characterized by wollastonite skarns. The skarn mineralogy of the occurrence was studied using a few samples from the mine dumps, since the outcrops are destroyed. The mineral assemblage of the skarns includes wollastonite, garnet, calcite, and epidote as skarn minerals, and pyrite, sphalerite, hematite, magnetite, galena and chalcopyrite as ore minerals.

Wollastonite is the major constituent of the skarns. It occurs as medium to coarse grained sub-parallel radiating crystals (Figure 6.23). It is associated with

hematite. Wollastonites are replaced by fine grained pyrite crystals.. The ore minerals are commonly observed as replacing wollastonite.

Garnet is very rare, and it occurs as fine to medium grained subhedral to euhedral crystals. Similar to garnets in the garnet-pyroxene skarns of Karamağara occurrence, they also show oscillatory zoning. The oscillatory zones are associated with iron-oxide minerals, mostly between two oscillatory zones. They are altered to epidotes and calcites. In places, they are replaced totally by calcites and only the pseudomorph are present. They are replaced by sphalerites along the fracture planes.

Epidotes are not abundant, and are observed as fine grained patches in the garnets. They are observed only as the alteration products of garnets, and are not present elsewhere.

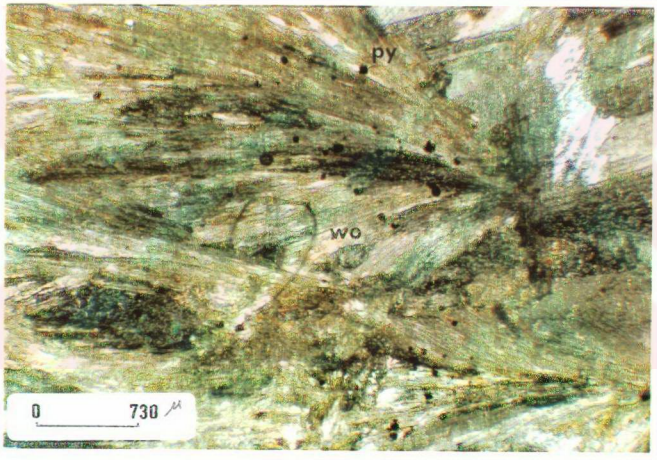

Figure 6.23. Photomicrograph showing wollastonite (wo) crystals replaced by fine grained pyrite (py) crystals

Calcite occurs as fine to medium grained anhedral crystals. They are formed by the alteration of clinopyroxenes and garnets. Sphalerite and galena mineralizations are associated with calcite.

Pyrite is the major ore mineral constituent of the Simlikurşun occurrence. It occurs as fine to medium grained anhedral crystals, or coarse grained anhedral masses. The fractures are very distinct. Pyrites are replaced by chalcopyrites along the fracture planes.

Sphalerite occurs as medium to coarse grained anhedral masses. It is gray in color and has low reflectance. It is associated with calcite and wollastonite, and is replaced by galena.

Hematite occurs as medium to coarse grained radiating laths. It shows more or less a folded structure similar to those observed in the Karamağara occurrence, and is termed as sinuous hematite. Hematites replace the specular magnetites, and the centers of the radiating laths are characterized by unreplaced islands of specular magnetite . They are cataclastically deformed, and highly fractured.

Magnetite occurs as fine to medium grained radiating laths usually replaced by hematites. It is specular magnetite with typical radiating and/or fibrous crystals. Since the magnetites are replaced by hematites, they are observed only where the hematites are observed.

Galena is not common in this occurrence, It occurs as medium to coarse grained subhedral crystals. It replaces sphalerite, and sphalerite may locally be observed as unreplaced island within the galena.

Chalcopyrite occurs as fine to medium grained anhedral crystals. It is usually associated with pyrite, and dominate in places where the pyrite is the dominant mineral.

6.4. Discussion

6.4.1. Mineral paragenesis

In the studied districts, the minerals in the skarnized marbles are formed in a sequence from earlier to later as hematite I, garnet, pyroxene, quartz I, magnetite, wollastonite, hematite II, pyrrhotite, pyrite I, epidote, tremolite, calcite, chalcopyrite+sphalerite, galena, pyrite II, quartz II, chalcopyrite, chlorite, chalcocite, and goethite. The presence of specular magnetite indicates that the hematite may have been precursor iron-oxide, and later, under more reducing conditions, it was

converted to magnetite totally (these were later replaced by hematites). This phenomenon is also mentioned in Ban Ban Zinc deposit of S. Queensland (Australia, Ashley, 1980) and skarn deposits of Yerington district (Nevada, Harris and Einaudi, 1982). The replacement of garnet-pyroxene skarn assemblages by specular magnetite indicates that garnets and pyroxenes predate the magnetite mineralization. Quartz is the next mineral in the paragenesis, and it occurs also throughout the epidote skarn formation. Wollastonite contains many fine grained pyrite crystals in it, and radiating laths of hematites between the radiating crystals, thus this indicates that wollastonite is followed by hematite and pyrite. Pyrite is closely associated with pyrrhotite in these assemblages, but it is difficult to determine which one is earlier. There is no obvious replacement textures between these two minerals. Garnet-pyroxene skarn assemblages are replaced by epidote. Epidote is the next mineral, and tremolites formed after epidote. Calcite is formed by the alteration of calc-silicate minerals, it is associated with sulfide minerals. Chalcopyrite is the next mineral that coexists with pyrite and sphalerite. The relationships between sphalerite and chalcopyrite show that chalcopyrite began to form earlier than sphalerite but continued with sphalerite formation. It is evident from the unreplaced islands of sphalerite in galena that galena was formed later than sphalerite. However, it should be emphasized that galena formation took place just after the sphalerite, since these two always present together. The replacement of sphalerite and galena by chalcopyrite indicates that a new chalcopyrite formation began. The pyrite that formed during the sericitic alteration stages dominates in the assemblage and replace other minerals. This period indicates the association of later pyrite (pyrite II) with later quartz assemblage. All these were later overprinted by chlorite, so chlorite is the next mineral to form. Chalcocite and goethite represent the supergene minerals formed during the late alteration stages.

6.4.2. Skarn stages

The petrographical examinations show substantial differences in skarn stages. Although there is an overlap of stages (that is, a stage was incomplete at the onset of a new stage) the petrographic relationships indicate that the earliest stage was the replacement of initially recrystallized meta-carbonate by a garnet dominated assemblage. This stage is termed as the garnet stage. A later stage that consists

mainly of epidote and tremolite with calcite and quartz is termed as epidote stage. The stage in which Fe-sulfides (pyrrhotite and pyrite), chalcopyrite, galena and sphalerite is termed as the sulfide stage. The next stage, chlorite, calcite and quartz is termed the chlorite stage. On the other hand an apparent final stage is dominated by chalcocite and goethite is termed as supergene stage. These stages are present throughout all skarn types with variations within the stages and type of skarns.

The products of garnet stage are not abundant volumetrically compared to the products of other stages. Although it was overprinted by later stages, it is well developed along the margins of granites at Evciboyuntepe, Radarbaca, Barajdoğusu, Özgebaca, and Karamağara occurrences. It is dominated by grandite (grossular andradite) with clinopyroxene, magnetite, hematite I and II, pyrite I, primary quartz and calcite. Most of the iron-oxide minerals are also associated with the garnet stage. The fluid inclusion studies on garnets show that the homogenization temperature is about 500°C (Sağıroğlu, 1982). This temperature represents the minimum temperature of formation, so they should be formed at temperatures higher than 500°C (around 600°C, Sağıroğlu, 1982).

The epidote stage is the next stage overprinting the products of the garnet stage. The products of the epidote stage are volumetrically the most abundant compared to other stages. It is characterized by the assemblage of epidote and tremolite with calcite and quartz. The assemblage of epidote stage is present at Bayramali, Çiçeklitepe, Çukurmaden, Evciboyuntepe, Peynirliktepe and Radarbaca occurrences in the Akdağmadeni district, and at Akçakışla, Barajdoğusu and Özgebaca occurrences in the Akçakışla district. Epidote is the most common mineral that is observed at each occurrence, but tremolite is locally absent. The products of epidote stage are not observed in the Keskin district. The homogenization temperatures in the epidotes and amphiboles in this stage range from 460°C to 490°C (Sağıroğlu, 1982), and the formation temperatures were estimated as 450°C to 500°C (Sağıroğlu, 1982).

Sulfide stage is the next stage overprinting the epidote stage. The assemblage of sulfide stage occurs as replacing the epidote stage assemblage, even in places the sulfide stage assemblages crosscut the garnet stage assemblages. The sulfide stage is dominated by sphalerite and galena; pyrite II, chalcopyrite, quartz and calcite. Most

of the calcic exoskarns in Akdağmadeni, Akçakışla and Keskin districts, contain the dominant sulfide stage assemblage of sphalerite-galena-pyrite, and chalcopyrite. The precipitation of sulfides in the sulfide stage is strongly controlled by later retrograde alteration of early garnet stage assemblages (that forms the epidote skarns), mainly of clinopyroxenes, but petrographical studies showed that the epidote stage assemblages are not related to mineralization. The sulfide mineralization took place just after the epidote stage. The sulfide mineralization is associated mainly with calcite, tremolite and rarely with epidote. These minerals were formed by the alteration of pyroxenes, this means that the ore-forming processes were controlled in some way by clinopyroxene, and that the ore-forming fluid was not in equilibrium with clinopyroxene and the fluids reacted with pyroxenes to form epidote and tremolite that causing precipitation of sulfides. The sulfide minerals along the fractures of the clinopyroxenes, and epidotized and tremolitized clinopyroxenes associated with sulfide minerals support this argument. Similar observations are also mentioned in Nakatatsu Zn-Pb skarns in Japan (Shimizu and Iiyama, 1982), Central Mining district in New Mexico (Burt, 1972 in Shimizu and Iiyama, 1982), Mason Valley Mine in Nevada (Einaudi, 1977), and Yeonhwa-Ulchin skarns in South Korea (Yun and Einaudi, 1982). Garnet and clinopyroxene predate sulfide deposition in skarns. Burt (1977) proposed that these silicates may exert a chemical control on later fluids and therefore on the sulfide minerals that were formed. The experimental studies on the stability of clinopyroxene solid solutions (Gamble, 1982; Burton et. al., 1982) indicated that clinopyroxene may behave as an ideal solution with respect to Fe^{+2}- Mg^{+2} exchange that controls the clinopyroxene composition and sulfide precipitation. The zones of most abundant sulfides correlate with the zones of the most altered pyroxenes This is not unique to the skarns in the studied areas, similar observations are reported from several Pb-Zn skarns from Yeonhwa-Ulchin district, South Korea (Yun and Einaudi, 1982), Mason Valley, Nevada (Einaudi, 1977), and Central Mining district, New Mexico (Burt, 1972 in Shimizu and Iiyama, 1982). In order to emphasize the significance of pyroxene, a representative clinopyroxene alteration reaction is (Yun and Einaudi, 1982).

$$CaFeSi_2O_{6(hed.)} + 2HSO_4^- + 4H^+ \Leftrightarrow FeS + 2SiO_2 + H_2S + Ca^{+2} + 2H_2O + 4O_2 \quad (1)$$

This reaction shows that clinopyroxene is replaced by iron sulfide and quartz if ore fluids contain specified proportion of oxidized sulfur species (HSO4). A

representative reaction for deposition of sulfides from chloride complexes in the presence of reduced sulfur species is (Yun and Einaudi, 1982):

$MeCl_{2(aq)} + H_2S_{(aq)} \Leftrightarrow MeS + 2H^+ + 2Cl^-$ (2).

Reaction (2) shows that the deposition of sulfides could result from (1) an increase in the concentration of (H2S) due to reduction of sulfate (equation (1)), and (2) a increase in the concentration of Cl^- (Yun and Einaudi, 1982). An increase in the reduced sulfur is the most effective process for the deposition of sulfides (Andersen, 1973; Barnes, 1979).

The chlorite stage is observed as overprinting the products of the epidote and garnet stages. This stage is characterized by chlorite observed along the fractures of epidotes and pyroxenes. Sağıroğlu (1982) termed this stage as chlorite-epidote stage, and proposed that it is the most important stage in the sulfide mineralization. However, the presence of chlorites mainly along the fractures of epidotes, tremolites and clinopyroxenes, and rare associations with sulfide minerals indicate that the chlorite stage is not the main stage in which the sulfide mineralization took place. The homogenization temperatures in this stage range from 310°C-430°C (Sağıroğlu, 1982). Supergene stage is the last stage overprinting the earlier stages. The products of this stage are characterized by goethite and chalcocite.

6.4.3. Significance of chalcopyrite exsolutions

The sphalerite in many cases, contain chalcopyrite in the form of exsolutions. The exsolutions are commonly observed along the crystallographic directions, or along the margins of sphalerite. They are also present in the pre-existing fractures. The presence of chalcopyrite exsolutions is most probably related to compositional or structural adjustments as they cool from the temperatures of initial crystallization. In exsolution, one phase is expelled from another, often in a characteristic pattern. This form of chalcopyrite in sphalerite is termed as "chalcopyrite disease" (Craig and Vaughan, 1981) and is ascribed to exsolution on the cooling of the minerals after emplacement. However, experimental studies (Wiggins and Craig, 1980) showed that chalcopyrite will not dissolve in sphalerite in significant amounts unless the temperature is above 500°C. These data and numerous studies on Pb-Zn bearing ore deposits in volcanics and carbonates indicated that temperature dependent exsolution

alone is not adequate to explain the formation of these intergrowths. Instead, the chalcopyrite is formed by epitaxial growth during sphalerite formation, or by replacement as copper-rich fluids reacted with the sphalerite after the formation (Craig and Vaughan, 1981). Therefore, this indicates that chalcopyrite and sphalerite in the studied districts are coeval.

6.4.4. Significance of morphological instabilities and anomalies in garnets

Garnet morphology puts constraints on the garnet growth rates and emphasize the importance of growth kinetics during hydrothermal system evolution. An understanding of the processes that control the morphological characteristics of metamorphic and/or hydrothermal minerals such as garnets and pyroxenes may potentially give important information about essential parameters such as the crystal growth rates and consequently the chemical potentials of mineral forming components, and the evolution of hydrothermal system. Garnets in the studied districts form subhedral to euhedral outlines except where they are massive. They form an interlocking mosaic texture. Fracturing is common, and the minerals exhibit strong oscillatory zoning with strong anisotropy and moderate birefringence. The hydrothermal experiments (Zimmernink, 1985) showed that the anisotropism and birefringence occur in garnets of variable grossular-andradite composition, but it is not characteristic for pure end members of the series. For the development of birefringent crystals, chemical conditions with high growth rates were essential like the garnets in Santender skarn deposits in Peru (Zimmernink, 1985). The optical examination of the oscillatory zones show that many are quite narrow, and exhibit sharp contacts between the rather dark and the light colored bands. In addition, the light colored bands oscillate with very thin dark colored bands giving rise to a complex, non-periodic, fluctuating zonation patterns. The zonal fluctuation may be explained by the cyclical variations in the composition of the hydrothermal solutions controlled probably by hydrofracturing. This would suggest that the zoning is externally controlled, and initiated by the onset of hydrofracturing in the skarn hydrothermal system that caused rapid crystal growth and/or rapid changes of composition in the hydrothermal solutions. Lessing and Standish (1973) showed that similar parameters controlled the garnet zonation at Crested Butte skarns in Colorado.

The euhedral garnet crystals in the recrystallized carbonate-rich rocks of the studied areas frequently display spectacular, oscillatory zonation patterns normal to the crystal surfaces. These garnets, occasionally display morphological changes from regular planar to non-planar surfaces. As it was described in the petrographical examination of garnets (section 6.2.4., 6.2.7, and 6.3.2.) of this study, the garnet morphology exhibits some instabilities such as transition from planar surface to cellular structures (Figure 6.14), and dissolution structures (Figure 6.15). Planar surfaces are characterized by the regular sequentially developed facets. Figure 6.14 display both chemical zonation patterns and growth morphologies outlined by the zonation patterns. It also shows the typical hopper-morphology (Figure 6.24) (as defined by Jamtveit and Andersen, 1992; Jamtveit et al., 1993) of fresh skarn garnets with breakdown of central dodecahedral crystal surface to a cellular structure. Figures 6.14 and 6.15 clearly show a transition from a planar to a cellular morphology. The cellular morphology of the garnet is characterized by the surface-parallel striations (Figure 6.11) caused by the oscillations in the chemical composition, which emphasize that the cellular surface is a growth phenomenon rather than a resorption/dissolution controlled feature (Jamtveit and Andersen, 1992) usually following the planar structures at the edges. Figure 6.15 shows the dissolution structures between two individual light colored bands indicating increasing development of new garnet faces.

In general, the garnet growth starts with the dodecahedral crystal shape with planar structures during the hopper stage (Jamtveit and Andersen, 1992). The reason why the cellular surface developed at crystal surfaces simultaneously with nearly planar surfaces at the edges may be that the transition from a dodecahedral crystal to the more spherical ikositetrahedron, would require more rapid addition of material (and thus much more rapid growth rate) to the central parts of the crystal surfaces relative to the edges and apexes (Jamtveit et al., 1993). In similar manner, well defined morphological transitions from planar to cellular structures in the garnets of the studied area especially in the Barajdoğusu, Özgebaca, and to some extent Karamağara occurrences suggest increasing growth rate with time. Thus, the increase in growth rate for these garnets may well have been associated with the sudden changes in the composition of garnets. The increase in the growth rate would enable rapid mineral formation that may cause the clogging of the hydrothermal system leading to hydrofracturing. The consequences of high growth rate result in many changes in the

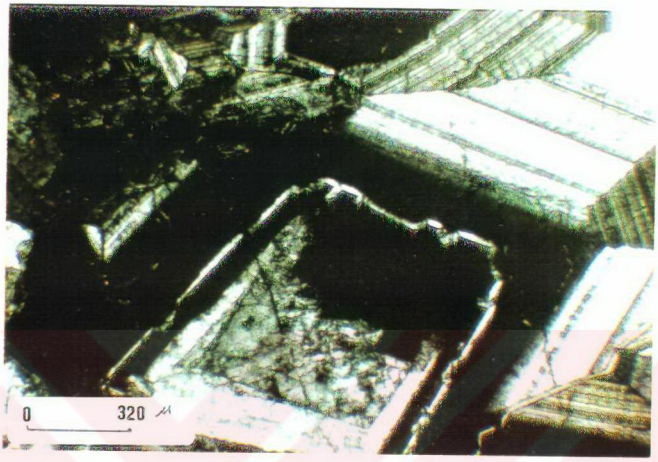

Figure 6.24. Photomicrograph showing hopper-like morphology of garnets.

hydrothermal system, and this strongly affects the chemical potentials of the garnet forming components in the system such as periodic changes in the oxygen fugacity of the system (Yardley et al., 1991). Therefore, it is notable that the hydrothermal system was under the effect of high fluid flow and high growth rate at least for the Barajdoğusu, Özgebaca and Karamağara occurrences.

Morphological transitions may potentially serve to understand the garnet growth rate and thus the rate of change in the physico-chemical variables during evolution of hydrothermal system in the garnet bearing occurrences of the studied areas. The observations presented here suggest that the garnets experienced overstepping in the garnet forming reaction at some stage during their growth.

6.4.5. Constraints about epidotes and epidote skarns

The epidote skarns which consist predominantly of epidote, and minor amounts of clinopyroxene, tremolite and quartz, can be used to investigate the oxidation state

of the hydrothermal systems. Occurrences of epidote in skarn deposits might be a rough indicator of the oxidation state of the hydrothermal system that formed the epidotes, because the epidote (plus quartz) has a restricted stability in oxidizing conditions as qualitatively shown in Figure 6.25. This figure illustrates that epidote is stable relatively high oxygen fugacities. Shimazaki (1980), in his studies concerning the general features of the skarn deposits related to acid magmatism in Japan, suggested that the epidote skarns in Japan could be formed under a relatively high oxidation state. He proposed that the original skarn forming fluid prevailing in the region is presumed to have been oxidizing, based on the presence of abundant epidote skarn around the deposits.

The epidote skarns are the products of retrograde skarn formation and this implies that they were under the influence of fluid flow into the skarns regardless of temperature (Figure 6.25). This could only be achieved by the superimposed permeability. The fluid flowing into the skarns is probably the meteoric water, causing the increase in the oxygen fugacity of the hydrothermal system (Jamtveit and Hervig, 1994, based on oxygen isotope studies). Therefore, the epidote skarns are said to be formed at relatively high oxidation state following the garnet stage. The high oxidation states cause the sulfur in the hydrothermal fluids to remain in the oxidized state, and sulfides can not form. This may be the reason why the products of the epidote stage are not associated with sulfide mineralization in the studied skarns. The sulfides were formed as replacing the assemblage of epidote stage during low oxidation states (sulfide stage). Therefore, Bayramali, Çukurmaden, Evciboyuntepe, Peynirliktepe occurrences (Akdağmadeni district), Akçakışla, Barajdoğusu and Özgebaca occurrences (Akçakışla district), Karamağara and Simlikurşun occurrences (Keskin

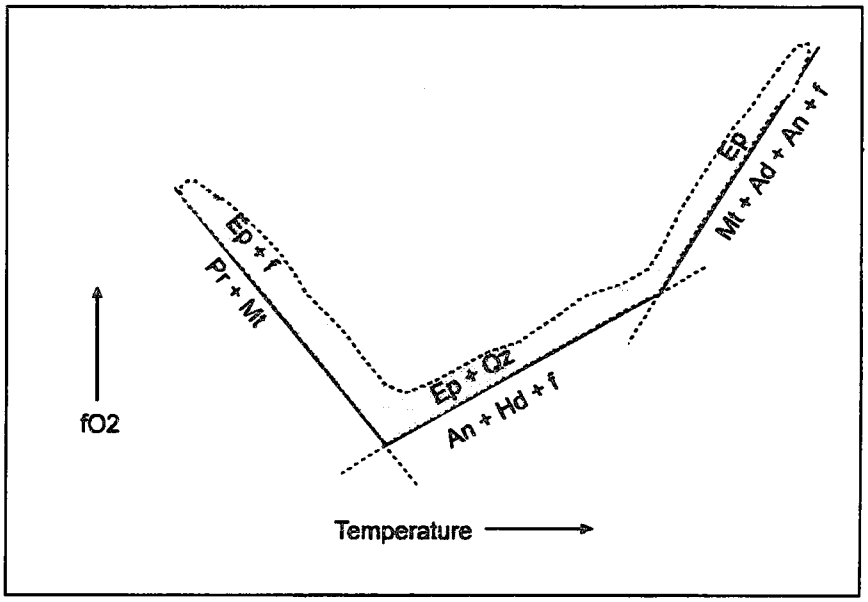

Figure 6.25. A schematic oxygen fugacity-temperature relationship of epidote (After Shimazaki, 1980). Ad: andradite, An: anorthite, Ep: epidote, Hd: hedenbergite, Mt: magnetite, Pr: prehnite, Qz: quartz, f: aqueous fluid.

CHAPTER 7

MINERAL CHEMISTRY OF SKARNS

The geochemical characteristics of the skarns in the studied districts are different in each district. The variations are caused by a number of factors, such as magma type, depth at which the pluton was emplaced, composition of host rock, oxidation potential of the hydrothermal system, and degree of meteoric water influx, or combinations of them. Since skarn minerals occur throughout the skarn system, and display significant solid solutions, their chemical compositions are the potential indicators of the complex interaction between these variables. The minerals which are most useful for the evaluation of these variables are garnets, pyroxenes and amphiboles (Meinert, 1983) since these show marked compositional variability. Amphiboles are more difficult to portray graphically because they have structural as well as compositional variations. Zaharikov (1970) was the first geologist to point out the correlation between skarn mineralogy and the skarn types based on compositional variations of minerals. His observations were extended by Burt (1972 in Shimuzu and Iiyama, 1982), Meinert et al. (1980), Einaudi et al. (1981), and Einaudi and Burt (1982) to correlate a wide variety of deposits to mineralogical variations in skarn types.

The skarn minerals studied in this section occur in calcic exoskarns resulting from the reaction of marbles with hydrothermal fluids. Garnet and pyroxene represent the earliest metasomatic products which were later overprinted by epidote skarn assemblages, and their compositions could yield insights into the geochemical conditions in the hydrothermal system. Therefore, the mineral chemistry part of this study aims to underline some of the distinctive features of garnets and pyroxenes, and to some extent epidote compositions based on electron microprobe (EMP) analyses. It also focuses on some key factors such as rate of flow of hydrothermal fluid and growth rate of minerals that may be responsible for the observed variations.

7.1. Analytical methods

The analyses were done on 19 relatively fresh samples of which 7 contain only garnets, 4 only pyroxenes and 3 only epidotes. In addition to these, 1 sample (R3) contain both pyroxenes and epidotes, and 4 samples (Ö5, B17, B20 and B23) contain both pyroxenes and garnets. The samples were selected by petrographical studies of 130 thin sections from the occurrences in the Akdağmadeni, Akçakışla and Keskin districts. The minerals were analyzed by using a Scanning Electron Microscope (JEOL JSM35) specially designed for Electron Microprobe Analysis (EMP) in the geochemistry laboratories of the Department of Earth Sciences, Keele University, England. The mineral chemical analyses were conducted according to general scheme adopted at Keele University for the preparation of rock samples prior to analysis. The Appendix 1 describes the procedures and methods applied for sample preparation and microprobe analysis.

This chapter is based on the microprobe analyses of a total of 211 points on garnet, pyroxene and epidote from the selected samples. Of these, 126 analyses are for garnets, 53 analyses for pyroxenes and 32 for epidotes. 15 samples are mainly from the garnet-pyroxene skarns in the Bayramali (1 sample), Çiçeklitepe (1 sample) Evciboyuntepe (4 samples), Radarbaca (1 sample), Barajdoğusu (3 samples), Özgebaca (4 samples) and Karamağara (1 sample), 4 from the epidote skarns in the Çiçeklitepe (1 sample), Çukurmaden (1 sample), Peynirliktepe (1 sample) and Radarbaca (1 sample). The analyses were conducted from core to rim for the garnets to detect the rimward compositional variations in individual minerals, but this method was not applied for pyroxenes and epidotes. Several lines of sections were used on a single mineral to check the presence of systematic variations on a single grain. Figure 7.1 illustrates the notations and abbreviations used in the tables

The garnet crystals with good zoning patterns were chosen for EMP analyses because this allowed to locate the approximate position of the core and rim sections of the garnets during analyses. The EMP analyses of the garnets were done on several line of sections (microprobe traverses) normal to the oscillatory zones to obtain the precise variations from core to rim on a single grain. The EMP results were then recalculated by using a software called Minpet 2.0, to determine the compositions of garnets in terms of mole % of end members (grossular (Gr), andradite (Ad), pyrope

(Py), spessartine (Sp), uvarovite (Uv) and almandine (Alm)). The composition of each point along microprobe traverses is expressed as mole % of these garnets. For example, the garnet with the composition of 3.88% grossular, 94.20% andradite, 1.00% pyrope, and 0.90% spessartine (in Table 7.1, E8-1-1-18) is denoted as $Gr_{3.88}Ad_{94.20}Py_{1.00}Sp_{0.90}$.

The pyroxenes were not analyzed by EMP from core to rim because the pyroxene morphology is not obvious as that of garnet, thus analysis points usually were chosen at the core, near the edge and halfway between the two. Similar procedures were applied for the epidote analyses. The colored spots on the altered pyroxenes were also analyzed separately to obtain the compositional differences. The results of EMP analyses were recalculated by using the software Minpet 2.0.

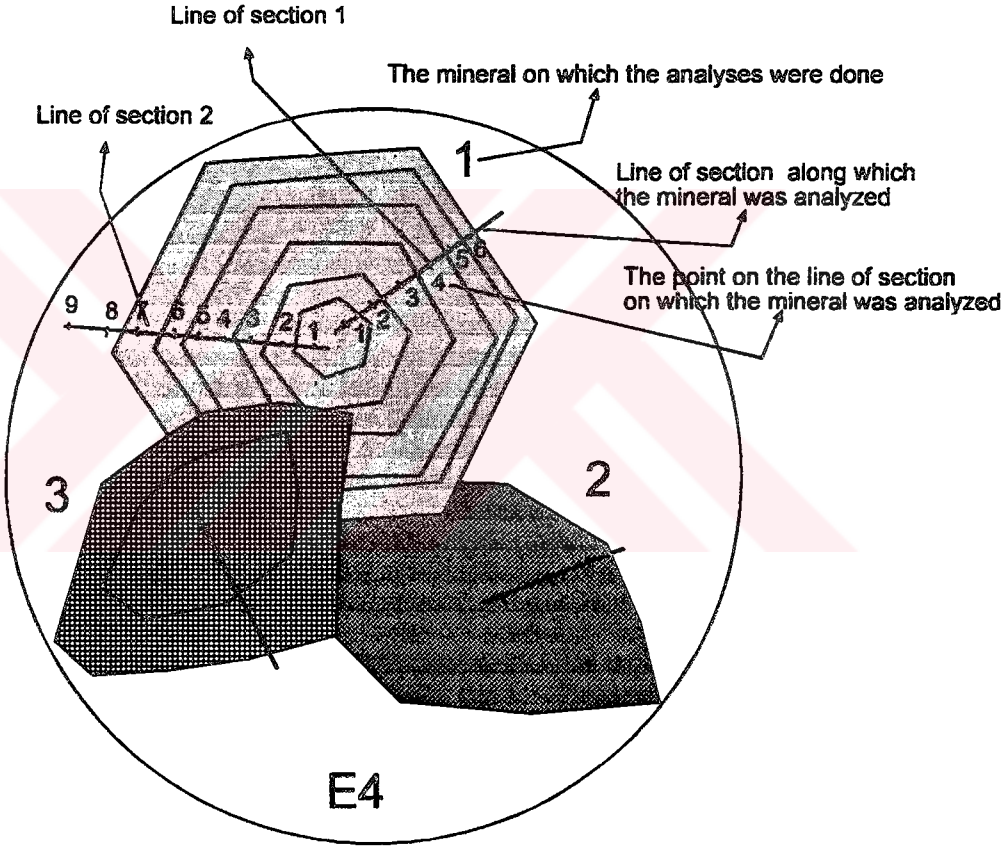

Evciboyuntepe occurrence, sample 4, mineral 1, line of section 1, point 4

Figure 7.1. The notations and abbreviations used in the tables for the mineral chemistry data.

7.2. Objectives of mineral chemistry in the skarns

The EMP studies documented the existence of compositional heterogeneity in the garnets and pyroxenes of the studied areas. As discussed in the petrography section, most of the garnets display oscillatory zoning from core to rim. Zoned crystals intrigue the geologists primarily because they contain information concerning the mineral paragenesis. Their occurrence was used as evidence for disequilibrium as well as equilibrium conditions of formation (Barton et al., 1963 in Lessing and Standish, 1973; Lessing and Standish, 1973; Nakano et al. 1989; Jamtveit, 1991; Yardley et al., 1991; Jamtveit et al., 1992;Jamtveit et al., 1993; Jamtveit et al., 1995; Polvates et al., 1996).

Garnet chemistry comprises the examination of the complex compositional zonation pattern of garnets in the studied areas. The main objectives of studying garnet chemistry is (1) to obtain compositional data on the garnets in each district, (2) to identify the garnets using nomenclature of Deer et al. (1982), and (3) to understand the possible mechanisms that formed the oscillatory zoning. This also helps to (1) determine the records of the geochemical evolution of the hydrothermal system that produced the skarns in studied areas, and (2) to understand the underlying geological processes.

Clinopyroxenes occur throughout the skarn system as prograde minerals partly or completely altered by later events, and their evolution can help to evaluate the complex interactions between the skarn forming hydrothermal fluid and the minerals. Therefore, the EMP analyses were performed not only on the fresh pyroxenes but also on the altered ones especially those altered to epidotes. Pyroxene compositions both within individual pyroxene grain and among the individual grains within a granular aggregate may provide constraints on the mechanism controlling the pyroxene composition, and on the evolution of the skarn forming fluid (Nakano, 1989; Nakano et al., 1989).

Einaudi and Burt (1982), following the studies done by Meinert (1980) and Einaudi et al. (1981) argued that the compositions of pyroxenes are strongly correlated to the dominant metal that skarns contain. They showed that johannsenitic pyroxenes

accompany Pb-Zn deposits, whereas diopsidic-ferrosalitic pyroxenes are present in Cu-Fe deposits. Many studies on skarn mineralogy is consistent with this correlation (e.g. Einaudi et al., 1981; Einaudi, 1982a; Yun and Einaudi, 1982; Meinert, 1987; Newberry et al., 1991; Nakano et al., 1994). The skarns in the studied districts are classified as Pb-Zn skarns based on their dominant metal they contain, the compositions of the pyroxenes in this study have a special importance to confirm whether the skarns in the Akdağmadeni, Akçakışla and Keskin districts are of Pb-Zn type based on their pyroxene compositions. Therefore, pyroxene microprobe data in this study serve to determine (1) the compositions of pyroxenes, and (2) identify pyroxenes using the nomenclature of Deer et al. (1982), and (3) present the Mn/Fe, and Mg/Fe ratio variations for each occurrence.

Epidotes occur throughout the skarn system as retrograde minerals replacing the earlier skarn assemblages. Their compositions may help to differentiate the skarn occurrences containing these skarns. In order to present the epidote compositions, chemical analyses of allanite, zoisite, clinozoisite, and epidote (Deer et al., 1962) was plotted on a trapezoidal diagram whose corners are occupied by Mn-Al, Mn-Fe, Fe and Al (Figure 7.2). The compositional boundaries were drawn based on the these clusters (Figure 7.2). The varieties of epidotes analyzed in this thesis, then were classified according to this diagram.

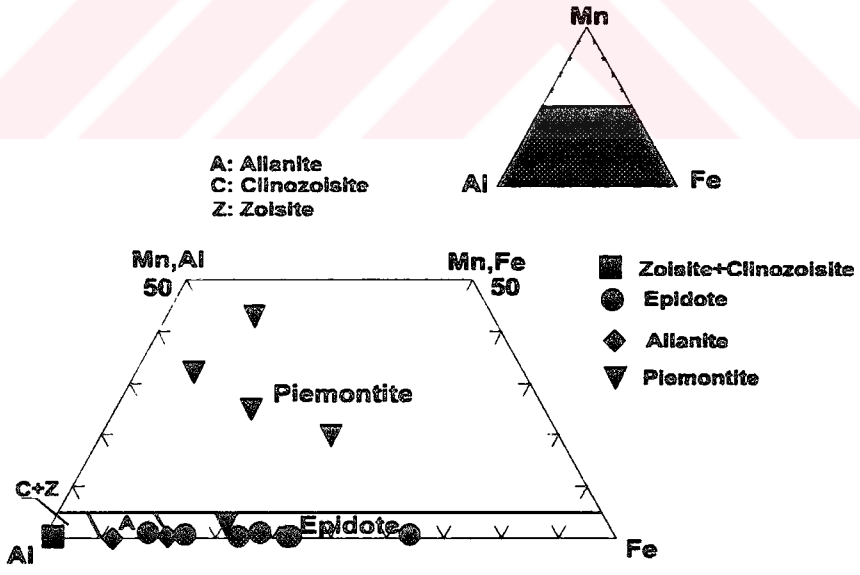

Figure 7.2. The Mn-Al, Mn-Fe, Fe and Al trapezoidal diagram showing the classification of the epidotes (Analyses from Deer et al., 1962)

7.3. Akdağmadeni district

The mineral chemistry studies in the Akdağmadeni district include the chemistry of garnet, pyroxene and epidotes. A total of 90 points were analyzed on these minerals. A total of 32 points were analyzed for garnets only in the samples selected from the Evciboyuntepe occurrence, since the garnets in the Radarbaca occurrence were almost completely overprinted by epidote skarn assemblages during retrograde alterations. A total of 26 points were analyzed for pyroxenes in the samples selected from Bayramali, Çiçeklitepe and Radarbaca occurrences. A total of 32 points were analyzed for epidotes in the samples selected from Çiçeklitepe, Çukurmaden, Peynirliktepe and Radarbaca occurrences.

7.3.1. Chemistry of garnets

The results of garnet analyses in the Akdağmadeni district are given in Table 7.1. The garnets were analyzed for SiO_2, TiO_2, Al_2O_3, $Fe_2O_{3(T)}$, MnO, MgO, and CaO. The results of EMP analyses in the garnets indicate that SiO_2 contents range from 30.67 to 40.62%. TiO_2 contents of the garnets range from 0.0 to 1.24%. Al_2O_3 compositions range from 0.0 to 18.89%. Fe_2O_3(T) contents range from 1.37 to 30.34%. MnO and MgO contents are almost equal to each other, and range from 0.0 to 2.54% and 0.0 to 2.99%, respectively. CaO contents range from 29.33 to 39.42%.

Al_2O_3 displays significant relationships with $Fe_2O_{3(T)}$, SiO2, CaO, and MnO (Figure 7.3). Al_2O_3 increases with MnO, CaO and SiO_2, however, it decreases as $Fe_2O_{3(T)}$increases (Figure 7.3). This results in the oscillations in grossular and andradite. There is an increase in $Fe_2O_{3(T)}$ contents of garnets from core to rim (Figure 7.4) except for sample E3-3-1. This is the most significant chemical variation along the analyzed garnets. This shows that Al and Fe (as total iron) are the two elements of the garnets that are substituting or replacing each other in the same system throughout the metasomatism in the Akdağmadeni district. In Figure 7.4 the x-axes represent the line of section (traverse) along which the mineral was analyzed, and the y-axes represent the Al_2O_3 and $Fe_2O_{3(T)}$ contents at the analyzed points along the line of section. In these diagrams, Al_2O_3 and $Fe_2O_{3(T)}$ appear as the mirror images of each other. In a similar

ıalysis of garnets in the Akdağmadeni district from core to rim

E3-3						E4-1					E4-1	
1	1	1	1	1	1	1	1	1	1	1	2	2
1	4	5	6	12	13	1	2	6	9	11	5	8
35.48	36.36	36.25	35.78	36.27	36.15	39.84	40.28	40.14	38.67	39.35	40.62	40.49
-	-	-	0.24	-	-	0.39	0.27	0.29	-	-	-	-
-	1.23	4.54	5.50	4.60	6.18	17.33	17.67	18.00	10.48	6.99	18.89	18.28
30.33	29.50	24.08	22.13	23.91	22.32	7.15	6.75	7.23	16.34	19.95	4.71	6.25
0.40	0.78	0.65	0.79	0.60	1.19	0.75	0.66	0.72	2.21	0.85	0.86	0.64
-	-	-	-	-	-	-	0.28	0.23	-	-	-	-
34.70	34.21	35.57	35.20	35.64	35.69	36.06	35.94	36.03	35.67	35.31	36.03	36.46
100.93	102.43	101.76	99.66	101.03	101.53	101.54	101.86	102.66	103.38	102.46	101.13	
												102.14
6.341	6.327	6.185	6.181	6.221	6.128	6.09	6.128	6.065	6.154	6.434	6.132	
-	-	-	0.032	-	-	0.045	0.032	0.033	-	-	-	6.099
-	0.253	0.914	1.12	0.931	1.235	3.123	3.168	3.207	1.966	1.347	3.362	-
4.539	4.294	3.437	3.197	3.43	3.166	0.915	0.859	0.914	2.175	2.728	0.595	3.247
-	-	-	-	-	-	0.766	0.161	-	-	0.13	0.204	0.788
4.126	3.93	3.17	2.981	3.19	2.948	0.766	0.607	0.688	1.903	2.245	0.333	0.142
0.062	0.215	0.093	0.117	0.088	0.171	0.098	0.085	0.093	0.299	0.118	0.111	0.566
-	-	-	-	-	-	-	0.064	0.053	-	-	-	0.082
6.653	-	6.504	6.156	6.551	6.483	5.907	5.858	5.833	6.084	6.186	5.829	-
												5.885
100	93.85	77.18	71.98	78.91	73.30	20.62	19.45	20.24	50.10	63.3	13.73	
-	4.28	21.25	26.07	19.77	24.18	77.75	78.05	77.32	45.21	32.77	48.40	17.92
-	1.86	1.56	1.94	1.32	2.57	1.62	1.42	0.55	4.68	1.84	1.86	84.40
-	-	-	-	-	-	-	-	0.88	-	-	-	1.86

Table 7.1. Cont.

Sample #	E4-1		E7-1			E8-1						E8-2			
Line of Sec.	2	2	1	1	1	1	1	1	1	1	1	1	1	1	1
Probe	10	12	1	11	13	1	2	8	16	18	22	1	4	6	7
SiO_2	37.97	39.02	39.33	39.63	39.88	39.75	40.06	38.71	37.67	37.10	37.39	38.74	36.04	38.89	37.11
TiO_2	-	-	1.23	0.31	-	0.37	-	-	-	-	-	0.33	-	-	-
Al_2O_3	6.62	0.93	16.18	16.51	16.88	4.76	4.25	6.59	1.62	1.03	0.67	7.22	5.00	0.90	0.62
$Fe_2O_{3(T)}$	19.31	26.55	2.95	3.24	2.89	22.68	22.59	20.03	26.39	26.38	27.07	19.01	22.68	26.61	26.60
MnO	0.75	0.21	-	-	-	0.67	0.32	2.53	0.56	0.44	0.94	0.60	0.64	0.45	0.75
MgO	-	-	1.92	2.04	2.98	0.33	-	-	-	0.22	-	0.23	-	-	-
CaO	34.36	33.89	39.42	39.11	37.35	34.68	33.90	30.92	34.17	34.21	32.99	35.72	34.54	34.49	33.24
TOTAL	99.02	100.62	101.06	100.87	100.00	103.27	101.1	98.81	100.42	99.40	99.08	101.88	98.91	101.36	98.33
Number of cations based on 24 (O)															
Si	6.434	6.726	5.998	6.036	6.119	6.519	6.708	6.531	6.546	6.53	6.63	6.35	6.254	6.691	6.618
Ti	-	-	0.142	0.036	-	0.047	-	-	-	-	-	0.041	-	-	-
Al	1.323	0.19	2.909	2.965	3.054	0.92	0.798	1.312	0.332	0.215	0.141	1.405	1.023	0.183	0.131
Fe_T	2.737	3.829	0.377	0.426	0.383	3.112	3.164	2.827	3.835	3.948	4.104	2.606	3.292	3.829	3.967
$Fe^{+2}{}_{calc}$	0.088	0.418	-	-	-	0.287	0.563	0.571	0.092	0.059	0.211	-	-	0.255	0.146
$Fe^{+3}{}_{calc}$	2.291	2.892	0.333	0.366	0.328	2.419	2.194	1.92	3.199	3.244	3.231	2.268	2.829	3.038	3.257
Mn	0.108	0.032	-	0.465	-	0.094	0.047	0.363	0.083	0.066	0.143	0.084	0.095	0.067	0.114
Mg	-	-	0.438	-	0.539	0.083	-	-	-	0.059	-	0.056	-	-	-
Ca	6.239	6.261	6.441	6.382	6.148	6.096	6.083	5.589	6.534	6.431	6.267	6.274	6.497	6.357	6.353
End members of garnet															
Andradite	65.05	94.73	10.30	11.22	9.89	74.32	72.97	59.92	91.22	94.20	96.23	62.02	74.85	94.95	96.46
Grossular	33.28	4.72	83.34	81.98	80.08	22.86	17.67	25.59	7.49	3.88	1.54	35.74	23.66	4.01	1.77
Spessart.	1.7	0.50	-	-	-	1.32	0.69	5.55	1.27	1.00	2.22	1.31	1.45	1.03	1.76
Pyrope	-	-	6.36	6.79	10.11	1.49	-	-	-	0.90	-	0.88	-	-	-

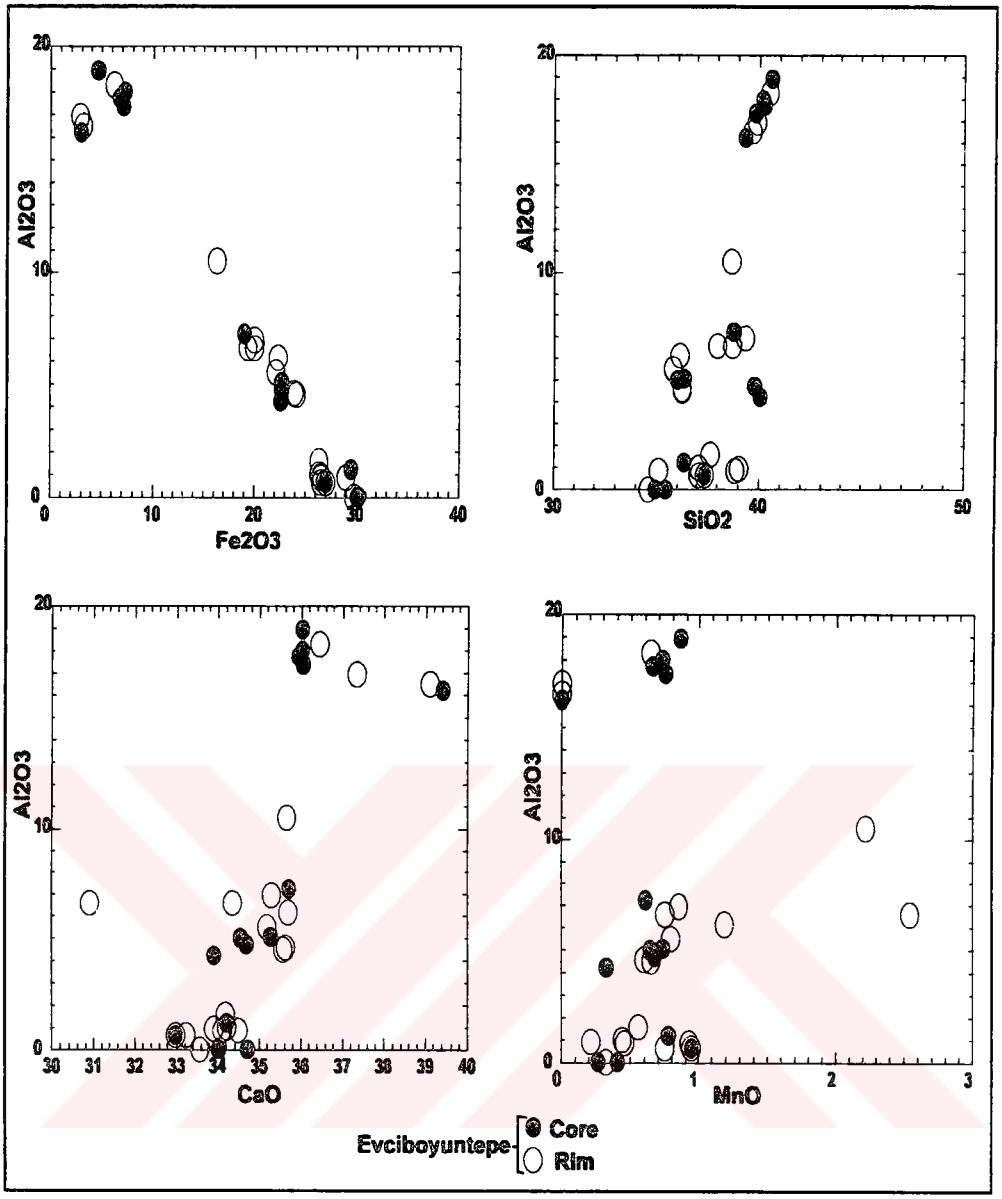

Figure 7.3. The relationships of Al_2O_3 contents with $Fe_2O_{3(T)}$, SiO_2, CaO and MnO contents in the garnets.

other. In a similar manner, the positive relationships of Al_2O_3 with MnO, CaO, and SiO_2 indicate that MnO, CaO, and SiO2 decrease from core to rim in the garnets. $Fe_2O_{3(T)}$ displays additional significant relationships with CaO, MnO, SiO_2 ,and MgO in the garnets. $Fe_2O_{3(T)}$ content decreases with the increase in MgO, MnO, SiO_2, and CaO contents (Figure 7.5).

The similar phenomena are also observed in many skarn districts in the world, such as Darwin Pb-Zn-Ag skarn, California-USA (Newberry et al., 1991), Ban Ban zinc skarn, Queensland-Australia (Ashley, 1980), Santender skarn deposit, Peru, (Zimmermink, 1985), Skarn deposits in Oslo Rift, Norway (Jamtveit et al., 1993;1994), Crested Butte skarns, Colorado-USA (Lessing and Standish, 1973) Chichibu Mine, Central Japan (Nakano et al., 1989), Turgai garnet skarns, Russia (Polvates et al., 1996). They explain this relationship is due to the exchange between Al^{+3} and Fe^{+3} in the garnet composition during metasomatic processes leading to skarn formation. Lessing and Standish (1973) proposed in their studies in the Crested Butte, Colorado-USA that this exchange is strongly controlled by the oxygen fugacity of the entire skarn system. Since Ca is a component supplied by the wall rocks, the rimward depletion (Figure 7.3) of CaO (except for E3-3-1)indicate that the garnets become less calcic from core to rim most probably due to decreasing interactions between hydrothermal fluids and wall rocks. Therefore, it is possible to say that contribution of wall rocks to the hydrothermal fluid decreases during the skarnization in which the garnets are formed.

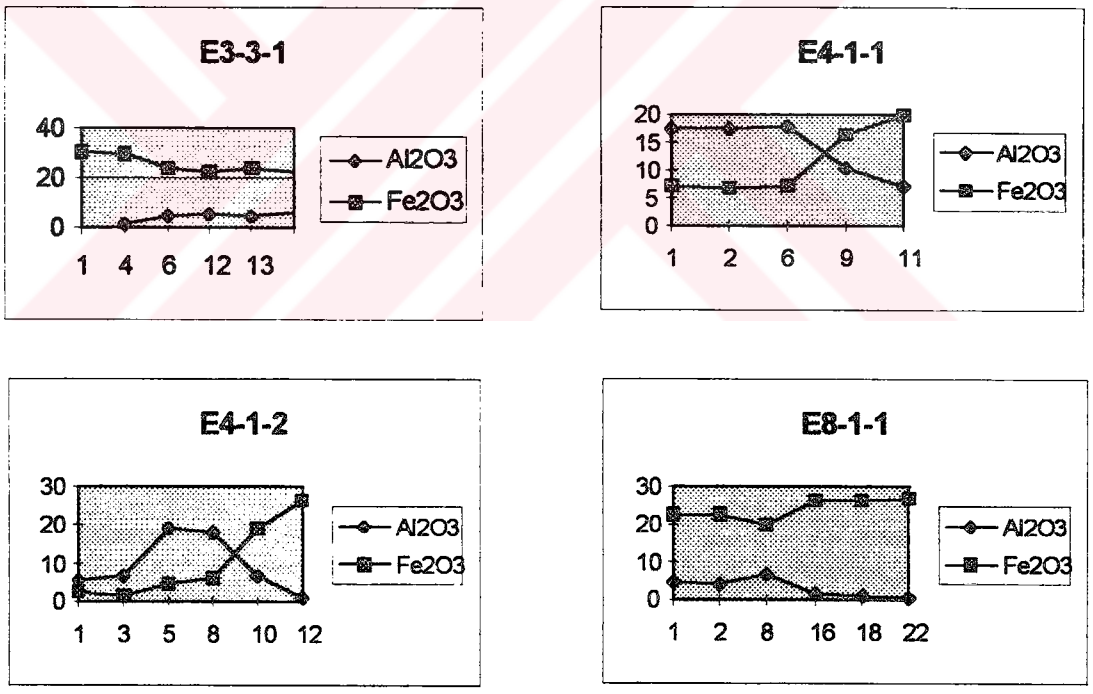

Figure 7.4. Al_2O_3 and $Fe_2O_{3(T)}$ microprobe garnet traverses from core to rim in the Akdağmadeni district

The recalculations based on major oxide data and cations were made by Minpet 2.0 using the nomenclature of Deer et al. (1982). The recalculations show that the garnets in the Akdağmadeni district contain grossular ($Ca_3Al_2(SiO_4)_3$), andradite ($Ca_3Fe_2(SiO_4)_3$), spessartine ($Mn_3Al_2(SiO_4)_3$) and pyrope ($Mg_3Al_2(SiO_4)_3$) end members. The grossular mole percent of the garnets range from 0.0 to 83.34%. The andradite mole percent of garnets range from 0.0 to 100%. The pyrope and spessartine mole percent of garnets are very low compared to andradite and grossular mole percents, and they range from 0.0 to 10.11% and 0.0 to 5.55%, respectively.

The garnets in the Akdağmadeni district are regarded as grossular-andradite (grandite) garnets, because of their high grossular-andradite contents, and low spessartine-pyrope-almandine (pyralspite) contents. In general, the garnets in the Akdağmadeni district have compositions ranging from almost pure andradite, Ad_{100} to almost pure grossular, $Gr_{83.34}Ad_{10.30}Py_{6.36}$. The compositional distribution of garnets are expressed in the ternary diagram as the proportions of their end members (grossular, andradite and pyralspite) (Figure 7.6). This figure shows that the garnet cores in the Evciboyuntepe are clustered more or less in two groups. Of these, first one is observed close to the grossular corner, and the second is observed close to the andradite corner of the diagram. Rim compositions of garnets plot close to the grossular and andradite corners of the diagram. However, most of the garnets analyzed in the rims are clustered close to the andradite corner of the diagram (Figure 7.6). This indicates that rim compositions of the garnets are usually represented by andradite-rich garnets in the Akdağmadeni district. By comparing the compositional distribution in the cores to the rims, it is possible to say that the there are oscillations between grossular and andradite contents of garnets from core to rim depending on the physico-chemical parameters that control the Al^{+3} and Fe^{+3} exchange in the hydrothermal system especially at the advanced stages of the skarnization in the Akdağmadeni district. However, it is also possible to say that the garnets become andradite-rich from core to rim (Figure 7.6) except for the sample E3-3-1. This is directly related to the rimward enrichment of $Fe_2O_{3(T)}$ contents in the garnets. Thus, oscillatory zones observed in the garnets are not only petrographical anomalies, but also chemically different zones that oscillate from core to rim.

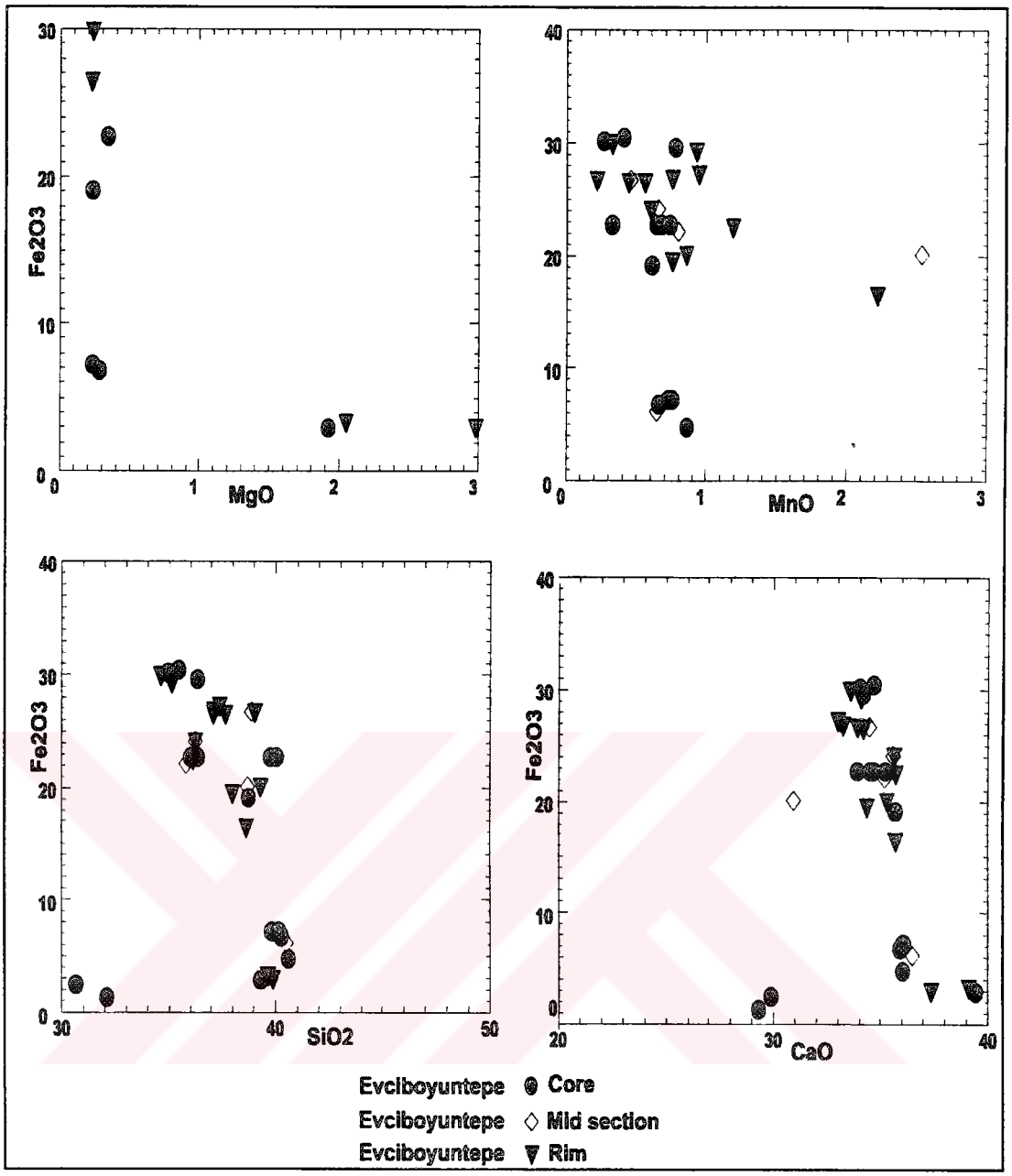

Figure 7.5. The relationships of $Fe_2O_{3(T)}$ contents with MgO, MnO, SiO2 and CaO contents in the garnets

The examination of Figure 7.7 shows that the grossular and andradite end-members of the garnets in the Akdağmadeni district is inversely related to each other. Grossular decreases as andradite increases (Figure 7.7).

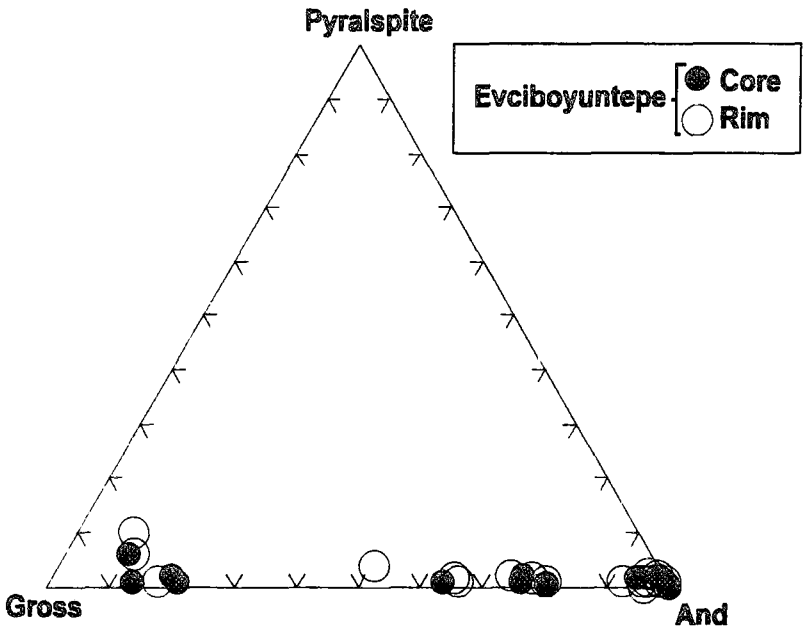

Figure 7.6. The compositional ternary variation diagram for the garnets in the Akdağmadeni district.

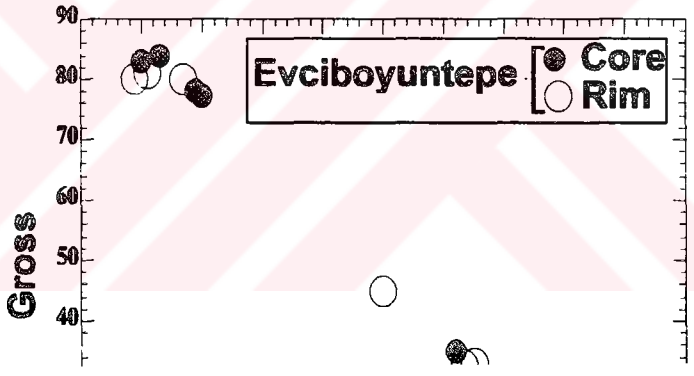

7.3.2. Chemistry of pyroxenes

The results of EMP analyses in the pyroxenes are given in Table 7.2. The pyroxenes were analyzed for SiO_2, TiO_2, Al_2O_3, $Fe_2O_{3(T)}$, MnO, MgO and CaO. The SiO_2 contents range from 39.94 to 54.24%, the lowest value observed in the Evciboyuntepe and the highest value in the Çiçeklitepe occurrence. TiO_2 contents of the pyroxenes are very low similar to those observed in several skarns in the world (Einaudi et al., 1981; Nakano et al., 1994). It is present only in the pyroxenes from the Evciboyuntepe occurrence. TiO_2 contents range from 0.63 to 0.69%. Al_2O_3 contents of the pyroxenes range from 0.0 to 19.09%, the lowest value observed in the Bayramali, and the highest in the Evciboyuntepe occurrence. $Fe_2O_{3(T)}$ contents have a range of 2.69 to 12.89%, the lowest value observed in the Evciboyuntepe and the highest in the Bayramali occurrence (Table 7.2). MnO contents of pyroxenes range from 0.0 to 14.47%. The lowest value is observed in the Evciboyuntepe and the highest value is observed in the Bayramali occurrence. MgO contents range from 1.88 to 12.92%, the lowest value observed in the Bayramali, and the highest in the Evciboyuntepe occurrence. CaO contents have a range of 20.10 to 39.61% the lowest value observed in the Bayramali and the highest in the Evciboyuntepe occurrence.

The binary plots between $Fe_2O_{3(T)}$ and other oxides are shown on Figure 7.8. The correlation matrix (Table 7.3) for the major oxides indicate that the correlation coefficient for $Fe_2O_{3(T)}$-SiO_2, $Fe_2O_{3(T)}$-MnO, $Fe_2O_{3(T)}$-CaO and $Fe_2O_{3(T)}$-MgO are -0.55, 0.58, -0.30, and -0.76, respectively.

The most striking feature of the Figure 7.8 is that the samples from different occurrences are clustered separately in the diagrams. They never show an overlapping pattern. This means that pyroxenes from these occurrences should also be clustered separately in the ternary Wo-En-Fs diagram as well.

The EMP data for the pyroxenes were recalculated in terms of wollastonite (Wo), enstatite (En) and ferrosilite (Fs) end-members using the Minpet 2.0. In general, wollastonite contents of the pyroxenes range from 46.18 to 51.52% with the lowest value observed in the Radarbaca and the highest in the Çiçeklitepe occurrence. Enstatite contents range from 6.50 to 37.85%, the lowest value in the Bayramali, and the highest in the Radarbaca occurrence (Table 7.2). Ferrosilite contents of the

Table 7.2. The results of EMP analyses of pyroxenes in the Akdağmadeni district

Sample#	Çİ8-2				Çİ8-2				Çİ8-2			Ba1-2	
Line of S.	1	1	1	1	2	2	2	2	3	3	3	1	1
Probe #	1	3	4	5	2	3	4	5	1	3	6	1	2
SiO_2	53.03	53.34	52.47	53.72	52.53	53.20	54.24	52.50	53.30	52.40	53.31	50.42	50.00
Al2O3	0.56	0.46	0.25	0.66	0.40	-	0.74	.0.52	0.54	0.30	0.64	1.08	0.29
$Fe_2O_{3(T)}$	8.04	8.90	9.97	10.80	11.04	10.31	8.17	8.98	9.20	7.25	9.90	12.27	11.30
MnO	0.99	1.49	0.90	0.41	0.35	0.57	1.49	0.52	0.51	1.12	0.50	11.10	12.14
MgO	12.28	11.63	11.06	11.15	10.39	11.23	12.35	12.12	11.88	12.33	10.87	3.30	3.61
CaO	24.40	25.96	24.23	25.04	24.29	24.66	24.52	23.46	23.67	24.21	24.71	21.07	21.72
TOTAL	99.30	101.72	98.91	101.78	99.00	99.97	101.51	98.63	99.10	97.61	99.93	99.26	99.48
Number of cations based on 6 (O)													
Si	1.994	1.972	1.997	1.991	2	2.002	1.993	0.1995	2.005	1.996	2.003	2.004	2.004
Al	0.025	0.02	0.011	0.029	0.018	-	0.032	0.023	0.024	0.014	0.028	0.051	0.014
Fe_T	0.253	0.275	0.317	0.335	0.351	0.325	0.251	0.285	0.289	0.237	0.311	0.408	0.379
Mn	0.032	0.047	0.027	0.013	0.012	0.018	0.047	0.017	0.016	0.036	0.016	0.374	0.412
Mg	0.688	0.641	0.628	0.616	0.59	0.63	0.677	0.687	0.667	0.701	0.609	0.196	0.216
Ca	0.983	1.029	0.988	0.995	0.991	0.995	0.965	0.955	0.954	0.989	0.995	0.898	0.933
Mg/Fe	2.71	2.33	1.98	1.83	2.82	1.93	2.69	2.41	2.3	2.95	2.21	0.48	0.56
Mn/Fe	0.13	0.17	0.08	0.03	0.03	0.05	0.18	0.05	0.05	0.15	0.05	0.33	1.08
End-members													
Wollast.	50.25	51.63	50.35	50.77	51.68	50.54	49.76	49.01	49.60	50.71	51.52	47.86	48.09
Enstat.	35.19	32.19	31.98	31.46	29.91	32.03	34.89	35.49	34.65	32.69	31.52	10.45	11.12
Ferrosil.	14.56	16.18	17.67	17.77	18.41	17.43	15.35	15.50	15.75	17.00	16.96	41.69	40.79

Table 7.2. Cont.

Sample#	Ba-1-2	Ba1-2								R3-2			
Line of S.	1	2	2	2	2	3	3	3	4	2	2	2	2
Probe #	4	1	2	3	1	2	3	1	5	1	2	4	5
SiO_2	50.08	50.38	49.27	50.99	51.18	50.93	50.09	49.84	52.79	54.15	53.84	52.38	51.65
Al2O3	0.25	0.34	2.75	0.30	0.28	0.51	-	-	0.30	0.81	-	3.37	0.28
$Fe_2O_{3(T)}$	12.76	11.89	12.10	11.20	11.29	12.35	10.67	12.89	12.15	6.82	6.90	5.83	7.22
MnO	11.33	9.38	11.39	14.21	12.86	11.09	14.47	10.23	9.83	3.24	3.31	3.35	4.24
MgO	3.70	5.26	3.78	2.11	2.90	4.03	2.59	3.58	5.37	12.91	11.85	12.27	10.48
CaO	22.17	21.15	20.45	22.23	22.72	22.79	22.13	21.95	22.19	22.67	23.45	20.83	24.46
TOTAL	100.29	98.74	99.74	101.04	101.23	101.70	99.95	98.49	103.10	100.60	99.3	99.03	98.33
Number of cations based on 6 (O)													
Si	1.993	2.008	1.956	2.022	2.015	1.991	2.008	2.009	2.012	2.008	2.017	1.963	1.988
Al	0.012	0.016	0.128	0.014	0.013	0.024			0.013	0.036		0.149	0.013
Fe_T	0.425	0.396	0.402	0.371	0.372	0.404	0.358	0.435	0.388	0.212	0.216	0.183	0.232
Mn	0.382	0.317	0.383	0.474	0.429	0.367	0.492	0.349	0.318	0.102	0.105	0.107	0.138
Mg	0.22	0.903	0.224	0.125	0.17	0.235	0.155	0.215	0.305	0.714	0.664	0.686	0.601
Ca	0.946	0.027	0.87	0.945	0.959	0.955	0.951	0.948	0.906	22.674	0.941	0.836	1.008
Mg/Fe	0.52	2.30	0.55	0.33	1.15	0.58	0.43	0.49	0.79	3.36	3.07	3.74	2.6
Mn/Fe	0.89	0.8	0.95	1.27	1.15	0.9	1.37	0.80	0.82	0.48	0.48	0.58	0.59
End-members													
Wollast	47.95	46.82	46.31	49.40	49.71	48.68	48.55	48.68	47.30	47.12	48.89	46.18	50.92
Enstat.	11.15	16.20	11.92	6.50	8.82	11.99	7.91	11.05	15.94	37.35	34.40	37.85	30.35
Ferrosil.	40.90	36.98	41.77	44.10	41.47	39.33	43.54	40.27	36.76	15.35	16.71	15.97	18.73

pyroxenes range from 15.35 to 44.10%, the lowest value observed in the Radarbaca and Çiçeklitepe, and highest value in the Bayramali occurrence.

Table 7.3. The correlation matrix for the major oxides in pyroxenes from the Akdağmadeni district.

	SiO_2	Al_2O_3	Fe_2O_{3T}	MnO	MgO	CaO
SiO_2	1					
Al2O3	-0.59	1				
Fe_2O_{3T}	-0.55	-0.08	1			
MnO	-0.83	0.30	0.58	1		
MgO	0.86	-0.27	-0.76	-0.97	1	
CaO	0.77	-0.52	-0.30	-0.77	0.70	1

Pyroxenes in the Akdağmadeni district are classified as diopside and hedenbergite based on their distribution in ternary En-Fs-Wo diagram of Morimoto et al. (1988) (Figure 7.9). The clinopyroxenes from the Radarbaca and Çiçeklitepe occurrences plot in the diopside field, clinopyroxenes from the Bayramali plot completely in the hedenbergite field (Figure 7.9).

The pyroxenes that are clustered in the diopside and hedenbergite field are called Ca-pyroxenes (Morimoto et al., 1988), and are the products of diopside-hedenbergite series. They are further classified as diopside, hedenbergite and johannsenite which are the mostly occurring clinopyroxenes in the skarns. These pyroxenes are expressed by ternary proportions of their Mg-Fe-Mn contents (Einaudi et al., 1981). These are classified in a ternary diagram whose corners are occupied by Mg (diopside, Di), Fe (hedenbergite, Hd) and Mn (johannsenite, Jo) (Figure 7.10). Figure 7.10 shows that the pyroxenes from the Bayramali, Çiçeklitepe and Radarbaca occurrences are clustered in different parts of the ternary diagram. The pyroxenes from the Bayramali occurrence plot close to the johannsenite corner indicating that the pyroxenes are johannsenitic in the Bayramali occurrence. However, those from the

Çiçeklitepe and Radarbaca occurrences plot within diopsides, but those from Radarbaca occurrence have more MnO contents (Figure 7.10).

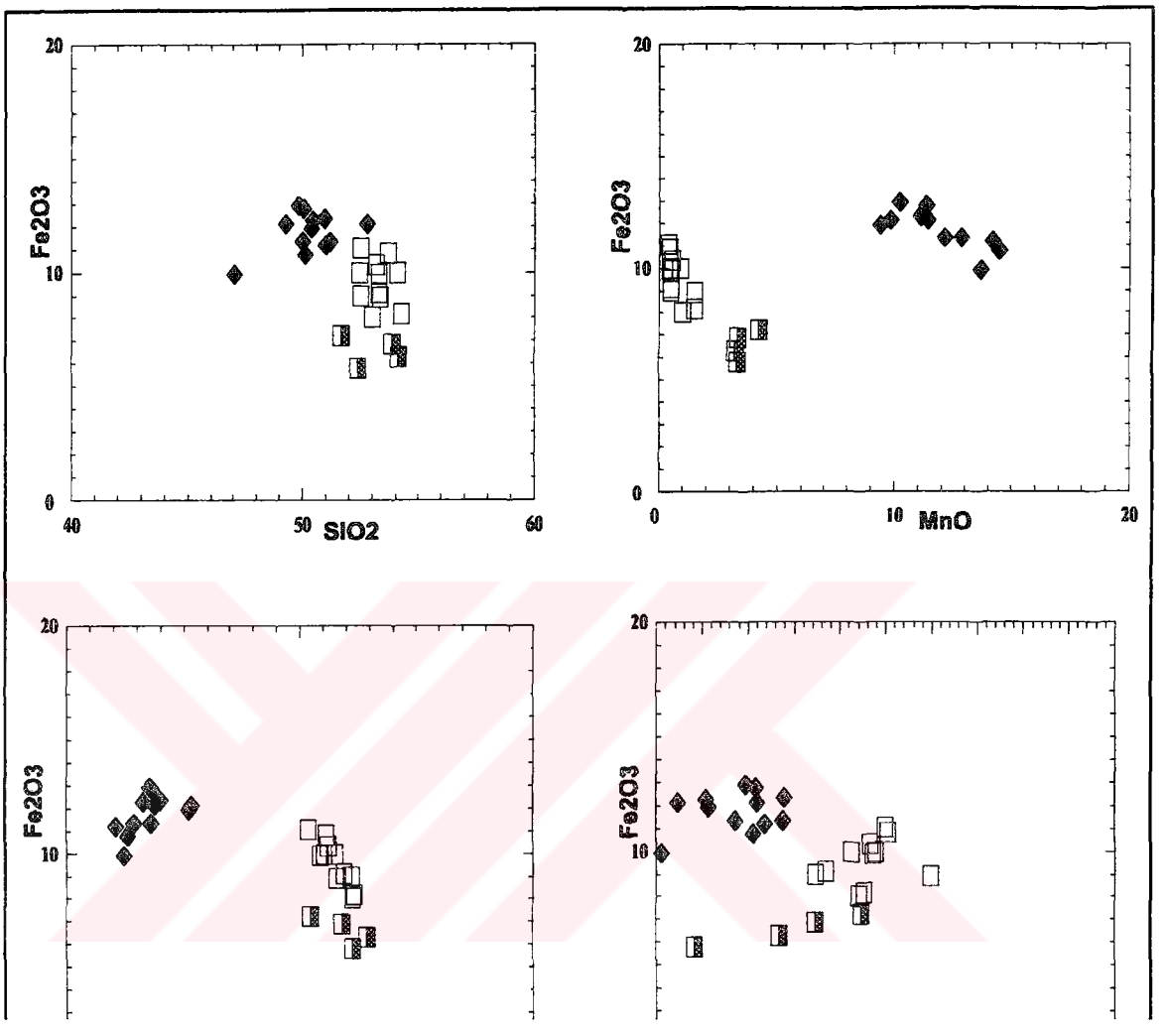

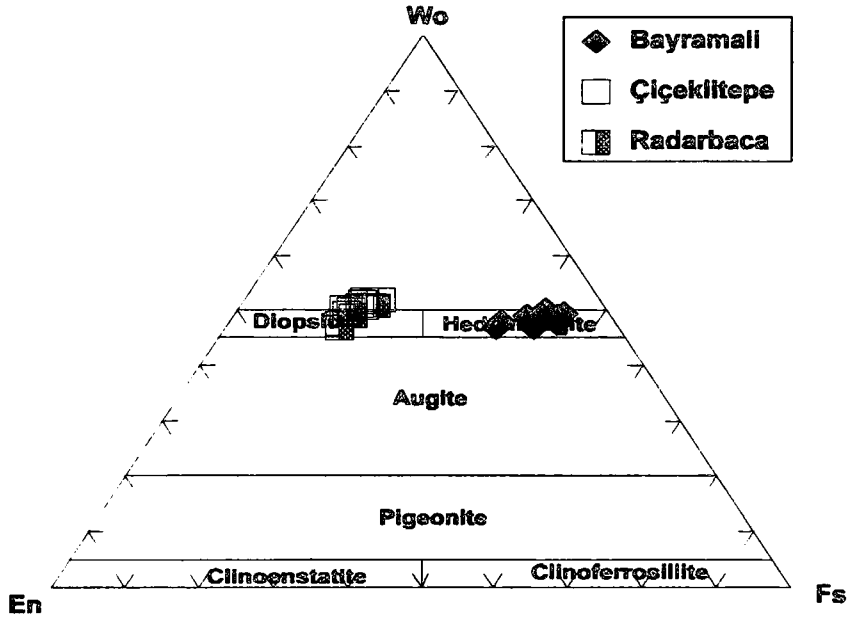

Figure 7.9. The ternary En-Fs-Wo diagram (En: Enstatite, Fs: Ferrosilite, Wo: Wollastonite, fields from Morimoto et al., 1988) showing the classification of pyroxenes in the Akdağmadeni district.

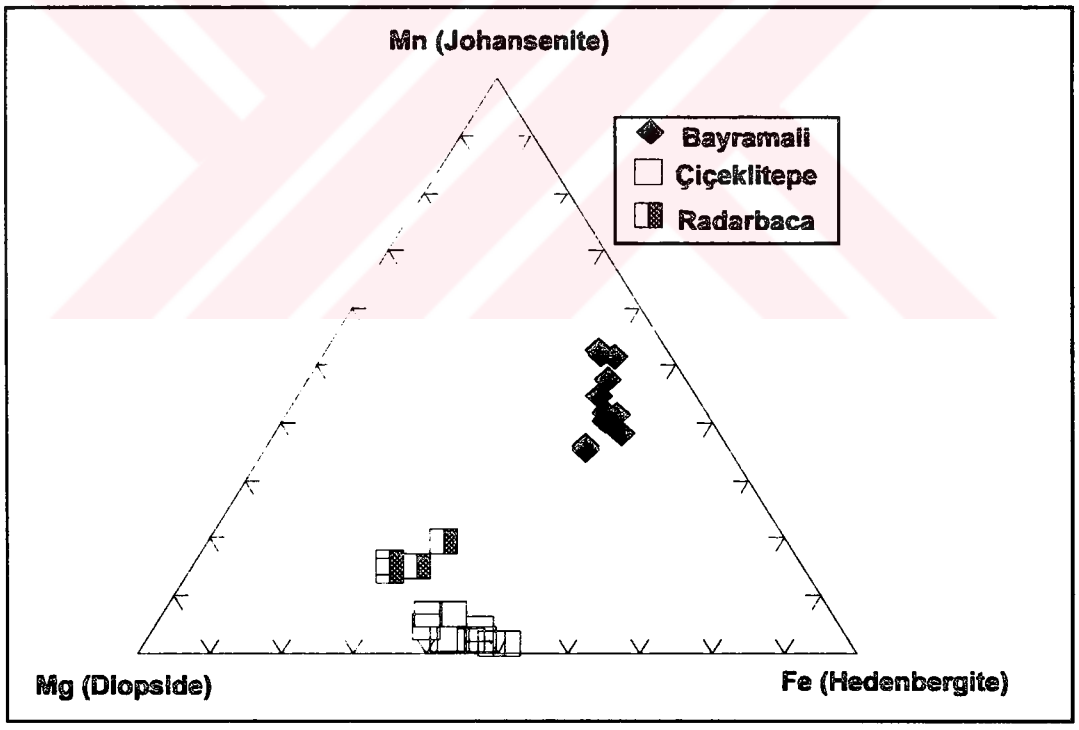

Figure 7.10. Mg-Fe-Mn ternary diagram for the classification of pyroxenes in the Akdağmadeni district.

The comparison of the distribution of the pyroxenes in the Akdağmadeni district with the pyroxenes from several skarns (Einaudi et al. 1981) shows that the pyroxenes from the Bayramali occurrence display a pattern within the distribution pattern of the pyroxenes observed in the major Zn-Pb skarns of the world (Figure 7.11). On the other hand, the pyroxenes from the Radarbaca occurrence fall within the fields of the major Zn-Pb and W-skarns in the world (Figure 7.11). The pyroxenes from the Çiçeklitepe occurrence fall within the fields of in the major Cu-, W- and Fe-skarns of the world (Figure 7.11). Therefore, it is proposed that Pb-Zn skarns in the Akdağmadeni district has also some W , Fe and Cu imprints that should be investigated in detail.

7.3.3. Chemistry of epidotes

Epidotes in the Akdağmadeni district were analyzed for SiO_2, Al_2O_3, $Fe_2O_{3(T)}$, MnO, MgO and CaO. The results of EMP analyses for epidotes in the Akdağmadeni district are shown in Table 7.4. SiO_2 contents of epidotes range from 38.22 to 41.77%, the lowest value observed in the Çukurmaden, the highest in the Çiçeklitepe occurrence. Al_2O_3 contents range from 21.63 to 26.65%, the lowest and highest values observed in the Çiçeklitepe occurrence. $Fe_2O_{3(T)}$ contents ranges from 8.63 to

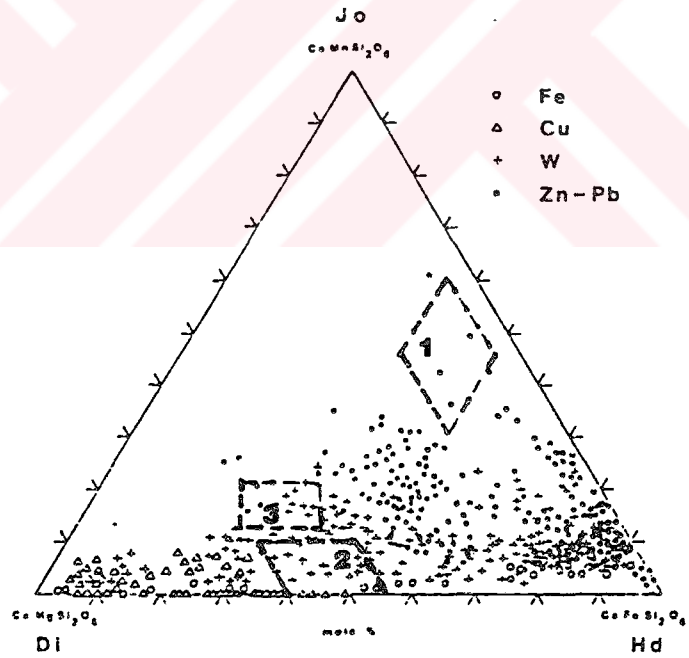

Figure 7.11. The Mg-Fe-Mn ternary diagram for major skarn types in the world (taken from Einaudi et al., 1981), dashed lines encircle the areas for the pyroxenes from the Bayramali (1), Çiçeklitepe (2), and Radarbaca (3) occurrences

Table 7.4. Results of EMP analyses for epidotes in the Akdağmadeni district (Çi: Çiçeklitepe, Çu: Çukurmaden, KP: Peynirliktepe, R: Radarbaca occurrences)

Sample #	Çi1-2					Çu4-1				Çu4-2		KP1-1	KP1-2			
Line of sec.	4	4	4	5	5	1	1	2	2	1	1	1	1	1	2	2
Probe #	1	4	5	3	4	3	4	1	2	1	2	2	2	3	1	2
SiO2	41.38	39.63	39.61	38.99	39.95	39.65	38.22	38.97	39.24	39.64	39.98	39.73	40.28	39.39	39.43	39.23
Al2O3	24.65	24.26	23.14	23.24	23.76	25.32	23.51	25.60	25.45	23.94	24.53	24.11	24.98	22.82	24.25	21.63
$Fe_2O_{3(T)}$	12.50	11.43	12.81	12.69	12.27	10.05	11.37	9.39	9.25	12.40	12.05	11.51	11.53	13.35	11.43	14.32
MnO	0.98	0.34	0.59	0.66	1.13	0.65	0.28		0.35	0.42	0.37	0.61	0.54	-	-	-
MgO	-	-	-	-	-	-	-	-	-	0.34	0.33	-	-	-	0.58	-
CaO	23.19	23.72	22.75	23.65	23.71	24.30	23.76	23.32	23.25	23.68	24.04	24.08	24.30	23.51	23.90	23.56
TOTAL	102.69	99.38	99.15	99.23	100.80	99.97	97.38	97.70	97.52	100.42	101.29	100.40	101.63	99.07	99.59	98.74
Number of cations based on 13(O)																
Si	3.289	3.258	3.291	3.254	3.263	3.229	3.226	3.231	3.254	3.253	3.242	3.252	3.243	3.28	3.243	3.302
Al	2.309	2.351	2.266	2.287	2.287	2.431	2.339	2.502	2.488	2.315	2.345	2.327	2.371	2.243	2.353	2.146
Fe	0.831	0.786	0.89	0.886	0.838	0.684	0.803	0.651	0.641	0.851	0.817	0.788	0.766	0.931	0.786	1.009
Mn	0.066	0.023	0.042	0.047	0.078	0.045	0.02	-	0.024	0.029	0.025	0.042	0.037	-	0.041	-
Mg	-	-	-	-	-	-	-	-	-	0.04	0.04	-	-	-	-	-
Ca	1.975	2.09	2.025	2.116	2.075	2.12	2.149	2.072	2.066	2.082	2.089	-	-	-	-	-

Table 7.4. Cont.

Sample #	KP1-2	R3-1						R3-2					Çİ1-2		
Line of sec.	3		3	3	1	1	2	2	1	1	1	3	3	1	1
Probe #	1	1	3	2	3	1	3	1	3	4	2	3	1	2	4
SiO2	39.30	39.41	40.27	41.01	40.39	40.13	41.70	40.43	41.25	40.21	39.09	39.69	41.77	40.73	41.34
Al2O3	22.12	23.26	24.16	26.96	23.65	25.61	25.02	23.94	26.33	23.99	21.82	24.42	26.67	25.81	23.74
$Fe_2O_{3(T)}$	14.07	13.01	12.02	8.63	12.54	10.07	12.25	12.02	9.98	12.07	13.69	11.42	10.02	10.95	13.56
MnO	0.21	1.08	0.59	1.10	0.51	1.10	1.01	0.73	0.57	0.44	-	0.72	1.29	0.95	0.31
MgO	-	-	-	-	-	-	-	-	-	-	-	-	0.29	-	-
CaO	23.15	23.58	24.54	23.67	24.08	23.73	23.80	23.72	23.99	23.87	23.48	23.46	22.57	23.01	23.78
TOTAL	98.85	100.58	101.57	101.36	101.17	100.65	103.78	100.85	102.13	100.58	98.09	99.70	102.61	101.45	102.99
Number of cations based on 13(O)															
Si	3.299	3.256	3.259	3.254	3.287	3.246	3.292	3.287	3.271	3.275	3.304	3.26	3.293	3.267	3.302
Al	2.188	2.265	2.304	2.522	2.269	2.242	2.328	2.294	2.461	2.303	2.174	2.363	2.478	2.441	2.235
Fe	0.988	0.899	0.814	0.573	0.853	0.681	0.809	0.817	0.662	0.822	0.968	0.784	0.661	0.734	0.906
Mn	0.015	0.076	0.04	0.074	0.035	0.076	0.068	0.051	0.038	0.03		0.05	0.086	0.065	0.021
Mg	-	-	-	-	-	-	-	-	-	-	-	-	0.034	-	-
Ca	-	2.08	2.128	2.013	2.1	2.057	2.013	2.066	2.038	2.083	2.127	2.064	1.906	1.978	2.032

Table 7.5. Correlation matrix for the major oxides in epidotes from the Akdağmadeni district

	SiO_2	Al_2O_3	$Fe_2O_{3(T)}$	MnO	MgO	CaO
SiO_2	1					
Al_2O_3	0.55	1				
$Fe_2O_{3(T)}$	-0.25	-0.9	1			
MnO	0.56	0.55	-0.32	1		
MgO	0.18	0.27	-0.20	0.13	1	
CaO	-0.04	0.02	-0.07	-0.12	-0.08	1

14.32%, the lowest value observed in the Çukurmaden and the highest in the Radarbaca occurrences. MnO contents range from 0.0 to 1.29%, the lowest value observed in Peynirliktepe and Radarbaca, highest value in the Çiçeklitepe occurrence. MgO and CaO contents range from 0.0 to 0.33% and 22.57 to 24.54%, respectively. The lowest and highest MgO contents are observed in the Çukurmaden occurrence. The lowest CaO content is observed in the Çiçeklitepe, and the lowest content is observed in the Radarbaca occurrence.

Significant relationships are observed between Al_2O_3, $Fe_2O_{3(T)}$, and MnO and contents of epidotes. Al_2O_3 contents decrease as $Fe_2O_{3(T)}$ contents increase, but it increases with MnO content. $Fe_2O_{3(T)}$ contents slightly decrease as MnO content increase (Figure 7.12). The correlation matrix shows the coefficients between SiO_2, Al_2O_3, $Fe_2O_{3(T)}$, MnO, MgO and CaO (Table 7.4). The most significant relationship is observed between Al_2O_3 and $Fe_2O_{3(T)}$. The correlation coefficient for these represent maximum observed negative correlation (-0.9). The maximum observed positive correlation occurs between Al_2O_3 and MnO (0.55). The Mn-Al, Mn-Fe, Fe and Mn classification diagram indicates that the samples plot in the epidote field of the diagram (Figure 7.13), and they are classified as epidote.

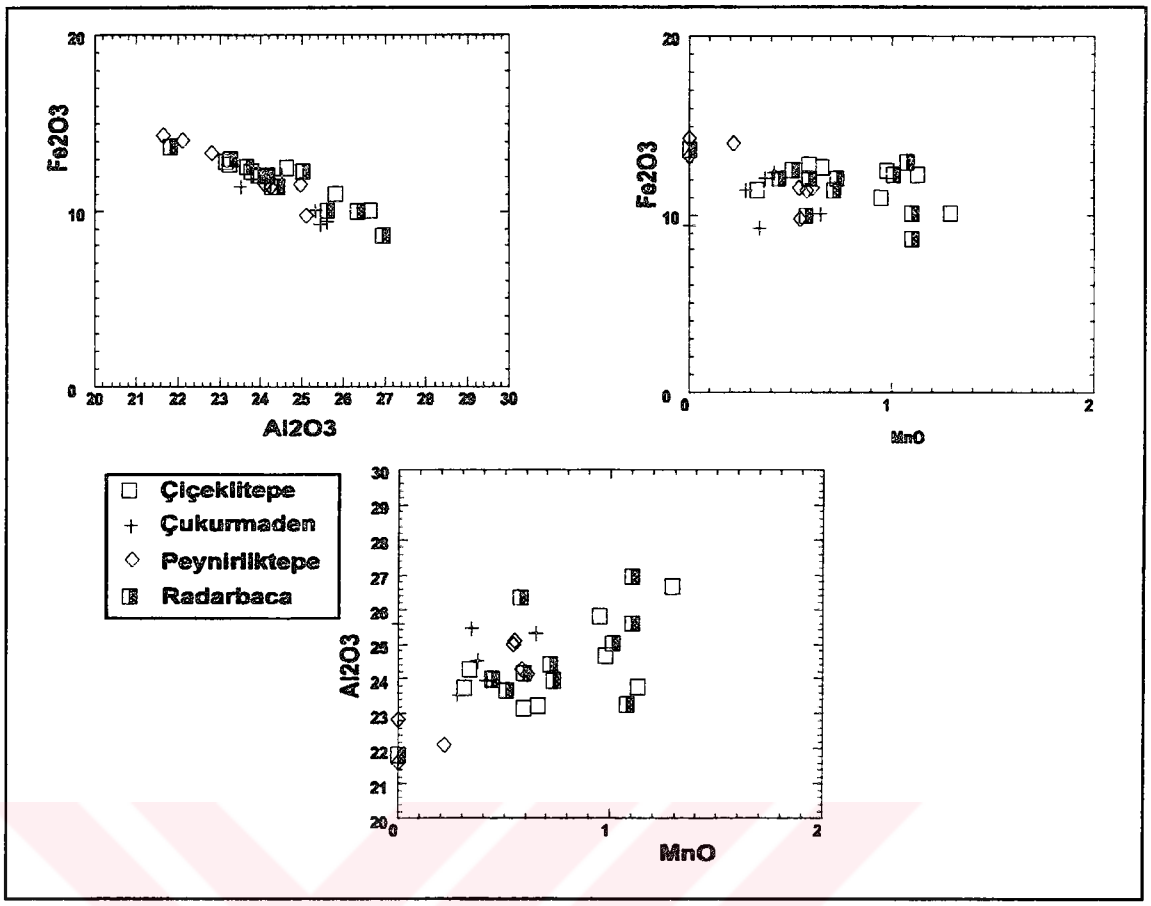

Figure 7.12. The relationships between Al_2O_3, $Fe_2O_{3(T)}$ and MnO in epidotes

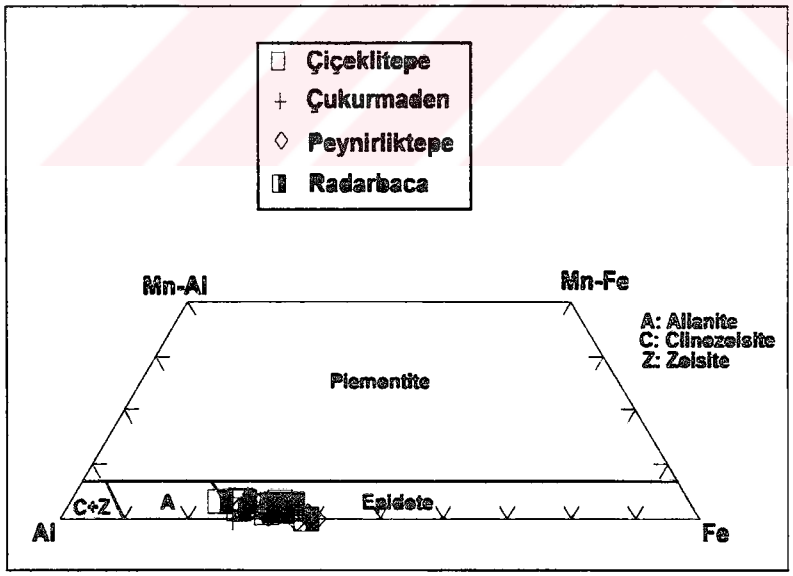

Figure 7.13 Mn-Al, Mn-Fe, Fe and Al classification diagram for the epidotes

7.4. Akçakışla district

The mineral chemical analyses in the Akçakışla district are based on garnets and pyroxenes. A total of 97 points were analyzed along several lines of sections on these minerals. A total of 70 points on garnets and a total of 27 points on pyroxenes were analyzed in the samples selected from the Barajdoğusu and Özgebaca occurrences.

7.4.1. Chemistry of garnets

The garnets were analyzed for SiO_2, TiO_2, Al_2O_3, $Fe_2O_{3(T)}$, MnO, MgO, and CaO. The results of analyses are given in Table 7.6. SiO2 contents of the garnets range from 35.14 to 40.54%. The highest and lowest values are observed in the Barajdoğusu occurrence. TiO_2 contents range from 0.0 to 2.55%, the highest value observed in the Özgebaca occurrence. Al_2O_3 contents have a range of 0.0 to 20.68%, the lowest and highest values observed in the Barajdoğusu occurrence. $Fe_2O_{3(T)}$ contents of the garnets range from 2.70 to 28.00%. Similar to SiO_2 and Al_2O_3, the highest the lowest values observed in the Barajdoğusu occurrence. The MnO, MgO and CaO contents of the garnets range from 0.0 to 6.33%, 0.0 to 0.77%, and 29.21 to 38.15%, respectively.

Al_2O_3 contents of the garnets display significant relationships with $Fe_2O_{3(T)}$, SiO_2, MnO and CaO (Table7.7). Al_2O_3 contents increases with SiO_2, MnO and CaO contents. However, Al_2O_3 contents are negatively correlated to $Fe_2O_{3(T)}$ contents (-0.99, Table 7.7) (Figure 7.14). In contrast to Al_2O_3 contents, $Fe_2O_{3(T)}$ contents are negatively correlated to SiO_2, MgO and CaO (Table 7.7 and Figure 7.15) $Fe_2O_{3(T)}$ and

Table 7.6. The results of microprobe analyses of garnets from core to rim in the Akçakışla district (B: Barajdoğusu and Ö: Özgebaca occurrences)

Sample #	Ö5-1				Ö5-1			Ö5-2						Ö6-1	Ö6-2
Line of Sec.	1	1	1	1	2	2	2	1	1	1	1	1	1	1	1
Probe	1	6	8	11	1	4	10	1	3	6	8	12	14	1	1
SiO_2	38.75	39.98	39.09	38.12	38.21	39.81	39.09	39.52	39.85	37.43	39.81	38.05	39.14	37.63	36.70
TiO_2	0.88	0.50	0.78	0.42	-	0.58	0.61	0.42	0.87	-	-	-	-		-
Al_2O_3	13.17	14.56	11.9	8.58	15.25	14.38	9.65	14.24	13.53	1.29	5.94	3.35	7.27	1.42	-
$Fe_2O_{3(T)}$	11.16	9.98	12.95	16.41	9.49	10.58	15.34	10.46	11.50	25.63	21	23.78	19.38	25.85	26.00
MnO	2.20	1.32	1.37	1.17	0.24	1.41	1.29	1.17	1.02	0.99	0.65	1.39	2.70	1.13	1.15
MgO	0.33	0.4	-	-	-	0.37	0.24	0.23	-	0.25	-	-			0.26
CaO	33.56	35.02	34.86	35.38	36.00	34.66	34.01	35.18	35.28	33.60	35.39	34	33.50	35.19	33.07
TOTAL	100.05	101.76	100.95	100.08	99.19	101.79	100.23	101.22	102.05	99.24	102.79	100.52	101.99	101.50	99.18
Number of cations based on 24 (O)															
Si	6.157	6.214	6.237	6.301	6.07	6.2	6.368	6.185	6.213	6.589	6.507	6.524	6.406	6.5	6.564
Ti	0.106	0.059	0.095	0.053	-	0.06	0.075	0.05	0.102	-	-	-	-	-	-
Al	2.472	2.669	2.244	1.673	2.857	2.641	1.855	2.627	2.486	0.268	1.146	0.677	1.404	0.291	-
Fe_T	1.486	0.1298	1.728	2.27	1.261	1.379	2.091	1.369	1.5	3.773	2.87	3.41	2.653	-	4.189
$Fe^{+2}{}_{calc}$	0.179	-	0.191	-	0.182	-	-	0.29	0.034	0.034	0.075	-	-	0.173	-
$Fe^{+3}{}_{calc}$	1.143	-	1.338	1.119	0.866	0.283	-	1.045	3.198	2.286	2.862	-	-	3.289	3.829
Mn	0.297	0.174	0.185	0.164	0.033	0.151	0.179	0.156	0.136	0.149	0.091	0.203	0.375	0.166	0.175
Mg	0.08	0.093	-	-	-	0.086	0.058	0.055	-	0.068	-	-	-	-	0.071
Ca	5.723	5.832	5.96	6.297	6.131	5.783	5.937	5.9	5.894	6.337	6.199	6.245	5.875	6.514	6.338
End members of garnet															
Andradite	34.14	29.98	39.94	54.20	28.50	31.40	49.37	31.32	34.26	92.69	69.26	81.91	62.97	90.25	100
Grossular	59.67	65.64	57.04	43.24	70.96	64.09	46.78	65.03	63.44	4.00	29.30	14.94	31.03	5.75	-
Spessart.	4.86	3.53	3.12	2.56	0.54	3.09	2.90	2.55	2.30	2.27	1.44	3.15	6.0	2.50	-
Pyrope	1.33	1.15			-	1.42	0.95	0.92	-	1.04	-	-	-	-	-

Table 7.6. Cont.

Sample #	ö9-1						Ö9-2						B17-1		
Line of sec.	1	1	1	1	1	1	2	2	2	2	2	2	1	1	1
Probe	2	1	4	9	10	11	1	2	4	7	9	10	1	2	6
SiO_2	36.00	38.10	38.46	38.96	38.48	36.12	40.20	40.01	39.03	39.24	37.08	37.35	36,83	37,85	37,98
TiO_2	-	1.86	1.93	1.92	2.55	1.53	0.75	1.10	0.47	0.31	0.30	-	-	-	-
Al_2O_3	-	14.30	14.36	14.46	14.45	13.93	14.55	14.68	13.07	16.80	7.94	7.45	2,25	1,62	2,52
$Fe_2O_{3(T)}$	28.17	8.90	8.77	9.13	9.23	9.56	10.62	9.55	11.98	7.1	18.73	17.35	24,61	25,97	24,69
MnO	0.69	-	-	-	-	-	-	-	-	0.65	6.33	5.00	0,68	0,65	0,66
MgO	-	0.47	0.63	0.77	0.61	0.38	0.27	0.32	0.31	-	-	0.29	0,43	0,30	0,31
CaO	33.57	35.39	34.57	35.80	35.98	35.56	36.03	35.26	35.48	35.27	29.21	29.45	34,52	34,20	34,95
TOTAL	98.43	99.02	98.72	101.04	101.3	99.08	102.42	100.92	100.34	99.37	99.59	96.89	99,32	100,60	101,11
Number of cations based on 24 (O)															
Si	6.514	6.058	6.09	6.067	6.002	6.09	6.206	6.219	6.188	6.128	6.284	6.365	6,433	6,565	6,512
Ti	-	0.223	0.236	0.23	0.3	0.184	0.087	0.129	0.056	0.037	0.039	-	0,464	0,332	0,510
Al	-	2.68	2.68	2.654	2.658	2.624	2.648	2.69	2.443	3.092	1.586	1.699	3,594	3,768	3,541
Fe_T	4.264	1.184	1.175	1.189	1.205	1.251	1.372	1.241	1.588	0.927	2.684	2.474	0,105	0,161	
$Fe^{+2}{}_{calc}$	-	0.146	0.315	0.146	0.152	0.103	0.276	0.406	0.148	0.184	0.111	0.193	3,077	3,223	3,031
$Fe^{+3}{}_{calc}$	3.899	0.908	0.727	0.913	0.919	1.03	0.944	0.704	1.262	0.646	2.204	1.997	0,101	0,096	0,095
Mn	0.106	-	-	-	-	-	-	-	-	0.087	0.909	0.722	0,111	0,078	0,080
Mg	-	0.113	0.149	0.18	0.143	0.091	0.063	0.076	0.075	-	-	0.074	6,462	6,358	6,420
Ca	6.508	6.029	5.865	5.973	6.013	6.087	5.959	5.873	6.028	5.902	5.304	5.377	-	-	-
End members of garnet															
Andradite	99.168	26.85	26.42	27.09	27.29	29.03	31.09	28.37	36.37	21.04	59.52	59.77	87,46	91,08	86,21
Grossular	-	71.3	71.09	69.98	70.38	69.49	67.85	70.36	62.40	77.50	25.85	27.32	9,37	6,26	11,13
Spessart.	-	-	-	-	-	-	-	-	-	1.46	14.63	11.70	1,52	1,47	1,44
Pyrope	-	1.85	2.49	2.93	2.33	1.48	1.06	1.27	1.23	-	-	1.21	-	-	-

Table 7.6 Cont.

Sample #	B17-1									B17-2			B17-2			B17-4
Line of sec.	1	1	1	1	1	1	1	1	1	1	1	1	1	1	1	1
Probe	8	9	11	14	16	17	18	20	21	1	4	6	7	9	11	1
SiO_2	37,34	37,65	38,29	37,86	38,25	39,16	38,54	37,79	37,60	39.59	37.36	37.82	37.08	37.70	38.85	38.69
TiO_2	-	-	-	-	-	-	-	-	-	-	-	-	-	-	-	-
Al_2O_3	1,55	3,96	2,80	4,53	2,40	0,42	6,41	0,60	0,64	0.58	0.29	0.52	1.15	1.43	0.65	1.49
$Fe_2O_{3(T)}$	25,82	23,54	24,68	22,86	25,70	24,34	20,86	24,81	27,55	27.49	27.24	27.37	27.15	26.78	27.74	27.06
MnO	0,69	0,61	0,57	0,61	0,82	1,46	0,83	0,06	0,27	0.41	0.47	0.37	0.28	0.27	0.50	0.34
MgO	0,37	0,28	0,34	0,30	-	0,30	0,27	-	-	0.43	-	0.39	0.31	-	-	-
CaO	34,31	35,65	34,87	35,69	35,77	34,95	35,96	34,97	34,77	34.91	34.21	34.94	35.44	35.38	34.73	35.00
TOTAL	100,08	101,71	101,54	101,85	102,93	100,63	102,87	98,24	100,82	103.41	99.57	101.50	101.44	101.86	102.48	102.60
Number of cations based on 24 (O)																
Si	6,496	6,371	6,518	6,375	6,472	6,759	6,336	6,472	6,562	6.672	6.585	6.556	6.432	6.487	6.66	6.595
Ti	0,318	0,791	0,561	0,898	0,478	0,086	1,242	0,602	0,131	-	-	-		-	-	-
Al	3,756	3,333	3,515	3,219	3,637	3,513	2,868	3,554	4,022	0.115	0.061	0.107	0.236	0.29	0.132	0.3
Fe_T	0,161	0,143	0,151	0,138	0,156	0,151	0,120			3.874	4.016	3.968	3.939	3.584	3.976	3.858
$Fe^{+2}{}_{calc}$	3,219	2,856	3,015	2,761	3,110	3,015	2,475	3,137	3,433	-	0.172	0.169	0.168	0.165	0.17	0.165
$Fe^{+3}{}_{calc}$	0,102	0,088	0,082	0,087	0,117	0,213	0,115	0,091	0,040	3.328	3.441	3.382	3.348	3.299	3.4	3.302
Mn	0,095	0,071	0,086	0,076		0,077	0,066			0.059	0.086	0.055	0.041	0.04	0.073	0.05
Mg	6,396	6,465	6,361	6,439	6,486	6,468	6,334	6,416	6,502	0.108	-	0.101	0.082	-	-	-
Ca										6.304	6.46	6.49	6.587	6.524	6.378	6.392
End members of garnet																
Andradite	91,40	79,13	84,93	76,33	87,24	90,23	67,51	96,34	94,09	96.79	98.35	97.07	93.74	92.28	96.42	92.03
Grossular	5,62	18,47	12,50	21,20	10,98	6,03	29,72	2,26	2,90	0.62	0.55	0.57	4.40	7.11	2.45	7.19
Spessart.	1,55	1,33	1,25	1,32	1,78	2,15	1,77	1,40	0,61	0.91	1.10	0.83	0.61	0.61	1.13	0.78
Pyrope	1,44	1,07	1,31	1,15	-	1,59	1,01	-	-	1.68	-	1.57	1.25	-	-	-

			B20-1			B20-1		B20-1	B23-1	
1	1	1	1	1	1	1	1	1	1	1
8	10	13	1	3	4	6	8	10	2	4
39.23	38.85	37.64	36.66	37.86	39.19	39.34	37.37	39.16	37.02	39.17
-	-	-	-	0.26	-	-	-	-	-	-
1.44	5.00	7.38	0.21	1.40	5.163	11.34	8.94	3.44	1.972	6.08
26.81	22.33	19.25	26.47	25.20	21.316	14.20	20.01	22.94	26.52	20.41
0.48	0.62	0.28	0.60	0.50	1.521	1.23	0.63	0.3	-	-
-	-	-	0.31	-	-	-	-	0.27	-	-
35.19	34.34	34.80	33.95	35.07	33.071	33.57	34.27	34.51	35.62	34.72
03.17	101.18	99.80	98.23	100.31	100.261	99.70	101.23	100.63	101.15	100.39
5.611	6.498	6.315	6.569	6.55	6.591	6.349	6.175	6.628	6.401	6.53
-	-	-	-	0.03	-	-	-	-	-	-
0.287	0.987	1.461	0.045	0.28	1.023	2.158	1.742	0.687	0.402	1.195
3.779	3.124	2.702	3.966	3.64	2.998	1.917	2.766	3.247	3.835	2.846
0.167	0.25	0.23	0.169	-	-	-	-	-	-	-
3.985	2.47	2.334	3.38	3.13	2.622	1.702	2.402	2.813	3.274	2.483
0.07	0.089	0.04	0.092	0.07	0.217	0.169	0.088	0.043	-	-
-	-	-	0.085	-	-	-	-	0.069	-	-
6.355	6.154	6.256	6.519	6.50	5.959	5.807	6.068	6.258	6.6	6.201
92.22	74.00	62.46	98.77	91.08	72.49	44.42	59.29	80.95	89.57	68.19
6.69	24.57	36.90	-	7.79	24.60	52.74	39.26	17.29	10.43	31.81
1.09	1.43	0.64	-	1.13	2.91	2.84	1.45	0.67	-	-
-	-	-	1.23	-	-	-	-	1.09	-	-

			B23-2			
1	1	1	1	1	1	1
10	16	18	2	6	10	11
8.56	39.58	37.93	39.19	40.54	40.33	39.58
-	-	-	0.83	-	0.77	0.85
0.05	18.42	6.94	18.91	19.23	20.68	19.94
3.55	5.06	19.25	4.21	4.20	2.70	2.84
0.35	0.27	0.27	0.23	0.23	0.20	0.25
-	-	-	-	-	-	0.25
6.43	36.62	34.84	37.44	37.73	37.57	37.22
6.96	99.97	99.24	100.81	101.94	102.28	100.96
.945	6.092	6.399	5.979	6.079	5.981	5.977
-	-	-	0.096	-	0.087	0.098
.644	3.343	1.381	3.398	3.399	3.616	3.549
.458	0.652	2.716	0.537	0.527	0.336	0.36
-	-	-	-	-	-	-
0.41	0.583	2.36	0.48	0.472	0.302	0.282
.046	0.036	0.039	0.03	0.03	0.025	0.032
-	-	-	-	-	-	0.057
.107	6.04	6.298	6.12	6.063	5.971	6.022
0.36	14.93	64.50	12.33	12.33	7.56	8.23
8.88	84.47	35.50	87.18	87.27	92.01	90.30
0.76	0.60	-	0.48	0.50	0.43	0.52
-	-	-	-	-	-	0.95

Akdağmadeni district, they appear as the mirror images of each other for the same point along the traverse in the sense that Al_2O_3 contents increase if $Fe_2O_{3(T)}$ contents decrease or vice versa.

The recalculations of the EMP data using Minpet 2.0 show that the garnets in the Akçakışla district contain grossular, andradite, pyrope and spessartine end-members. The mole percents of grossular range from 0.0 to 92.01%, the highest value observed in the Barajdoğusu occurrence. Mole percent of andradite ranges from 0.0 to 100%, pyrope from 0.0 to 2.93%, and spessartine 0.0 to 14.63%, the highest values observed in the Özgebaca occurrence. In general, the composition of garnets in the Akçakışla district ranges from pure andradite (Ad_{100}) and $Ad_{99.23}Sp_{0.77}$ to $Gro_{92.01}Ad_{7.56}Sp_{0.43}$. The garnets are termed as grandite based on these compositions. The garnets scatter between andradite and grossular corners in the Gross-And-Pyralspite ternary diagram (Figure 7.17).

Table 7.7. Correlation matrix for the major oxides in the garnets from the Akçakışla district.

	SiO_2	Al_2O_3	TiO2	$Fe_2O_{3(T)}$	MnO	MgO	CaO
SiO_2	1						
Al2O3	0.60	1					
TiO2	0.09	0.39	1				
$Fe_2O_{3(T)}$	-0.63	-0.99	-0.45	1			
MnO	-0.04	0.02	-0.20	-0.04	1		
MgO	0.10	0.10	0.78	-0.13	0.34	1	
CaO	0.34	0.42	0.27	-0.43	-0.77	-0.14	1

The garnet cores in the Akçakışla district are either grossular-rich or andradite-rich. The Barajdoğusu occurrence is characterized by andradite-rich core sections (Figure 7.17). The garnets analyzed in the core sections from the Özgebaca occurrence plot in the diagram close to grossular corner of the diagram. Therefore, it could be proposed that the garnets in the Barajdoğusu samples began to be formed from a hydrothermal fluid with high fO_2, but those in the Özgebaca samples began to be formed from a hydrothermal fluid with low fO_2 , or the relatively high Al_2O_3 contents

of the garnet cores at Özgebaca are considered to be controlled by the composition of minerals in the original metamorphic rocks during initial metamorphic reactions.

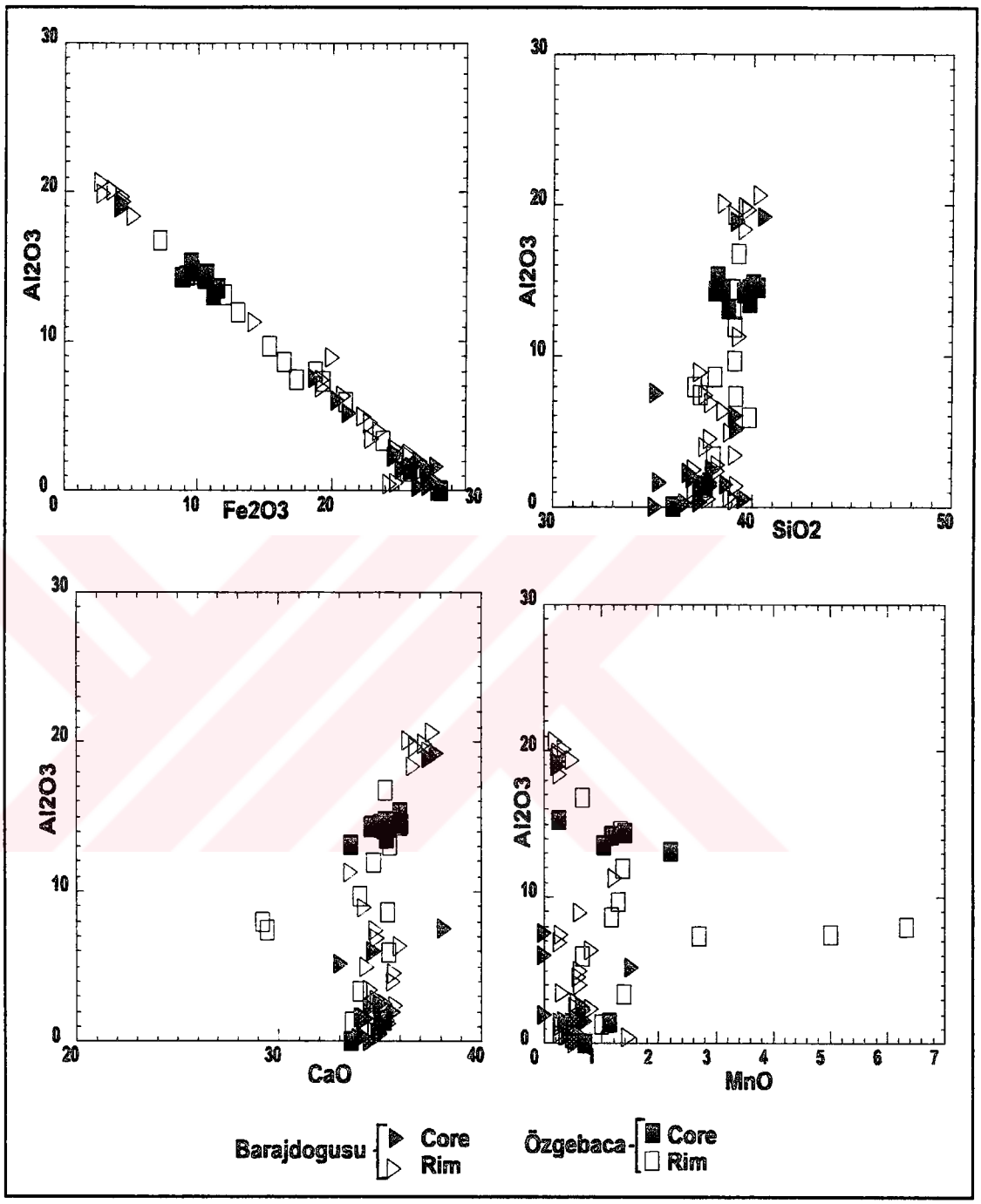

Figure 7.14. The relationships of Al_2O_3 with Fe2O3, SiO2, MnO and CaO in the garnets of the Akçakışla district.

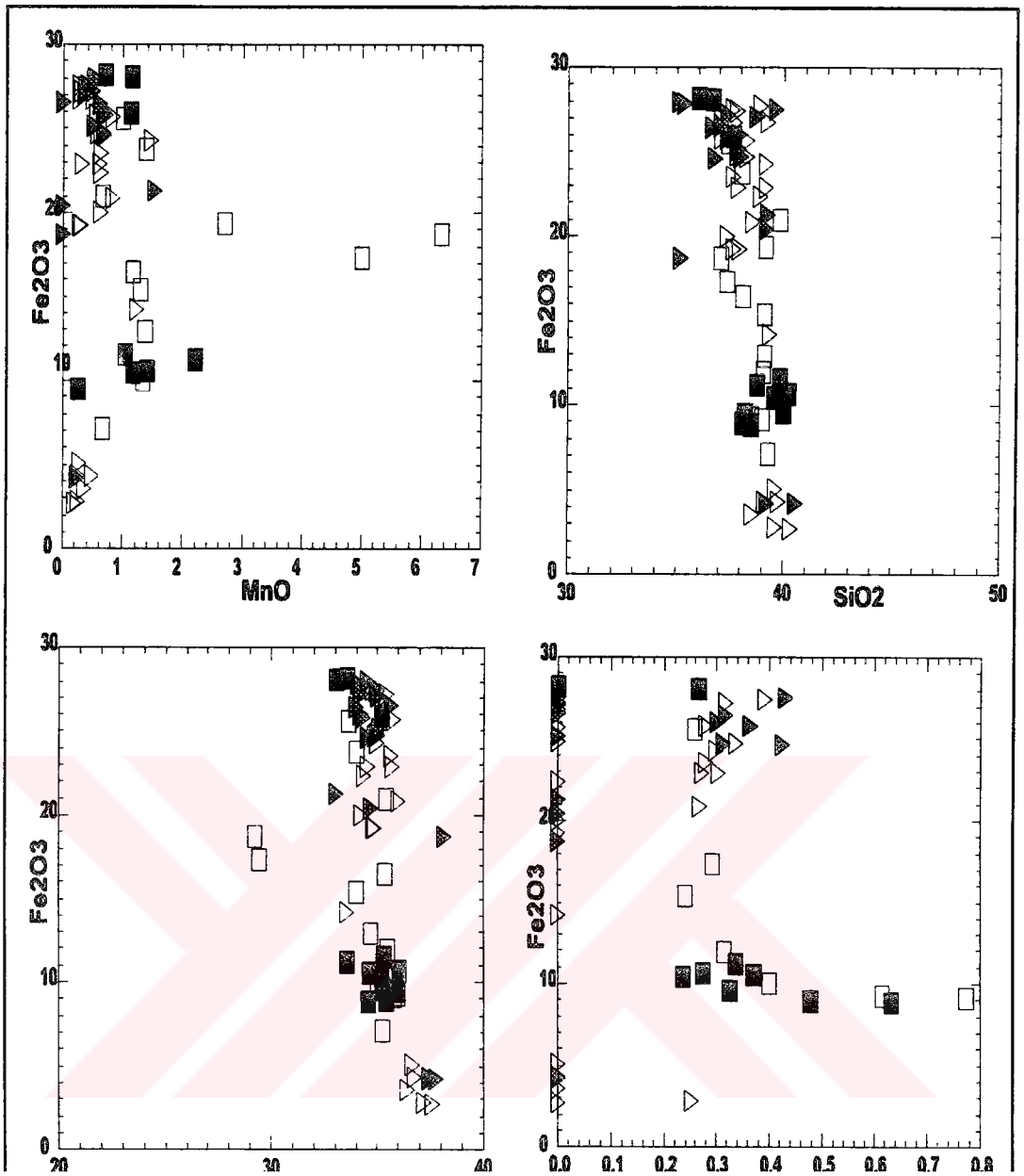
Fe2O3
MnO
Fe2O3
SiO2
Fe2O3
Fe2O3

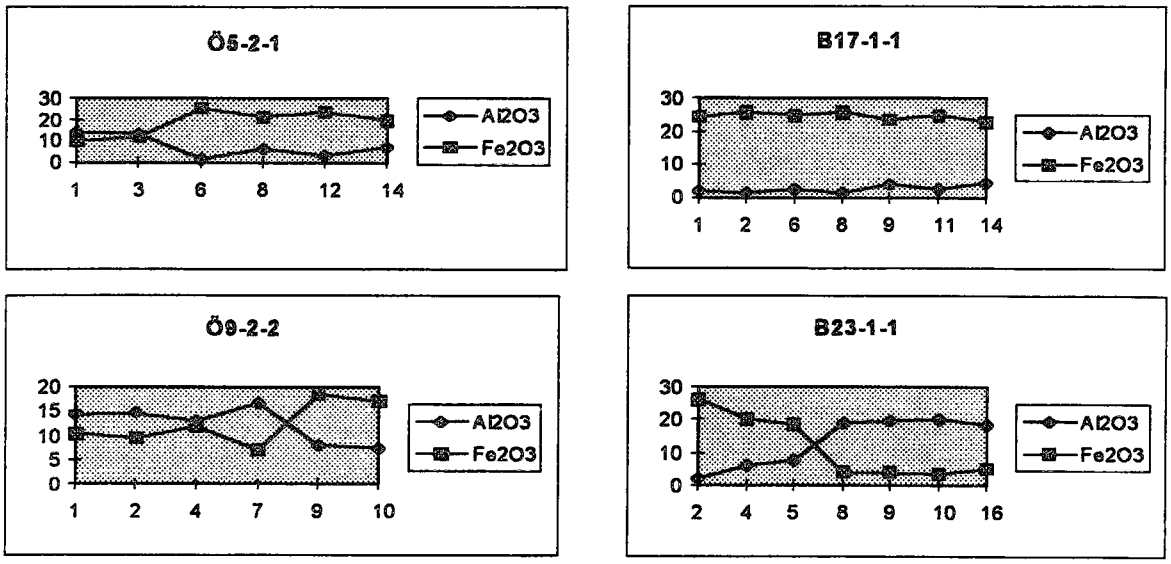

Figure 7.16. Al_2O_3 and $Fe_2O_{3(T)}$ microprobe garnet traverses from core to rim in the Akçakışla district .

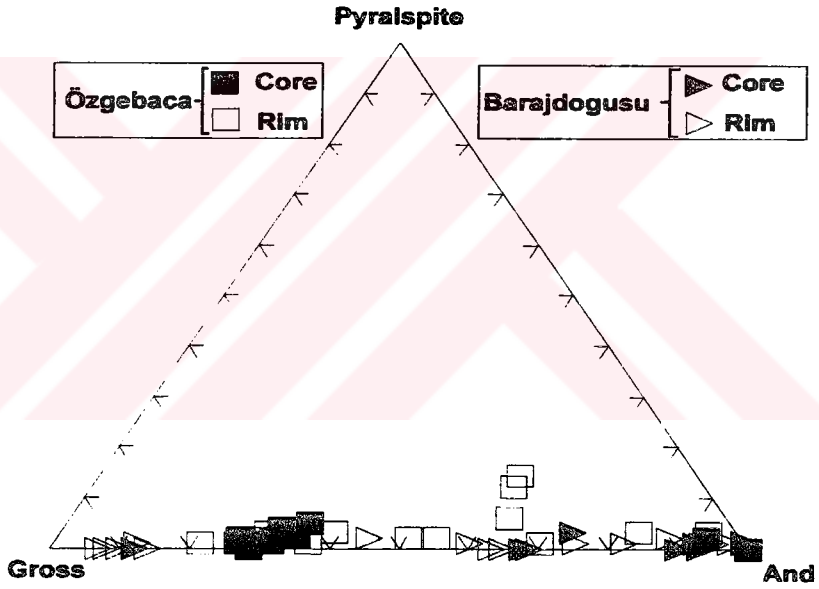

Figure 7.17. The compositional ternary variation diagram for the garnets in the Akçakışla occurrence

In general, the compositions of garnets in the rims display an overlapping pattern from grossular corner to andradite corner of the diagram. This indicates that the garnet compositions oscillate between grossular and andradite in the rims. It could also be seen in the rims that the grossular-rich points of the Özgebaca samples shifted

towards andradite corner, and andradite-rich points of the Barajdoğusu samples shifted towards grossular corner of the diagram compared to cores (Figure 7.17). This is the result of Al^{+3} and Fe^{+3} exchange between the hydrothermal fluids and the wall rocks. Since this exchange is strongly controlled by the oxygen fugacity of the hydrothermal system, oxygen fugacity of the system changed periodically during the formation of garnets.

The grossular and andradite compositions of samples are inversely related to each other. This relationship is shown in Figure 7.18. This figure indicates that the Barajdoğusu and Özgebaca occurrences are clustered in two different groups, this grouping becomes more obvious for core sections of both occurrences (Figure 7.18). Figure 7.16, 7.17 and 7.18 indicate that the grossular and andradite contents oscillate from core to rim depending on the oscillations in Al_2O_3 and $Fe_2O_{3(T)}$ contents. This is evident by the presence of compositional zoning in the garnets.

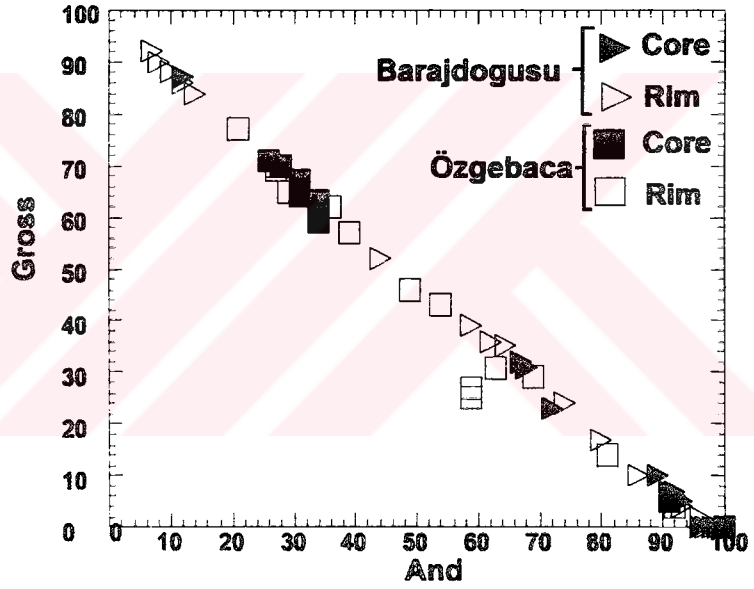

Figure 7.18. The relationships between grossular and andradite contents in the Akçakışla district.

7.4.2. Chemistry of pyroxenes

The results of EMP analyses in pyroxenes from the Akçakışla district are given in Table 7.8. Pyroxenes were analyzed for SiO_2, TiO_2, Al_2O_3, $Fe_2O_{3(T)}$, MnO, MgO,

CaO, Na_2O, and K_2O. The SiO_2 contents of pyroxenes range from 35.52 to 57.26%, the lowest and the highest values observed in the Barajdoğusu occurrence. TiO_2 contents are present mainly in the samples from the Özgebaca occurrence with a range of 0.24 to 27.6%. Al_2O_3 contents range from 0.27 to 12.37%, the lowest values observed in Barajdoğusu and the highest in the Özgebaca occurrence. $Fe_2O_{3(T)}$ contents of pyroxenes range from 1.14 to 26.97%, with the lowest and highest values observed in the Barajdoğusu occurrence. MnO bearing pyroxenes are mainly from the Barajdoğusu occurrence, and MnO contents of these range from 0.0 to 15.22%. The lowest and highest MnO compositions are observed in the Barajdoğusu occurrence. MgO contents range from 0.0 to 23.40%, the lowest and highest values observed in the Barajdoğusu occurrence (Table 7.8). CaO content has a range of 0.0 to 34.95%, the lowest and highest values observed in the Barajdoğusu occurrence. Na_2O and K_2O contents of the pyroxenes are quite high compared to Na_2O and K_2O contents of pyroxenes in the several skarns in the world (Nakano et al., 1994). They both are present in the pyroxenes from the Barajdoğusu occurrence. Na_2O and K_2O contents have a ranges of 0.0 to 2.17 and 0.0 to 0.81, respectively.

The binary plots between the $Fe_2O_{3(T)}$ and SiO_2, MnO, MgO illustrate the relationships between these components (Figure 7.19). The correlation matrix gives statistical relationships between these major oxides as well (Table 7.9). SiO_2 and MgO is negatively correlated with $Fe_2O_{3(T)}$ (Figure 7.19, and Table 7.9) This negative correlation is higher with respect to SiO2 (-0.88, Table 7.9) (Figure 7. 19). The $Fe_2O_{3(T)}$-MgO- and -SiO_2 plots illustrate that the samples from the Barajdoğusu occurrence is clustered in three distinct groups (Figure 7.19). $Fe_2O_{3(T)}$ is positively correlated with CaO (0.47, Table 7.9). On the other hand, the samples form the Özgebaca occurrence all plot together in the binary plots (Figure 7. 19). These groups are controlled by $Fe_2O_{3(T)}$, MgO, and CaO content of the pyroxenes.

The EMP data for pyroxenes are calculated with respect to Wo, En and Fs end-members (Table 7.8) and plotted on the Wo-En-Fs ternary diagram (Figure 7.20) Pyroxenes in the Akçakışla district contain wollastonite up to 62% (Table 7.8). Wollastonite contents of the pyroxenes range from 0.0 to 61.04%. Enstatite content ranges from 0.0 to 57.03%. The highest and the lowest enstatite contents are observed in the Barajdoğusu occurrence. Ferrosilite contents range from 1.77 to

37.98%, the lowest and highest values observed in the Barajdoğusu occurrence (Table 7.8).

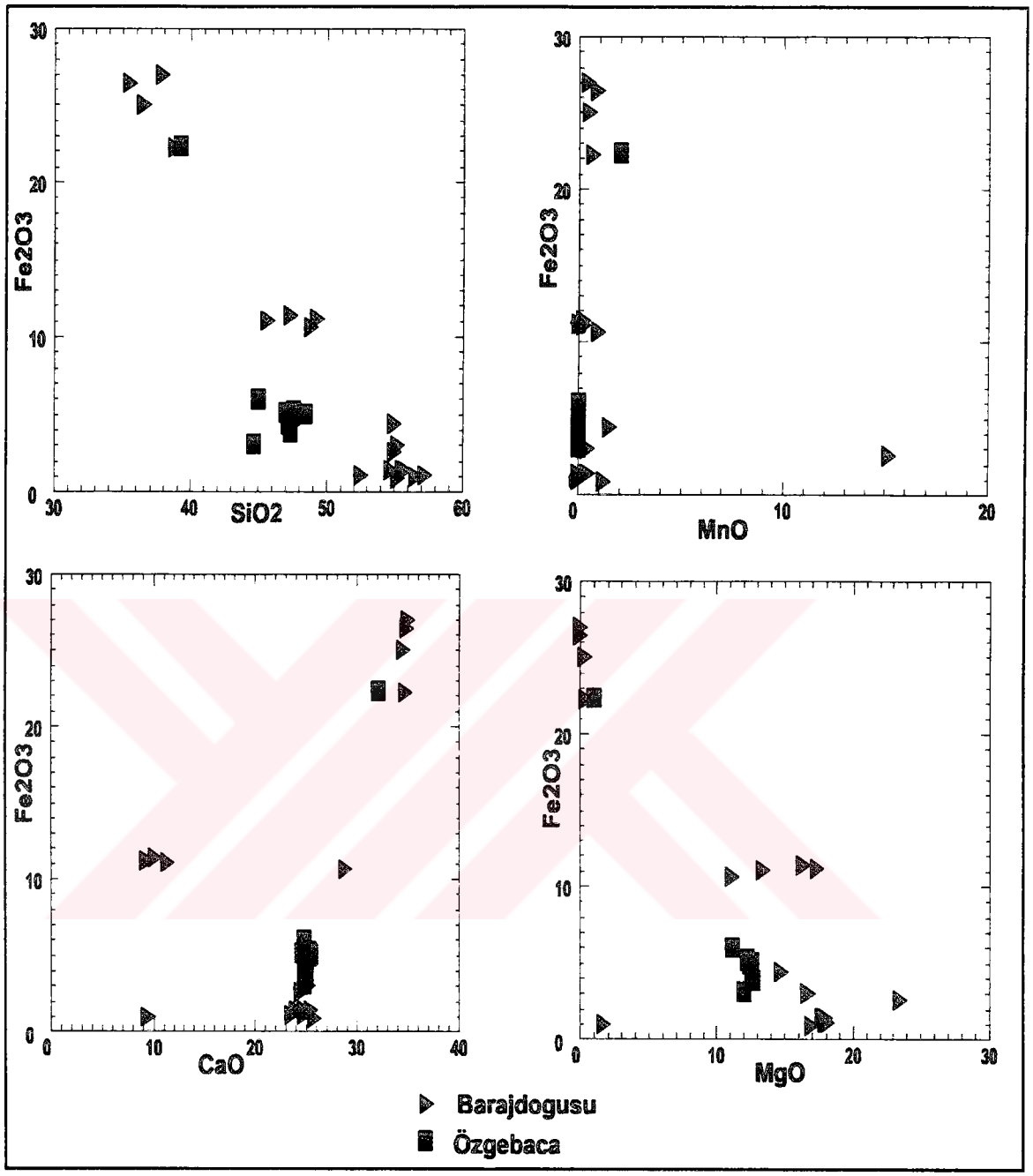

Figure 7.19. The relationships between $Fe_2O_{3(T)}$ and SiO_2, MnO and CaO in pyroxenes from the Akçakışla district

Table 7.8. The results of EMP analyses for pyroxenes in the Akçakışla district

Sample	Ö2-2			Ö2-2							Ö6-2	B11-3		
Section #	1	1	1	2	2	3	3	3	4	6	3	1	1	1
Probe #	1	2	4	1	3	1	3	4	1	2	3	1	3	4
SiO_2	47,62	47,16	47,02	44,69	47,49	47,39	45,02	48,47	47,35	47,18	39,17	47,32	49,28	45,70
TiO_2	0,75	0,64	0,79	2,76	0,80	0,73	0,62	0,88	0,49	0,31	-	0,49	0,23	0,40
Al_2O_3	8,52	7,96	9,27	12,37	10,14	8,72	11,20	9,00	9,22	10,52	5,39	12,12	8,58	14,77
$Fe_2O_{3(T)}$	5,32	4,42	5,12	3,08	4,98	5,14	6,01	5,10	3,85	5,00	22,39	11,41	11,19	11,06
MnO	-	-	-	-	-	-	-	-	-	-	2,02	0,20	-	0,24
MgO	12,23	12,58	12,19	12,01	12,40	12,23	11,11	12,57	12,64	12,51	1,00	16,35	17,30	13,38
CaO	25,21	24,92	24,56	24,80	25,38	25.31	24,78	25,48	25,03	25,18	32,10	10,12	9,39	11,33
Na_2O	-	0,33	0,34	-	0,43	-	-	-	-	-	-	1,71	0,64	2,17
K_2O	-	-	-	-	-	-	-	-	-	-	-	0,23	0,20	0,30
TOTAL	99,65	98,01	99,29	99,71	101,62	99,52	98,74	101,50	98,58	100,7	102,07	99.95	96,84	99,38
Number of cations based on 6(O)														
Si	1,768	1,778	1,75	1,647	1,749	1,759	1,692	1,761	1,763	1,728	1,622	1,733	1,838	1,686
Tl	0,021	0,018	0,022	0,076	0,024	0,02	0,018	0,024	0,014	0,009	-	0,014	0,007	0,011
Al	0,373	0,354	0,407	0,537	0,415	0,382	0,496	0,386	0,405	0,454	0,263	0,52	0,378	0,642
Fe_T	0,165	0,139	0,16	0,095	0,152	0,16	0,189	0,155	0,12	0,153	0,775	0,327	0,349	0,342
Mn	-	-	-	-	-	-	-	-	-	-	0,071	0,006	-	0,008
Mg	0,677	0,707	0,677	0,66	0,675	0,677	0,623	0,681	0,702	0,683	0,062	0,887	0,962	0,736
Ca	1,003	1,007	0,979	0,98	0,987	1,006	0,998	0,991	0,989	0,989	1,424	0,395	0,376	0,448
K	-	-	-	-	-	-	-	-	-	-	-	0,011	0,01	0,014
Na	-	-	-	-	-	-	-	-	-	-	-	0,121	0,046	0,154
Mg/Fe	4.10	5.08	4.23	6.94	4.44	4.23	3.29	4.39	5.85	4.46	0.08	2.71	2.75	2.15
Mn/Fe	0.0	0.0	0.0	0.0	0.0	0.0	0.0	0.0	0.0	0.0	0.09	0.01	0.0	0.0
End-members														
Wollast.	54.42	54.31	53.94	56.46	54.52	54.6	55.14	54.27	54.85	54.16	61.04	24.13	22.26	29.23
Enstat.	36.75	38.17	37.27	38.05	37.08	36.73	34.41	37.25	38.56	37.44	2..67	54.23	57.03	48.00
Ferrosil.	8.83	7.52	8.8	5.49	8.40	8.67	10.45	8.48	6.59	8.4	36.29	21.64	20.71	22.77

Table 7.8. Cont.

Sample	B17-1		B17-1		B20-3		B23-1				B23-4		
Section #	3	3	4	4			2	2	2	2			
Probe #	3	4	2	4	1	4	1	2	6	7	1	2	3
SiO_2	38,75	35,52	37,85	36,48	57,26	55,00	54,75	52,65	48,86	55,60	55,73	55,26	54,96
TiO_2	-	-	-	-	-	-	-	-	-	0,27	-	-	-
Al_2O_3	0,42	1,55	0,66	2,94	0,79	2,27	0,40	2,02	1,15	1,46	0,37	0,86	0,27
$Fe_2O_{3(T)}$	22,25	26,42	26,97	24,99	1,14	2,61	1,41	1,14	10,70	1,44	1,41	2,99	4,43
MnO	0,68	0,87	0,41	0,48	-	15,22	-	-	0,95	0,46	-	0,46	1,49
MgO	0,41	-	-	0,32	18,13	23,4	17,68	17,89	11,11	17,82	17,90	16,64	14,71
CaO	34,72	34,90	34,95	34,56	24,85	-	24,79	23,57	28,83	24,03	25,50	25,22	24,82
Na_2O	-	-	-	-	-	0,46	-	-	-	-	0,50	-	-
K_2O	-	-	-	-	-	-	-	0,818	-	-	-	-	-
TOTAL	97.23	99,26	100,84	99.77	102,17	98.96	99,03	98,08	101,6	101,08	101,41	101,43	100,68
Number	of	cations	based on	6(O)									
Si	1,624	1,58	1,644	1,583	2,01	2,016	1,99	1,936	1,863		1,99	1,982	2,008
Al	0,21	0,081	0,034	0,151	0,033	-	0,17	0,088	0,052		0,016	0,035	0,012
Fe_T	0,798	0,983	0,979	0,907	0,034	0,07	0,43	0,044	0,341		0,042	0,09	0,136
Mn	0,024	0,033	0,015	0,018	-	0,081	-	-	0,031		-	-	0,046
Mg	0,026	-	-	0,021	0,949	0,853	0,958	0,981	0,631		0,953	0,89	0,802
Ca	1,559	1,663	1,626	1,607	0,935	0,921	0,966	0,929	1,178		0,976	0,969	0,972
K								0,038					
Mg/Fe	0.03	0.0	0.0	0.02	27.91	12.18	2.22	24.52	1.85		22.69	9.88	5.89
Mn/Fe	0.03	0.33	0.01	0.01	0.0	1.15	0.0	0.0	0.09		0.0	0.0	0.33
End-members													
Wollast.	65.25	62.08	62.02	62.94	48.75	34.33	49.09	47.74	53.98	47.75	49.51	49.37	49.70
Enstat.	1.08	-	-	0.82	49.48	45.88	48.71	50.44	28.95	49.28	48.34	45.34	41.0
Ferrosil.	33.67	37.62	37.98	36.24	1.77	19.79	2.20	1.82	17.07	2.97	2.15	5.29	9.30

Table 7.9. Correlation matrix for the major oxides in the pyroxenes from the Akçakışla district.

	SiO_2	TiO_2	Al_2O_3	$Fe_2O_{3(T)}$	MnO	MgO	CaO	Na_2O	K_2O
SiO_2	1								
TiO_2	-0.11	1							
Al2O3	-0.03	0.06	1						
$Fe_2O_{3(T)}$	-0.88	-0.43	-0.07	1					
MnO	0.16	-0.36	-0.06	-0.04	1				
MgO	0.78	0.05	0.01	-0.79	0.27	1			
CaO	-0.49	0.15	0.00	0.47	-0.03	-0.19	1		
Na_2O	0.23	-0.19	0.01	-0.14	-0.03	-0.19	-0.65	1	
K_2O	0.40	-0.24	-0.06	-0.23	-0.16	-0.44	-0.56	0.92	1

Pyroxenes in the Akçakışla district are classified as diopside, hedenbergite, and augite based on their distribution in ternary En-Fs-Wo ternary diagram of Morimoto et al. (1988) (Figure 7.20). Pyroxenes from the Barajdoğusu occurrence are clustered in two groups. One of them plot in the diopside field, another plot in the augite field. (Figure 7.20). In general, pyroxenes from the Özgebaca occurrence plot close to diopside field (Figure 7.20). High Ca contents in these pyroxenes are related to alteration of pyroxenes to calcites during the retrograde alteration stages. The presence of considerable amounts of augite in the pyroxenes at the Barajdoğusu occurrence is related to alteration, and to substitution of Ca by Na, and substitution of Mg (or Fe) by Al in the clinopyroxenes.

The Mg-Fe-Mn (diopside-hedenbergite-johannsenite) ternary diagram shows that the pyroxenes in the Akçakışla district are mostly diopsides and hedenbergites (Figure 7.21). Two groups observed in Figure 7.20 are also obvious in this diagram. Most of the samples plot close to diopside corner. The pyroxenes from the Barajdoğusu occurrence plot in two distinct areas, some of them are close to diopside corner, and some are close to hedenbergite corner of the diagram (Figure 7.21).

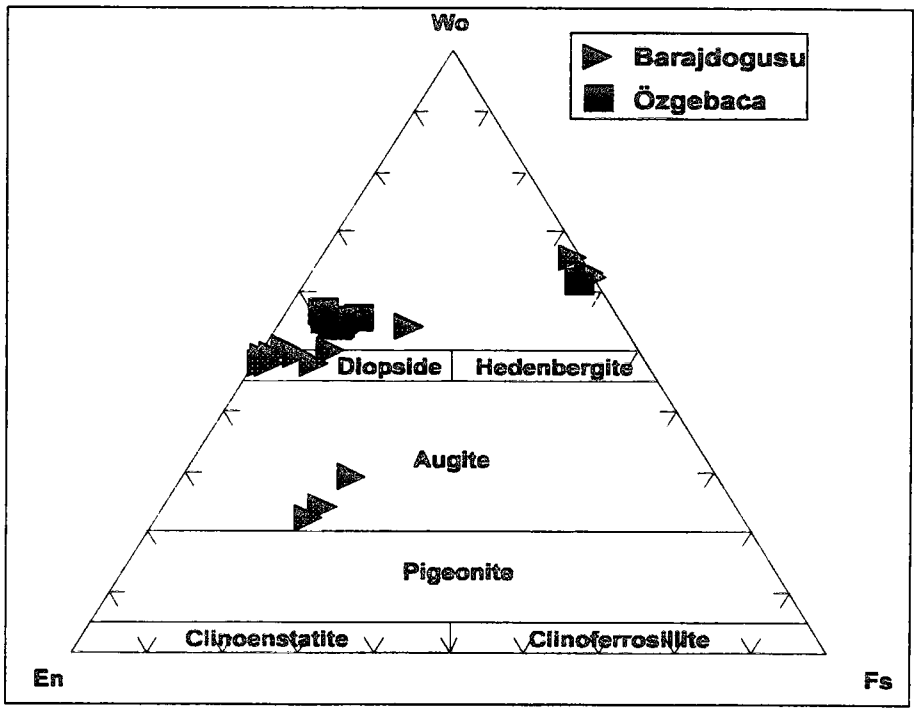

Figure 7.20. The ternary En-Fs-Wo ternary diagram (En: Enstatite, Fs: Ferrosilite, Wo: Wollastonite; Fields from Morimoto et al., 1988) illustrating the classification of pyroxenes in the Akçakışla district.

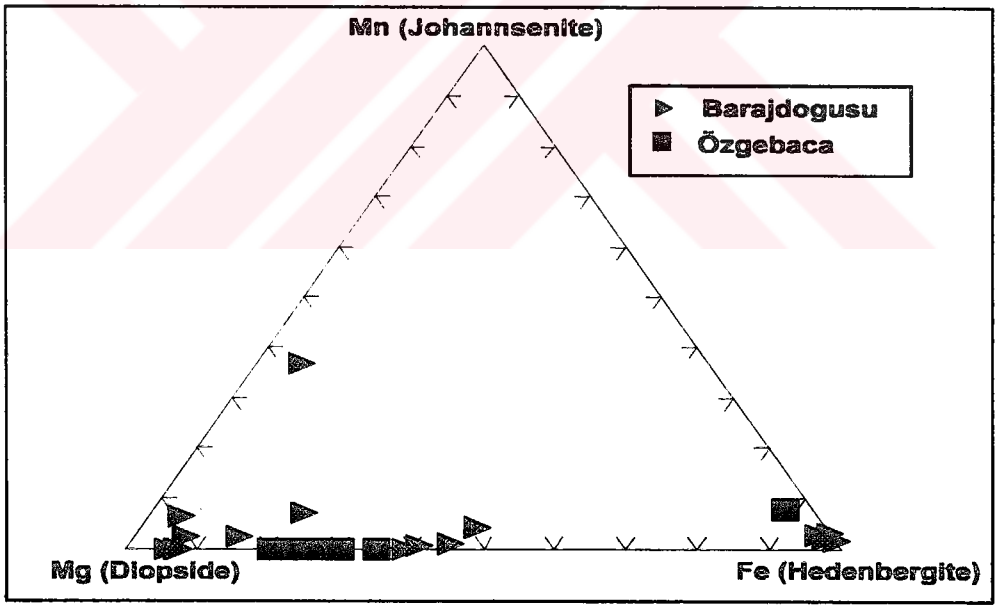

Figure 7.21. Mg-Fe-Mn ternary diagram for the classification of pyroxenes in the Akçakışla district

The comparison of the distribution of the pyroxenes in the Akçakışla district with the pyroxenes from several skarns (Einaudi et al., 1981) shows that the pyroxenes from the Barajdoğusu and Özgebaca occurrences display a pattern within the distribution pattern of the pyroxenes observed in the major Cu- and Zn-Pb skarns in the world (Figure 7.22). Therefore, it is proposed that the samples the Barajdoğusu occurrence has some Cu imprints at least based on their pyroxene compositions.

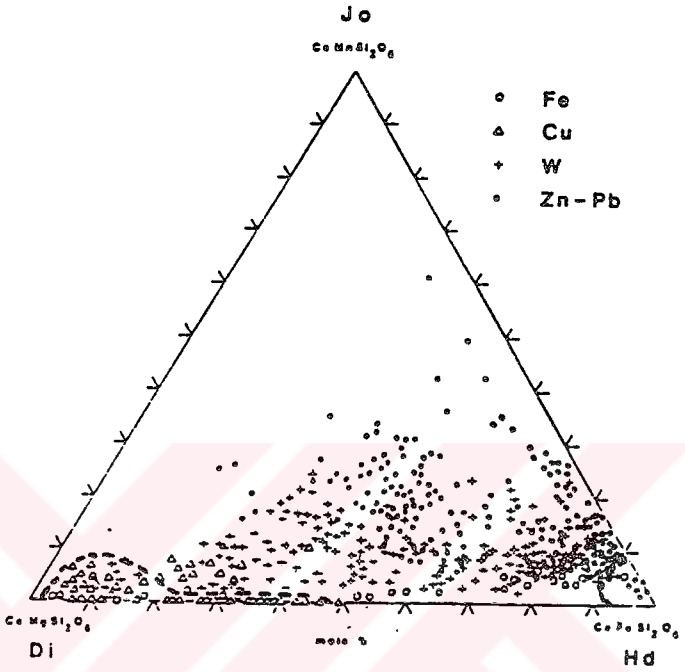

Figure 7.22. Fe-Mg-Mn ternary diagram for pyroxenes from the major skarn types in the world (After Einaudi, et al., 1981), dashed lines encircle the areas for the pyroxenes from the Akçakışla district.

ses of garnets from core to rim in the Keskin district (IK: Karamağara occurrence)

					IK4-1			
1	1	1	1	1	2	2	2	2
7	8	10	14	16	5	9	10	12
8,80	39,65	38,99	40,23	38,26	37,85	38,57	38,53	35,83
1,16	11,57	11,85	7,41	6,52	11,65	7,86	0,56	0,56
4,28	13,68	13,24	16,90	19,28	13,60	17,12	28,35	27,07
,69	1,67	1,17	1,25	0,84	1,29	1,27	1,26	1,00
-	-	-	1,43	-	-	-	-	0,24
6,38	36,55	36,07	32,13	35,26	35,21	34,90	35,27	34,04
02,30	103,11	101,32	99,35	100,15	99,60	99,73	103,97	98,74
,204	6,248	6,223	6,605	6,4	6,188	6,407	6,549	6,432
-	-	-	-	-	-	-	-	-
,103	2,149	2,23	1,434	1,286	2,209	1,54	0,113	0,119
,91	1,802	1,767	2,232	2,697	1,86	2,378	4,289	4,065
-	-	-	0,426	0,117	-	-	-	-
,666	1,548	1,554	1,623	2,346	1,626	2,706	3,431	3,445
,228	0,222	0,141	0,174	0,118	0,179	0,179	0,182	0,152
-	-	-	0,35	-	-	-	-	0,063
,233	6,171	6,37	5,652	6,321	6,169	6,211	6,423	6,548
4,97	42,21	41,62	59,28	65,37	42,70	58,17	96,98	96,86
1,50	54.30	55,89	32,24	32,80	54,50	39,04	0,27	-
,53	3.49	2,49	2,82	1,84	2,81	2,80	2,76	2,24
-	-	-	5,66	-	-	-	-	0,91

Table 7.10. Cont.

Sample #	IK4-1		IK4-2					IK4-2		IK4-2		
Line of sec.	2	2	2	2	2	2	2	2	2	1	1	1
Probe	13	14	1	2	5	7	10	11	12	2	3	4
SiO_2	38,76	37,20	38,99	37,10	37,58	38,86	36,96	39,28	37,41	36,17	37,54	38,25
Al2O3	8,81	-	9,21	5,17	3,47	7,25	2,33	3,78	-	-	7,97	7,98
$Fe_2O_{3(T)}$	16,76	27,65	16,32	20,60	23,84	19,22	24,55	21,97	26,88	27,16	16,81	18,23
MnO	2,47	0,96	1,10	0,76	1,11	1,02	0,83	1,72	1,01	0,76	1,08	1,06
MgO	-	-	-	-	-	-	-	-	0,29	-	-	-
CaO	34,24	33,85	36,13	34,74	35,57	36,76	34,66	33,05	33,70	33,32	34,85	36,72
TOTAL	101,02	99,65	101,75	98,37	101,57	103,09	99,34	99,79	99,52	97.41	98.25	102.24
Number of cations based on 24 (O)												
Si	6,357	6,555	6,34	6,394	6,39	6,333	6,487	6,626	6,626	-	-	-
Ti	-	-	-	-	-	-	-	0,032	-	-	1,587	1,54
Al	1,702		1,729	1,049	0,695	1,392	0,482	0,752	-	4,122	2,377	2,502
Fe_T	2,299	4,115	2,22	2,97	3,39	2,62	3,604	3,099	3,982	-	-	0,108
$Fe+2_{calc}$		0,015	0,097		0,145	0,113	-	0,429	0,004	3,518	2,069	2,16
$Fe+3_{calc}$	2,006	3,485	1,931	2,569	2,909	2,267	3,079	2,289	3,395	0,117	0,154	0,148
Mn	0,343	0,138	0,151	0,111	0,16	0,14	0,124	0,246	0,152	-	-	-
Mg	-	-	-	-	-	-	-	-	0,076	6,48	6,312	6,442
Ca	6,017	6,487	6,294	6,415	6,492	6,419	6,517	5,974	6,394	0,352	-	-
End members of garnets												
Andradite	54,85	100	53,08	71,80	81,44	62,87	87,05	78,08	99,10	100.00	57.39	59.31
Grossular	39,76	-	44,57	26,50	16,15	35,00	11,08	17,97	-	-	40,22	38,45
Spessart.	5,39	-	2,35	1,70	2,41	2,14	1,86	3,96	0,90	-	2,39	2,24
Pyrope	-	-	-	-	-	-	-	-	-	-	-	-

Table 7.11. Correlation matrix for the major oxides analyzed in the garnets of the Keskin district.

	SiO_2	Al_2O_3	$Fe_2O_{3(T)}$	MnO	MgO	CaO
SiO_2	1					
Al_2O_3	0.70	1				
$Fe_2O_{3(T)}$	-0.71	-0.99	1			
MnO	-0.27	-0.12	0.14	1		
MgO	-0.09	-0.23	0.19	0.41	1	
CaO	0.26	0.53	-0.48	-0.31	-0.58	1

SiO_2content of the garnets range from 34.60 to 40.23%. Al_2O_3 contents range from 0.0 to 11.85%. $Fe_2O_{3(T)}$ contents range from 13.24 to 28.35. MnO is present as less than 4 % in the garnets, and it has a range of 0.76 to 3.11%. MgO contents range from 0.0 to 1.43%. CaO contents range from 32.13 to 36.72% in the garnets (Table 7.10).

The relationships of Al_2O_3 contents with $Fe_2O_{3(T)}$, SiO_2, MnO and CaO contents are notable in the garnets. Al_2O_3 contents is negatively correlated to $Fe_2O_{3(T)}$ contents (Table 7.11) (Figure 7.23). This negative relation between Al_2O_3 and $Fe_2O_{3(T)}$ in the garnets Al_2O_3 is due to Al^{+3} and Fe^{+3} exchange or the changes in the Al/Fe ratio in the hydrothermal fluid from which the garnet is formed. This relation is well observed in the microprobe traverses (Figure 7.24). Figure 7.23 and 7.24 show that Al2O3 and $Fe_2O_{3(T)}$ contents oscillate from core to rim. This gives way to consequent oscillations in the compositions of garnets between grossular and andradite.

Al_2O_3 contents are positively correlated to SiO_2 contents (0.70, Table 7.11), and SiO_2 increases with Al_2O_3 contents. This is more pronounced in the garnet rims (Figure 7.23). Al_2O_3 contents are positively correlated to CaO contents in the garnets (0.53, Table 7.11) (Figure 7.23). Thus, it is possible to say that CaO contents also oscillate from core to rim together with Al_2O_3 from core to rim. Since the Ca is a component supplied from the wall rocks, the Ca depletion in the garnet composition from core to rim shows that the interactions between hydrothermal fluid and the wall rocks decreased during the formation of garnets. Thus, this results in the formation of

less calcic garnets in the Keskin district. The relationships between Al_2O_3 contents and MnO contents are not significant (-0.12, Table 7.11).

Similar to Al2O3 contents, $Fe_2O_{3(T)}$ also display some relationships with SiO_2, MnO, MgO and CaO in the garnets. $Fe_2O_{3(T)}$ contents are negatively correlated to SiO2 (-0.71, Table 7.11) and CaO contents (-0.48, Table 7.11). $Fe_2O_{3(T)}$ contents do not display significant relationships with MgO and MnO contents (Table 7.11 and Figure 7.25). The garnets show a scattered distribution pattern in the $Fe_2O_{3(T)}$-MgO diagram (Figure 7.25).

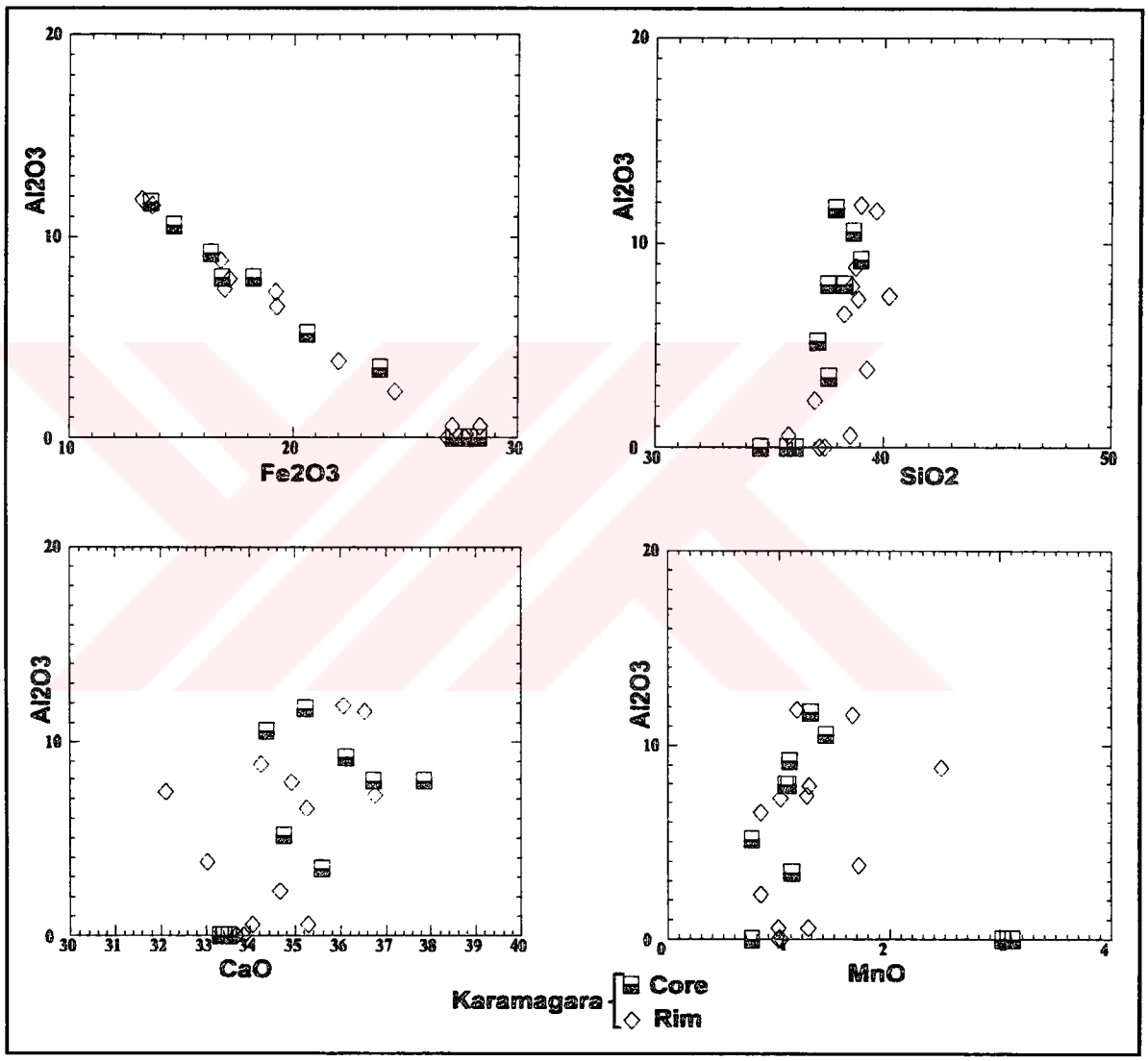

Figure 7.23. The relationships between Al_2O_3 and other major oxides in the garnets from the Keskin district

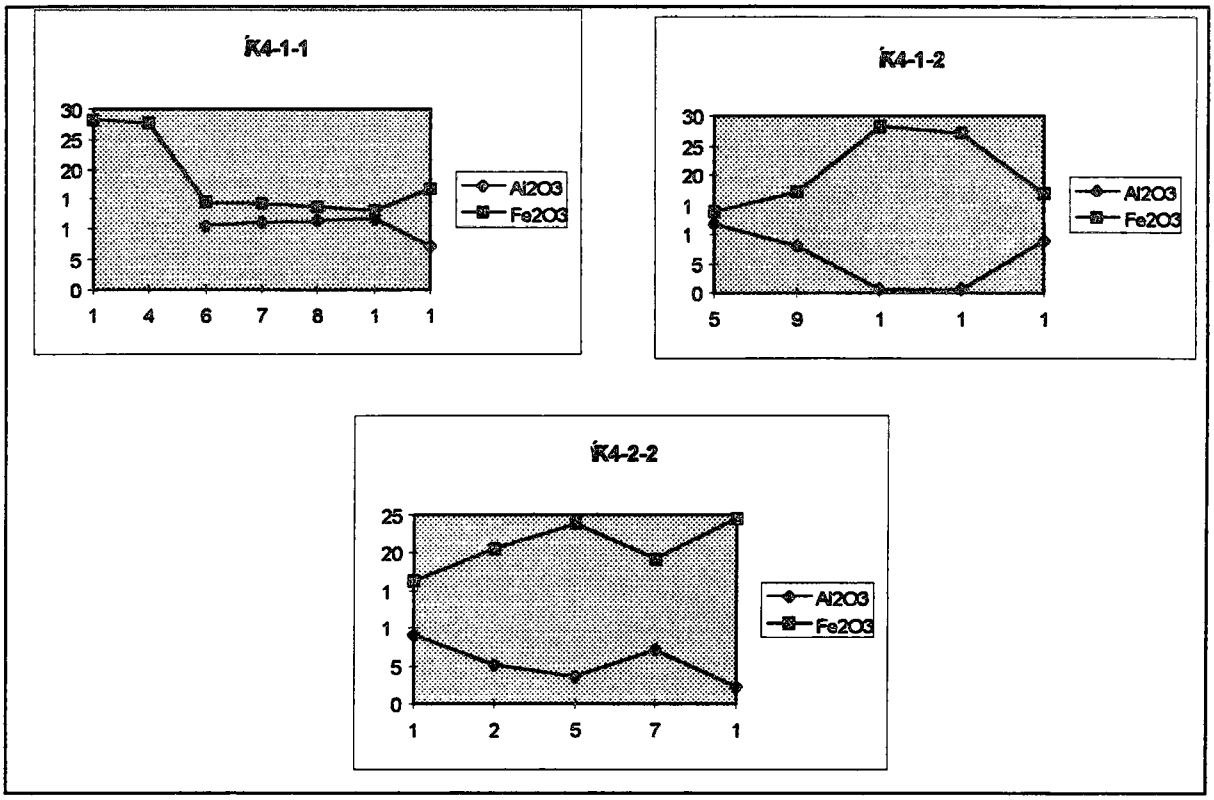

Figure 7.24. Microprobe traverses from core to rim in the Keskin district

The recalculation of EMP data in the Table 7.10 shows that the garnets in the Keskin district contain grossular, andradite, pyrope and spessartine. Grossular ranges from 0.0 to 55.89%, and andradite ranges from 41.62 to 100%. Pyrope and spessartine range from 0.0 to 5.66%, and 0.0 to 5.39%, respectively. In general the garnets in the Keskin district ranges from pure andradite (Ad_{100}) to $Gr_{55.89}Ad_{41.62}Sp_{2.49}$. Thus, the garnets in the Keskin district are termed as grandite garnets except for those with 100% andradite. The Gross-And-Pyralspite ternary diagram (Figure 7.26) for the garnets show that they are clustered between Ad_{40} to Ad_{100}. The garnet cores are characterized by grandite garnets with $Gr_{40}Ad_{60}$ to Ad_{100} compositions. The rims and cores of garnets show more or less an overlapping distribution. This is due to the oscillations between Al_2O_3 and $Fe_2O_{3(T)}$ contents of garnets from core to rim.

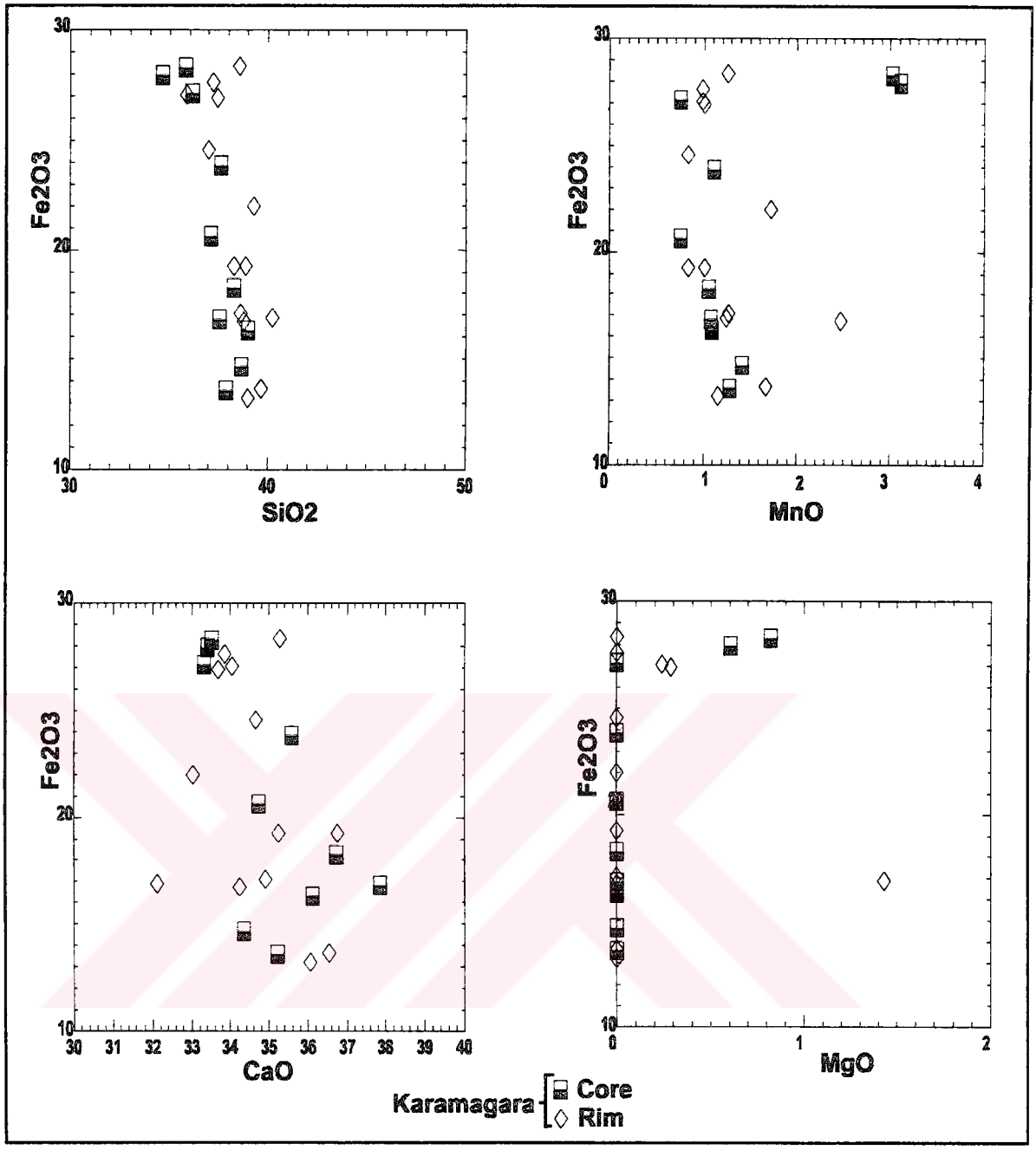

Figure 7.25. The relationships between $Fe_2O_{3(T)}$ and other major oxides in the garnets from the Keskin district

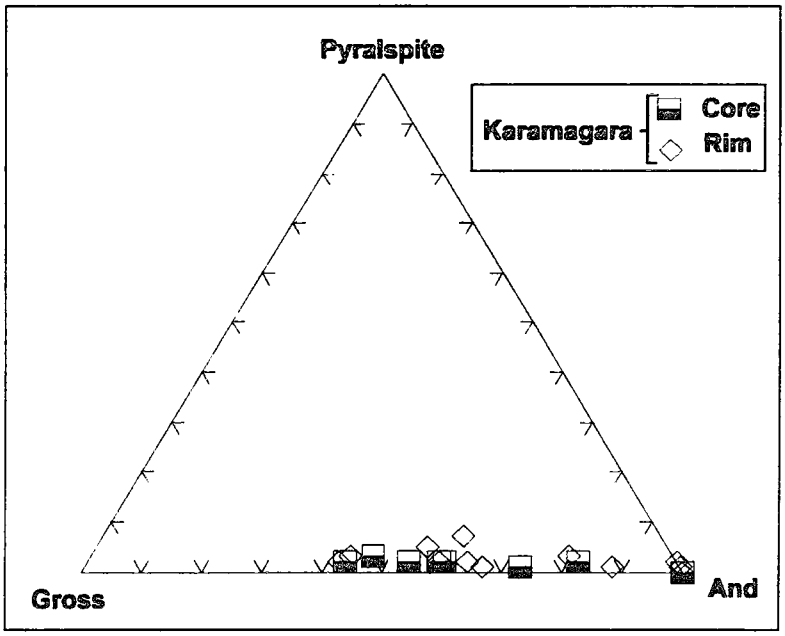

Figure 7.26. Gross-And-Pyralspite ternary diagram for the garnets in the Keskin district

The relationships between grossular and andradite are similar to those observed in other districts. They are inversely related to each other (Figure 7.27). The grossular contents decrease as andradite contents increase in the garnet compositions. Figure 7.24 , 7.26 and 7.27 indicate that grossular and andradite end-members oscillate in the garnets from core to rim. This results in the formation of oscillatory zoning in the garnets of the Keskin district.

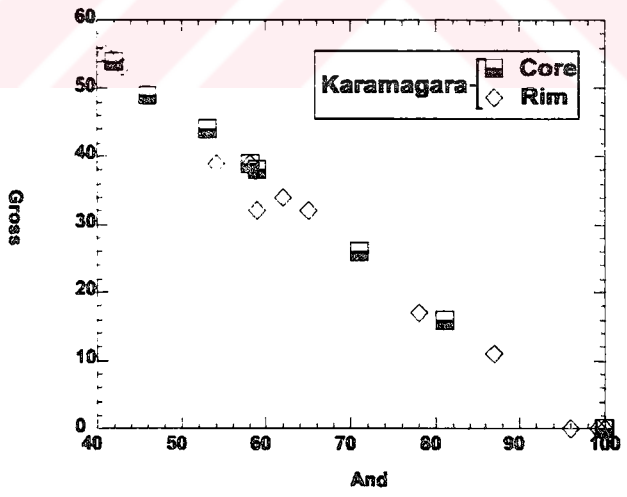

Figure 7.27. The relationships between andradite and grossular contents of the garnets in the Keskin district.

7.6. Discussion

7.6.1. Constraints about oscillatory zoning in garnets

The oscillatory zoning is a particular class of non-equilibrium texture, and it is well developed in minerals that show solid solutions such as garnets and pyroxenes formed in a range of open-system environments. The oscillatory zoning acts both as an indicator of infiltration metasomatism where it is found, and an argument against a metamorphic origin in rocks from which it is absent (Yardley et al., 1991). Oscillatory zoning is best known from skarn garnets and pyroxenes. Examples of oscillatory zoning in garnets using EMP and petrographical microscope are described from the Evciboyuntepe occurrence in the Akdağmadeni district, Barajdoğusu and Özgebaca occurrences in the Akçakışla district, and Karamağara occurrence in the Keskin district. The EMP studies show that the zoning in the garnets in these occurrences, is in the form of compositional zoning formed by the oscillations between Al_2O_3 and $Fe_2O_{3(T)}$ and hence grossular and andradite contents of the garnets caused by the oscillations in the oxidation potential of the hydrothermal system in which the garnet was formed.

The critical factor yielding the development of oscillatory zoning is that growth is formed under non-equilibrium conditions, and thus the meaning of the term "open system" should be discussed. The open system refers to a chemical system in which the material is either added or removed from the system. In this section, the open system refers to the system where the fluid introduced is not in chemical equilibrium with the pre-existing assemblage of phases. According to Ortoleva et al. (1987), the essential requirements for the formation of oscillatory zoning are: chemical disequilibrium and some sort of noise in the system that help to initiate the zoning.

Oscillatory zoning can reflect externally imposed fluctuations in some thermodynamic parameters (P, T, f_{O2}, etc.) in the hydrothermal system, or may arise from local disequilibrium between an individual crystal and the adjacent fluid medium. In the garnets of the studied areas, it seems that the cause of oscillations is externally controlled in skarns because all of the zoned garnets display similar zoning patterns. Also, it is evident from the microprobe traverses that the Al_2O_3 and $Fe_2O_{3(T)}$ contents of the zoned garnets in the occurrences are negatively correlated with each other

implying an exchange between cations of these oxides. The zoning, therefore reflects either changes in the activity ratio; a_{Fe+3}/a_{Al+3} as described by Yardley et al. (1991), or changes in the distribution of Al and Fe cations between fluid and mineral. The zonal oscillations, therefore may be explained by cyclical variations in the composition of the hydrothermal fluid. These variations involve decrease or increase in the amount of iron accompanied with the increase and decrease of aluminum, or change in the oxidation state of iron which also controls the amount of iron present in the hydrothermal fluid (Lessing and Standish, 1973; Yardley et al. ,1991). Ferric iron fits into the R+3 lattice site of garnet, but ferrous iron does not normally enter this site (Lessing and Standish, 1973).

Optical examination of oscillatory zones (Figure 5.11, 5.12, 5.14 and 5.15) shows that they are quite narrow and exhibit sharp contacts. This would suggest a rapid crystal growth and/or rapid changes in the composition of hydrothermal fluid. The study of Figure 5.11 and 5.12 indicates that the chemical variations that controlled the oscillatory zoning, are not gradational, but abrupt. This is most probably related to the relative activities of the Al and Fe cations in the hydrothermal fluid which is strongly controlled by the oxidation state of the fluid (Jamtveit, 1991). In the view of these chemical settings, it is here proposed that the oscillations reflect fluctuations in a_{Fe+3} in the fluid phase as a consequence of rapid changes in the oxidation state of the fluid (of the cations, Fe is the most susceptible cation to changes in the oxidation state of the hydrothermal fluid. As shown by Jamtveit (1991), the composition of solid solution series like grossular-andradite binary system may be very sensitive to small changes in the hydrothermal fluid composition, and any change in this system is recorded as the formation of compositionally different garnets as observed in the garnets of the

high Al_2O_3 contents of the garnet cores are considered to be controlled by wall rocks in the original rocks during initial metamorphic reactions that cause metasomatism (Jamtveit, 1991). Most skarns in the world have an early metamorphic stage and this results in grossularitic garnet cores which was subsequently overprinted by metasomatic/magmatic fluids resulting in more andraditic rims (Meinert, 1997; written comm.). The zoning is considered to be compositional mostly controlled by the relative activities of trivalent Al and Fe (mainly of Fe), and the Al-Fe partitioning between garnet and solution. Thus, it is necessary to discuss the factors controlling the changes in the activities and Al-Fe partitioning. In their studies, Jamtveit et al. (1995) discussed the factors controlling the above parameters in zoned grossular-andradite garnets in the hydrothermal systems using the solid solution-aqueous solution equilibria, grossular-andradite (grandite) binary system. They proposed that that the Al-Fe partitioning in the solution is sensitive to variations in pH, fO_2 and Cl^- activity, due to differences in aqueous complexation behavior between Al and Fe. In order to better understand the relative effects of T, pH, fO_2 and, Cl^- the calculated Al-Fe partitioning between garnet and aqueous solutions should be examined. The complex relationships concerning total mole fraction of aluminum $X_{Al}T$ and total mole fraction of grossular $X_{gro}T$ are shown in Figure 7.27 and Figure 7.28. These figures indicate that for grossular-rich (X_{gro}>0.4) garnet compositions, the Al-Fe fractionation between garnet and hydrothermal solution is very sensitive to variations in temperature, pH, fO_2, and salinity. For example for a given pressure, the T decrease corresponds to increase in the total mole fraction of Al in the aqueous solution, and enable the Fe rich garnet to form (Figure 7.28). The pressure has less pronounced effects on the Fe-Al partitioning between garnet and the aqueous solution. The most pronounced effects

Barajdoğusu samples and Evciboyuntepe (except for Özgebaca and Karamağara, since the garnets in these occurrences are not andradite-rich compared to

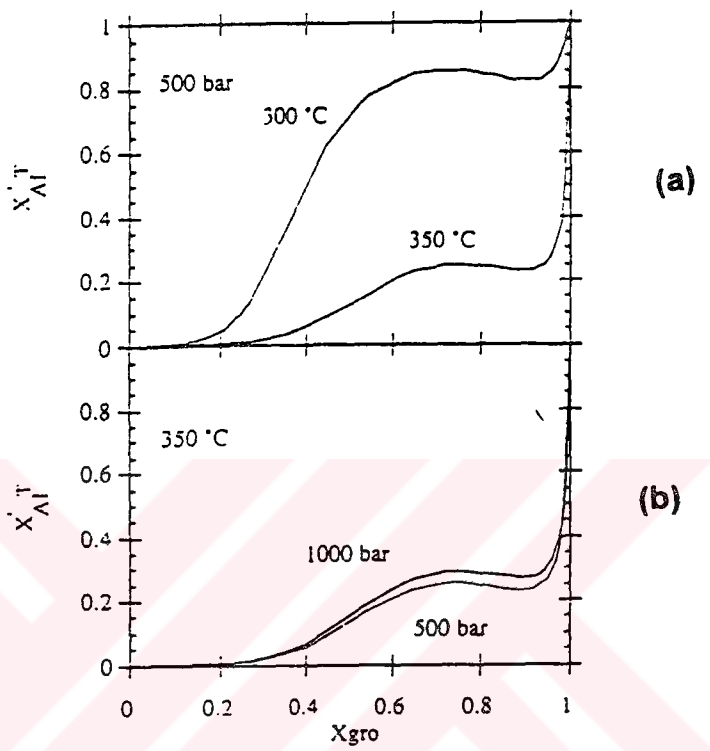

Figure 7.28. Calculated Al-Fe partitioning between garnet and aqueous solutions at neutral pH=5.5, $fO_2=10^{-32}$ and $[Cl]^T \cong 1.0$. (a): effect of varying T, (b): effect of pressure (After Jamtveit et al., 1995).

other occurrences) indicate that the garnet compositions were controlled partly by the system in which the temperature is lower and oxygen fugacity is higher, and salinity is high compared to that of core composition garnets. The relative enrichment of grossularitic garnets in the Özgebaca and Karamağara occurrences could possibly be related to the initial contact metamorphism controlled by initial protolith composition rich in Al that cause aluminum enrichment in the garnet cores (Yardley et al., 1991; Jamtveit et al., 1992; Meinert, 1997 written comm.).

The possible causes of the changes in pH, T, P, fO_2, and salinity need to be discussed to understand the causes of the garnet zonation in the skarns of the studied districts. The common processes such as boiling, fluid mixing, temperature and pressure fluctuations would have the potential to cause fluctuations in the garnet composition (Jamtveit, 1991; Jamtveit, et al., 1995). Boiling of magmatically

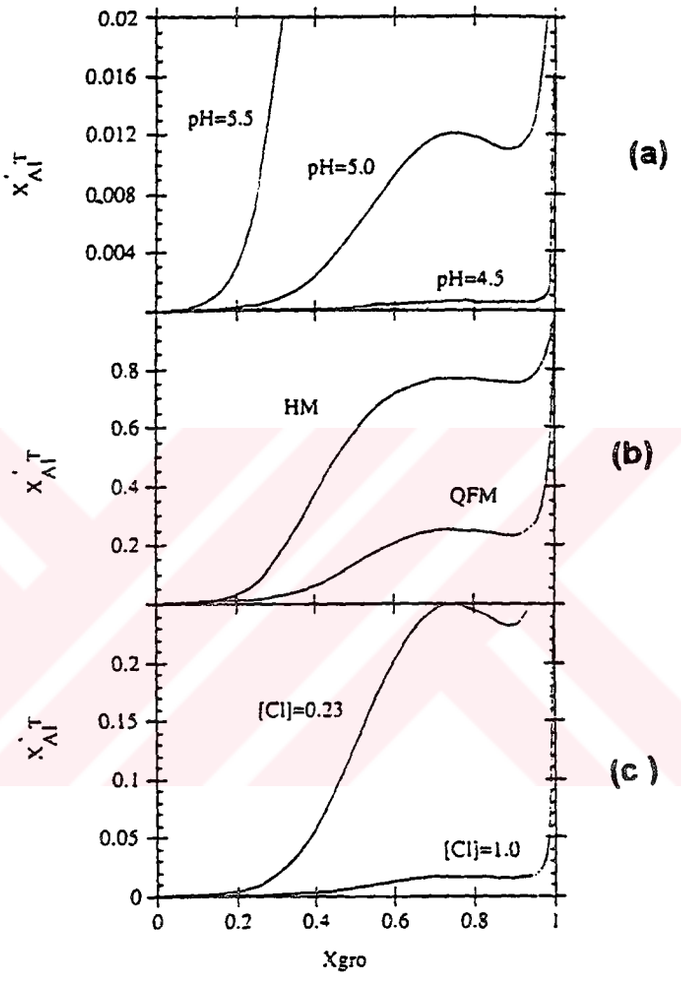

Figure 7.29. Calculated Al-Fe partitioning between garnet and aqueous solutions at 350°C, 500 bar, (a) effect of pH at $fO_2=10^{-32}$ and $[Cl]^T \cong 1.0$, (b) effect of fO_2 at pH=5.5 and $[Cl]^T \cong 1.0$ at $fO_2=10^{-28}$, (c): effect of salinity at pH=5.5 and $fO_2=10^{-32}$ (HM: hematite buffer, QFM: Quartz-fayalite-magnetite buffer) (After Jamtveit et al., 1995).

dominated fluid would normally result in oxidation and pH increase in the liquid phase as CO_2 and reduced species such as H_2 and H_2S are fractionated into the vapor phase (Drummond and Ohmoto, 1985). Mixing with meteoric fluids would lead to a salinity decrease and oxidation (Jamtveit et al., 1995). Both of these variables act together and force garnet solution towards more andradite-rich garnet compositions. The andradite enrichment from core to rim is probably related to increase in the total mole fraction of Fe in the solution and mixing with the meteoric water at the later stages of garnet formation in the garnet bearing skarns of the studied areas. The hydrothermal system becomes oxidized due to mixing with the meteoric water (Jamtveit and Hervig, 1994; Jamtveit et al., 1995) thus the Al/Fe partition work for the iron, and iron is oxidized to form ferric iron. It is this oxidized iron that can enter the structure of the garnets. In the previous paragraphs it was emphasized that the ferrous iron can not enter the R+3 site of the garnet structure but the ferric iron can. This makes the garnet compositions more iron-rich and andraditic as the oxidation continues. Therefore, all these indicate that the garnet compositions in the studied areas are somewhat akin to an open system or oxidation and, are externally controlled at least for the late-stage garnet formations. The influx of meteoric water begins during these stages. The major role of meteoric water influx is to oxidize the hydrothermal system (Jamtveit and Hervig, 1994), and to control Al-Fe partitioning, and Al/Fe exchange between the garnet and the hydrothermal fluid.

The extent of fluid mixing is strongly controlled by hydrofracturing (Jamtveit and Andersen, 1991; Jamtveit et al., 1993). Jamtveit et al. (1995) indicated that high growth rates give way to the clogging of the flow system, decrease in permeability, and build-up of fluid pressure that leads to hydrofracturing and new period of high fluid flow and mineral formation (Jamtveit et al., 1995). In the garnets of the studied areas, there is a number indications of high flow rate and hydrofracturing. As discussed in the petrography chapter, many morphological instabilities such as dissolution structures and cellular structures appear in the zoned garnets, and they are interpreted so as to be indication of high flow rate in the hydrothermal system (as suggested by Jamtveit and Andersen, 1992; Jamtveit et al., 1993). Also, the presence of microfractures in the garnets described in the petrography section are the direct indications of the effects of extensive hydrofracturing in the hydrothermal system. In this respect, the garnet-

pyroxene skarns in the Evciboyuntepe occurrence (Akdağmadeni district), Barajdoğusu and Özgebaca occurrences (Akçakışla district), and Karamağara occurrence in the Keskin district were formed in a hydrothermal system where the composition of the fluid changes frequently because of high flow rates, and high growth rates. The hydrofracturing may lead to flow of meteoric water into the hydrothermal system (Jamtveit and Hervig, 1994), and lead to salinity, temperature and pH variations as well as oxidation. In the studied districts, these physico-chemical parameters may cause changes in the total mole fraction of Al in the solution that changes the Al/Fe partitioning between garnet and solution, and hence changes the compositions of garnets formed from these solutions.

Kwak and Tan (1981) proposed that if andradite dominates particularly at garnet cores, the skarn is closer to the granite contact. In this respect, the relative enrichment of andradite in the garnet cores in the Barajdoğusu and Evciboyuntepe occurrences, and enrichment of grossular in cores in the Özgebaca and to some extent Karamağara occurrences could indicate the garnet-pyroxene skarns in the Barajdoğusu and Evciboyuntepe occurrence were formed close to the plutonic contacts, and thus the Al^{+3}/Fe^{+3} partition was controlled by magmatic waters derived from the pluton. Therefore, by considering only the garnet compositions and Kwak and Tan's (1981) suggestion, it is possible to differentiate the garnet-pyroxene skarns as proximal and distal relative to each other. However, Meinert (1997, written comm.) suggests that the millimeter and micrometer scale zonation patterns are of a mystery, and the statement such as Fe-rich cores being close to the pluton is not always systematic, and is not likely to be a productive line of inquiry. It is very clear from Figure 3.2 that the Özgebaca is also very close to the granite contact. Therefore, Kwak and Tan's (1981) suggestion can not be accepted. Instead, it is proposed here that the andradite-rich core compositions are controlled by oxidation potential of the hydrothermal system.

7.6.2. Na_2O-K_2O and Al_2O_3 contents of skarn pyroxenes

The total alkali content of the pyroxenes in the Barajdoğusu occurrence are quite high compared to the total Na2O and K2O content (0.02 to 0.11 in Brijraj et al., 1988; 0.0 to 1.15 in Nakano et al., 1994) of common skarn pyroxenes in the literature. The total alkali contents of the studied pyroxenes in the Barajdoğusu occurrence

range from 0.0 to 2.47%. Based on the total alkali contents, Brijraj et al. (1988) proposed that low alkali contents in the pyroxenes suggest that iron is present as nearly as Fe+2. By contrast, high total alkali contents of the pyroxenes in the Barajdoğusu occurrence could indicate that iron exists as Fe^{+3} (Brijraj et al., 1988). As diopside favors the ferric state of iron (Fe^{+3}) while hedenbergite favors the ferrous state of iron (Fe^{+2}) (Nakano et al., 1994), in the Barajdoğusu occurrence, the diopside component predominates over the hedenbergite component in the clinopyroxene composition (Figure 7.20 and 7.21) (as suggested by Brijraj et al., 1988).

7.6.3. Mg/Fe and Mn/Fe ratios of pyroxenes

The EMP studies show that the Mg/Fe ratios vary widely in the pyroxenes from studied the occurrences. The Mg/Fe ratio of pyroxenes range from 0.0 to 27.91 (Table 7.7) (Bayramali: 0.33 to 2.30, Çiçeklitepe: 1.83 to 2.71, Radarbaca: 2.60 to 3.74, Barajdoğusu: 0.0 to 27.91, and Özgebaca: 0.08 to 6.94). However, their Mn/Fe ratio is relatively restricted for each occurrence. The Mn/Fe ratio of pyroxenes range from 0.0 to1.37 (Bayramali:0.8 to 1.37, Çiçeklitepe: 0.03 to 0.17, Radarbaca: 0.48 to 0.59, Barajdoğusu: 0.0 to 1.15, and Özgebaca: 0.0 to 0.09). These ratios are used as a parameter to differentiate the skarns in the literature (Nakano et al., 1994). The occurrences differ clearly from each other by their ratios as given above. Those with high Mn/Fe ratio indicate the johannsenitic pyroxenes and those with high Mg/Fe ratio indicate diopsidic pyroxenes. In the Bayramali, Çiçeklitepe and Barajdoğusu occurrences, johannsenites with considerable amounts of diopside and hedenbergite components are present. Such pyroxenes characteristically are associated with Pb-Zn sulfides. An extreme example appear in the Bayramali where the pyroxenes contain unusual Mn/Fe ratios (1.37) and they cover a very wide area in the diopside-johannsenite-hedenbergite diagram (Figure 7.9).

Several models are possible to account for the wider variation in the Mg/Fe ratio of pyroxenes than in their Mn/Fe ratio. Nakano et al. (1994) noted that Mg has a higher tendency to be concentrated in the clinopyroxene whereas Mn has a lesser tendency. Therefore, if skarn pyroxene crystallizes from a relatively homogeneous fluid with respect to Mg-Mn-Fe proportions, then the Mg fraction in the fluid would be readily modified. This leads to the formation of a fluid with relatively homogeneous Mn/Fe ratio but with variable Mg/Fe ratio according to the modification of the Mg fraction in

the original fluid. A suite of pyroxenes when formed from fluid with a variable Mg fraction would have a positive Fe-Mn (or negative Mg-Mn relation) (Nakano, 1991); The Mn/Fe ratio in pyroxenes is dependent on Mg-fraction in the original fluid. Nakano (1989) proposed a fluctuation model to account for the local variation of pyroxene formation (including Mg/Fe variations) in terms of the associated fluid composition. This model assumes a cation exchange equilibrium of Mg, Mn, and Fe between growing pyroxene and surfaces and the hydrothermal fluids. According to this model, large heterogeneous clinopyroxene compositions can be produced simultaneously by the unsystematic fluctuation of fluid compositions about the mean solution component concentrations, although the mechanism of fluctuation remains unknown.

A negative relationship occurs between Fe_2O_3 and MgO (Figure 7.8 and 7.19), that is the magnesium content decreases with increase in iron content. This result verifies the fact that the fluids depositing pyroxene in calcic exoskarns are "depleted first in the Mg and then in Fe, so that finally only Mn remains to form johannsenite" (Burt, 1977). Therefore, Burt (1977), Einaudi et al. (1981), Einaudi (1982a), and Meinert (1987) argued that the johannsenitic bearing pyroxenes are found commonly in the skarns distal to the pluton, and diopsidic pyroxenes are likely to be found at proximal skarns. However, Yun and Einaudi (1982), suggested that the Mg enrichment in skarn pyroxenes is related to the increasing dolomitic wall rock control of fluid compositions, and is not related to the oxidation state of the of the fluid phase.

The composition of pyroxene forming fluid would have been changed by various factors including the dissolution and composition of host minerals (Nakano, 1989), migration processes (infiltration and diffusion), and fluid-pyroxene partitioning of the elements (Nakano et al., 1994). Among these, the dissolution and composition of host minerals, and fluid-pyroxene partitioning of the elements seem to be more appropriate to explain the compositional heterogeneity of the skarn pyroxenes within the occurrences. Since the compositional differences are commonly observed in each occurrence, region-wide systematic changes in fluid composition seem be true , and it should also be considered that the dolomitic wall rocks could play a part in the original Mg fraction of pyroxene forming fluid, and partitioning of elements between fluid and growing pyroxene.

The association of diopsidic pyroxene and andraditic garnet in Cu-skarns with slightly later quartz-magnetite-sulfide assemblages is consistent with relatively high oxidation states. This relative high oxidation state of Cu-skarns can also be inferred from the common presence of hematite (Einaudi, 1982a). In the Barajdoğusu occurrence, diopsidic pyroxene, andradite and hematite are present. Therefore, it could be proposed that the Barajdoğusu occurrence was under the influence of relatively high oxidation state compared to other occurrences. Under oxidizing conditions, first diopside is precipitated from the pyroxene forming fluid. As noted by Burt (1977), the Mg is depleted first and diopside is formed; the next cation, Fe, is ready to be used up by hedenbergite formation. But under oxidizing conditions, Fe in solution favors andradite relative to hedenbergite (Meinert, 1987) since the iron is present as Fe+3, it is used up by the ongoing andradite formation. This also explains the coexistence of diopside with andraditic garnet in the Barajdoğusu occurrence.

CHAPTER 8

GEOCHEMICAL SIGNATURE OF GRANITOIDS ASSOCIATED WITH SKARN OCCURRENCES.

Many ore deposits are directly related to magmatic activity, and the genetic association between magmatism and mineralization is generally accepted. Most major skarn deposits occur in carbonate rocks, close to but usually not within the associated pluton. The broad correlations between igneous composition and skarn type were described by several workers (Zharikov, 1970; Shimazaki, 1975, 1980; Einaudi et al., 1981; Kwak and White, 1982; Meinert, 1983; Newbery and Swanson, 1986; Newbery, 1987; Meinert, 1990; 1993; 1995). Averages of large amounts of data for each skarn type can be summarized on a variety of compositional diagrams to show distinctions between the skarn types. In other words, the range in igneous compositions associated with skarns makes it possible to address the relationship between the composition of igneous rocks and the metal content of the associated skarns.

This section aims to present the chemical classification of the granitoids from the Akçakışla district, and investigate the genetic association between skarn occurrences in three districts and intrusive rocks associated with or nearby them by major and trace element chemistry data compiled from several studies. The geochemical data for the granitoids of the Akdağmadeni district (Table 8.1) are from Tülümen (1980), of the Akçakışla district from Erler (unpublished data) and from this study (Table 8.2), and of the Keskin district (Table 8.3) from Bayhan (1989) (Keskin Pluton).

8.1. Analytical methods

The samples from the Akçakışla Granite were analyzed for major and trace elements using ARL 8420 XRF spectrometer in the Department of Earth Sciences at the University of Keele (England). The whole rock geochemistry analyses, like other analyses, were conducted according to general scheme adopted at Keele University for the preparation of rock samples prior to analysis. The XRF analyses of major elements were done by squashed fused beads, and trace elements by

Table 8.1. Major and trace element analysis of samples from the granitoids within the Akdağmadeni district (After Tülümen, 1980)

SAMPLE	122A	104A	146A	137A	152A	80A	167A	AK1	58A	136A	26A	73A	149A	82A	172A	136A
SiO2	66,99	73,45	55,23	66,01	70,42	68,08	68,76	63,6	67,42	65,71	68,75	73,83	65,19	67,81	67,92	65,71
TiO2	0,16	0,06	1,19	0,49	0,28	0,19	0,1	0,26	0,16	0,21	0,15	0,09	0,21	0,17	0,19	0,21
Al2O3	16,48	14,08	26,53	15,24	15,59	15,77	15,71	17,09	16,39	16,57	15,22	14,26	16,81	15,78	15,59	16,58
Fe2O3T	1,27	0,36	2,77	5,18	1,98	0,86	0,89	1,98	0,48	1,41	1,33	0,64	1,59	1,31	1,49	1,41
MnO	0,03	0	0,02	0,46	0,03	0,02	0,01	0,04	0,02	0,02	0,02	0,02	0,02	0,02	0,02	0,02
MgO	0,36	0,16	0,92	2,51	0,71	0,44	0,3	1,24	0,49	0,66	0,68	0,33	0,59	0,48	0,71	0,66
CaO	1,71	0,35	1,65	1,23	2,2	2,07	0,13	2,46	1,02	2,3	1,62	0,29	2,02	1,58	1,7	2,3
Na2O	7,42	4,9	2,95	4,5	4,39	7,1	11,41	7,44	7,73	8,08	7,4	4,69	8,13	7,51	7,06	8,08
K2O	5,27	6,42	6,84	4,15	4,07	5,31	2,61	5,7	6,16	4,9	4,75	5,82	5,28	5,21	5,17	4,9
P2O5	0,06	0,02	0,27	0,12	0,09	0,08	0,02	0,11	0,06	0,08	0,06	0,02	0,08	0,08	0,09	0,08
TOTAL	99,75	99,8	98,37	99,89	99,76	99,92	99,94	99,92	99,93	99,94	99,98	99,99	99,92	99,95	99,94	99,95
Rb	217,3	276,7	257,1	272,1	220,8	130,1	101	243,7	210,8	209,7	258,5	270,5	244,8	222,5	159,4	209,7
Sr	413	49,5	453,8	287,9	522,7	542,1	26,9	546	506	494,4	312,4	54,2	511,7	316,3	405	494,4
Ba	513,7	94,3	904,7	690	629,5	448,8	95,3	823,7	751	695,2	223,9	343	661,9	419,4	621,8	695,2
Zr	109,1	91,3	295,4	215,2	138,7	123	1168	158,6	160,5	149,5	147,8	95,9	134,6	142,2	119,6	149,5

Table 8.2. Major and trace element analyses from the Akçakışla Granite (samples from A-8 to Ö-1 from Erler, unpublished data)

SAMPLE	A-8	S-8	A4/74	A-12	A-13	A-14	Ö-1	A-25	A-26	A-27	A-28
SiO2	66,8	63.85	67,41	62,88	68,91	67,73	69,21	70,8	66,61	66,27	67,96
TiO2	0,39	0,49	0,34	0,44	0,33	0,33	0,32	0,35	0,46	0,47	0,34
Al2O3	16,18	17,28	16,87	17,92	15,04	16,65	16,26	15,11	16,29	16,42	16,1
Fe2O3T	3,07	3,14	2,17	3,24	2,3	2,55	2,11	2,01	3,18	3,16	2,85
MnO	0,05	0,04	0,03	0,05	0,05	0,04	0,02	0,02	0,04	0,05	0,06
MgO	1,7	2,06	1,4	2	1,02	1	0,86	0,42	1,19	1,09	0,71
CaO	2,55	3,22	2,45	3,4	2,07	2,28	1,65	1,54	2,92	2,84	2,17
Na2O	4.43	4.58	4.19	4,62	3,67	4,47	3,73	3,87	4,6	4,67	4,47
K2O	4.56	4,44	4,64	4,93	5,28	4,56	5,06	5,02	4,23	4,21	5,24
P2O5	0,25	0,3	0,17	0,33	0,2	0,17	0,12	0,06	0,2	0,21	0,19
LOI	0,1	0,26	0,42	0,39	0,64	0,16	0,38	0,49	0,35	0,49	0,22
TOTAL	100,8	99,66	100,1	100,2	99,51	99,94	99,72	99,69	100,07	99,88	100,3
Rb	226	182	241	198	213	244	261	220	194	212	272
Sr	633	796	574	888	546	608	463	393	641	626	591
Ba	985	1149	948	1459	724	994	1094	965	961	991	1143
Zr	194	306	223	198	184	189	274	227	190	185	212
Y	27	27	28	25	28	28	30	17	18	17	16
Nb	26	37	39	14	45	29	35	20	24	22	25
Cu	28	36	27	28	34	24	33	10	5	4	5
Pb	19	39	33	18	35	37	35	26	22	29	34
Zn	29	60	23	37	43	48	101	37	42	32	48

Table 8.3. Major and trace element analyses from the Keskin Pluton (After Bayhan, 1989)

SAMPLE	KE-31	KE-33	KE-40	KE-41	KE-43	KE-45	KE-47	KE-48	KE-50	KE-53	KE-55	KE-62	KE-69
SiO2	72,67	73,4	72,34	74,04	70,9	72,63	69,04	70,48	74,46	71,36	71,64	71,48	72,07
TiO2	0,29	0,16	0,28	0,17	0,21	0,21	0,37	0,24	0,16	0,24	0,32	0,21	0,16
Al2O3	13,77	13,26	14,2	12,86	14,1	14,02	16,23	16,76	13,26	14,25	14,84	13,6	12,44
Fe2O3T	0,99	1,9	3,05	1,79	2,54	2,335	3,86	3,1	2,33	2,2	3,05	2,87	2,4
MnO	0,36	0,05	0,07	0,02	0,04	0,05	0,08	0,07	0,04	0,45	1,85	3,37	0,05
MgO	0,29	0,51	0,66	0,32	0,75	0,57	1,17	0,73	0,45	0,65	0,93	0,69	0,56
CaO	1,69	1,85	2,1	1,65	2,06	1,51	2,82	2,81	1,85	2,57	2,91	2,43	2,33
Na2O	3,35	3,28	3,95	3,11	2,89	3,77	3,32	3,76	3,37	3,37	3,29	3,23	3,19
K2O	4,58	4,08	3,76	5,45	5,38	3,72	3,97	2,86	3,73	2,43	3,45	2,95	4,05
LOI	0,55	0,44	0,93	0,35	0,54	1,82	0,53	0,62	0,59	0,52	0,31	0,28	0,37
P2O5	0	0	0	0	0	0	0	0	0	0	0	0	0
TOTAL	98,54	98,93	101,34	99,76	99,41	100,64	101,39	101,43	100,24	98,04	102,59	101,11	97,62
Rb	147	175	110	241	267	126	152	115	147	126	147	163	105
Sr	154	114	85	186	214	172	186	136	156	142	192	214	126
Ba	546	437	1037	437	382	926	982	585	818	607	547	491	362

pressed powder pellets. The Appendix 2 describes the procedures and methods applied for sample preparation and XRF analysis.

8.2. Geochemistry of the Akçakışla Granite

In order to see the overall trends and possible genetic relationships, Harker diagrams were used. On the Harker diagrams, SiO_2 against other major oxides of the Akçakışla Granite, usually display linear correlations with Al_2O_3, $Fe_2O_{3(T)}$, MgO, CaO and P_2O_5. However for TiO_2, Na_2O and K_2O the relationship is relatively scattered (Figure 8.1a and 8.1b). These diagrams suggest a continuous fractional crystallization from a single magma. Harker diagrams of the selected trace elements are given in Figure 8.1b. In this diagram, Rb, and Nb increase with SiO_2. However, Ba and Sr decrease as the SiO_2 increases (Figure 8.1b).

The samples from the Akçakışla Granite are classified as subalkaline according to Irvine and Baragar's (1971) total alkalies-silica diagram (Figure 8.2), and are classified as calcalkaline according to AFM diagram (Figure 8.2) of Irvine and Baragar (1971). The Akçakışla Granite is classified as adamellite to quartz monzonite based on the Debon and Le Fort (1983) Q-P diagram (Figure 8.3). The mol. Al_2O_3 / (Na_2O+K_2O+CaO) is less than 1.1. Gençalioğlu Kuşcu (1997) showed that it contains normative diopside, and does not contain normative corundum. It contains more than 3.2% Na_2O in samples with approximately 5% K_2O. All these reveal that the Akçakışla Granite display I-type characteristics defined by Chappel and White, 1974.

8.3. Correlations between skarns and associated granitoids

The correlations between skarns and associated granitoids are described by Shimazaki (1980); Kwak and White (1982); Meinert (1983), Newberry and Swanson (1986), Newbery et al. (1990), Meinert (1993; 1995). Meinert (1995) classified the granitoids associated with various skarns types based on Harker type variation diagrams. However, in these diagrams the distinctions between the skarn types are not clear except for Fe and Au (Meinert, 1995), Cu and Zn, Mo and Sn (Meinert, 1993) skarns.

In general, the granitoids associated with the Pb-Zn skarns in the Akdağmadeni, Akçakışla and Keskin districts are classified as subalkaline based on total alkalies-silica (TAS) (Figure 8.2), and calcalkaline based on the AFM diagrams of Irvine and Baragar (1971) (Figure 8.2). Although some of the granitoids in the studied districts may show both S-and I-type characteristics, in

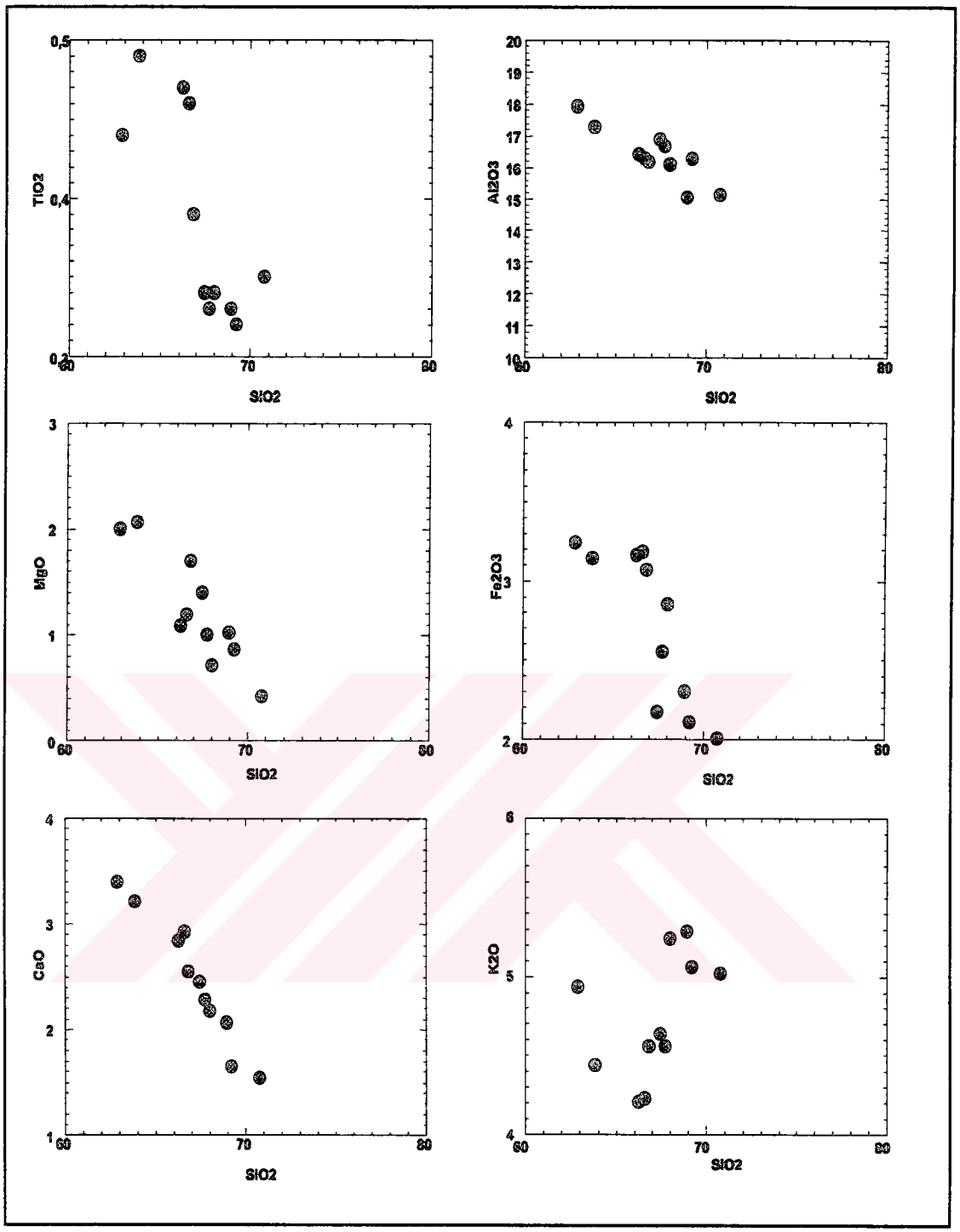

Figure 8.1a. Harker diagrams for the major elements from Akçakışla Granite

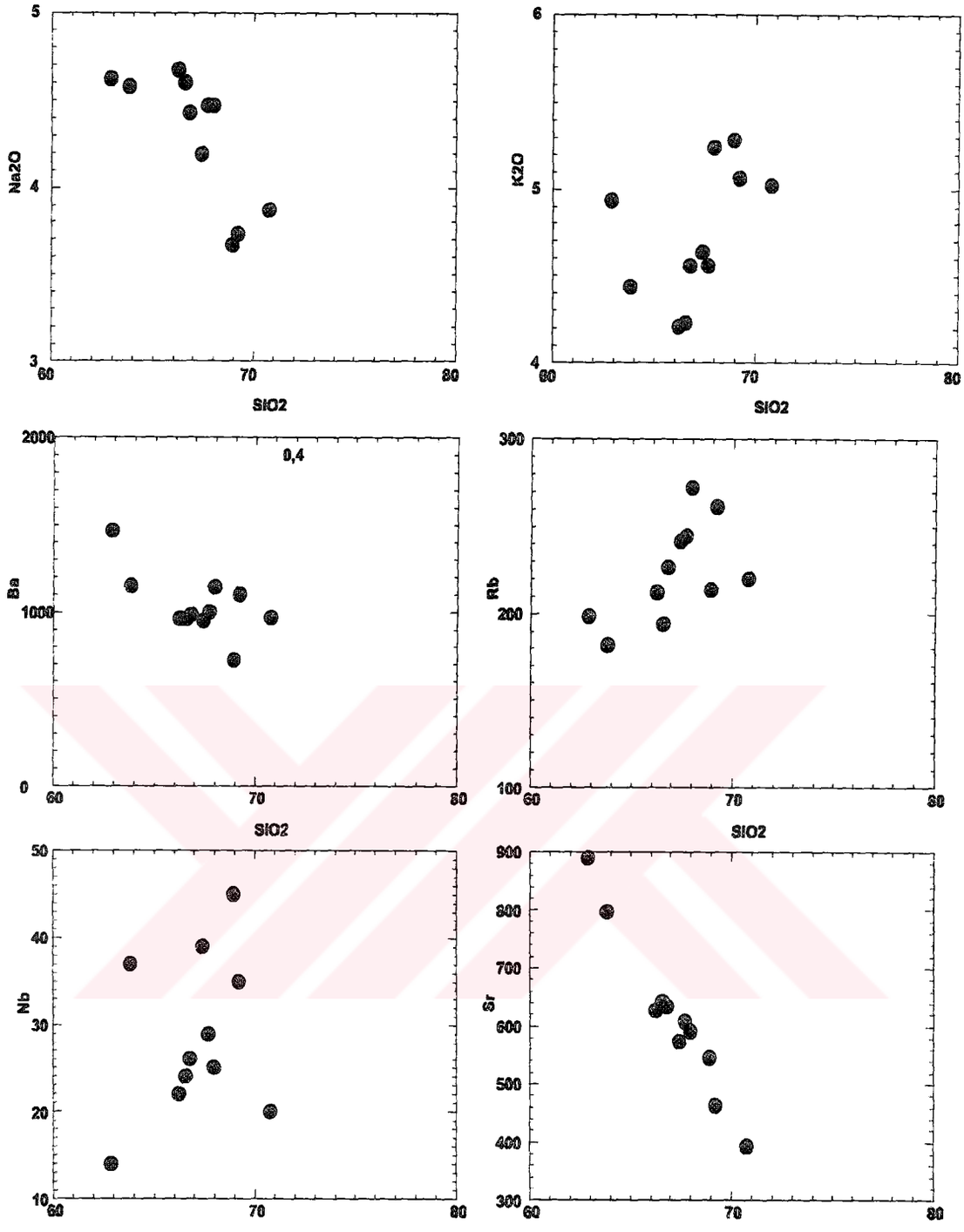

Figure 8.1b. Harker diagrams for the major and trace elements from the Akçakışla district

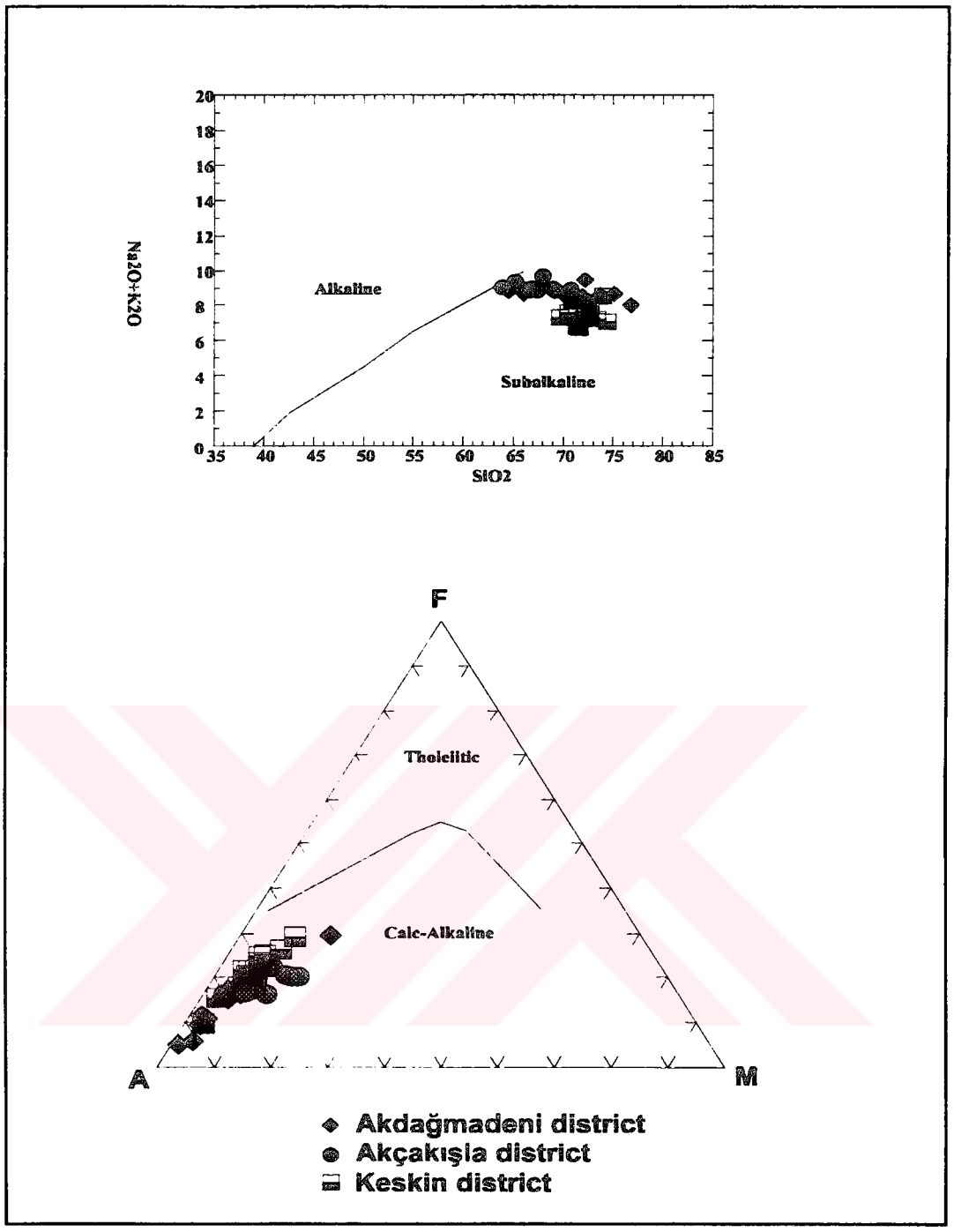

Figure 8.2. Total alkalies-silica diagram of Irvine and Baragar (1971) classifying subalkaline and calcalkaline natures of the granitoids within the studied districts.

general, granitoids in all three districts display I-type characteristics defined by Chappel and White (1974). The mol Al_2O_3 / (Na_2O+K_2O+CaO) ratio is less than 1.1 for the Akdağmadeni and Keskin (S-type characteristics), and more than 1.1 for

the Akçakışla district. They contain more than 3.2% Na2O in the samples with approximately 5% K2O (I-type characteristics).

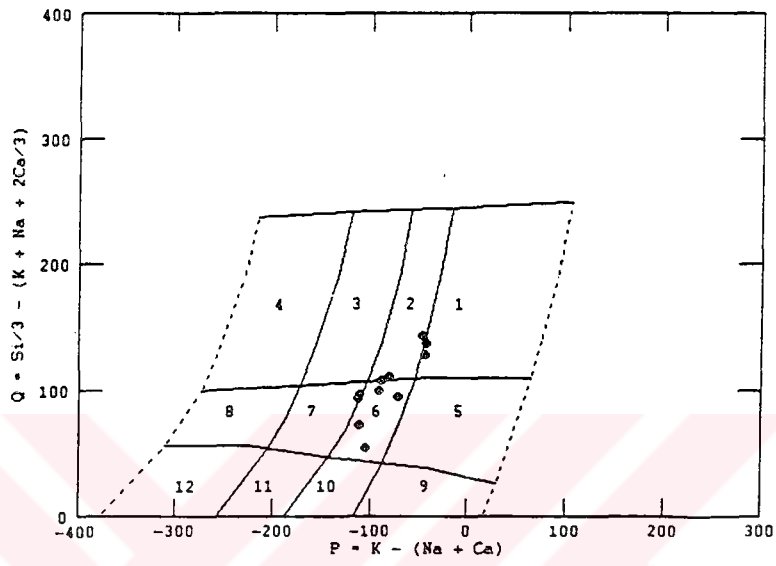

Figure 8.3. Q-P diagram of Debon and Le Fort (1983) showing the composition of samples from Akçakışla Granite

In order to correlate the skarns with the associated granitoids in the studied districts, the Harker diagrams similar to those proposed by Meinert (1993;1995) were used. In these diagrams, the SiO_2 contents of the granitoids associated with Zn-skarns range from 56 to 77% (with a mean of 68.7%), with Cu-skarns from 55 to 72% (with a mean of 64.9%), with W-skarns from 53 to 76 % (with a mean of 70.7%), with Mo-skarns from 65 to 77% (with a mean of 73.7%), and with Sn-skarns 65 to 77% (with a mean of 73.7%). The MgO contents of the granitoids associated with Zn-skarns range from 0.0 to 4.2% (with a mean of 1.0%), with Cu-skarns from 0.5 to 3.9% (with a mean of 1.8), with W skarns from 0.0 to 3.6% (with a mean of 0.7%), with the Mo-skarns from 0.0 to 2.7% (with a mean of 0.5%), and with Sn-skarns from 0.0 to 1.1% (with a mean of 0.3). The K_2O contents of the granitoids associated with Zn-skarns range from 1.9 to 10.0% (with a mean of

4.8%), with Cu-skarns from 2.0 to 5.5% (with a mean of 3.6%), with W-skarns from 2.5 to 6.3% (with a mean of 4.5%), with Mo-skarns from 2.8 to 8.5% (with a mean of 4.7%), and with Sn-skarns from 2.7 to 6.0% (with a mean of 4.7%).

The MgO vs. $SiO_2$and K_20 vs SiO_2 diagrams indicate that the granitoids from the Akçakışla districts plot separately, but those from the Keskin and the Akdağmadeni district plot together, and they usually display a scattered distribution pattern. These diagrams reveal significant relationships between the skarns and associated granitoids in the studied districts. The granitoids from the studied districts plot in the field where granitoids associated with Zn, W and Sn-skarns are shown (Figure 8.4b). The mean MgO, K_2O and SiO_2 values for the granitoids within the studied districts are also plotted in the MgO vs SiO_2 and K_20 vs SiO_2 diagrams. These diagrams show that the granitoids from the Akdağmadeni, Akçakışla and Keskin district also display distribution patterns similar to granitoids associated with W-Zn skarns, Zn skarns, and Mo+Sn skarns, respectively (Figure 8.4a and 8.4b). Based on this, it is proposed that the skarns in the Akdağmadeni and Keskin districts have some W and Mo imprints, respectively. The ($Fe_2O_{3(T)}$+CaO+Na_2O/K_20) vs SiO_2 plot shows that the granitoids within the Akdağmadeni and Akçakışla districts exhibit distribution patterns of plutons associated with the Zn-W and Zn skarns (Figures 8.4a and 8.4b). The skarns in the Keskin district plot in an unidentified part of the diagram. This indicates that the skarns in the Akdağmadeni district have some W imprints that should be investigated in detail. Meinert (1983) described that although there do not appear to be significant differences in total alkali contents of the intrusions related to W, Zn-Pb, Mo, and Sn-skarns, the ratio of K_20 to Na_2O varies. For example, plutons associated with W, Zn-Pb and Cu-skarns, the ratio is close to 1.0, whereas plutons associated with Mo and Sn skarns are characterized by high K_20/Na_2O ratios with an average of 1.60 (Meinert, 1983). This would indicate that the plutons associated with Mo and Sn-skarns are more differentiated than those of other skarn types. In similar manner, the K_20/Na_2O ratios of granitoids in the Akdağmadeni, Akçakışla Granite and the Keskin Pluton may possibly provide information about the metals that skarns contain. The average K_2O/Na_2O ratio of the Keskin Pluton is 1.23 close to that of Mo and Sn-skarns. On the other hand, the average K_2O/Na_2O ratios of Akçakışla Granite and Akdağmadeni granitoid are below 1.0, they are 0.70 and 0.90, respectively. The average ratio of Akçakışla Granite is very close to 1.0 indicating that it could be associated with Cu (and W ?) as well as Pb and Zn.

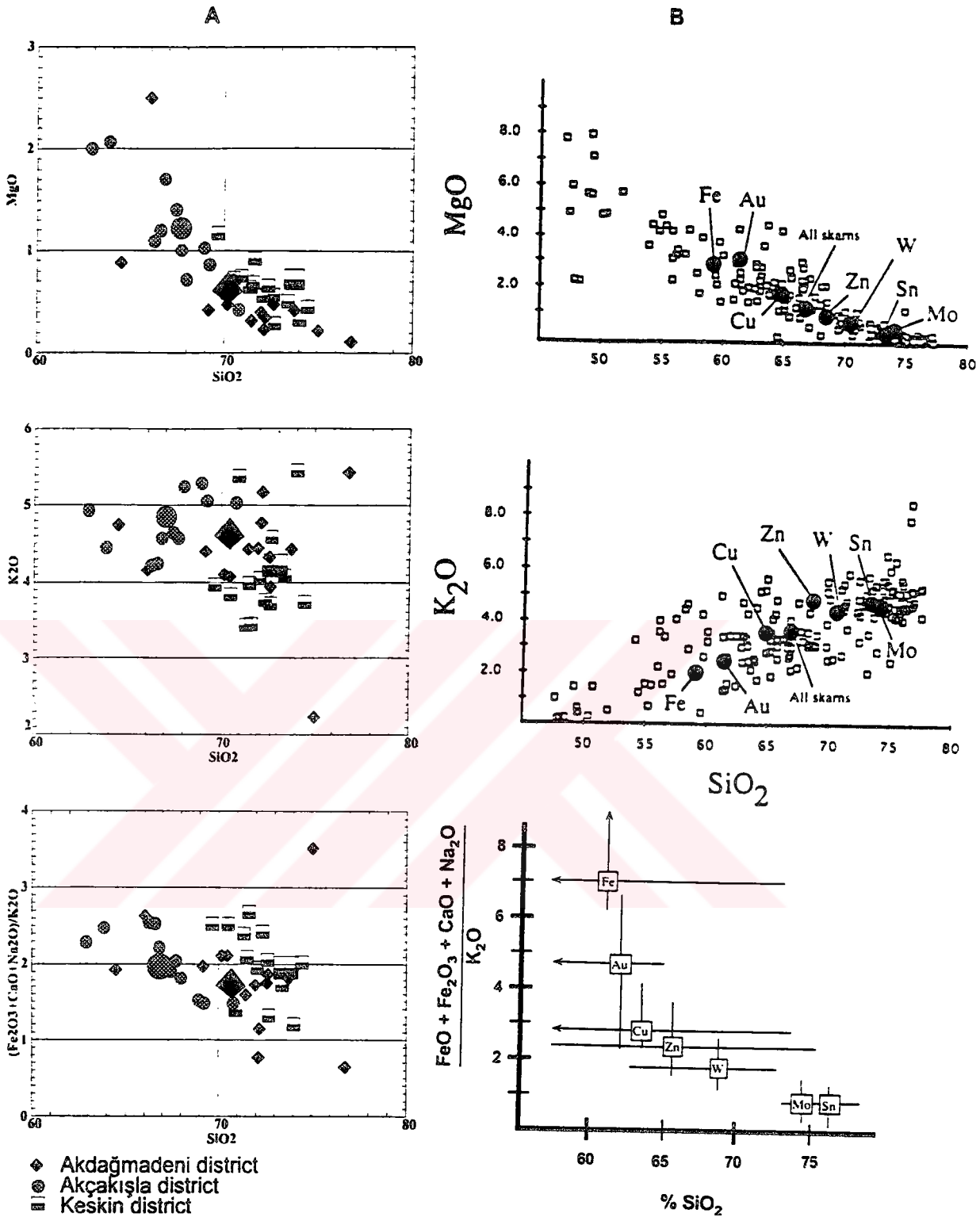

Figure 8.4. Harker diagrams, (A): for granitoids associated with skarns in the studied districts (larger symbol represents mean values), (B) for the granitoids with different skarn types in the world (After Meinert, 1993;1995)

Another approach to understanding the relationships between the skarns and associated granitoids is to examine the trace element diagrams. The variation of mobile, large-ion lithophile elements such as K, Rb, Sr relative to immobile, high-field strength elements such as Zr and Nb help to distinguish granitoids associated with various skarns. Mean Zr content of the granitoids associated with various skarn types do not vary significantly, however, their distribution patterns in Rb/Sr vs Zr plot show significant variations (Figure 8.5). According to these diagrams, the distribution pattern of the granitoids within the Akdağmadeni are similar to granitoids associated mainly with Zn, and W and Cu, but the plot of average Rb/Sr to average Zr indicates that they resemble to those associated with Zn skarns only. The distribution pattern of the Akçakışla Granite is similar to granitoids associated with Cu-skarns only (Figure 8.5). These diagrams reveal that the Pb-Zn skarns in the Akdağmadeni and Akçakışla districts may have some Cu and W imprints (Figure 8.5). The granitoids within the Keskin district are not shown in Figure 8.5 because of the absence of Zr analyses. The importance of differentiation process can be measured by plotting Rb/Sr against Zr. Ba is also one of the distinguishing elements that discriminate the Cu-skarns from other type of skarns. Ba can substitute for K in both K-feldspar and in mica. Following the crystallization of orthoclase and mica, Ba is depleted. Thus, the intermediate-composition plutons associated with Cu and Zn-skarns are the only ones enriched in Ba even though granitoids associated with Sn and W contain more orthoclase (Meinert, 1995). The plot of Ba against Zr show the relationships skarns and Ba contents (Figure 8.6a, 8.6b). According to this diagram, the granitoids associated with Cu and Zn skarns represent those with higher Ba contents, and granitoids associated with Sn, W and Mo skarns with low Ba contents (Figure 8.6b). Figure 8.6 shows that the granitoids within the Akdağmadeni and Akçakışla districts display similar to those associated with W and Zn+Cu skarns respectively. The relative enrichment in the Ba content of the granitoids within the Akçakışla district, and relative depletion in the Ba content of the granitoids within the Akdağmadeni district could be used as an evidence to propose that the skarns within the Akdağmadeni and Akçakışla districts (Figure 8.6a) may have a W and Cu components, respectively that should investigated in detail.

8.4. Discussion

In terms of major and trace-element data there are differences among the granitoids associated with the skarns in the studied districts. There are three general group of plutons, and the distinction between them is based largely on the major element data. As a whole, the groups display geochemical characteristics of the plutons similar to those associated with Zn, W, Mo and Sn-skarns based on Harker diagrams (Figure 8.4a and 8.4b; Figure 8.5a and 8.5b; Figure 8.6a and 8.6b). By combining these diagrams, it is proposed that the skarns within the Akdağmadeni district are mainly of W+Zn skarns, those within the Akçakışla are mainly of Zn skarns, and those within the Keskin district are of probably Zn-skarns with some Mo+Sn imprints. This would probably indicate that some other elements like Mo and Sn could also be associated within the skarns in the Keskin district. The association of hypothermal Mo deposit (MTA, 1965; Tümer, 1984) around the Hüseyinbeyobası (to the northeast of the Keskin district) area, may support this argument. The detailed

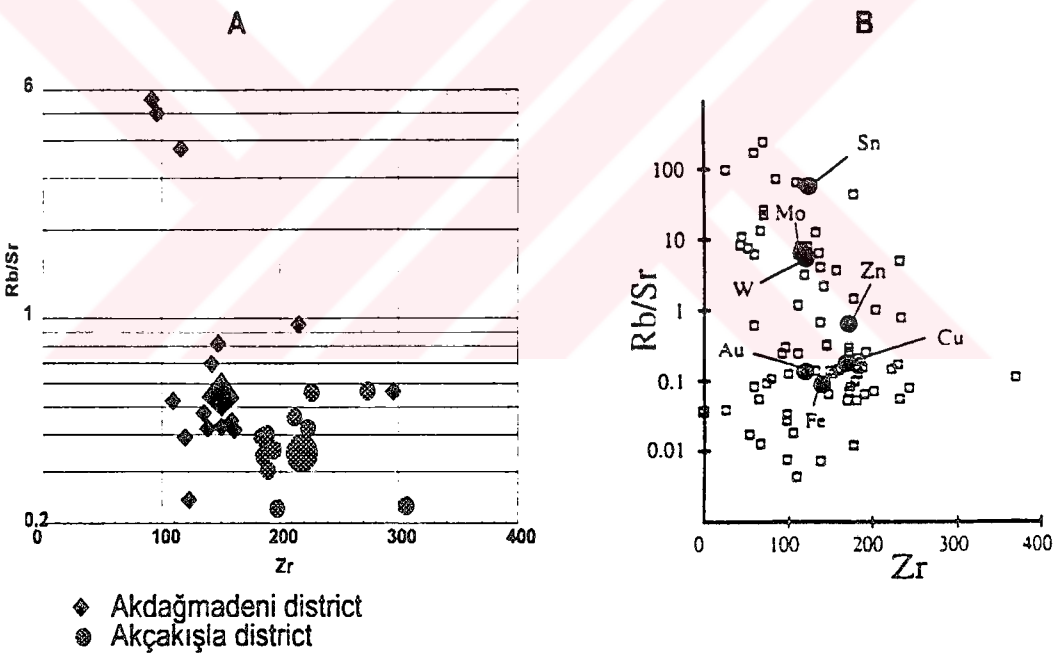

Figure 8.5. Trace-element discrimination diagrams showing the relationships between Rb/Sr and Zr content of the granitoids associated with skarns (Larger symbol represents mean values), (A): data from the granitoids within the Akdağmadeni and Akçakışla, districts, (B) data from Meinert (1995).

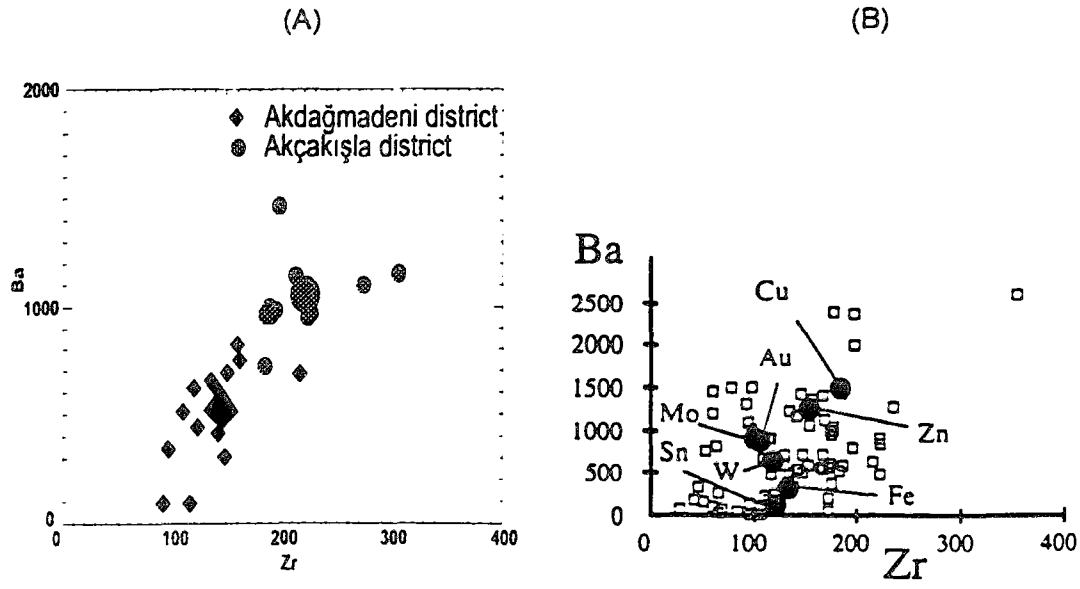

Figure 8.6. Ba-Zr content of granitoids associated with skarns (Larger symbol represents mean values), (A) data from the studied districts, (B) data from Meinert (1995)

geochemical studies on the Keskin Pluton in the Keskin district and in the Hüseyinbeyobası area may provide clues about the mineralizations in both areas. The trace element variation diagrams for the granitoids (Figure 8.5a and8.5b; Figure 8.6a and 8.6b) show that the granitoids in the Akdağmadeni and Akçakışla districts have the geochemical signatures of the plutons associated with Zn, Cu, and W skarns. This also helps to understand the possible association of W and Mo-skarns in the Akdağmadeni and Cu-skarns in the Akçakışla districts. In general, the study of these diagrams reveal that W and Mo skarns are associated with the granitoids within the Akdağmadeni and Keskin districts, respectively. Zn+Cu skarns are associated with the granitoids within the Akçakışla districts. Zn-skarns are observed in both Akdağmadeni and Akçakışla districts. However, all these correlations are based on the major and trace element contents of granitoids associated with skarns within the Akdağmadeni, Akçakışla and Keskin districts, and better results could be obtained only if the skarns and associated granitoids are systematically sampled, and geochemically analyzed.

The K_2O/Na_2O ratio of the Akçakışla Granite shows that skarns associated with the Akçakışla Granite should contain Cu and W elements as well as Pb-Zn elements. The association of Cu in this district was also discussed in the mineral chemistry section in that these are associated with diopsidic pyroxenes, which are the mostly found pyroxenes in the Cu-skarns.

CHAPTER 9

CONCLUSIONS

This study is based on the petrographical, mineralogical and geochemical examination of samples from 6 skarn occurrences (Bayramali, Çiçeklitepe, Çukurmaden, Peynirliktepe, Radarbaca, and Tunca) within the Akdağmadeni, 3 occurrences (Akçakışla, Barajdoğusu and Özgebaca) within the Akçakışla and 2 occurrences (Karamağara and Simlikurşun) within the Keskin district. The Akdağmadeni, Akçakışla and Keskin districts are within the Central Anatolian Crystalline Complex (CACC). The skarns are observed along the contacts of granitoids and marbles of the Gümüşler and Aşıgediği metamorphics within the studied districts

Both endoskarns and exoskarns occur within the studied districts. Endoskarns are present only in the Akçakışla district and represent the skarnization of the Akçakışla Granite. Exoskarns are observed at all districts, and they are classified as calcic exoskarns. Three types of exoskarns were identified as garnet-pyroxene, epidote and wollastonite skarns. The garnet-pyroxene skarns are observed only in Evciboyuntepe and Radarbaca occurrences of the Akdağmadeni district. Those of the Akçakışla district are observed in Barajdoğusu and Özgebaca occurrences, and those of the Keskin district are observed only in the Karamağara occurrence. The epidote skarns expose at Akdağmadeni and Akçakışla districts are superimposed on the garnet-pyroxene skarns. The wollastonite skarns observed only in the Simlikurşun occurrence.

The garnet-pyroxene skarns are composed of garnet as predominant mineral associated with pyroxene. Magnetite, hematite, pyrrhotite, and some pyrite are the characteristic metallic minerals observed in the garnet-pyroxene skarns. These represent the early formed prograde skarn assemblage. The epidote skarns include epidote, pyroxene, wollastonite, tremolite, calcite, chlorite, quartz, and sulfide minerals (sphalerite, galena, chalcopyrite, pyrite). The early formed mineral assemblages (garnet and pyroxene) were re-equilibrated by subsequent hydrothermal solutions, and altered to mineral assemblage of epidote skarns.

Wollastonite skarns consist mainly of wollastonite associated with pyrite, sphalerite, hematite and magnetite. The petrographical studies showed that the minerals above were formed in a sequence from earlier to later as hematite-I, garnet, pyroxene, quartz-I, wollastonite, magnetite, hematite-II, pyrrhotite, pyrite-I, epidote, tremolite, calcite, chalcopyrite+sphalerite, galena, pyrite-II, quartz-II, chalcopyrite, chlorite, chalcocite, and goethite. Substantial differences exists between skarn stages. These are from earliest to latest; (1) a garnet dominated assemblage termed as the garnet stage, (2) epidote and tremolite dominated stage with calcite and quartz-II termed as epidote stage, (3) pyrite-II, chalcopyrite, galena and sphalerite dominated stage termed as the sulfide stage, (4) chlorite, calcite dominated stage with quartz-II termed as the chlorite stage, and (5) the final chalcocite and goethite dominated stage termed as the supergene stage.

The optical examination of the oscillatory zones in garnets showed that many are quite narrow, and exhibit sharp contacts between the dark and light colored bands giving rise to a complex, non-periodic, fluctuating zonation pattern. The zonal fluctuation is explained by the cyclical variations in the composition of the hydrothermal solutions controlled by fracturing. It is proposed that the zoning is externally controlled, and initiated by the onset of fracturing in the skarn hydrothermal system. The presence of morphological instabilities such as dissolution structures, striations, and cellular structures and well defined morphological transitions from planar to cellular structures in the garnets in the Barajdoğusu, Özgebaca, and Karamağara occurrences indicate high flow rates and rapid crystal growths. The high growth rates result in many changes in the hydrothermal system such as periodic changes in the chemical potentials of the garnet forming components and in the oxygen fugacity of the system

The Pb-Zn occurrences are hosted by the exoskarns within the studied districts. The mineralizations in the Akdağmadeni district appear as a series of lenses parallel to each other. Two types as mineralizations were formed, one at high temperatures with magnetite (martitized), hematite-I and II, and pyrite-I, and the other at low temperatures with pyrite-II, sphalerite, galena and chalcopyrite. The mineralizations in the Akçakışla district occur in three different zones as hematite, pyrite-hematite and sphalerite zones. The mineralizations in the Keskin district occur as pockets and lenses within the skarnized rocks. They are characterized by dominant galena and hematite, with subordinate sphalerite, magnetite and pyrite,

The sulfide minerals are observed as replacing wollastonite and to some extent garnet-pyroxene skarns during the retrograde stages.

The garnets in all districts are regarded as grossular-andradite (grandite) garnets, because of their high grossular-andradite contents, and low spessartine-pyrope-almandine (pyralspite) contents. The composition of garnets range from Ad_{100} to $Gro_{83.34}Ad_{10.30}Py_{6.36}$ in the Akdağmadeni, $Ad_{99.23}Sp_{0.77}$ to $Gro_{92.01}Ad_{7.50}Sp_{0.43}$ in the Akçakışla, and Ad_{100} to $Ad_{40}Gro_{60}$ in the Keskin district. The compositions of garnets change from core to rim. The compositional zoning in the garnets is formed by the oscillations of Al_2O_3 and total iron as $Fe_2O_{3(T)}$ contents, and hence oscillations of grossular and andradite contents of the garnets.

The oscillatory zoning in garnets reflects changes in the activity ratio (a_{Fe+3}/a_{Al+3}), changes in the distribution of Al and Fe cations between fluid and mineral, and changes in the in the oxidation potential controlled mainly by the changes in the oxygen fugacity of the hydrothermal system. The relative enrichment of andraditic garnets in the rim compositions of Barajdoğusu and Evciboyuntepe samples indicate that the garnet compositions were controlled partly a system with lower temperatures, higher oxygen fugacities, and lower salinities compared to that of core compositions garnets. The relative enrichment of grossularitic garnets in the Özgebaca and Karamağara occurrences is possibly related to the initial contact metamorphism controlled by Al-rich protolith composition that cause aluminum enrichment in the garnet cores.

The EMP analyses of the pyroxenes from the Akdağmadeni and Akçakışla districts indicated that the compositions of pyroxenes are different. The Wo-En-Fs diagram showed that the wollastonite content of pyroxenes ranges from 0.0 to anomalously high 61.04%, enstatite content from 0.0 to 57.03%, and ferrosilite content from 1.77 to 44.1%.Based on the above compositions, the pyroxenes in the Akdağmadeni district are classified as diopside and hedenbergite, and in the Akçakışla as diopside. They are also classified using Di-Hd-Jo diagram. In the Akdağmadeni district, the pyroxenes in the Bayramali occurrence are mainly johannsenitic typical for Pb-Zn sulfide associations, those in the Çiçeklitepe and Radarbaca occurrences are diopsidic. In the Akçakışla district, the pyroxenes in the Barajdoğusu and Özgebaca occurrences range from hedenbergite to diopside. The association of diopsidic pyroxene and andraditic garnet with slightly later quartz-magnetite-sulfide assemblages in skarns of the Barajdoğusu occurrence indicates

a Cu potential. This association also showed that Barajdoğusu occurrence was under the influence of relatively high oxidation state compared to other occurrences.

The correlations between skarns and associated granitoids within the studied districts were made by using Harker type diagrams. ($Fe_2O_{3(T)}$ +CaO+Na_2O)/K_2O vs SiO_2 diagram shows that that the granitoids within the Akdağmadeni and Akçakışla districts exhibit characteristic distribution patterns of the plutons associated with W, Zn and W skarns, respectively. MgO vs SiO_2 diagram shows that the plutons within the Akdağmadeni, Akçakışla and Keskin districts are associated with W, Zn+Cu, and Mo+Sn skarns, respectively. The K_2O vs SiO_2 diagram indicates that the granitoids within the Akdağmadeni, Akçakışla and Keskin districts are associated with W, Zn and Mo+Sn skarns, respectively, The Rb/Sr vs Zr diagram indicates that the granitoids within the Akdağmadeni and Akçakışla districts are associated with W and Zn+Cu, respectively. The Ba vs Zr diagram for the same granitoids indicates that they are associated with W+Mo and Zn+Cu skarns, respectively. The K_2O/Na_2O ratio of the Akçakışla Granite shows that the Pb-Zn skarns have some Cu imprints.

REFERENCES

Abrecht, J., 1985. Manganiferous pyroxenes and pyroxenoids from three Pb-Zn-Cu skarn deposits, Contrib. Mineral. Petrol, v.89, p. 379-393

Akgün, F., Olgun., E., Kuşcu., İ., Toprak., V., and Göncüoğlu, M.C., 1995. Orta Anadolu Kristalen Kompleksinin "Oligo-Miyosen" örtüsünün stratigrafisi, çökelme ortamı ve gerçek yaşına ilişkin yeni bulgular, TPJD Bull., v. 6/1, p. 51-68.

Akıman, O., Erler, A., Göncüoğlu, M.C., Güleç, N., Geven, A., Türeli, T.K., and Kadıoğlu, Y.K., 1993, Geochemical characteristics of granitoids along the western margin of the Central Anatolian Crystalline Complex and their tectonic implications. Geol. Journ., v.28, p. 371-382.

Andersen, G.M., 1973. The hydrothermal transport and deposition of galena and sphalerite near 100°C. Econ. Geol., v. 75, p. 480-492.

Arslanpay, D. and Yıldırım, D.,1978. Ankara-Keskin Denek madeni bakır-kurşun-çinko aramaları jeofizik induklem polarizasyon (I.P) etudu. M.T.A. Rep. no. 6334, 19 p.

Ashley, P.M., 1980. Geology of the Ban Ban zinc deposit; A suifide bearing skarn, Southeast Queensland, Australia. Econ. Geol., v., p.15-29.

Atabey, E., Tarhan, N., Akarsu, B., and Taşkıran, A., 1987. Şereflikoçhisar , Panlı (Ankara), Acıpınar (Niğde)örelerinin jeolojisi. M.T.A. Rep. no. 8155, 59 p.

Ataman, G., 1972. Ankara'nın güneydoğusundaki granitik-granodiyoritik kütlelerden Cefalıkdağ'ın radyometrik yaşı hakkında ön çalışma. Hacettepe Üniversitesi Yerbilimleri, v.2, p. 44-49.

Atkinson, W.W., Jr., and Einaudi, M.T., 1978. Skarn formation and mineralization in the Contact Aureole at Carr Fork, Bingham, Utah: Econ. Geol., v. 73, no. 7, p. 1326-1365.

Ayan, M., 1963. Contribution a l'etude petrographique et géologique de la region située au nord-est de Kaman. M.T.A. Bull., v. 115, 332 p.

Ayhan, G., 1976. Yozgat-Akdağmadeni-Akçakışla köyü manyetit zuhuru prospeksiyon raporu. M.T.A. Rep. no. 1402,

Bailey, E. and McCallien, W.J., 1950. Ankara melanjı ve Anadolu Şaryajı. M.T.A Bull., v. 40, p. 12-22.

Barnes, H.L., 1979. Solubilities of ore minerals. In H.L. Barnes (ed.) Geochemistry of hydrothermal ore deposits, 2nd ed., New York, Wiley, p. 404-460.

Bartholomé, P., 1970. Minerais et skarns dans les auréoles de métamorphisme. Mineral. Deposita, v. 5., p. 345-353.

Bayhan, H., 1987. Cefalıkdağ ve Baranadğ plutonlarının petrografik ve kimyasal-mineralojik ozellikleri. Türkiye Jeol. Kur. Bull., v. 30/31, p. 11-16.

Bayhan, H. and Tolluoğlu, A.Ü., 1987. Çayağazı syenitoidinin (Kırşehir kuzeybastısı) mineralojik ve jeokimyasal özellikleri. Hacettepe Üniversitesi Yerbilimleri, v. 14, p. 109-120.

Bayhan, H., 1988. Bayındır-Akpınar (Kaman) yöresindeki alkali kayaçların jeokimyası ve kökensel yorumu. Türkiye Jeol. Kur. Bull., v. 31, p. 59-69.

Bayhan, H.,1989. Keskin sokulumunun (Ankara) petrografik ve kimyasal-mineralojik özellikleri. Hacettepe Üniversitesi Yerbilimleri, v.15, p. 29-36.

Brijraj, K. D., Okrusch, M., Olesch, M., 1988. Mineralogy and genesis of zoned skarns from Chaur Hill, Himachal Himalaya, India. Neues Jahrbuch Miner. Abh. V. 158 (3), p. 211-224.

Burt, D.M., 1977, Mineralogy and petrology of skarn deposits. Soc. Italiana Mineralogia Petrolgia Rendiconti, v. 33, p. 859-873.

Burt, D.M., 1982, Skarn deposits - Historical bibliography through 1970: Econ. Geol., v. 77, p. 755-763.

Burton, J.C., Taylor, L.A., and Chou, I-Ming, 1982, The fO_2-T and fS_2-T stability relations of hedenbergite and of hedenbergite-johannsenite solid solutions, Econ. Geol., v. 77, p. 764-783.

Buseck, P.R., 1966, Contact Metasomatism and ore deposition: Conception Del Oro, Mexico. Econ. Geol., v. 61, p. 644-666.

Çağatay, A., and Teşrekli, R., 1979, Vitişenit minerali içeren Keskin-Karamağara kurşun-çinko zuhurunun mineralojisi ve kökeni. Türkiye Jeol. Kur. Bull., v. 22, p. 203-208.

Çavuşoğlu, H.,1967. Keskin-Denek Pb-Zn madenleri ve civarının jeolojik yapısı hakkında rapor. M.T.A. Rep. no. 3871, 18 p.

Chappel, B.W. and White, A.J.R., 1974. Two contrasting granite types: expanded abstract. Pacific Geology, v. 8, p.173-174.

Cornwall, H.R., 1982.Petrology and geochemistry of igneous rocks : Ray porphyry copper district, Pinal County, Arizona. In S.R. Titley (ed.) Advances in the geology of the porphyry copper deposits, Southwestern United States, Arizona Univ. Press., p. 259-274.

CENTO, 1964, Symposium on mining and the base metals, held in Ankara, Turkey, proceedings, p. 25-34.

Craig, J.R., and Vaughan, D.J., 1981, Ore microscopy and petrography, John Wiley & Sons, New York, 406p.

Dalkılıç, F., 1986. Petrography and geochemistry of felsic intrusive rocks from northeast of Kaman region (Kırşehir-Turkey), M.Sc Thesis, Middle East Technical University, Ankara, 113 p.

Deer, W.A., Howie, R.A., and Zussman, J., 1962. Rock forming minerals, vol. 1. Ortho- and ring silicates. William Clowes and Sons, London, 333 p.

Deer, W.A., Howie, R.A., and Zussman, J., 1982. Rock forming minerals, 2nd ed. Vol. 1A: Orthosilicates, Longman, London, 913 p.

Debon, F. and Le Fort, P., 1983. A Chemical and mineralogical classification of common plutonic rocks and associations. Transactions of the Royal Society of Edinburgh: Earth Sciences, v. 111, p. 135-149.

Dick, L.A., and Hodgson, C.J., 1982, The Mac Tung W-Cu(Zn) contact metasomatic and related deposits of the northeastern Canadian Cordillera. Econ. Geol., v. 77, p. 845-867.

Drummond, S.E. and Ohmoto, H., 1985. Chemical evolution and mineral deposition in boiling hydrothermal systems. Econ. Geol., v. 80, p. 126-147.

Egeran, N. and Lahn, E., 1951. Note on the tectonic position of the Northern and Central Anatolia. M.T:A. Bull., v. 41, p. 23-27.

Einaudi, M.T., 1977, Petrogenesis of copper-bearing skarn at the Mason Valley mine, Yerington district, Nevada. Econ. Geol., v. 72, p. 769-795.

Einaudi, M.T., 1982a,Garnet and pyroxene compositions in skarn deposits. Carnegie Institution of Washington Yearbook, v. 81, p. 320-324.

Einaudi, M.T., 1982b, General Features and Origin of Skarns Associated with Porphyry Copper Plutons, southwestern North America in Advances in Geology of the Porphyry Copper Deposits, Southwestern U.S. In S.R.Titley (Ed), Univ. Arizona Press, p.185-209.

Einaudi, M.T., and Burt, D.M., 1982, Introduction-terminology, classification, and composition of skarn deposits. Econ. Geol., v. 77, p. 745-754

Einaudi, M.T., Meinert, L.D., and Newberry, R.J., 1981, Skarn deposits: Econ. Geol., 75th Anniv. Vol., p. 317-391.

Erentöz, C., 1961. 1/500 000 ölçekli Türkiye Jeoloji haritası, Sivas paftası, M.T.A. Publ., Ankara.

Erentöz, C. and Ternek, Z., 1962. 1/500 000 ölçekli Türkiye Jeoloji haritası, Adana paftası, M.T.A. Publ., Ankara.

Ergintav, T.Y., 1987. Geology of Akçakışla-Eynelli region near Akdağmadeni between Yozgat and Sivas, M.Sc. thesis, Middle East Technical Univ., Ankara, 72p.

Erkan, Y., 1976. Kırşehir çevresindeki rejyonel metamorfik bölgede saptanan izogradlar ve bunların petrolojik yorumları. Hacettepe Universitesi Yerbilimleri, v. 2(1), p. 213-218.

Erkan, Y., and Ataman, G., 1981, Orta Anadolu Masifi (Kırşehir yöresi) metamorfizma yaşı üzerine K/Ar yöntemi ile bir inceleme. Hacettepe Üniversitesi Yerbilimleri, v.8, p. 27-30.

Erler, A., Akıman, O., Unan, C., Dalkılıç , F., Dalkılıç, B., Geven, A., and Önen, P., 1991, Kaman (Kırşehir) ve Yozgat yörelerinde Kırşehir.Masifi magmatik kayaçlarının petrolojisi ve jeokimyası. Doğa, v. 15, p. 76-100.

Erler, A., and Bayhan, H., 1995. Orta Anadolu Granitoidleri'nin genel değerlendirilmesi ve sorunları. Hacettepe Üniversitesi Yerbilimleri, v.17, p. 49-67.

Erler, A., Kuşcu, İ., Dirik, K., Ulu, Y., and Yavuz, N., 1996. Orta Anadolu Kristalen Karmaşığının Metalojenisi. O.D.T.Ü. Araş. Fonu Projesi, 39p.

Erler, A. and Göncüoğlu, M.C., 1996.

Gamble, R.P., 1982. An experimental study of sulfidation reactions involving andradite and hedenbergite, Econ. Geol., v.77, p. 784-797.

Gençalioğlu-Kuşcu, G. and Floyd, P.A., 1995. Preliminary data on petrography and geochemistry of dacites and rhyodacites from Saraykent region, Yozgat, Central Anatolia, Turkey. In Ö. Pişkin, M. Ergün, M.Y. Savaşçın, and G. Tarcan (eds.), International Earth Sciences Colloquium on the Egean region-1995, p. 399-413.

Gençalioğlu-Kuşcu, G., and Floyd, P.A., 1996. Upper Cretaceous pyroclastic rocks in the Akdağmadeni region, Central Anatolia, Turkey. The physics of the Explosive Volcanic Eruptions, Arthur Holmes European Research Conference Abstracts vol. P.26.

Geven, A., 1992. Mineralogy, petrography and geochemistry of Cefalıkdağ Plutonic rocks (Kaman Region-central Anatolia), Ph.D Thesis, Middle East Technical University, Ankara, 165 p.

Göncüoğlu, M.C., 1977, Geologie des westlichen Niğde Massivs, Ph.D Thesis, Bonn University, 167 p.

Göncüoğlu, M.C., 1986, Orta Anadolu Masifi'nin güney ucundan jeokronolojik yaş bulguları. MTA Bull., v.105/106, p. 111-124.

Göncüoğlu, M.C., Toprak, V., Kuşcu, İ., Erler, A., and Olgun, E., 1991. Orta Anadolu Masifi'nin batı bölümünün jeolojisi, Bölüm 1: Güney Kesim. TPAO Rep., No. 2909, 140p.

Göncüoğlu, M.C., Erler, A., Toprak, V., Yalınız, K., Olgun, E., and Rojay, B., 1992, Orta Anadolu Masifi'nin batı bölümünün jeolojisi, Bölüm 2: Orta Kesim. TPAO Rep.No. 3155, 76 p.

Göncüoğlu, M.C., Erler, A., Toprak, G.M.V., Olgun, E., Yalınız, K., Kuşcu, İ., Köksal, S., and Dirik, K., 1993. Orta Anadolu Masifi'nin orta bölümünün jeolojisi, Bölüm 3: Orta Kızılırmak Tersiyer baseninin jeolojik evrimi. TPAO Rep. No. 3313, 104 p.

Göncüoğlu, M.C., Dirik, K., Erler, A., Yalınız, K., 1994. Orta Anadolu Masifinin doğu bölümümün jeolojisi, Bölüm 4: Orta Anadolu Masifinin sivas Baseni ile olan ilişkisi. ODTÜ-AGUDOS rep. 135 p.

Görür, N., Oktay, F.Y., Seymen, İ., and Sengör, A.M.C., 1984, Paleotectonic evolution of Tuzgölü Basin Complex, central Turkey. In: J.E. Dixon and A.H.F. Robertson (eds.) The geological evolution of the Eastern Meditterranean, Geol. Soc. Spec. Publ., 17, Blackwell, Oxford, 81-96.

Güleç, N., 1994. Rb-Sr isotope data from the Ağaçören granitoid (East of Tuzgölü): Geochronological and genetic implications. Doğa, v. 3, p. 39-43.

Gündoğdu, M. N., Bros, R., Kuruç, A., and Bayhan, H., 1988. Bayındır feldispatoidli siyenitlerinin Rb-Sr tümkaya sistematiği (Kaman-Kırşehir). Hacettepe Üniv. Yerbilimleri 20.Yıl Simp. Abstracts, p.55.

Harris, N.B. and Einaudi, M.T., 1982, Skarn deposits in the Yerington District, Nevada: Metasomatic skarn evolution near Ludwig. Econ. Geol., v. 77, p. 877-898.

Irvine, T.N. and Baragar, W.R.A., 1971. A guide to the chemical classification of the common volcanic rocks. Canadian Journal of Earth Sciences, v. 8, p. 523-548.

James, L.P., 1976, Zoned alteration in limestone at porphyry copper deposits, Ely, Nevada. Econ. Geol., v. 71, p. 488-512.

Jamtveit, B., 1991, Oscillatory zonation patterns in hydrothermal grossular andradite garnet, nonlinear dynamics in regions of immiscibility,. American Mineralogist, v. 76. (7 8). p. 1319-1327.

Jamtveit, B., and Andersen T. B., 1992, Morphological instabilities during rapid growth of metamorphic garnets. Phys.and Chem. of Minerals, v. 19. (3), p. 176-184.

Jamtveit, B., Bucher N. K., and Stijfhoorn D. E., 1992, Contact metamorphism of layered shale carbonate sequences in the Oslo Rift, I, Buffering, infiltration, and the mechanisms of mass transport: J. Petrol., v. 33 (2), p. 377-422.

Jamtveit, B., Wogelius R. A, and Fraser D. G., 1993, Zonation patterns of skarn garnets, records of hydrothermal system evolution. Geology, v. 21. (2), p. 113-116.

Jamtveit, B. and Hervig, R. L., 1994, Constraints on transport and kinetics in hydrothermal systems from zoned garnet: Science, v. 263. (5146). p. 505-508.

Jamtveit, B., Ragnarsdattir, K.V., and Wood, B.J., 1995, On the origin of zoned grossular-andradite garnets in hydrothermal systems. Eur. J. Mineral., v. 7, p. 1399-1410.

Jensen,M.L. and Bateman, A.M.,1979. Economic mineral deposits, John Wiley and Sons, New York, 593 p.

Kadıoğlu, Y.K. 1991. Geology, petrography and geochemisrty of Ağaçören (Aksaray) magmatic rocks, M.Sc. Thesis, Middle East Technical University, Ankara, 141 p.

Kadıoğlu, Y.K., 1996. Genesis of Ağaçören Intrusive Suite and its enclaves (central Anatolia): Constraints from geological, petrographic, geophysical, and geochemical data, Ph.D. Thesis, Middle East Technical University, Ankara, 242 p.

Kato, Y., 1991, Textural and compositional changes of clinopyroxene replaced by garnet in the Mozumi deposit, Kamioka Mine, Japan, Skarns-Their genesis and metallogeny, Theophrastus Publ., Athens, 459 p.

Kerrick, D. M., 1974, Review of metamorphic mixed-volatile (H_2O-CO_2) equilibria. American Mineralogist, v. 59, p. 729-762.

Kesler, S.E., Jones, L.M, and Walker, R.L., 1975, Intrusive rocks associated with porphyry copper mineralization in island arc areas. Econ. Geol., v.70, p. 515-526.

Ketin, İ., 1955. Yozgat bölgesinin jeolojisi ve Orta Anadolu masifinin tektonik durumu. Türkiye Jeol. Kur Bull., v. 6, 1-40.

Ketin, İ. and Erentöz, C., 1961. 1/500 000 ölçekli Türkiye Jeoloji haritası, Sinop paftası, M.T.A. Publ., Ankara.

Ketin, İ., 1963. 1/500.000 ölçekli Türkiye Jeoloji Haritası, Kayseri Paftası. M.T.A. Publ., 83 p.

Ketin, İ., 1966. Tectonic units of Anatolia (Asia Minor). M.T.A. Bull., v. 66, 23-34.

Koçak, K., and Leake, B.E., 1994. The petrology of the Ortaköy district and its ophiolite at the western edge of the Middle Anatolian Massif. Turkey. J. African Earth Sci., v.18, 163-174.

Korzhinskii, D.S., 1970. Theory of metasomatic zoning. Oxford Univ. Press. London, 162 p.

Köksal, S., 1996. The geological and petrological characteristics of the İdiş Dağı-Avanos area (Nevşehir-central Anatolia), M. Sc. Thesis Middle East Technical Univ., Ankara, 141 p.

Kovenko, V., 1939a. Denek madenlerinin ziyareti hakkında muhtıra. M.T.A. Rep. no. 844, 4 p.

Kovenko, V., 1939b. Denek Kurşun madenine yapılan ziyaret hakkında kısa muhtıra. M.T.A. Rep no. 967, 4 p.

Kovenko, V., 1940. Denek kurşun madenine yapılan ziyaret hakkında rapor. M.T.A. Rep. no. 1140, 3 p.

Kovenko, V., 1947, Kuzey Anadolu bölgesinin bazı kurşun-çinko ve antimuan madenleri (Denek, Akdağ, Turhal). M.T.A. Bull., v. 1(37), p. 61-96.

Kuşcu, İ and Demirci, C., 1995. Tectonostratigraphy of the Keskin area, Kırıkkale, Turkey. 2nd International Symposium on the Geology of the Eastern Mediterranean Region, Abstracts vol., p. 14, Jerusalem, Israel.

Kuşcu, İ and Erler, A., 1996. Metallogeny of the Central Anatolina Crystalline Complex, Turkey. Mineral Exploration '96: The third International conference, Brisbane, Australia, Abstracts vol. p. 33.

Kuşcu, İ. and Erler, A., 1997. Mineralizations in the Central Anatolian Crystalline Complex: Metallogeny of a collision related setting. The Geological Society, Mineral Deposits Studies Group 1997 Annual Meeting, Glasgow, United Kingdom, Abstracts vol., p. 74.

Kwak, T.A.P., 1986, Fluid inclusions in skarns (carbonate replacement deposits). J. Metamorphic Geol., v. 4, p. 363-384.

Kwak, T.A.P., and Tan., T.H., 1981, The geochemistry of zoning in skarn minerals at the King Island (Dolphin Mine). Econ. Geol., v. 76, p. 468-497.

Kwak, T.A.P. and White, A.J.R., 1982. Contasting W-Mo-Cu and W-Sn-F skarn types an related grantoids. Mining Geology, v., 32, p. 339-351.

Lessing, P. and Standish, R.P., 1973. Zoned garnet from Crested Butte, Colorado. American Mineralogist., v. 58, p. 840-842.

Meinert, L.D., 1980.Evolution of metasomatic fluids by transport over large distances: An example from the Paymaster zinc skarn, Esmeralda Co., Nevada, vol., Geol. Soc. America, Abstracts with programs v. 12., 373-408.

Meinert, L.D., Newberry, R.J., and Einaudi, M.T.,1980. An overview of W, Cu, and Zn-bearing skarns. In Western North America. In Field C and Silberman, M., (eds.), Mineral Deposits of the Pacific Northwest, U.S. Geol.Survey Open File Rep. 81-355, p. 303-327.

Meinert, L.D., 1983, Variability of skarn deposits-Guides to exploration in Boardman, S.J., (ed.), Revolution in the Earth Sciences, Kendall-Hunt Publishing Co., p. 301-316.

Meinert, L.D., 1987, Skarn zonation and fluid evolution in the Groundhog Mine, Central Mining District, New Mexico. Econ. Geol., v. 82, p. 523-545.

Meinert, L.D., 1990, Skarn deposits in Nevada - Geology, mineralogy, and petrology of Au, Cu, W, and Zn skarns: In L.D.Meinert, G.L. Myers, and, J.W. Brooks (eds.), Skarn deposits in Nevada , Great Basin Symposium - Geology and ore deposits of the Great Basin, Geological Society of Nevada Fieldtrip #2 Guidebook, p. 41-72

Meinert, L.D., 1992, Skarns and skarn deposits. Geoscience Canada, v. 19, p. 145-162.

Meinert, L.D., 1993, Igneous petrogenesis and skarn deposits. In R.V. Kirkham, W.D. Sinclair, R.I. Thorpe, and J.M.Duke, (eds.), Geol. Assoc. Can. Special Paper, v. 40, p. 569-583.

Meinert, L.D., 1995, Compositional variation of igneous rocks associated with skarn deposits - Chemical evidence for a genetic connection between petrogenesis and mineralization. In Thompson, J.F.H., (eds.), Magmas, fluids, and ore deposits, Min. Assoc. Canada Short Course Series, v. 23, p. 401-418.

Meinert, L.D., 1997. Skarns and skarn deposits. Http://www.wsu.edu:8080/~meinert/about skarn.html.

Millet, F., 1938. Denek simli kurşun madeni hakkında rapor. M.T.A. Rep. no. 779, 7 p.

Morimoto, N., Frabies, J., Ferguson, A.K., Ginzburg, I.V., Ross, M., Siefert, F.A., Zussman, J., Aoki, K., and Gottardi, G., 1988. Nomenclature of pyroxenes. American Mineralogist v.73, p.1123-1133.

M.T.A., 1965. Türkiye volfram ve molibden yatakları. M.T.A. Publ., no 128, 12 p.

Mutschler, F., Wright, E., Ludington, S. and Abbott, J., 1981. Granite molybdenum systems. Econ. Geol., v. 76, p.874-897.

Nakano, T., 1982. Genesis of skarn developed in diorite porphyry at the Kamaishi Mine, Japan, (Abstract). Ph.D. Thesis, University of Tsukuba, Tsukuba, 162 p.

Nakano, T., 1989. Fluctuation model for compositional heterogeneity of skarn clinopyroxenes. Geochemical Journal, v. 23, p. 91-99.

Nakano, T., Takahara, H., and Nishida, N., 1989. Intra crystalline distribution of major elements in zoned skarn in the Chichibu Mine, Central Japan: Illustration by color coded maps. Canadian Mineralogist., v. 27, p. 499-507.

Nakano, T., 1991. An antipathetic relation between the hedenbergite and johannsenite components in skarn clinopyroxenes from the Kagata tungsten deposit, Central Japan. Canadian Mineralogist, v. 29, p. 427-434.

Nakano, T., Yoshino, T., Shimazaki, H., and Shimuzu, M., 1994. Pyroxene composition in the classification of skarn deposits. Econ. Geol., v. 89, p. 1567-1580.

Newberry, R.J., 1982. Tungsten-bearing skarns of the Sierra Nevada, The Pine Creek Mine, California. Econ. Geol., v. 77, p. 823-844.

Newberry, R.J. and Swanson, S.E., 1986. Scheelite skarn granitoids: An evolution and roles of magmatic source and process, Ore Geology Reviews, v. 1., p. 57-81.

Newberry, R.J., 1987. Use of intrusive and calc-silicate compositional data to distinguish contrasting skarn types in the Darwin polymetallic skarn district, California, U.S.A. Mineral. Deposita, v. 22, p. 207-215.

Newberry, R.J., Burns, L.E., Swanson, S.E., and Smith, T.E., 1990. Comparative petrologic evolution of the Sn and W granites of the Fairbanks-Circle area, Interior Alaska. In H.J. Stein and J.L., Hannah (eds.) Ore bearing granite systems; Petrogenesis and mineralizing processes. Geol. Soc. America Spec. Paper v. 246, p. 121-142.

Newberry, R.J., Einaudi, M.T., and Eastman, H.S., 1991. Zoning and genesis of the Darwin Pb-Zn-Ag skarn deposit, California: A reinterpretation based on new data. Econ. Geol., v. 86, p. 960-982.

Ortoleva, P., Merino, E., Moore, C. and Chadam, J., 1987. Geochemical self-organ,sation I: Reaction transport feedbacks and modeling approach. American J. of Sci. v. 287, p. 979-1007.

Özcan, A., Göncüoğlu, M.C., Turhan, N., Şentürk, K., Uysal, Ş. And Işık, A., 1990. Konya-Kadınhanı-Ilgın dolayının temel jeolojisi. M.T.A. Rep. no. 9535, 139 p.

Özkan, H.M.and Erkan, Y.,1994. A petrological study on a foid syenite intrusion in central Anatolia (Kayseri, Turkey). Doğa, v.3, 45-55.

Özkazanç, F., 1980. Ankara-Keskin-Denek madeni manyetik etüd raporu. M.T.A. Rep. no. 6764, 8 p.

Park, C.F. and McDiarmid, R.A., 1975. Ore Deposits, Freeman, San Fransisco, 512 p.

Paolo, S., 1909. Akdağ gümüş madeni raporu, M.T.A. Rep. no., 392.

Perry, D.V., 1969. Skarn genesis at the Christmas mine, Gila County, Arizona. Econ. Geol., v. 64, p. 255-270.

Picot, P. and Johan, Z., 1982. Atlas of ore minerals. Elsevier, Orleans, 458 p.

Pilz, R., 1936. Akdağmadeni hakkında rapor. M.T.A. Rep. no. 898, 5 p.

Pollak, A., 1958. 1957 yılında Akdağmadeni-Yıldızeli sahasında yapılan jeolojik prospeksiyon hakkında rapor. M.T.A. Rep. no. 2679,

Polvates, Y.A., Bakhtin, A.I., Polvates, Z.I., and Lapotin, O.N., 1996. Garnets as an indicator of physicochemical conditions of magnetite-bearing skarn deposit formation. Geology of Ore Deposits, v. 38(2), p. 163-167.

Sağıroğlu, A., 1982. Contact metasomatism and ore deposition of the lead-zinc deposits of Akdağmadeni, Yozgat, Turkey, Ph.D. Thesis, University of London, London, 314p.

Sağıroğlu, A., 1984a. Akdağmadeni (Yozgat) kurşun-çinko yataklarında cevherleşme. Jeoloji Müh., v. 21, p.15-27.

Sağıroğlu, A., 1984b. Akdağmadeni, (Yozgat) cevherleşmelerinde görülen değişik skarn oluşuklarının özellikleri ve irdelenmesi. Türkiye Jeol. Kur. Bull., v. 27, p. 69-80.

Sağıroğlu, A., 1984c. Akdağmadeni (Yozgat) kontakt metasomatik yataklarında sıvı kapanım çalışmaları. Türkiye Jeol. Kur. Bull., v. 27, p. 141-144.

Sato, K., 1980. Tungsten skarn deposit of the Fujigatani mine, Soutwest Japan. Econ. Geol., v. 75, p. 1066-1082.

Seymen, İ., 1981. Kaman (Kırşehir) dolayında Kırşehir masifinin stratigrafisi ve metamorfizması. Türkiye Jeol. Kur. Bull., v.24, p. 7-14.

Seymen, İ., 1982. Kaman dolayında Kırşehir masifinin jeolojisi, Docentlik Tezi, İstanbul Tek. Üniv., İstanbul, 164 p.

Şengör, A.M.C. and Yılmaz, Y., 1981. Tethyan evolution of Turkey: A plate tectonic approach. Tectonophysics, v. 75., p. 181-241.

Shimazaki, H., 1975. The ratios of Cu/Zn-Pb of pyrometasomatic deposits in Japan and their genetic implications. Econ. Geol., v. 70, p. 717-724.

Shimazaki, H., 1980. Characteristics of skarn deposits and related acid magmatism in Japan. Econ. Geol., v. 75, p. 173-183.

Shimuzu, M. and Iiyama, T., 1982. Zinc-lead skarn deposits of the Nakatatsu Mine, Central Japan. Econ. Geol., v. 77, p. 1000-1012.

Tekeli, O., Varol, B., Gökten, E., Kesgin, Y., Özaksoy, V. and Işık, V., 1992. Sivas havzasının batı kesiminin jeolojisi. TPAO Rep. no. 3173, 147 p.,

Tülümen, E., 1980. Akdağmadeni (Yozgat) yöresinde petrografik ve metalojenik incelemeler, Ph.D. Thesis, Karadeniz Tek. Üniv., Trabzon, 157p.

Tümer, L., 1984. Türkiye molibden envanteri, M.T.A. Publ. No. 191, 35 p.

Türeli, T.K., 1991. Geology, petrology, and geochemistry of Ekecikdağ plutonic rocks (Aksaray region, central Anatolia), Ph.D. Thesis, Middle East Technical Univ., Ankara, 194 p.

Türeli, T.K. and Göncüoğlu, M.C., 1993. Ekecikdağ Granitoyidinin petrolojisi ve kökeni (Orta Anadolu Kristalen Kütlesi Batısı). M.T.A. Bull., v. 115, p. 15-28.

Tüysüz, O., 1993. Karadenizden Orta Anadoluya bir jeotravers: Kuzey Neotetisin tektonik evrimi. TPJD Bull., v. 5(1), p. 1-33.

Tüysüz, O., Dellaloğlu, A.A. and Terzioğlu, N., 1995. A magmatic belt within the Neotethyan suturre zone and its role in the tectonic evolution of northern Turkey. Tectonophysics, v. 243. P. 173-191.

Vache, R., 1963. Akdağmadeni kontak yatakları ve bunların Orta Anadolu Kristalinine karşı olan jeolojik çerçevesi. M.T.A. Inst. Bull., v. 60, p. 22-36.

Vidale, R., 1969. Metasomatism in a chemical gradient and the formation of calc-silicate bands. American J. Sci., v. 267, p. 857-874.

White, A.J.R:, Beams, S.D. and Cramer, J.J:, 1977. Granitoid types and mineralization with special reference to tin. In N. Yamada (ed.), Plutonism in relation to volcanism and metamorphism, 7th CPPP Meeting, Toyama, Japan, p. 89-100.

Wiggins, L.B., and Craig, J.R., 1980, Reconnaissance of the Pb-Zn-S system: Sphalerite phase relationships. Econ. Geol., v. 75, p. 742-752.

Yalınız, M.K., Göncüoğlu, M.C. and Floyd, P.A.,1994. Geochemical characteristics and geodynamic interpretation of supra-subduction Sarıkaraman Ophiolite, Central Anatolia, Turkey. International Volcanological Congress, Ankara, Abstracts vol. 144 p.

Yalınız, M.K., Göncüoğlu, M.C. and Floyd, P.A., 1995. Petrology of plagiogranites of Sarıkaraman ophiolites (Central Anatolia) and their tectonic significance within the Eastern Mediterranean ophiolites. EUG 8th Biannual meeting, Strasbourg, Terra Abstracts vol. 179p.

Yalınız, M.K. Floyd, P.A. and Göncüoğlu, M.C., 1996. Supra-subduction zone ophiolites of Central Anatolia: Geochemical evidence from the Sarıkaraman Ophiolite, Aksaray, Turkey. Mineral. Mag., v. 60, p. 697-710.

Yardley, B.W.D., Rocehelle, C.A., Barnicoot, A.C., and Lloyd, G.E., 1991. Oscillatory zoning in metamorphic minerals: As an indicator of infiltration metasomatism., Mineral. Mag., v. 55. 357-365.

Yun, S., and Einaudi, M.J., 1982, Zinc-lead skarns of the Yeonhwa-Ulchin district, South Korea. Econ. Geol., v.77, p. 1013-1032.

Zharikov, V.A., 1970, Skarns. International. Geol. Rev., v. 12, p. 541-559, 619-647, 760-775.

Zimmermink, W.G., 1985. Optical anomalies of garnets in the skarn deposit of Santender, Peru. N. Jb. Miner. Mh., v. 5, p. 221-233.

APPENDIX 1

MICROPROBE ANALYSES

1.1. Sample preparation

The microprobe analyses were made on 33 selected fresh, doubly polished thin sections. The samples were polished in the laboratories of the M.T.A Institute. completed sections (2.6 cm by 4.8 cm) were coated in carbon, by using an Edwards S150B sputter vacuum coater to provide a conductive layer to minimize charge build up under the electron beam.

1.2. Microprobe analyses

Microprobe data were collected on a JEOL JSM35 Scanning Electron Microscope running link QX2000 energy dispersive analytical software at Keele University. The operating conditions were as follows; The beam current was 15 kV. Normally a probe session would begin with a gain calibration for a certain element. The primary standard used was diopside for the minerals to be analyzed. Following successful calibration of the instrument, routine analyses would proceed. SiO2, Al2O3, TiO3, Fe2O3, FeO, MnO, MgO, CaO, Na2O and K2O major oxides were analyzed, and calibrated according to standard used.

The data was then corrected by a theoretical ZAF correction procedure using a computer software developed by David Emley. Individual analyses of garnets, pyroxenes, amphiboles and epidotes are given in the following tables in Appendix 2. The molecular proportions were calculated on the basis of the number of oxygen atoms. These are 6 for pyroxenes, 24 for garnets, 23 for amphiboles and 13 for epidotes.

APPENDIX 2

WHOLE ROCK GEOCHEMISTRY ANALYSES

2.1. Preliminary preparation

The rock samples were prepared for analysis in the following way: (a) samples were washed and scrubbed under the tap to remove all extraneous materials such as soil and lichen, (b) samples were cut into blocks on the diamond saw to remove the weathered materials from the margin, and to reduce samples to manageable fragments ready for the "Denbigh fly-press splitter", (c) the samples were split into fragments of 1-2 cm diameter pieces. Any remaining weathered material was removed at this stage, (d) A sturtevant Jaw-crusher of 5x7.5 cm size was used to reduce the split samples to a 6 to 10 mm size rock chips, suitable for Tema mill, (e) the rock chips were then homogenized by cone-and-quartering. Any remaining weathered material was picked out at this stage too. An approximately 100 g of sample was prepared by this method for further reduction by Tema mill (f) the sample was ground in the Tema mill for 50 to 60 seconds to reduce the chips to a fine powder of around 120 microns. After this stage, the sample were ready to prepare for major and trace element analysis by XRF.

2.2. Preparation of samples for trace and major element analyses

About 20 g of rock powder was dried at 110°C for about two hours to remove adsorbed water. After cooling in desiccator for about 15 minutes, an accurately weighted 4 g of rock powder within the platinum crucible was ignited at 1000°C for 30 minutes. After cooling in a desiccator for about 15 minutes the crucible and ignited powder was reweighted and the "loss on ignition (LOI) of the sample was calculated.

The trace and major element analyses were done by using the pressed powder pellets and fused squash beads.

The procedure for the preparation of pellets are given as follows: 10 g of rock powder was mixed with 10 drops of 2% moviol solution an mixed in an agate mortar

with the pestle until homogeneous. The material was then transferred to the die and placed between two tungsten carbide formers and pressed at 20 tons/sq-inc for 4 minutes. The sample pellets were then removed from the press and placed in an oven at 110°C overnight.

The procedures for squashed fused beads are as follows: 0.7 g ignited powder and 3.5 g spectroflux was mixed. When completely mixed, the sample-flux was transferred to a platinum-gold crucible and heated over a meker burner until the mixture was molten. Beads were formed by pouring the melt into die, and immediately after pressing the melt within the aluminum plunger for a few seconds. The bead is strengthened by a previously inserted bounding ring.

2.3. X-Ray Fluorescence analysis (XRF)

X-Ray fluorescence analyses for both trace and major elements was performed on ARL 8420 spectrometer in the Department of Earth Sciences at the University of Keele (England). The x-ray tube used was a Matchlett 75 kv rhodium end-window type. The diagramization of both trace and major element results, and the calculation of normative mineral compositions were carried out by using software developed by David Emley.

VITA

İlkay KUŞCU was born in Kozağaç-Burdur in 20.10.1967. After graduation from the Burdur Cumhuriyet Lisesi in 1984, he entered the Department of Geological Engineering Department , Middle East Technical University. He graduated from this department in July 1989. In the same year he joined the Department of Geological Engineering, Middle East Technical university as a teaching assistant, and he has been working in the same department since then. He had the M.S. degree in the Department of Geological Engineering, Middle East Technical University in February 1992. In the same year he began his Ph. D. studies at the Department of Geological Engineering, Middle East Technical University. He married in August 1994.

İlkay Kuşcu has 4 papers, all of which are published n the national journals. He has 11 presentations at international conferences and 3 presentations at national conferences. A total of 2 papers are currently in review in international journals.